TECHNISCHE UNIVERSITÄT MÜNCHEN

Ingenieurfakultät Bau Geo Umwelt

Lehrstuhl für Siedlungswasserwirtschaft

„Sequential Managed Aquifer Recharge Technology (SMART) – The role of dissolved organic carbon composition and concentration on trace organic chemical transformation“

Karin Elisabeth Hellauer

Vollständiger Abdruck der von der Ingenieurfakultät Bau Geo Umwelt der Technischen Universität München zur Erlangung des akademischen Grades eines

Doktors der Naturwissenschaften (Dr. rer. nat.)

genehmigten Dissertation.

Vorsitzende:	apl. Prof. Dr. rer. nat. habil. Brigitte Helmreich
Prüfer der Dissertation:	1. Prof. Dr.-Ing. Jörg E. Drewes
	2. Prof. Dr.-Ing. Martin Jekel
	3. Prof. Dr. Martin Elsner

Die Dissertation wurde am 05.12.2018 bei der Technischen Universität München eingereicht und durch die Ingenieurfakultät Bau Geo Umwelt am 04.03.2019 angenommen.

Für meine wunderbare Familie und meine großartigen Freunde

“It's the possibility of having a dream come true
that makes life interesting.”

Paulo Coelho, The Alchimist

Abstract

Managed aquifer recharge (MAR) systems such as induced bank filtration or surface spreading techniques are often used as part of a drinking water treatment train. They are known to provide an efficient barrier for trace organic chemicals (TOrCs) which could be detected in the aquatic environment e.g. due to the discharge of wastewater treatment plants. The removal of TOrCs during MAR is assigned to biotransformation rather than sorption, whereby a co-metabolic process is assumed. This indicates the important role of dissolved organic carbon (DOC) serving as primary substrate. It was previously shown that the biodegradation of TOrCs during MAR is enhanced under carbon-limited as well as oxic redox conditions resulting in a highly diverse microbial community with broad metabolic capabilities. Based on these results, the sequential managed aquifer recharge technology (SMART) was established which is characterized by two infiltration steps with an intermediate aeration to establish prevailing carbon-limited and oxic conditions in the second system. The SMART concept results in an improved removal of many moderately degradable TOrCs in comparison to a conventional operated MAR. However, factors triggering this enhanced transformation of TOrCs are still poorly understood and need to be further investigated. Thus, the scope of this dissertation project was to test the applicability of the SMART concept in the case study Berlin and to investigate more mechanistically the role of the dissolved organic carbon (DOC) on the transformation of TOrCs.

The first objective was to validate the applicability of the SMART concept under different conditions for the case study of Berlin. Therefore, laboratory- as well as field-scale experiments were performed. The laboratory-scale soil column experiment consisted of four parallel systems each comprised of two columns operated in series. Between both columns different intermediate treatment steps were applied in order to adjust the predominant redox conditions, namely: i) no aeration (representing conventional bank filtration), ii) aeration with air, iii) aeration with pure oxygen, and iv) oxidation with ozone. Even though carbon-limited and oxic conditions did only partly prevail in these laboratory-scale SMART systems, the transformation of targeted TOrCs was equal or better in comparison to a system mimicking conventional bank filtration. At field-scale, the SMART approach was compared to a conventional operated MAR facility. Oxic and carbon-limited conditions solely prevailed at the SMART field site resulting in a better performance regarding TOrCs transformation in comparison to conventional MAR. Both, at laboratory- as well as field-scale, several compounds such as 4-Formylaminoantipyrine, gabapentin or benzotriazole exhibited a significantly better removal during SMART in comparison to conventional MAR treatment.

The second objective of this study aimed at understanding the effect of biodegradable DOC composition as well as concentration on TOrCs removal more mechanistically. Thus, the fate of the effluent organic matter (EfOM) serving as primary substrate for microorganisms also engaged in TOrC transformation was monitored using Fourier transform ion cyclotron resonance mass spectrometry (FT-ICR-MS) in combination with spectroscopic methods within a simulated SMART system. These structural changes were further linked to the different behavior of TOrCs throughout the infiltration as well as the prevailing microbiome. A correlation between molecular compositions with distinct clusters

of TOrCs as well as microbial phyla was observed suggesting that the application of FT-ICR-MS analyses in combination with 16S rRNA amplicon sequencing can help to elucidate the influence of DOC composition on TOrCs transformation. A second laboratory-scale experiment was conducted to investigate the influence of the concentration of highly refractory primary substrate on the transformation of TOrCs. These results indicated that TOrCs transformation does not always rely on the principle of co-metabolism, hence metabolic degradation seems to be more probable under extremely carbon-depleted conditions (at biodegradable DOC concentrations of ≤ 0.7 mg/L).

The third objective was the characterization of oxic and carbon-limited conditions for TOrC biotransformation using redox and bulk organic parameters and biomolecular methods. The approach taken followed the principle of oligotrophy and copiotrophy which describes the two trophic strategies of microorganisms in ecosystems. While copiotrophic organisms grow in nutrient rich environments, oligotrophic organisms prefer nutrient-poor conditions. The trophic strategy of an organism is represented in its genome, hence, information derived from bacterial genomes could be used to predict their preferred lifestyle. This concept could be used to asses prevailing carbon conditions in MAR systems. A set of genomic markers characteristic for oligotrophic or copiotrophic organisms was identified and further used to establish a Bayesian model. This model could be used to successfully predict prevailing carbon conditions using (meta)genomic datasets to confirm the presence or absence of favorable carbon-limited conditions.

This dissertation thesis provides new insight into the biotransformation of TOrCs in natural treatment systems with the focus on SMART as well as the role of DOC concentration and its composition on TOrCs transformation. The applicability of SMART and its great potential compared to conventionally operated MAR facilities could be demonstrated. FT-ICR-MS analyses in combination with 16S rRNA amplicon sequencing was applied for the first time to elucidate the influence of DOC composition on TOrCs transformation. Furthermore, low concentration of highly refractory biodegradable DOC used as feed water might establish conditions that favor metabolic TOrC transformation during MAR where the microbial community present is able to use TOrCs as sole carbon source. Observed differences between TOrCs transformation even under similar boundary conditions emphasize the need to further study the metabolic potential within the prevailing microbial community and its influence on TOrCs biodegradation pathways. Furthermore, a Bayesian network model was established which allows the prediction of favorable carbon-limited conditions based on (meta)genomic data.

Zusammenfassung

Naturnahe Aufbereitungsverfahren wie die Uferfiltration sind häufig ein wichtiger Bestandteil der Trinkwasseraufbereitung. Diese Verfahren sind bekannt für die effektive Entfernung von Spurenstoffen, welche meist über den Ablauf von Kläranlagen in die aquatische Umwelt gelangen. Der Abbau solcher Spurenstoffe findet dabei neben der Sorption, hauptsächlich durch Biotransformation statt. Dabei wird angenommen, dass der Abbau co-metabolisch erfolgt, weshalb der gelöste organische Kohlenstoff als Primärsubstrat bei der Entfernung der Spurenstoffe eine bedeutende Rolle spielt. Bisherige Studien haben gezeigt, dass vorherrschende kohlenstoffarme sowie oxische Bedingungen in solchen naturnahen Aufbereitungsverfahren zu einem verbesserten Spurenstoffabbau führen. Dies kann mit der Entwicklung einer diversen mikrobiellen Gemeinschaft, die ein großes metabolisches Potential aufweist, begründet werden. Aufgrund dieser Erfahrungen wurde ein sequentielles Verfahren entwickelt (*engl.:* sequential managed aquifer recharge technology, SMART), das durch die Kombination zweier Infiltrationsschritte mit einer Zwischenbelüftung, die zu den bevorzugten kohlenstoffarmen und oxischen Bedingungen im zweiten System führen, gekennzeichnet ist. Das SMART Verfahren zeichnet sich im Vergleich zu konventionell betriebenen Verfahren durch eine verbesserte Entfernung von vor allem moderat abbaubaren Spurenstoffen aus. Faktoren, die den Abbau von Spurenstoffen während naturnaher Aufbereitung beeinflussen sind jedoch kaum verstanden und bedürfen deshalb weitergehenden Untersuchungen. Die Schwerpunkte dieses Dissertationsprojektes sind einerseits die Anwendbarkeit von SMART am Fallbeispiel Berlin zu untersuchen sowie den Einfluss des gelösten organischen Kohlenstoffes auf die Transformation der Spurenstoffe mechanistisch aufzuklären.

Die erste Zielstellung war die Validierung des SMART Konzeptes unter verschiedenen Bedingungen anhand des Fallbeispiels Berlin. Dafür wurden sowohl Labor- als auch Feldversuche durchgeführt. Der Laborversuch bestand aus vier parallel betriebenen experimentellen Aufbauten aus je zwei mit Sand gefüllten Säulen. Zwischen den beiden Säulen fanden unterschiedliche Zwischenbehandlungen statt, um die vorherrschenden Redoxbedingungen zu manipulieren: i) keine Belüftung (repräsentativ für eine konventionelle Uferfiltration), ii) Belüftung mit Luft, iii) Belüftung mit reinem Sauerstoff sowie iv) Oxidation mit Ozon. Obwohl in den SMART Systemen bevorzugte kohlenstofflimiterte und oxische Bedingungen nur teilweise vorlagen, zeigte sich ein gleicher oder besserer Abbau untersuchter Spurenstoffe verglichen mit der konventionellen Uferfiltration. Während des Feldversuchs konnten kohlenstofflimitierte und oxische Bedingungen für das SMART Verfahren im Vergleich zu einer konventioneller MAR Fahrweise etabliert werden was zu einem gleichen oder verbesserten Abbau biologisch abbaubarer Spurenstoffe in SMART führte. Sowohl bei den Labor- als auch den Feldversuchen zeigten einige Stoffe, darunter 4-Formylaminoantipyrin, Gabapentin oder Benzotriazol eine signifikant verbesserte Entfernung im SMART Verfahren verglichen mit dem konventionellen Betrieb.

Eine weitere Zielstellung dieser Arbeit war die mechanistische Aufklärung des biologisch abbaubaren organischen Kohlenstoffs bezüglich seiner Komposition sowie Konzentration auf die Spurenstoffentfernung. Dabei wurde die Veränderung des organischen Materials,

welches als Primärsubstrat dient, in einem simulierten SMART System im Labormaßstab untersucht. Dies erfolgte mittels FT-ICR-MS (*engl.:* Fourier-transform ion cyclotron resonance mass spectrometry) in Kombination mit spektroskopischen Verfahren. Diese strukturellen Veränderungen wurden mit dem unterschiedlichen Verhalten einzelner Spurenstoffe sowie der Zusammensetzung der dominierenden mikrobiellen Gemeinschaft in Verbindung gebracht, wodurch ein Zusammenhang zwischen der molekularen Komposition des Primärsubstrats mit Gruppen von Spurenstoffen sowie mikrobiellen Stämmen herausgearbeitet werden konnte. Dies zeigt, dass die Kombination aus FT-ICR-MS sowie 16S rRNA Amplikon Sequenzierung genutzt werden kann, um den Einfluss der Komposition des gelösten organischen Kohlenstoffs und der mikrobiellen Gemeinschaft auf den Spurenstoffabbau zu erklären. Ein weiterer Versuch im Labormaßstab diente dazu, den Einfluss der Konzentration von refraktärem Primärsubstrat auf die Transformation von Spurenstoffen zu untersuchen. Die Ergebnisse zeigten, dass die Entfernung der Spurenstoffe nicht immer einem co-metablischem Prozess folgen, sondern, dass unter stark kohlenstofflimitierten Bedingungen auch ein metabolischer Abbau stattfinden kann.

Die dritte Zielstellung galt der Charakterisierung von oxischen und kohlenstoff-limitierten Bedingungen mittels Redox- und organischen Summenparametern sowie biomolekularen Methoden. Der Ansatz beruht auf dem Prinzip der Oligotrophie und Copiotrophie, die unterschiedliche Ernährungsstrategien von Organismen in Ökosystemen beschreiben. Während copiotrophe Organismen eine nährstoffreiche Umgebung bevorzugen, wachsen oligotrophe Organismen bevorzugt unter nährstoffarmen Bedingungen. Die Ernährungsstrategie eines jeden Organismus ist in dessen Genom repräsentiert, so dass Informationen des bakteriellen Genoms genutzt werden können, um die jeweilige Ernährungsstrategie zu bestimmen. Dieses Konzept könnte genutzt werden, um die vorherrschenden Bedingungen hinsichtlich Kohlenstoffverfügbarkeit in naturnahen Aufbereitungsverfahren auf der biomolekularen Ebene zu beschreiben. Eine Auswahl an genomischen Markern, welche charakteristisch für oligotrophe bzw. copiotrophe Organismen sind, konnten dabei identifiziert werden. Anhand dieser Marker wurde ein Bayesian Modell entwickelt, das für die Vorhersage vorherrschender Bedingungen auf Basis von (Meta)genomdaten genutzt werden kann.

Die Ergebnisse dieser Dissertation liefern neue Einblicke hinsichtlich der Biotransformation von Spurenstoffen während einer naturnahen Trinkwasseraufbereitung mit Fokus auf dem SMART Konzept, wobei insbesondere die Rolle der Konzentration und Komposition des gelösten organischen Kohlenstoffs auf den Spurenstoffabbau aufgeklärt werden konnte. Die Vorteile des SMART Verfahrens hinsichtlich einer Spurenstoffentfernung im Vergleich zu konventionellen Aufbereitungsverfahren konnte herausgestellt werden. Des Weiteren wurden strukturelle Veränderungen der Komposition des gelösten organischen Kohlenstoffs beim Spurenstoffabbau durch die Einsatz der FT-ICR-Massenspektrometrie herausgearbeitet und diese durch die Kombination mit 16S rRNA Amplikon Sequenzierung mit der Zusammensetzung der mikrobiologischen Gemeinschaft korreliert. Weiterhin konnte gezeigt werden, dass die Entfernung von Spurenstoffen unter sehr kohlenstoffarmen Bedingungen nicht immer mit einem co-metablischen Abbau zu erklären ist und die vorherrschende mikrobielle Gemeinschaft in der Lage zu sein scheint, Spurenstoffe als alleinige Kohlenstoffquelle zu nutzen.

Unterschiede in der Entfernungsleistung von Spurenstoffen unter ähnlichen Umweltbedingungen in unterschiedlichen Systemen unterstreicht die Notwendigkeit detailliertere Untersuchungen des metabolischen Potenzials der vorherrschenden mikrobiellen Gemeinschaft durchzuführen. Ebenso gelang es innerhalb dieses Dissertationsvorhaben, ein Bayesian Model zu entwickeln, das zur Vorhersage dominanter Umgebungsbedingungen in biologisch aktiven Systemen hinsichtlich der Kohlenstoffverfügbarkeit genutzt werden kann.

Author contributions

This cumulative dissertation is based published peer-reviewed research papers as well as papers in preparation, which are presented in the same or similar form as published in chapters 4 to 8.

Paper I:

Hellauer, K., Mergel, D., Ruhl, A.S., Filter, J., Hübner, U., Jekel, M., Drewes, J.E., 2017. Advancing Sequential Managed Aquifer Recharge Technology (SMART) Using Different Intermediate Oxidation Processes. *Water* 9 (3), 221.

- Chapter 4
- Author contribution: Karin Hellauer, Aki S. Ruhl, Uwe Hübner, Martin Jekel and Jörg E. Drewes conceived and designed the experiment; Dorothea Mergel, Karin Hellauer and Josefine Filter performed the experiments; Dorothea Mergel and Karin Hellauer analyzed the data; Josefine Filter, Aki S. Ruhl and Martin Jekel contributed reagents, materials and analysis tools; Aki S. Ruhl performed the HPLC–MS/MS analysis; Karin Hellauer wrote the paper Jörg E. Drewes and Uwe Hübner supervised this study and reviewed the manuscript. The final version was approved by all authors.

Paper II:

Hellauer, K., Karakurt, S., Sperlich, A., Burke, V., Massmann, G., Hübner, U., Drewes, J.E., 2018. Establishing sequential managed aquifer recharge technology (SMART) for enhanced removal of trace organic chemicals: Experiences from field studies in Berlin, Germany. *Journal of Hydrology* 563, 1161–1168.

- Chapter 5
- Author contribution: Karin Hellauer, Alexander Sperlich, Victoria Burke, Gudrun Massmann, Uwe Hübner and Jörg E. Drewes conceived and designed the experiment; Sema Karakurt, Victoria Burke and Karin Hellauer performed the experiment; Sema Karakurt, Victoria Burke and Karin Hellauer analyzed the data; Alexander Sperlich, Gudrun Massmann and Jörg E. Drewes contributed reagents, materials and analysis tools; Karin Hellauer wrote the paper; Jörg E. Drewes, Uwe Hübner, Alexander Sperlich, Viktoria Burke and Gudrun Massmann supervised this study and reviewed the manuscript.

Paper III:

Hellauer, K., Uhl, J., Lucio, M., Schmitt-Kopplin, P., Wibberg, D., Hübner, U., Drewes, J.E., 2018. Microbiome-Triggered Transformations of Trace Organic Chemicals in the Presence of Effluent Organic Matter in Managed Aquifer Recharge (MAR) Systems. *Environmental Science & Technology* 52 (24), 14342–14351.

- Chapter 6
- Author contribution: Karin Hellauer, Uwe Hübner and Jörg E. Drewes conceived and designed the experiment; Karin Hellauer performed the experiment; Jenny Uhl performed the FT-ICR-MS measurements. Both authors contributed equally; Marianna Lucio performed the multivariate analyses; Karin Hellauer, Daniel Wibberg, Jenny Uhl and Marianna Lucio analyzed the data; Philippe Schmitt-Kopplin provided the reagents and equipment for FT-ICR-MS measurements; Uwe Hübner and Jörg E. Drewes supervised the study; Jenny Uhl, Philippe Schmitt-Kopplin, Daniel Wibberg, Uwe Hübner and Jörg E. Drewes reviewed the manuscript.

Paper IV:

Hellauer, K., Martínez Mayerlen, S., Drewes, J.E., Hübner, U., 2019. Biotransformation of trace organic chemicals in the presence of highly refractory dissolved organic carbon. *Chemosphere* 215, 33–39.

- Chapter 7
- Author contribution: Karin Hellauer and Uwe Hübner conceived and designed the experiment; Sara Martínez Mayerlen and Karin Hellauer performed the experiment and analyzed the data; Uwe Hübner supervised the study; Karin Hellauer wrote the paper. Uwe Hübner and Jörg E. Drewes reviewed the paper.

Paper V:

Hellauer, K., Michel, P., Holland, S.I., Hübner, U., Drewes, J.E., Lauro, F.M., Manefield, M.J., in preparation. Genomic Bayesian networks identify trophic strategies in microbiomes of managed aquifer recharge (MAR) systems. *The ISME Journal*.

- Chapter 8
- Author contribution: Karin Hellauer, Uwe Hübner and Michael J. Manefield conceived and designed the experiments; Karin Hellauer performed the experiments; Karin Hellauer, Sophie Holland and Federico M. Lauro analyzed the data; Philipp Michel performed the Bayesian network analysis and implemented this part in the paper; Karin Hellauer wrote the paper; Uwe Hübner, Michael J. Manefield and Federico M. Lauro supervised the study; Uwe Hübner, Jörg E. Drewes, Federico M. Lauro and Michael J. Manefield reviewed the paper.

Further related scientific contributions

Publication:

- Hettwer, Karina; Jähne, Martin; Frost, Kirstin; Giersberg, Martin; Kunze, Gotthard; Trimborn, Michael; Reif, Martin; Türk, Jochen; Gehrmann, Linda; Dardenne, Freddy; Croock, Femke de; Abraham, Marion; Schoop, Anne; Waniek, Joanna J.; Bucher, Thomas; Simon, Eszter; Vermeirssen, Etienne; Werner, Anett; **Hellauer, Karin**; Wallentits, Ursula; Drewes, Jörg E.; Dietzmann, Detlef; Routledge, Edwin; Beresford, Nicola; Zietek, Tamara; Siebler, Margot; Simon, Anne; Bielak, Helena; Hollert, Henner; Müller, Yvonne; Harff, Maike; Schiwy, Sabrina; Simon, Kirsten; Uhlig, Steffen. 2018. Validation of *Arxula* Yeast Estrogen Screen assay for detection of estrogenic activity in water samples: Results of an international interlaboratory study. *Science of the Total Environment* 621, 612-625

Oral presentations:

- **Hellauer, K.**; Uhl, J.; Lucio, M.; Schmitt-Kopplin, P.; Hübner, U.; Drewes, J.E.: Characterizing the transformation of natural organic matter in managed aquifer recharge systems. 13th European Fourier Transform Mass Spectrometry Workshop, Freising (Germany), 23.-27.04.2018.
- Fajnorová S.; Hübner U.; Herzog B.; Müller J.; **Hellauer K.**; Miklos D.; Drewes J.E.; Wanner J.: Fate of antibiotic resistance during advanced wastewater treatment. Vodárenská biologie (Water Supply Biology), Prague (Czech Republic), 06.-07.02.2018
- Drewes, J.E.; **Hellauer, K.**; Karakurt, S.; Zhiteneva, V.; Hübner, U.: Multibarrieren-Aufbereitungsverfahren zur Wasserwiederverwendung auf Basis einer Grundwasseranreicherung. Wassersprachliche Aussprache – WAT, 30.11.2017.
- **Hellauer, K.:** Transformation of trace organic chemicals in natural treatment systems. JAMS – Joint Academic Microbiology Seminars, Sydney (Australia), 31.10.2017.
- Drewes, J.E.; **Hellauer, K.**; Karakurt, S.; Zhiteneva, V.; Regnery, J.; Hübner, U.: Sequential Managed Aquifer Recharge Technology (SMART) For Enhanced Micropollutant Removal from Laboratory Studies to Full-scale Applications. IWA 10th Micropol & Ecohazard Conference, Vienna (Austria), 17.-20.09.2017.
- Sperlich, A.; Karakurt, S.; **Hellauer, K**.; Hübner, U.; Gnirss, R.; Drewes, J.E.: Sequential managed aquifer recharge (SMART): Results of demonstration-scale operation in Berlin, Germany. IWA International Conference of Water Reclamation and Reuse, Long Beach (California, USA), 23.-27.07.2017.
- **Hellauer, K**.; Mergel, D.; Ruhl, A.S.; Filter, J.; Hübner, U.; Jekel, M.; Drewes, J.E.: Sequential Managed Aquifer Recharge Technology (SMART) – Principles, Performance, and Optimization Strategies. IWA International Conference of Water Reclamation and Reuse, Long Beach (California, USA), 23.-27.07.2017.

- Karakurt, S.; Sperlich, A.; **Hellauer, K.**; Hübner, U.; Jekel, M.; Drewes, J.E.: Großtechnische Validierung der sequentiellen Grundwasseranreicherung. Jahrestagung der Wasserchemischen Gesellschaft, Donaueschingen (Germany), 22.-24.05.2017.
- Drewes, J.E.; Hübner, U.; Regnery, J.; **Hellauer, K.**; Karakurt, S.; Zhiteneva, V.: Revisiting the Design and Operation of Biofiltration in Water Treatment. Seminar presentation, Tübingen (Germany), 12.05.2017.
- Drewes, J.E.; Regnery, J.; Hübner, U.; **Hellauer, K.**; Müller, J.; Li, D.: Revising the Design and Operation of Biofiltration in Water Treatment. Institutional Seminar Series Eawag (Switzerland), 15.11.2016.
- Drewes, J.E.; Regnery, J.; Hübner, U.; **Hellauer, K.**; Müller, J.; Li, D.: Revising the Design and Operation of Biofiltration in Water Treatment. Departmental Seminar Series Universität Duisburg-Essen (Germany), 24.10.2016.
- Drewes, J.E.; **Hellauer, K.**; Müller, J.; Li, D.; Regnery, J.; Hübner, U.: Tuning Microbial Function to Transform Micropollutants during Managed Aquifer Recharge and Engineered Biofiltration. SETAC Europe 25th Annual Meeting, Barcelona (Spain), 05.-07.05.2015.
- Drewes, J.E.; **Hellauer, K.**; Müller, J.; Regnery, J.; Li, D.; Hübner, U.: New Design Strategies for Managed Aquifer Recharge Systems and Biofiltration to Enhance Removal of Trace Organic Chemicals. Departmental Seminar. Department of Civil, Mining and Environmental Engineering, 18.09.2015.
- Drewes, J.E.; Li, D.; **Hellauer, K.**; Müller, L.: Microbial Metabolic Capabilities Including Antimicrobial Biosynthesis During Water Infiltration Revealed by Metagenomic and Transcriptomic Analyses. 3rd EDAR Conference, Wernigerode (Germany), 17.-21.05.2015.
- Drewes, J.E.; **Hellauer, K.**; Regnery, J.; Müller, J.; Hübner, U.: Modifikationen der künstlichen Grundwasseranreicherung zur verbesserten Entfernung von anthropogenen Spurenstoffen mit Hilfe von Metatranscriptomics. Jahrestagung der Wasserchemischen Gesellschaft, Schwerin (Germany), 11.-13.05.2015.

Posters:

- Hübner, U.; Karakurt, S.; Zhiteneva, V.; **Hellauer, K.**; Drewes, J. E.: Developing a novel multi-barrier treatment concept based on sequential managed aquifer recharge technology (SMART) for indirect potable reuse. 26. Tagung der Fachsektion Hydrogeologie e.V. in der DGGV e.V., Bochum (Germany), 21.-24.03.2018.
- **Hellauer, K.**, Seiwert, B., Reemtsma, T., Uhl, J., Schmitt-Kopplin, P., Wibberg, D., Winkler, A., Kalinowski, J., Drewes, J.E., Hübner, U.: The role of concentration and composition of bulk organic carbon for microbial degradation of trace organic chemicals in natural treatment systems. 11th IWA Microbial Ecology in Water Engineering & Biofilms, Copenhagen (Denmark), 04.-07.09.2016.

- **Hellauer, K.**; Hübner, U.; Müller, E.; Drewes, J.E.: Sequential managed aquifer recharge leads to a high diverse microbial community resulting in a better attenuation of moderate degradable trace organic chemicals (TOrC). 2nd conference of the Ecology of Soil Microorganisms, Prague (Czech Republic), 29.11.-03.12.2015.
- **Hellauer, K.**; Hübner, U.; Müller, E.; Drewes, J.E.: Diversity and function of microbial communities in charge of micropollutants degradation analyzed by shotgun and 16S rRNA metagenomic sequencing. 6th European Conference on Prokaryotic and Fungal Genomics, Göttingen (Germany), 29.09.-02.10.2015.
- **Hellauer, K.**; Hübner, U.; Müller, E.; Drewes, J.E.: Analysis of microbial community diversity and function responsible for transformation of micropollutants in MAR systems using next generation sequencing. Annual Conference 2015 of the Association for General and Applied Microbiology (VAAM), Marburg (Germany), 01.-04.03.2015.
- Drewes, J.E.; Vuono, D.; Regnery, J.; **Hellauer, K.**; Dong, L.: Design principles for enhanced transformation of chemicals of emerging concern in biological wastewater treatment systems. EU Athene Projekt „Wastewater Treatment Targeted Organic Mikropollutant Biodegradation“,11.-12.11.2014.

List of Contents

Abbreviations XXIII
List of Figures XXVII
List of Tables XXXI
Acknowledgements XXXIII
1 Introduction 1
2 Theoretical background 5
2.1. Trace organic chemicals in the aquatic environment 5
2.2. Managed aquifer recharge (MAR) 6
2.2.1. MAR definition, classification and performance 6
2.2.2. TOrCs removal in MAR systems 7
2.2.3. Role of dissolved organic carbon in managed aquifer recharge 11
2.3. Sequential managed aquifer recharge technology (SMART) 15
2.4. Combination of managed aquifer recharge with oxidation techniques 16
2.5. Trophic strategies of microorganisms in the environment 17
3 Research significance, objectives, and hypotheses 21
3.1. Objectives and hypotheses 21
3.2. Structure of the dissertation 22
4 Advancing sequential managed aquifer recharge technology (SMART) using different intermediate oxidation processes 25
4.1. Introduction 26
4.2. Material and methods 27
4.2.1. Soil column experiments 27
4.2.2. Aeration/Oxidation 27
4.2.3. Analytical methods 28
4.3. Results and discussion 28
4.3.1. Redox conditions 28
4.3.2. Removal of bulk organic parameters 30
4.3.3. Transformation of trace organic chemicals as a function of different oxidation techniques 31
4.4. Conclusions 38
5 Establishing sequential managed aquifer recharge technology (SMART) for enhanced removal of trace organic chemicals: Experiences from field studies in Berlin, Germany 39
5.1. Introduction 40

5.2. Material and methods 41
5.2.1. Field sites 41
5.2.2. Analytical methods 42
5.3. Results and discussion 43
5.3.1. Site characterization 43
5.3.2. Removal of bulk organic carbon 45
5.3.3. Redox conditions 46
5.3.4. Transformation of trace organic chemicals 47
5.4. Conclusions 51
6 Microbiome-triggered transformations of trace organic chemicals in the presence of effluent organic matter in managed aquifer recharge (MAR) systems 53
6.1. Introduction 54
6.2. Material and methods 55
6.2.1. Laboratory-scale column experiment 55
6.2.2. Analytics 56
6.2.3. Statistical analyses 58
6.3. Results and discussion 58
6.3.1. Long-term column characterization of column systems 58
6.3.2. Microbial community structure 61
6.3.3. Characterization of effluent organic matter (EfOM) 62
6.3.4. Fate of the EfOM and correlation with microbial community 63
7 Biotransformation of trace organic chemicals in the presence of highly refractory dissolved organic carbon 71
7.1. Introduction 72
7.2. Material and methods 73
7.2.1. Laboratory-scale column experiment 73
7.2.2. Analytics 74
7.3. Results and discussion 75
7.3.1. Bulk organic carbon and redox characteristics 75
7.3.2. Transformation of TOrCs as a function of different refractory biodegradable DOC concentrations under oxic conditions 77
7.3.3. Comparison of TOrCs transformation under oxic and carbon-limited conditions 80
7.4. Conclusion 83
8 Genomic Bayesian networks identify trophic strategies in microbiomes of managed aquifer recharge (MAR) systems 85

8.1. Introduction 86
8.2. Materials and methods 87
8.2.1. Bacterial genomes 87
8.2.2. Identification of genomic markers 89
8.2.3. Metagenomic dataset 89
8.2.4. Bayesian network analysis 90
8.2.5. Validation 91
8.3. Results 92
8.3.1. Identification of carbon-rich and carbon-limited preferring organisms 92
8.3.2. Characterization of genomic markers 93
8.3.3. Bayesian network analysis 95
8.4. Discussion 99
8.5. Conclusion 100
9 Discussion and outlook 103
9.1. Sequential managed aquifer recharge as promising tool for improved water quality 104
9.1.1. Transformation of TOrCs under oxic and carbon-limited conditions 104
9.1.2. Recommendations and improvements for future SMART applications 108
9.2. DOC composition and TOrCs transformation 110
9.2.1. Linkage between molecular components, microbial community and TOrCs 110
9.2.2. Co-metabolic vs metabolic TOrCs transformation 111
9.3. Identification of favorable carbon-limited (oligotrophic) conditions using genomic markers 112
9.4. Outlook 113
References 115
Appendix 135
SI Chapter 4: Advancing sequential managed aquifer recharge technology (SMART) using different intermediate oxidation processes 135
SI Chapter 5: Establishing sequential managed aquifer recharge technology (SMART) for enhanced removal of trace organic chemicals: Experiences from field studies in Berlin, Germany 139
SI Chapter 6: Microbiome-triggered transformations of trace organic chemicals in the presence of effluent organic matter in managed aquifer recharge (MAR) systems 149
SI Chapter 8: Genomic Bayesian networks identify trophic strategies in microbiomes of managed aquifer recharge (MAR) systems 163

Abbreviations

Terms

≈	Approximately
ARR	Aquifer recharge and recovery
BDOC	Biodegradable dissolved organic carbon
BF	Bank filtration
bgs	Below ground surface
BMBF	German Federal Ministry for Research and Education
BWB	Berliner Wasserbetriebe
c	Concentration
c_0	Initial concentration
cMAR	Conventional managed aquifer recharge
DAAD	German Academic Exchange Service
DIN	German industrial standard
DO	Dissolved oxygen
DOC	Dissolved organic carbon
D_{OW}	Octanol/water distribution coefficient
EN	European standard
ESI	Electrospray ionization
FT-ICR-MS	Fourier transform ion cyclotron resonance mass spectrometry
HA	Humic acids
HPLC-MS/MS	High pressure liquid chromatography coupled with tandem mass spectrometry
HRT	Hydraulic retention time
IBF	Induced bank filtration
ID	Inner diameter
ISO	International Organization for Standardization
k	Reaction rate constant
K_{OW}	Octanol/water coefficient
LBF	Lake bank filtration
LC-MS/MS	Liquid chromatography coupled with tandem mass spectrometry
log D_{OW}	Logarithmic octanol/water distribution coefficient

log K_{OW}	Logarithmic octanol/water coefficient
LOQ	Limit of quantification
MAR	Managed aquifer recharge
MP	Measuring point
n	Number of measurements
OW	Observation well
PBS	Phosphate buffered saline
POC	Particulate organic carbon
RBF	Riverbank filtration
SAT	Soil aquifer treatment
SFW	Surface water
SI	Supplementary information
SMART	Sequential managed aquifer recharge technology
SPE	Solid phase extraction
SUVA	Specific ultraviolet absorbance at 254 nm
$t_{1/2}$	Half-live
TEG	Observation well at Lake Tegel
TOrC	Trace organic chemical
TUM	Technical University of Munich
UNSW	University of New South Wales
UVA_{254}	Ultraviolet absorbance at 254 nm
WWTP	Wastewater treatment plant
Δ	Delta
λ [d^{-1}]	First-order rate constant
λ [nm]	Wavelength

Units

°C	Degree Celsius
µg	Microgram
µm	Micrometer
cm	Centimeter
d	Day

h	Height
kg	Kilogram
L	Liter
m	Meter
M	Molar mass
m^2	Square meter
mg	Milligram
ng	Nanogram
nm	Nanometer
s	Second
vol.-%	Percentage by volume

Chemicals

4-FAA	4-Formylaminoantipyrine
AMDOPH	1-acetyl-1-methyl-2-dimethyloxamoyl-2-phenylhydrazide
BaQD	1-(2-benzoic acid)-(1H,3H)-quinazoline-2,4-one
BaQM	1-(2-benzoic acid)-4-hydro-(1H,3H)-quinazoline-2-one
BQD	1-(2-benzaldehyde)-(1H,3H)-quinazoline-2,4-one
BQM	1-(2-benzaldehyde)-4-hydro-(1H,3H)-quinazoline-2-one
Fe	Iron
Mn	Manganese
MTBE	Methyl tert-butyl ether
N	Nitrogen
NH_4^+	Ammonium
NO_2^-	Nitrite
NO_3^-	Nitrate
O_2	Oxygen
O_3	Ozone
VSA	Valsartan acid

List of Figures

Figure 2-1: Scheme of a) metabolic and b) co-metabolic biotransformation of TOrCs in the presence of BDOC. 8
Figure 2-2: Schematic of factors affecting biotransformation of TOrCs during MAR. 9
Figure 2-3: Scheme of the DOC composition. 11
Figure 2-4: Schematic principle of the sequential managed aquifer recharge technology – SMART. 16
Figure 3-1: Overview of the structure of the dissertation. 24
Figure 4-1: Conceptual design of the laboratory-scale soil column set-up (h = 1.00 m, ID = 0.14 m; HRT ≈ 6 days). 27
Figure 4-2: DOC, oxygen and UV_{254} absorbance (a) in the first column as an average from four different systems and (b) in the second filtration step after aeration with air (*n* ≥ 5).30
Figure 4-3: DOC concentrations (a) and UV_{254} absorbance values (b) of the influent and the effluents of all four systems: Bank filtration (BF), sequential managed aquifer recharge technology (SMART) air, SMART O_2, SMART O_3 (*n* ≥ 16). Whiskers indicate maximum and minimum values. 31
Figure 4-4: Removal efficiency (%) of all quantified trace organic chemicals (TOrCs) which were not degraded below the limits of quantification (LOQ) in the first column (*n* ≥ 8). (* Venlafaxine was degraded below LOQ during ozonation whereas an increase of the concentration up to 65 ± 13 ng/L in the following filtration step was observed.) 32
Figure 4-5: Improved removal efficiency of sulfamethoxazole in the SMART air system; * mean value of first column effluents, *n* = 2. 33
Figure 4-6: Degradation of gabapentin in the second filtration step of all four systems: BF, SMART air, SMART O_2 and SMART O_3 (*n* ≥ 2). 35
Figure 4-7: The formation of valsartan acid (VSA) in the first filtration step (grey line, a) and the transformation of valsartan, candesartan and olmesartan (black lines, a). Valsartan acid was degraded in the second filtration step after aeration with air, oxygen or ozonation (b) *n* ≥ 4. 37
Figure 5-1: Location of the Lake Tegel, Berlin, Germany with the conventional MAR using pond infiltration site (cMAR site, lower right) and the SMART field site using lake bank filtrate for infiltration (top right) including measuring points (MP) with suction cups and dissolved oxygen sensors, observation wells (OW) and production wells. 42
Figure 5-2: Infiltration rates and groundwater levels in the observation wells during the course of the study at (a) the cMAR site and (b) the SMART site. 45
Figure 5-3: DOC concentrations in the recharge basins and groundwater during the course of the study at (a) the cMAR site and (b) the SMART site 45
Figure 5-4: DO concentrations in the recharge basins and groundwater during the course of the study at (a) the cMAR site and (b) the SMART site 47
Figure 5-5: Comparison of first-order removal rate constants from the cMAR site and the SMART site with literature data (*n* ≥ 6). 50
Figure 5-6: Removal of benzotriazole and metformin concentrations under adapted conditions at the cMAR site (left) and SMART site (right). Whiskers indicate the maximum and minimum concentrations observed and the horizontal line represents the median concentration (*n* ≥ 4). 51

Figure 6-1: Laboratory-scale column experiment consisting of two infiltration steps (system 1, gray, columns B01, B02; system 2, patterned, columns b1-b4) operated in series with an intermediate aeration (Eff. B02, gray patterned). System was fed with effluent of the WWTP Garching, Germany (WWTPE), with a flow rate of 60 (system 1) and 30 mL/h (system 2). 56
Figure 6-2: DOC concentration ($n \geq 12$) and $SUVA_{254}$ ($n \geq 11$) throughout the system with respect to the HRT. Box represents the 25–75 percentiles; whiskers indicate the maximum and minimum values. 59
Figure 6-3: Van Krevelen plot of the effluent organic matter (EfOM) measured in column feedwater showing the H/C and O/C ratios of each mass assigned to a specific elemental composition (CHO, CHNO, CHOS, CHNOS). Bubble sizes depict the absolute intensity of each mass. 62
Figure 6-4: On the basis of multiple coinertia analysis three distinct clusters of masses (diamonds) and OTUs (triangles) were identified according to the influent (Influent B0) and the first (B01, B02) and the second (b1-b4) infiltration system. Corresponding OTUs (B01–b4) and masses are connected by a line, whose length is proportional to the divergence between the data from the same sample. Van Krevelen diagrams, absolute numbers of masses and their elemental compositions, as well as taxonomy assignments representative for each cluster are shown. Total number of masses are given within each circle; abundance of microbial phyla or classes are shown as relative values. 65
Figure 6-5: On the basis of orthogonal partial least-squares (OPLS) regression clusters of masses and OTUs were identified according to the four categories of TOrCs and their behavior in MAR systems: (i) persistent, (ii) easily degradable, (iii) redox insensitive, (iv) redox sensitive. Van Krevelen diagrams, absolute numbers of masses and their elemental compositions, as well as taxonomy assignments representative for each cluster are shown. Total number of masses are given within each circle; abundance of microbial phyla or classes, respectively, are shown as relative values; consider that the microbiome of column B01 corresponds to the influent B0 and each column (B02-b4) to the effluent of the previous column (B01-b3). OPLS model gave the following values for the goodness of its fit and the goodness of the prediction: R^2Y(cum) = 0.9 and Q^2(cum) = 0.9. (*) Not considered for further discussions. 68
Figure 7-1: Laboratory-scale column experiment consisting of two parallel set-ups (pre-treatment and main experiment) fed with a) drinking water (DW) and b) humic acid solution spiked to drinking water (DW + HA). Columns DW and DW + HA were operated in duplicate (columns 1 and 2). 74
Figure 7-2: 3D-EEM of an influent and effluent sample from columns DW- (top) and DW + HA- (bottom) as well as the difference between the influent and effluent. Dashed lines indicate five characteristic regions previously summarized by Chen et al. (2003): 1) aromatic protein I; 2) aromatic protein II; 3) fulvic acid-like; 4) microbial by-product-like; 5) humic acid-like. Note the different intensity scales of DW (-0.2300–0.3700) and DW + HA (-1.290 - 4.580). 77
Figure 7-3: Transformation of targeted TOrCs in different columns under oxic redox conditions in the presence/absence of humic acid ($n \geq 9$). * removed below limit of quantification (LOQ) in most samples. Error bars indicate standard deviation. 78

Figure 7-4: Increased transformation of sulfamethoxazole from the conditioning phase until the end of the experiment (*n* = 3-4). Values of all four columns were averaged, error bars indicate standard deviation. 79
Figure 7-5: Transformation of selected TOrCs in biological treatment systems operating under carbon-limited and oxic (suboxic) redox conditions (Hellauer et al., 2018a; Hellauer et al., 2017; Müller et al., 2017); Stacked bars represent additive removal at different HRT; Error bars indicate standard deviation. $n \geq 4$. * mainly removed < LOQ; † no further transformation observed with longer HRT. 81
Figure 8-1: Workflow to generate a Bayesian network model. 90
Figure 8-2: TAN network graph for the prediction of the trophic strategies a) oligotrophy and b) copiotrophy. 97
Figure 8-3: CI network for the prediction of the trophic strategies a) oligotrophy and b) copiotrophy. 98
Figure 9-1: Comparison of first order removal rate derived from SMART and cMAR. Error bars indicate standard deviation; *significantly better transformed during SMART. Data derived from Hellauer et al. (2018a) (chapter 5). 105

List of Tables

Table 2-1: Characteristics of copiotrophic and oligotrophic organisms* 18
Table 4-1: Dissolved organic carbon (DOC) concentration and redox parameters measured in the system influents and effluents as well as after the aeration with air, pure oxygen or ozone respectively. 29
Table 5-1: Redox and bulk organic parameters of the feed water at the cMAR site (Lake Tegel water) and the SMART site (aerated Lake Tegel bank filtrate); LOQ = limit of quantification. 43
Table 5-2: First-order removal rate constants ƛ [d^{-1}], half-lives $t_{1/2}$ [h], and percentage removal after 200 cm of infiltration of all quantified TOrCs at both field sites. 48
Table 6-1: List of TOrCs investigated during this study ($n \geq 7$) 60
Table 7-1: Influent concentrations and LOQ of all targeted TOrCs ($n = 39$). 75
Table 7-2: Bulk organic and redox parameters of influents and effluents of columns DW and DW + HA. Influent values are given as mean ± standard deviation of both parallel columns receiving the same feed water ($n \geq 6$), effluent values are shown for each column ($n \geq 3$)..... 76
Table 7-3: Bulk organic carbon and redox conditions as well as TOrCs influent concentration of different systems. 81
Table 8-1: Characteristics to identify copiotrophic and oligotrophic organisms based on growth experiment. WWTPE: wastewater treatment plant effluent; WF: effluent of columns receiving WWTPE; DW: drinking water; DW+HA: drinking water augmented with humic acids. Numbers in parenthesis indicate species count based on picked colonies. 89
Table 8-2: Bacterial genomes used for identification of genomic markers, RefSeq Accession nr., date of download as well as the quality hits based on checkM v1.0.9 (Parks et al., 2015) are given..... 93
Table 8-3: Genome characteristics enabling differentiation between copiotrophs and oligotrophs including general parameters, protein localization and COG categories..... 94
Table 8-4: Relative abundance of COG categories of metagenomes. 95
Table 8-5: Performance indicators of three tested strategies..... 95
Table 8-6: Sensitivity analysis of TAN and CI network..... 96
Table 9-1: Removal of all targeted TOrCs throughout this dissertation project. 106

Acknowledgements

“I have always believed that if you put in the work, the results will come” (Michael Jordan). It is incredible, it`s done! This dissertation project wouldn`t have been possible without the support of so many people. I try to express my deepest respect to all of them who were part of this doctoral thesis.

First of all, I want to thank my doctoral supervisor Prof. Dr. Jörg E. Drewes who gave me the opportunity to start my dissertation project. Without his support I couldn’t be there where I am now. Jörg, even if I felt that I cannot fullfill your expectations sometimes, your honest, encouraging and positive feedback allowed me to take a step back, take a deep breath and say yes, it´s worth it. Thank you for your confidence throughout the last years.

Many thanks to my supervisor Dr. Uwe Hübner, who was always there for me for questions and other problems. Uwe, your patience, confidence, advice and support were incredible. I´m very thankful having you as my supervisor.

Furthermore, I want to thank Prof. Dr. Martin Elsner and Prof. Dr. Martin Jekel for being part of my committee. Mr. Jekel, thank you for your valuable input throughout my dissertation project and your time for taking part at my interim evaluation.

Special thanks belong to Prof. Dr. Brigitte Helmreich who always believed in me since I came to the chair as Bachelor student. Thank you, Brigitte, for everything!

I`m grateful to Prof. Dr. Dirk Muscat who was such a valuable mentor for me (and my husband). Dirk, you always found the right words to cheer me up and keeping me on the right track. Thank you for being my contact person for all concerns regarding the dissertation.

During my time as doctoral candidate, I spent a lot of time in Berlin. I want to thank all the people from the TU Berlin (TUB) including Josefine Filter, Dr. Aki S. Ruhl and Prof. Dr. Martin Jekel as well as the students Angelina Patel, Juki Sorgler and Dorothea Mergel for their support and great work. Many thanks to the colleagues from the Berlin Waterworks (BWB) Dr. Alexander Sperlich, Jörn Frankenstein and the students Fabian Thalman, Sema Karakurt, Maresa Kempin, Mareike Harder and Lotte Batzdorf. We had a really good time out there at the island. I know, that it was not always easy for all of you from the TUB and BWB as I couldn`t be present during our experiments all the time. But due to your great engagement all projects worked very well – thank you for that. In addition, I want to thank Dr. Victoria Burke and Prof. Dr. Gudrun Massmann from the Carl von Ossietzky Universität Oldenburg for their assistance and help during the field experiments in Berlin. I really enjoyed working with both of you.

I`m really grateful to Jenny Uhl, Dr. Marianna Lucio and Prof. Dr. Philippe Schmitt-Kopplin from the Research Unit Analytical BioGeoChemistry (BGC), Helmholtz Zentrum München. You welcomed me in your team like a fully new member. Your tireless support and encouragement were phenomenal. Thank you for the good times not only for professional discussions but also your summer and Christmas parties.

My stay at the University of New South Wales (UNSW), Sydney, Australia, was fantastic. Many thanks to Prof. Dr. Michael J. Manefield for giving me this great opportunity. Mike, it was a pleasure for me to work with you and your PhD student Sophie I. Holland and your colleague Assoc. Prof. Federico Lauro form the Nanyang Technological University in Singapore.

I further don`t want to miss to thank the TUM Graduate School for their financial encouragement for taking part at special training but also at international conferences as well as the German Academic Exchange Service (DAAD) for the financial support for my stay at the UNSW.

I also want to thank the colleagues Prof. Dr. Jörn Kalinowski, Anika Winkler and Dr. Daniel Wibberg from the Center for Biotechnology – CeBiTec – at Bielefeld University for their assistance in getting familiar with next generation sequencing and the data analysis.

The time at the Chair at Urban Water Systems Engineering was very intensive – familiar, funny, challenging, happy, exhaustive, … All members of the institute made my time unforgettable. Many thanks to Susanne Wießler and Marianne Lochner from the secretariat. I also want to say thank you to Hubert Moosrainer for his willingness to help all the time and his assistance regarding the set-up of the laboratory-scale experiment as well as my colleagues from the lab: Heidrun Mayrhofer, Ursula Wallentits, Wolfgang Schröder, Myriam Reif, Nicole Zollbrecht, Theresa Häufle, Nelly Krügel, Carolin Kocur, Dr. Carolin Heim, Dr. Bastian Herzog and Dr. Christian Wurzbacher. I really appreciate your absolute assistance for my issues. Thanks a lot to Johann Müller who performed all LC-MS/MS measurements and his support regarding the data evaluation. I also want to thank all the students I could work with during my time at the institute: Konstantin Wycik, Nathalie Vas, Franka Busch, Michael Osina and Sara Martínez Mayerlen. Of course, I`m very thankful to all of my PhD colleagues! Thank you, Nils Horstmeyer, Sema Karakurt, Veronika Zhiteneva and Johann Müller for our really good time in California and thanks to the research group “Advanced Water Treatment”. Dr. Bettina Mößnang and Dr. Carmen Leix, I´m so happy and grateful that we met each other. You always gave me the possibility to talk to you whenever it was necessary, and I could always rely on you. I`m still enjoying our “Prosecco evenings” and I´m looking for some more in the future. Many thanks to my colleague and friend Philipp Michel for his support and funny times in the office.

Last but not least I want to thank my wonderful family and fabulous friends. Mam and Pa, thank you for your inexhaustible trust in me throughout my life. Thank you, my siblings Andrea and Stephan for being there for me. Erich, I`m so thankful having you on my side. You always cheered me up when I was down, you always encouraged me to go on just setting one step after another. Your motivation, encouragement, and love helped me to go my way and finally, finish my dissertation.

1 Introduction

Trace organic chemicals (TOrCs) end up in the environment via wastewater discharge due to their inefficient removal or rather incomplete mineralization during conventional treatment in wastewater treatment plants (WWTPs) (Kasprzyk-Hordern et al., 2009; Luo et al., 2014). Therefore, TOrCs can be detected in the aquatic environment in a concentration range of several nanogram to microgram per liter (Gavrilescu et al., 2015; Stuart et al., 2012) which may result in ecotoxicological risks (Li, 2014; Petrie et al., 2015). Especially in areas in which surface water is used for public drinking water production the quality of this wastewater impacted source water is highly relevant for the final drinking water quality. As less is known about toxicological effects of TOrCs on human beings, no threshold values are established in Germany. However, for some emerging chemicals drinking water guidance values (LW_{TW}) as well as human health-based advisory values (GOW) have been proposed. Thus, it is noteworthy that an exceedance of a GOW has no immediate health relevance since the thresholds are set as precautionary values (Drewes et al., 2018).

Managed aquifer recharge (MAR) systems such as induced bank filtration (IBF) or surface spreading techniques are commonly applied techniques for public drinking water supply (Dillon et al., 2010; Hamann et al., 2016; Heberer et al., 2008; Sprenger et al., 2017). MAR is generally accepted as an efficient barrier for particulate and dissolved organic matter, TOrCs, pathogens, odor- and taste-causing compounds (Maeng et al., 2012a; Regnery et al., 2017; Tufenkji et al., 2002). To guarantee a high quality of the abstracted water with respect to microbial contaminants, a travel time in excess of 50 days is required in Germany. Even though microorganisms are removed to a large extent within this time period, some TOrCs are not or only poorly degraded (Hass et al., 2012; Heberer et al., 2004). Hence, an improved removal of TOrCs in MAR systems is of general interest and thus, the factors triggering the main attenuation mechanisms including sorption and, biotransformation (Alidina et al., 2014a) have to be better understood.

As shown by Regnery et al. (2015b), establishing lasting oxic and carbon-limited conditions seem to be advantageous for the attenuation of many TOrCs during MAR. Under these conditions, the structure of the microbial community prevailing in the system is more diverse (Li et al., 2013) and harbors an enhanced metabolic potential for the biodegradation of xenobiotics (Li et al., 2014a). Based on these findings, the sequential managed aquifer recharge technology (SMART) was established which is defined as a combination of two infiltration steps with an intermediate aeration resulting in favorable oxic and carbon-limited conditions that persist in a second infiltration step (Regnery et al., 2016). Thereby, biodegradable dissolved organic carbon (BDOC) is consumed within the first infiltration step usually resulting in predominant anoxic conditions due to rapid oxygen consumption. The abstracted water is subsequently subject to reaeration which leads to oxic and carbon-limited conditions in the second infiltration system (Regnery et al., 2016). This concept was tested successfully in Aurora, Colorado, USA, at the Prairie Waters Project full-scale MAR facility (Regnery et al., 2016).

Besides the concentration of the dissolved organic carbon (DOC), the composition of the background organic matter has a major impact on TOrCs transformation in MAR systems.

Alidina et al. (2014b) reported an enhanced transformation of TOrCs under more refractory conditions compared to easily degradable organic matter. Furthermore, because of the much lower availability of TOrCs in the aquatic environment (ng-µg/L) in comparison to the DOC (mg/L) (Maeng et al., 2010; Massmann et al., 2008a; Muntau et al., 2017), the concentration of TOrCs may not be sufficient to support microbial growth and thus, additional growth substrate by means of DOC is essential (Tran et al., 2013). Dalton et al. (1982) defined this consumption of rarely available substrate without any benefit to the organism in the presence of growth supporting materials as co-metabolism. Hence, DOC as primary substrate seems to play a dominant role in the biotransformation of TOrCs during MAR. Bearing in mind that the transformation of TOrCs may be co-metabolic, structural similarities between the primary substrate and TOrCs could be assumed. Thus, detailed analyses of the DOC as primary substrate and its role in shaping the microbiome regarding structure and functionality, are crucial to get a deeper understanding of the influence of DOC on TOrCs transformation within natural treatment systems. This includes further the presence and activity of enzymes potentially involved in TOrCs transformation and how these are affected by the concentration and composition of the DOC.

It is well established that microorganisms preferentially grow either in nutrient-rich or nutrient poor environments, describing two different trophic strategies, namely copiotrophy and oligotrophy (Koch, 2001; Poindexter, 1981). In SMART systems both conditions prevail with respect to the DOC availability: i) carbon-rich conditions in the first infiltration step (copiotrophic conditions) and ii) carbon-limited conditions in the second infiltration step (oligotrophic conditions). Thereby, carbon-limited, oligotrophic conditions in combination with oxic redox conditions resulted in an enhanced removal of many TOrCs (Regnery et al., 2016) which could be attributed to more diverse metabolic capabilities of the prevailing microbial community to degrade xenobiotics (Li et al., 2014a). As the trophic strategy of an organism is represented in its genome, information derived from the bacterial genomes can be used to predict the organism`s lifestyle as previously proposed for the marine environment (Lauro et al., 2009). This approach would be useful to assess prevailing carbon conditions in MAR to determine whether preferred conditions (carbon-limitation) for biodegradation of TOrCs are present or not. So far, carbon-limitation quantified as ΔDOC (BDOC) of less than 1 mg/L (Hoppe-Jones et al., 2012) which could only be assessed by differential measurements of the DOC concentration.

Even though MAR is capable of removing many TOrCs, there are still some compounds which show a persistent behavior during treatment, e.g. carbamazepine or primidone (Benotti et al., 2012; Clara et al., 2004; Maeng et al., 2011b). Therefore, a combination of MAR and other treatment technologies such as ozonation, could be considered. These so called hybrid systems are effective with respect to DOC removal as well as attenuating a broader spectrum of TOrCs (Hübner et al., 2012).

The aim of this dissertation project was, to initially investigate the applicability of SMART under operational and environmental conditions prevailing at groundwater recharge sites in Berlin, Germany. To do so, laboratory- (**chapter 4**) and field-scale experiments (**chapter 5**) were conducted. During the laboratory-scale experiment, the performance of SMART with respect to TOrCs transformation was investigated by applying different intermediate aeration strategies: i) no aeration (mimicking conventional BF), ii) aeration with air

(SMART air), iii) aeration with pure oxygen (SMART O_2), and iv) oxidation with ozone (SMART O_3). At field-scale, the SMART concept was tested after modification of an existing infiltration pond receiving bank filtered water and performance was compared to a conventionally operated MAR facility fed with surface water.

The second major aim focusses on elucidating on the role of the primary substrate composition (effluent organic matter, EfOM) during a simulated SMART approach and its correlation to TOrCs as well as how the organic matter shapes the microbiome during MAR (**chapter 6**). Therefore, Fourier-transform ion cyclotron resonance mass spectrometry (FT-ICR-MS) was applied in combination with spectroscopic methods as well as 16S rRNA amplicon sequencing. In addition, the influence of highly refractory DOC at low concentration on the biotransformation of TOrCs was studied (**chapter 7**). Soil columns were fed with different feed water matrices (drinking water and drinking water augmented with humic acids) representing refractory DOC as primary substrate. The scope was to assess the TOrCs biotransformation efficiency as a function of BDOC concentration bearing in mind, that the TOrCs transformation is driven by co-metabolic processes.

The characterization of prevailing carbon conditions by use of molecular biological techniques was the final aim of this dissertation project (**chapter 8**). As carbon-limited, oligotrophic conditions resulted in an enhanced removal of many TOrCs (e.g. Regnery et al. (2016)), monitoring of these conditions from an operational standpoint is warranted. The approach chosen relies on the principle of trophic strategies of microorganisms: copiotrophy and oligotrophy which could be predicted by use of genomic markers representing characteristic features of the bacterial genome (Lauro et al., 2009). This approach could be adapted for engineered filtration systems with the aim of determining prevailing carbon conditions not only via differential measurements of the DOC concentration, but also by use of genomic markers as a biomolecular screening tool of the system’s predominant microbiome.

2 Theoretical background

2.1. Trace organic chemicals in the aquatic environment

Pharmaceuticals, endocrine disrupting compounds, pesticides, industrial chemicals, surfactants and personal care products can be summarized, amongst others, as TOrCs. They enter the aquatic environment mainly through effluents of WWTPs since their removal is incomplete during conventional treatment (Kasprzyk-Hordern et al., 2009; Luo et al., 2014; Stuart et al., 2012). Thus, TOrCs occur in surface water, groundwater and even drinking water at concentrations ranging from ng/L to µg/L (Funke et al., 2015; Gavrilescu et al., 2015; Hass et al., 2012; Heberer, 2002; Lapworth et al., 2012; Massmann et al., 2008a; Stuart et al., 2012). Some compounds like carbamazepine (Clara et al., 2004), primidone (Kahle et al., 2009), acesulfame (Buerge et al., 2009), or oxypurinol (Funke et al., 2015) are widely used as anthropogenic or rather wastewater markers as they are ubiquitous in the aqueous environment. Jekel et al. (2015) proposed to differentiate between markers representing the source where they derived from (e.g., wastewater, urban run-offs or agriculture) and treatment processes they persist in (e.g., conventional biological wastewater, advanced treatment, BF and soil-aquifer treatment (SAT)). Accordingly, indicator chemicals can be used to assess the dimension of anthropogenic influence in distinct water bodies, to reveal most dominant sources of emission and additionally, to indicate the efficiency of an applied technique to remove them (Jekel et al., 2015).

The presence of TOrCs in the aquatic environment provides a potential risk to the environment which has been a key aspect of several reviews (Grenni et al., 2018; Li, 2014; Pal et al., 2014; Petrie et al., 2015) and studies (Archer et al., 2017; Bergheim et al., 2012; Brezina et al., 2017) during the recent past. Since TOrCs occur as complex mixtures in the aquatic environment, it has to be considered that the toxicity of compositions of different TOrCs to aquatic organisms may be higher than ecotoxicological effects observed for single compounds. This was shown for instance for carbamazepine in the presence of clofibric acid (Cleuvers, 2003). With respect to humans, health advisory values (german *gesundheitlicher Orientierungswert, GOW*) were established in Germany which are defined as a precautionary value for compounds whose human toxicity is not or only partially known yet and which can end up in drinking water (Umweltbundesamt, 2003). The last update of the list of compounds and their corresponding GOWs took place in February 2018 and lists 50 substances ranging from pharmaceuticals and pharmaceutical metabolites, industrial chemicals, to naturally-occurring chemicals. Several TOrCs which are commonly detected in WWTP effluents and surface water, like gabapentin, diclofenac, valsartan acid, primidone, carbamazepine or phenazone amongst others, are included in this list (Umweltbundesamt, 2018). For instance, valsartan acid (GOW = 0.3 µg/L), a metabolite of diverse sartanes could be detected in the Creek Gonna, Germany, downstream of a WWTP discharge at concentrations above 2 µg/L. After drinking water treatment following the Mülheim Process[1] valsartan acid was mainly removed (Nödler et al., 2013). However, concentrations measured in drinking water samples in Berlin, Germany, ranged from 57 to 72 ng/L. Even though concentrations are largely below the

[1] More details about the Mühlheim Process is given in Sontheimer et al. (1978)

GOW (0.3 µg/L), valsartan acid may be relevant for public drinking water suppliers as it shows persistent behavior during BF (Nödler et al., 2013). Another example is oxypurinol (GOW = 0.3 µg/L), which was intensively monitored in WWTP in- and effluents, surface waters, groundwater as well as drinking waters in Germany by Funke et al. (2015). They observed oxypurinol in two out of four groundwater samples with concentrations of 0.18 and 0.38 µg/L but also in three out of five drinking water samples with concentrations of ≤ 0.30 µg/L which is as high as the GOW suggested in 2018. Hence, the potential contamination risk of drinking water by TOrCs detected in surface and groundwater becomes obvious pointing out the necessity of their removal.

2.2. Managed aquifer recharge (MAR)

2.2.1. MAR definition, classification and performance

MAR is a natural treatment process which represent the recharge or storage of water in an aquifer with the purpose of subsequently recovering the water and/or water treatment (Sharma and Amy, 2010). Besides surface-spreading techniques as well as induced bank filtration (IBF) at rivers and lakes, well injection techniques (aquifer storage and recovery (ASR); aquifer storage, transfer and recovery (ASTR); aquifer storage as hydraulic barriers (AS)) are commonly referred to as MAR (Sprenger et al., 2017). During IBF, groundwater is abstracted from a well close to a river or lake resulting in infiltration of the river or lake water through the subsurface (Dillon, 2005). Surface spreading methods rely on the principle of the infiltration of surface water (e.g. aquifer recharge) or reclaimed water (SAT) through e.g. an infiltration pond to the aquifer followed by extraction via recovery wells (Amy and Drewes, 2007; Dillon, 2005). The travel times though the subsurface can range from days and weeks to months (Grünheid et al., 2005; Regnery et al., 2015a). Since well injection techniques were not considered within this dissertation project, they won`t be discussed any further.

Considering the situation in Europe, in 2013 224 MAR sites were active in 23 European countries with Germany, Netherlands, France, Finland, Sweden, Switzerland and Spain harboring most of the MAR sites considered (Sprenger et al., 2017). Furthermore, Sprenger et al. (2017) highlighted IBF as the most frequent MAR type followed by surface-spreading approaches such as infiltration ponds and SAT. An overview of worldwide MAR inventories is provided by the web-based MAR portal developed by Stefan and Ansems (2018). MAR types, their main objectives as well as the final use of the treated water is highlighted together with the water used as influent.

It is well established that MAR systems provide an efficient barrier for organic matter. Regnery et al. (2015a) reported a DOC removal of more than 40% during riverbank filtration (RBF) with a residence time of up to ten days. Grünheid et al. (2005) observed a removal of approximately 40% down to ≈ 4.7 mg/L during BF but also pond infiltration after travel times of ≈ 4 months and 50 days, respectively. Furthermore, an attenuation of 36 to 51% was reported at a SAT site in Braunschweig, Germany, with HRT of < 1 day (Muntau et al., 2017). The decrease in DOC usually comes along with an increase of specific UV absorbance (SUVA) indicating that the organic matter of the abstracted water has a more aromatic character due to the degradation of easily degradable DOC during MAR (Muntau et al., 2017; Regnery et al., 2015a). Besides organic matter, an efficient

removal of odor and taste causing compounds (Maeng et al., 2012a) have previously been reported. Furthermore, MAR systems have the capability to remove pathogens including protozoa like *Cryptosporidium* (Hiscock and Grischek, 2002; Ray et al., 2002) which are known to be not completely eliminated during certain disinfection processes like for instance chlorine (Korich et al., 1990). In addition, MAR can play a crucial role in the attenuation of TOrCs which will be discussed in the following section.

2.2.2. TOrCs removal in MAR systems

Investigating the performance of MAR with respect to TOrCs attenuation was the scope of several previous studies. For instance, Grünheid et al. (2005) observed a fast transformation of iopromide during IBF and pond infiltration of more than 80%. Similar results were obtained by Muntau et al. (2017), who detected iopromide biotransformation during SAT of more than 95%. In addition, efficient transformation (> 90%) was monitored for compounds like atenolol, metoprolol, sotalol as well as diclofenac amongst others (Muntau et al., 2017). While the same counts for atenolol at a full-scale RBF site, only moderate removal (25 - 90%) was measured for diclofenac (Regnery et al., 2015a). Even though MAR provides a great potential for the elimination of many TOrCs, some TOrCs like carbamazepine or primidone persist MAR treatment (Clara et al., 2004; Hass et al., 2012).

The attenuation of TOrCs during MAR but also the elimination of organic matter, pathogens, odor and taste are a result of several processes (physical, chemical, microbiological) taking place during subsurface travel, for instance filtration, dilution, biotransformation, adsorption, chemical precipitation and redox reactions (Hiscock and Grischek, 2002; Sharma and Amy, 2010). Thereby, sorption and biotransformation are known as important attenuation mechanisms for TOrCs (Alidina et al., 2014b; Maeng et al., 2011a) which will be discussed in more detail in the following section.

2.2.2.1. Sorption

Removal of TOrCs during MAR via sorption is often studied in abiotic laboratory-scale experiments, in which sorption coefficients K_d are used to assess the sorption tendency of an individual compound onto solids (Alidina et al., 2014a; Alidina et al., 2014b; Bertelkamp et al., 2014; Burke et al., 2013; Rauch-Williams et al., 2010). Thereby, a high K_d value indicates a strong sorption behavior of the targeted compound (Ternes et al., 2004). For instance, the β-blocker atenolol was found to exhibit strong sorption affinity with K_d value ranging from > 1.54 L/kg (Burke et al., 2013) to 2.32 L/kg (Alidina et al., 2014b) while more pronounced sorption capabilities were observed for metoprolol and propranolol (K_d > 2.47 L/kg; Burke et al. (2013)) as well as caffeine (K_d = 11.34 L/kg; Alidina et al. (2014b)). However, especially for positive charged TOrCs like atenolol, cation exchange processes have to be considered as a crucial factor for sorption (Schaffer et al., 2012). Besides K_d, the octanol/water coefficient (K_{OW}) as a measure of the hydrophilic (or hydrophobic) character of an individual compound is considered for estimating its sorption affinity. Thereby, a compound is denoted as mobile in the aquatic phase if its K_{OW} is low. While the K_{OW} describes the proportion of a neutral species dissolved in octanol and water, the distribution coefficient D_{OW} refers to the pH dependent ratio of the species in its ionized and uncharged form (Reemtsma et al., 2016). In general, the log K_{OW} (log P) or log D_{OW}

(log *D*) are applied (Alidina et al., 2014b; Bertelkamp et al., 2014; Maeng et al., 2011a; Rauch-Williams et al., 2010). However, the removal of most TOrCs in MAR systems could be attributed to biodegradation rather than sorption (Alidina et al., 2014a; Maeng et al., 2011a; Rauch-Williams et al., 2010) and therefore, biotransformation is considered as major attenuation mechanism in MAR.

2.2.2.2. Biotransformation

As TOrCs usually occur orders of magnitudes lower in the aquatic environment in contrast to DOC (Grünheid et al., 2005; Massmann et al., 2008a), TOrC concentrations are therefore not considered sufficient to support microbial growth. Thus, it is widely assumed that the transformation of TOrCs during MAR occurs via a co-metabolic (Clara et al., 2005; Rauch-Williams et al., 2010; Tran et al., 2013) rather than metabolic mechanism (Figure 2-1). Alidina et al. (2014a) emphasized the assumption of co-metabolic biotransformation. They showed that the transformation of TOrCs was not affected by pre-exposure of the microbial community to TOrCs which indicates, that the prevailing microbiome does not utilize them as major carbon source. Co-metabolism is defined as "the transformation of a non-growth substrate in the obligate presence of a growth substrate or another transformable compound" (Dalton et al., 1982). According to TOrCs transformation during MAR, TOrCs represent the non-growth substrates and hence, do not provide any benefit to the organism while BDOC is essential for supporting microbial growth and the expression of enzymes for transformation (Figure 2-1b). Hence, the primary substrate in terms of DOC is a crucial factor affecting the biotransformation of TOrCs during MAR. A co-metabolic transformation of several TOrCs has previously been shown by Li et al. (2016b) who observed co-metabolic biodegradation of MTBE[2] by *Pseudomonas* sp. DZ13 using *n*-alkanes as primary substrate. Furthermore, ibuprofen, paracetamol and naproxen could co-metabolically be transformed in cultures enriched with pentane, while nimesulide was slowly degraded and diclofenac was not transformed at all (Bragança et al., 2016). Based on a study by Arp et al. (2001), it seems likely that oxygenases are often involved in aerobic co-metabolic processes as shown for chlorinated solvents, e.g. trichlorethylene.

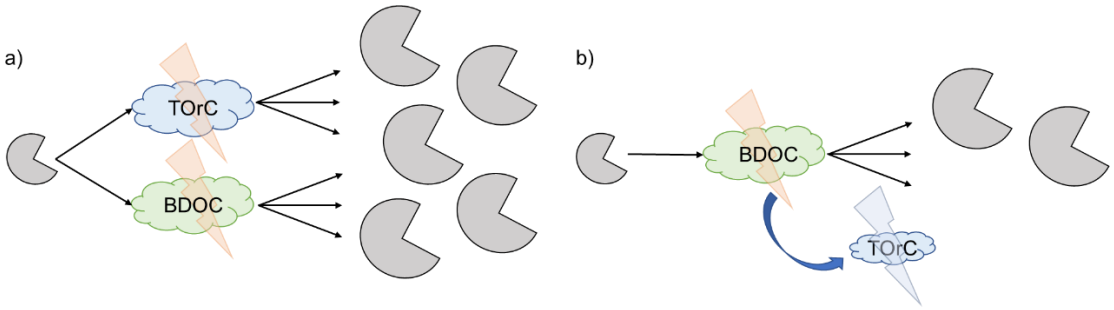

Figure 2-1: Scheme of a) metabolic and b) co-metabolic biotransformation of TOrCs in the presence of BDOC.

Besides the primary substrate (DOC), numerous additional aspects such as prevailing redox conditions (e.g. Massmann et al. (2008a)), temperature (e.g. Burke et al. (2014)),

[2] Methyl *tert*-butyl ether

and adaptation of the microbial community on primary substrate (Hoppe-Jones et al., 2012) affect the performance of MAR regarding TOrCs transformation. The interaction of these factors is schematically shown in Figure 2-2.

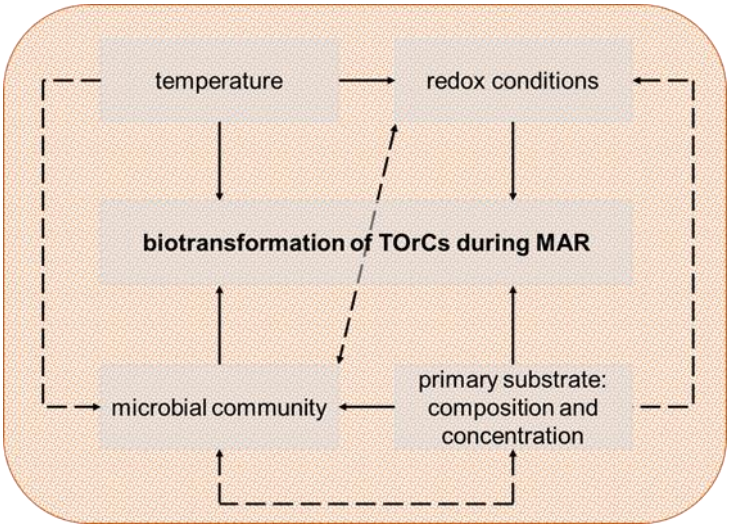

Figure 2-2: Schematic of factors affecting biotransformation of TOrCs during MAR.

a) Temperature

The influence of temperature on the transformation of TOrCs has been extensively studied within the last years. In laboratory-scale experiments, Burke et al. (2014) observed higher removal rate constants for most targeted compounds at 19.7 °C under oxic/penoxic[3] conditions in comparison to cold (6.5 °C), oxic/penoxic/suboxic conditions and similarly, Grünheid et al. (2008) showed a temperature dependent removal for compounds such as sulfamethoxazole. The increased removal as response to higher temperatures may be explained by an enhanced microbial activity at higher temperatures (Qiu et al., 2005). However, there are still compounds whose removal is not impacted by temperature variations either as they persist biodegradation, e.g. benzotriazole (Burke et al., 2014) or since they show high removal efficiency independently of ambient temperature, e.g. iopromide (Grünheid et al., 2008). A field study performed by Hoppe-Jones et al. (2010) emphasized reduced TOrCs transformation in winter compared to summer months for TOrCs gemfibrozil, ibuprofen, naproxen and TCEP which is in line with above mentioned laboratory-scale studies. Nevertheless, Alidina et al. (2015) did not observe an influence of temperature on attenuation of 16 out of 22 investigated TOrCs in a soil-column study. Only diclofenac, gemfibrozil, ketoprofen and naproxen showed an increased removal at 30 °C in comparison to 4 °C due to a stronger activity of the microbial community or a higher abundance of microorganisms associated with the transformation of these four compounds. On the contrary, better attenuation of oxybenzone and trimethoprim was observed at decreasing temperature maybe due to greater sorption (Alidina et al., 2015).

[3] Penoxic redox conditions are defined by Stuyfzand (1993) as oxygen availability close to oxic redox conditions and no observed nitrate reduction.

In addition to microbial activity, the temperature does strongly affect prevailing redox conditions within MAR. During winter at lower temperatures oxic redox-conditions prevailed over a longer travel time/distances, whereas during summer at higher temperatures less oxygen is dissolved in the influent and oxygen is rapidly consumed during infiltration (Henzler et al., 2016; Massmann et al., 2006). In a field study performed in Berlin, Germany, Maeng et al. (2010) pointed out that temperature fluctuations are more pronounced and thus, have a greater impact on prevailing redox conditions at a recharge site in comparison to BF. The higher availability of oxygen during winter results in a more efficient transformation of phenazone and phenazone-type pharmaceuticals pointing out a high redox dependency of individual TOrCs during MAR (Greskowiak et al., 2006; Massmann et al., 2006).

b) Redox conditions

Microbial degradation of organic compounds is associated with the utilization of terminal electron acceptors such as O_2, NO_3^-, SO_4^{2-}, Fe^{3+} or Mn^{4+} resulting in specific redox zones throughout the infiltration (Greskowiak et al., 2006; Gross-Wittke et al., 2010; Massmann et al., 2008a). The prevailing redox conditions were emphasized to be a crucial factor regarding TOrCs transformation during MAR (Wiese et al., 2011). It is well established, that phenazone is a highly redox sensitive compound which could be almost completely removed under prevailing oxic redox conditions during BF and aquifer recharge (Massmann et al., 2006; Massmann et al., 2008a) as well as during drinking water treatment (Reddersen et al., 2002). In addition, Burke et al. (2014) observed redox dependent transformation with higher removal rates under oxic/penoxic to suboxic redox conditions for several TOrCs such as iopromide, metoprolol, diclofenac or acesulfame. Furthermore, Regnery et al. (2015b) reported a strong influence of prevailing redox conditions on the transformation of gemfibrozil as well as diclofenac with decreasing removal efficiencies from oxic to suboxic to anoxic. However, Rauch-Williams et al. (2010) recognized faster removal under anoxic conditions for diclofenac which contradicts the studies from Regnery et al. (2015b) and Burke et al. (2014). Only few compounds are known to be better removed during anoxic recharge, such as sulfamethoxazole (Heberer et al., 2008), whereas Baumgarten et al. (2011) indicated oxic conditions are more favorable. To conclude, most studies are suggesting that oxic redox conditions are favorable for the transformation of most TOrCs during MAR.

c) Adaptation of the microbial community

Based on a study by Alidina et al. (2014a), an adaptation of the microbial community to TOrCs seems not to be required. They performed laboratory-scale experiments using different primary substrates (peptone/yeast, humic acids) which were operated for 310 days with or without a spike of selected TOrCs. Following this run-in phase, TOrCs were spiked to all columns for 60 days and the percentage removal of the parallel set-ups was compared. In the columns fed with humic acids, no differences for all studied TOrCs was observed, whereas in case of peptone/yeast columns only three out of eight targeted compounds showed a significantly different degradation (increased transformation in pre-exposed systems: sulfamethoxazole and oxybenzone; decreased attenuation in pre-exposed columns: methylparaben). Furthermore, the microbial community showed comparable characteristics in both systems. On the contrary, Baumgarten et al. (2011)

observed a long adaptation (> 2 years) for sulfamethoxazole in laboratory-scale column experiments. An increased transformation of TOrCs in laboratory-scale experiments fed with low and high BDOC substrate after an adaptation on the primary substrate over a period of more than three months was reported by Hoppe-Jones et al. (2012). This is in accordance to a study by Li et al. (2013) who observed a stable microbial community after 3 - 4 months. This indicates, that a proper adaptation of the microbial community to the boundary conditions, especially the primary substrate is essential for efficient TOrCs transformation in MAR.

d) Biodegradable dissolved organic carbon (BDOC)

Besides temperature and redox conditions as well as the adaptation of the microbial community to the primary substrate, the primary substrate itself plays an important role for the biotransformation of TOrCs regarding its concentration and composition. The role of (B)DOC as primary substrate during MAR will be reviewed in the following section (2.2.3).

2.2.3. Role of dissolved organic carbon in managed aquifer recharge

The transformation of TOrCs in MAR as a function of the available primary substrate was the scope of previously published research (e.g. Bertelkamp et al. (2016), Rauch-Williams et al. (2010), Alidina et al. (2014b)). As biotransformation was identified as the major removal mechanism for most TOrCs during MAR (Alidina et al., 2014a), the capability of the microbial community plays an essential role. Thus, the structure and function of the prevailing microbiome needs to be addressed which was done with respect to DOC availability (Bertelkamp et al., 2016; Drewes et al., 2014; Li et al., 2012; Li et al., 2013; Li et al., 2014a).

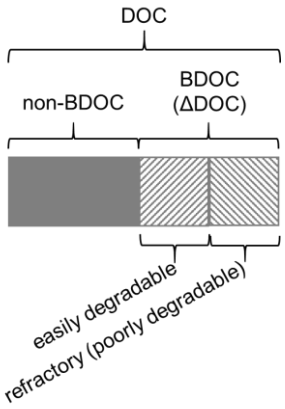

Figure 2-3: Scheme of the DOC composition.

The DOC as primary substrate in the feed water of MAR systems could be divided in a biodegradable fraction (further classified as BDOC or ΔDOC) and a fraction which persists microbial transformation (non-BDOC) (Figure 2-3). The BDOC is further shaped by easily degradable organic substances, as well as by refractory (poorly degradable) compounds such as humic acids. The proportion of non-BDOC and BDOC (easily degradable/refractory) depends on the makeup of the DOC and is highly site specific. For instance, the non-BDOC in riverbank filtrate in Berlin, Germany is with approximately 4.7 mg/L (Grünheid et al., 2005) slightly higher as observed in Aurora, CO, USA after infiltration at the South Plate river (approximately 3.3 – 4.4 mg/L; Regnery et al. (2015a)) and exceeds the non-BDOC concentration of approximately 2 mg/L observed in Shafdan, Israel after biofiltration and short-term SAT of a secondary treated effluent (Zucker et al., 2015).

2.2.3.1. Influence of DOC on TOrCs transformation during MAR

The transformation of TOrCs during MAR could significantly be influenced by applying DOC of different concentrations but also of diverse character (easily degradable vs. poorly degradable). Rauch-Williams et al. (2010) studied in laboratory-scale soil column

experiments the TOrCs transformation in the presence of four different primary substrates, namely hydrophobic acids (HPO-A), hydrophilic carbon (HPI), organic colloids as well as effluent organic matter (EfOM) and indicated the most refractory carbon source HPO-A as similarly or more efficient with respect to the transformation of biodegradable TOrCs. A better transformation of diclofenac, gemfibrozil and bezafibrate was observed in soil-columns mimicking MAR which were fed with surface water in comparison to surface water mixed with WWTP effluent (Maeng et al., 2012b). It was suggested that the transformation of TOrCs during MAR is influenced by the content of biodegradable compounds which were higher in EfOM in comparison to surface water (Maeng et al., 2012b). Comparable results for diclofenac and gemfibrozil but also for atenolol were obtained by Alidina et al. (2014b), who reported strongest transformation if the BDOC was mainly shaped by refractory carbon such as humic acids. In addition, the removal of diclofenac and gemfibrozil mainly decreased with increasing BDOC concentration. However, the effect of BDOC concentration seemed not to be as crucial as the BDOC composition for the attenuation of targeted compounds (Alidina et al., 2014b). In laboratory-scale experiments, Regnery et al. (2015b) monitored complete attenuation for TOrCs known as moderately degradable (diclofenac, gemfibrozil, naproxen) under oxic and low BDOC conditions, while removal under anoxic and high BDOC as well as suboxic and low BDOC conditions did not exceed ≈ 30%. Furthermore, Drewes et al. (2014) emphasized an increased transformation of biodegradable TOrCs if the primary substrate is characterized by low BDOC concentration with a high poorly degradable content. The higher fraction of refractory carbon in the primary substrate may promote a more diverse co-metabolic TOrCs transformation. This assumption was confirmed by experiments using a bench-scale moving bed biofilm reactor in which an increased transformation of several TOrCs (e.g. metoprolol, atenolol, iopromide) was observed with an increasing humic acid content (Tang et al., 2017).

2.2.3.2. Influence of DOC on prevailing microbial community

The concentration of the DOC significantly impacts the biomass distribution of the prevailing microbial community in MAR. The higher the BDOC concentration, the higher the total viable biomass (Li et al., 2013; Maeng et al., 2012b; Rauch-Williams et al., 2010; Rauch-Williams and Drewes, 2006). This relationship usually results in higher biomass in the shallow infiltration zone of MAR systems in comparison to greater depths (Li et al., 2012). Furthermore, the biomass depends on the character of the BDOC meaning, a more poorly degradable BDOC, e.g. hydrophobic acid fraction leads to a lower biomass in comparison to more easily available BDOC, e.g. hydrophilic carbon fraction (Rauch-Williams et al., 2010). Besides the total mass of the microbial community, the structure and functionality could be influenced by the nature of the primary substrate which further impacts the TOrCs transformation during MAR.

The structure of a prevailing microbiome could be assessed by 16S rRNA amplicon sequencing. A negative correlation between the diversity of the prevailing microbial community with the DOC concentration but also the biomass was observed in field- as well as laboratory-scale experiments by Li et al. (2012). Li et al. (2013) obtained significant differences of microbial community structure between the first centimeter of a simulated MAR system and 30 cm depth, whereas differences at greater depths (i.e., 60, 90, 120 cm)

were negligible. Independently of applied BDOC concentration the microbial community structures between depths of 30 and 120 cm were similar, whereas at the first centimeter distinct differences were observed between columns fed with low or moderate BDOC containing waters (Li et al., 2013). In accordance to Li et al. (2012), a less diverse microbial community prevails in the shallow sediments where the DOC concentration is highest (Li et al., 2013). Furthermore, moderate BDOC columns had lower diversity at one cm depth as low BDOC columns (Li et al., 2013). Li et al. (2013) explained this phenomenon by the parallel establishment of different microbial groups harboring diverse metabolic functions under highly refractory carbon conditions. *Proteobacteria*, *Bacteroidetes*, *Actinobacteria* and *Firmicutes* were the most abundant bacterial phyla in soil-column as well as field studies (Li et al., 2012), while *β-Proteobacteria* and *Bacteroidetes* (Li et al., 2013) as well as *γ-Proteobacteria* (Li et al., 2012) could be positively correlated with (B)DOC availability. Microbial phyla such as *Firmicutes*, *Planctomycetes* and *Actinobacteria* increased in their relative abundance under more refractory carbon conditions (40:60 PY:HA) leading to the assumption that these phyla may be able to transform BDOC of refractory character (Li et al., 2014a).

Where the structure of prevailing microbial communities is changing, the functionality may also vary. In a study by Li et al. (2014a), the microbial community structure and functionality was investigated in terms of different primary substrate compositions: 60:40 peptone/yeast (PY):humic acids (HA) and 40:60 PY:HA with low (BDOC ≈ 0.7 – 1.2 mg/L) and high (BDOC ≈ 1.6 mg/L) BDOC concentrations. Hence, the influence of the composition as well as concentration of BDOC on the microbial community could be determined. The main outcome of their experiment was that low BDOC conditions and a high fraction of HA resulted in a highly diverse microbial community having manifold metabolic capabilities regarding xenobiotic transformation. It may be suggested, that the diversity of the microbial community is directly correlated with the diversity of the metabolic functions within the microbiome. Based on metagenomic analyses performed by Li et al. (2014a), the metabolic capability for the biodegradation of xenobiotics is more diverse if the feed water is characterized by a higher refractory content and low BDOC concentration. Especially transformation processes which are catalyzed by Cytochrome P450 enzymes seem to be more likely under low BDOC conditions with higher HA content. Cytochrome P450 is known to be able to metabolize diclofenac (Prior et al., 2010) but also transform the anthropogenic marker carbamazepine (Golan-Rozen et al., 2011).

It becomes obvious that understanding the role of DOC in MAR systems with respect to the biotransformation of TOrCs is crucial. However, it still remains unclear which characteristics of the natural organic matter as primary substrate drive the removal of TOrCs in MAR systems. Methods to characterize the composition of the organic matter to further elucidate possible factors impacting the microbial community and hence, microbial capability for TOrCs degradation, will be specified in the following section.

2.2.3.3. Analytical techniques to elucidate the composition of DOC

For many years the characterization of the organic matter composition is of great interest with the purpose of i) monitoring changes of organic matter during MAR and thereby, tracking the performance of MAR systems (Drewes et al., 2006; Grünheid et al., 2005;

Stahlschmidt et al., 2016), ii) investigating similarities/differences between organic matter of diverse origin (natural organic matter (NOM), effluent organic matter (EfOM)) (Drewes and Croue, 2002) and their fate within MAR treatment (Maeng et al., 2008), iii) determining its influence on the structure and functionality of the prevailing microbial community (Li et al., 2012; Li et al., 2014a), as well as iv) studying the role of DOC and its components with respect to TOrCs transformation during MAR (Alidina et al., 2014b; Rauch-Williams et al., 2010).

Single fractions of the organic matter retained on XAD resins based on their size and polarity (Leenheer et al., 2000; Leenheer and Croué, 2003) could be used to assess the proportion of single fractions (hydrophobic and transphilic acids and neutrals, hydrophilic carbon) prior to and after MAR treatment as well as in the final drinking water source. Thereby, a higher removal of hydrophilic carbon during SAT was observed in comparison to the other fractions (Drewes et al., 2006). Furthermore, fractionating of the DOC was applied to investigate the influence of the different fractions (organic colloids, hydrophobic acids, hydrophilic carbon) on TOrCs transformation during MAR as previously done by Rauch-Williams et al. (2010).

Spectroscopic methods relying on the presence of light absorbing moieties (Minor et al., 2014), such as ultraviolet absorbance at 254 nm (UVA_{254}) and further, specific UV absorbance (SUVA) are often used (Drewes and Croue, 2002; Regnery et al., 2015a). Also liquid chromatography with organic carbon detection (LC-OCD) analyses (Baghoth et al., 2011; Grünheid et al., 2005) are commonly applied in characterizing DOC. It was shown that the SUVA as a measure of aromatic content of the DOC (Weishaar et al., 2003) increases during MAR indicating a stronger removal of aliphatic components throughout infiltration (Drewes et al., 2006; Regnery et al., 2015a). In addition, 3D-fluorescence measurement resulting in 3D-Excitation-Emission matrices (3D-EEM) with regions characteristic of diverse compound classes is a promising tool to derive a deeper understanding of DOC composition (Chen et al., 2003; Maeng et al., 2008; Maeng et al., 2012b; Stahlschmidt et al., 2016). It could be shown that EfOM is mainly shaped by humic-acid like but also protein-like (tryptophan-like) substances (Carvajal et al., 2017). Both could be removed during short- and long term SAT while humic-like substances showed a more significant attenuation with longer travel times (Amy and Drewes, 2007). Additionally, Stahlschmidt et al. (2016) highlighted that elucidating anthropogenic like components in different water sources is possible by applying 3D-EEM in combination with parallel factor analysis (PARAFAC), a statistical technique to identify and quantify components underlying in 3D-EEM (Murphy et al., 2013).

To identify functional groups of compounds present in DOC, Fourier-transform infrared spectroscopy (FT-IR) is commonly applied. In EfOM, prominent peaks characteristic for humic substances as well as proteins were identified (Drewes et al., 2006), which is in accordance to results observed by applying 3D-EEM (e.g. Carvajal et al. (2017)). Furthermore, a decrease of peak characteristics for aliphatic C-H bonds during SAT indicates removal of aliphatic moieties (Drewes et al., 2006), which could also be observed by applying SUVA as reported by Regnery et al. (2015a).

The performance of Fourier transform ion cyclotron resonance mass spectrometry (FT-ICR-MS) with the intent of deciphering DOC in the environment is of great interest (Minor

et al., 2014; Zwiener and Frimmel, 2004) due to its ultrahigh resolution and mass accuracy (Hertkorn et al., 2007; Hertkorn et al., 2008; Sleighter and Hatcher, 2007). Gonsior et al. (2011) and Tseng et al. (2013) for instance, used ESI-FT-ICR-MS for the characterization of EfOM. Especially in combination with nuclear magnetic resonance spectroscopy (NMR), FT-ICR-MS will provide a great insight into the complexity of organic matter (Dvorski et al., 2016; Hertkorn et al., 2013; Schmitt-Kopplin et al., 2010).

Considering the above mentioned techniques, the composition of the DOC changes from easily degradable to more refractory harboring more aromatic moieties during MAR. Furthermore, the methods applied were suitable to highlight that DOC mainly composed of refractory substances is more favorable for TOrCs transformation. However, a link between characteristic structures and components of the DOC and the biodegradation of TOrCs is still missing. Therefore, further research using techniques with the capability of identifying molecular structures and more likely functional groups in combination with quantitative analyses of TOrCs within MAR systems are needed.

2.3. Sequential managed aquifer recharge technology (SMART)

Based on the findings of previous studies reporting that low BDOC concentrations (Drewes et al., 2014; Regnery et al., 2015b) and high oxygen availability are favorable for the transformation of most TOrCs (Burke et al., 2014; Massmann et al., 2008a; Regnery et al., 2015b) the **S**equential **M**anaged **A**quifer **R**echarge **T**echnology (**SMART**) was established by Regnery et al. (2016). The SMART concept consists of two infiltration steps, e.g. IBF followed by aquifer recharge, with an intermediate aeration (Figure 2-4). The following characteristics are specific of SMART (Regnery et al., 2016):

- Elevated concentration of BDOC in the influent of the first infiltration system;
- Anoxic redox conditions during the first infiltration system due to rapid oxygen depletion as a result of a high concentration of easily degradable BDOC;
- Prevailing oxic redox conditions in the second infiltration step due to reaeration of the filtrate after the first infiltration system;
- Maintaining carbon-depleted (low BDOC concentration), oxic conditions in the second infiltration system since the easily degradable BDOC is already removed during the first infiltration step.

The SMART concept was successfully demonstrated in Aurora, Colorado, USA at the full-scale MAR facility Prairie Waters Project. Thereby, abstracted river BF after short travel times (5 – 7 days) is collected and pumped to an artificial aquifer recharge (ARR) facility for subsequent infiltration. For well to moderately degradable compounds (e.g., caffeine, diclofenac, gemfibrozil and naproxen) an incomplete attenuation was monitored during the first infiltration step (short RBF), while an efficient transformation occurred during the second infiltration step (ARR) (Regnery et al., 2016). In comparison to other advanced treatment techniques, SMART requires no addition of chemicals, only little maintenance effort, and finally exhibits a low energy demand (Regnery et al., 2016).

Although SMART performs well for many TOrCs, some compounds persist even throughout the sequential treatment approach, e.g. carbamazepine and primidone. Thus, SMART could be combined with alternative treatment processes such as ozonation (Huber

et al., 2003). The combination of MAR with ozonation, a so-called hybrid system, will be discussed in the following section.

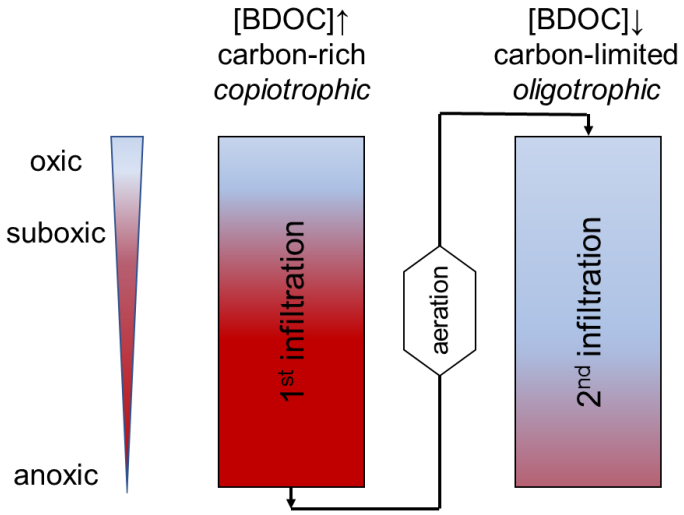

Figure 2-4: Schematic principle of the sequential managed aquifer recharge technology – SMART.

2.4. Combination of managed aquifer recharge with oxidation techniques

Ozonation is a well-established technique to efficiently oxidize many TOrCs from WWTP effluents (Hollender et al., 2009; Huber et al., 2005; Ternes et al., 2003) and during drinking water treatment (Huber et al., 2003; Ternes et al., 2002). Furthermore, ozonation is known to have the capability for diminishing estrogenic activity of hormones (Huber et al., 2004) as well as antibacterial activity (Suarez et al., 2007). The transformation of a substance in water via ozonation depends on its reactivity against ozone. Electron-donating groups such as olefins, aromatics and amines but also sulfur containing compounds are generally more affine to reactions with ozone (Hübner et al., 2015; von Gunten, 2003a), while the removal efficiency of TOrCs by ozonation strongly depends on applied ozone dosages (Hollender et al., 2009; Huber et al., 2005; Ternes et al., 2002).

TOrCs can be classified based on their second-order rate constant as fast reacting ($k_{O3} > 10^4$ $M^{-1}s^{-1}$, e.g. carbamazepine, diclofenac, sulfamethoxazole), moderately reacting (10^2 $M^{-1}s^{-1} < k_{O3} < 10^4$ $M^{-1}s^{-1}$, e.g. metoprolol) or slowly reacting ($k_{O3} < 10^2$ $M^{-1}s^{-1}$, e.g. iopromide) compounds (Hollender et al., 2009; Hübner et al., 2012). Due to the decomposition of ozone in water, hydroxyl radicals (·OH) are formed and thus, oxidation of compounds may not solely be attributed to ozone but also ·OH (von Gunten, 2003a), which is of general interest for slow reacting compounds, e.g. iopromide due to their oxidation by ·OH (Huber et al., 2003; Huber et al., 2005).

TOrCs are more likely transformed as completely mineralized during ozonation (Huber et al., 2003). However, toxicity of formed transformation products is often not known (Lajeunesse et al., 2013; McDowell et al., 2005). The persistence of ozonation transformation products from ozone reactions with TOrCs containing the four different reactive functional groups (olefins, aliphatic amines, aromatics, sulfur-containing

compounds) was the main focus of a review by Hübner et al. (2015). They predicted by use of the biodegradability probability program (BIOWIN) and the Eawag Biocatalysis/Biodegradation Database (Gao et al., 2010) (formerly known as University of Minnesota Pathway Prediction System (UM-PPS), Ellis et al. (2008)) an enhanced biodegradability of most detected olefin-derived transformation products, while the majority of transformation products derived from aliphatic amines exhibited no better biodegradability. Even if the reaction of ozone with aromatic compounds is highly complex, Hübner et al. (2015) were able to indicate an increased biodegradability after aromatic ring cleavage. However, tools to predict biodegradability used by Hübner et al. (2015) were not sufficient to derive information on biodegradation behavior of transformation products from sulfur-containing compounds. The removal of carbamazepine and its transformation products derived from ozonation of secondary effluent in subsequent laboratory-scale SAT was the scope of a study performed by Hübner et al. (2014). They detected a sufficient removal of the main transformation products BQM[4], BaQM[5] as well as BQD[6] during soil column infiltration, while BaQD[7] exhibited reduced biodegradation capabilities. In addition to the transformation of TOrCs, ozonation results in an increase of biodegradable organic carbon like organic acids, aldehydes and ketones (Hammes et al., 2006) which is also reflected in an elevated biochemical oxygen demand (BOD_5) (Lester et al., 2013). This could be confirmed by Hübner et al. (2014), who observed a stronger DOC attenuation during SAT for ozonated in comparison to non-ozonated secondary effluent.

Even though, coupling ozonation and MAR combines i) the potential of oxidation via ozone to attenuate many TOrCs with ii) the advantage of MAR regarding its biodegradation capabilities (Hübner et al., 2012; 2014; 2016), the formation of bromate during ozonation of bromide-containing waters is of concern and should not be neglected as its removal during drinking water treatment is challenging (von Gunten, 2003b).

2.5. Trophic strategies of microorganisms in the environment

It is widely accepted, that microorganisms follow a specific strategy regarding the utilization of nutrients – e.g. DOC – depending on their availability in the environment. Organisms may preferentially grow in nutrient limited, oligotrophic, environments, so called oligotrophs, while others grow with high levels of nutrients, so called copiotrophs (Koch, 2001; Poindexter, 1981). There are several characteristics which are specific for oligotrophs and organisms settled in copiotrophic environments, respectively. Based on studies by Fierer et al. (2007) and Lauro et al. (2009), properties of copio- and oligotrophic organisms are listed in Table 2-1.

[4] 1-(2-benzaldehyde)-4-hydro-(1H,3H)-quinazoline-2-one
[5] 1-(2-benzoic acid)-4-hydro-(1H,3H)-quinazoline-2-one
[6] 1-(2-benzaldehyde)-(1H,3H)-quinazoline-2,4-one
[7] 1-(2-benzoic acid)-(1H,3H)-quinazoline-2,4-one

Table 2-1: Characteristics of copiotrophic and oligotrophic organisms*

Characteristics	Copiotrophs	Oligotrophs
Growth rate	high	low
Population size	highly fluctuating due to "feast and famine" strategy	constant resulting in an equilibrium
Cultivation	easy; fast growing colonies in nutrient rich media	difficult; slow growing colonies in nutrient poor media
Stress tolerance	low	high
Cell morphology	low surface area to volume ratio	high surface area to volume ratio
Substrate affinity	low	high
rRNA operon number	many	few
Genome size	large	small

*list adopted from Fierer et al. (2007) and Lauro et al. (2009).

The classification in high and low availability of nutrients, however, is very variable. As summarized by Schut et al. (1997), the definition of oligotrophic bacteria ranges from < 1 mg C/L up to several mg C/L and included the differentiation "obligate" and "facultative" oligotrophs, which highlights that oligotrophic bacteria may also be able to grow under higher nutrient concentrations ("facultative" oligotrophs). Fierer et al. (2007) classified soil bacteria in copio- and oligotrophs based on the net mineralization rate of carbon. Thereby, *Acidobacteria* were identified as oligotroph while *β-Proteobacteria* and *Bacteroidetes* could be assigned to copiotrophic organisms. Nevertheless, this classification has to be critically assessed since a phylum contains a diverse consortium of microorganisms exhibiting a wide range of physiological attributes and hence, could harbor different trophic strategies (Trivedi et al., 2013).

The terms "oligotroph" and "copiotroph" are often used in conjunction with describing prevailing conditions in MAR as a function of DOC availability. For instance, Regnery et al. (2016) specifies the conditions in the second infiltration system of SMART as oligotroph due to less available BDOC serving as electron donor (BDOC ≤ 1.0 mg/L) (cf. Figure 2-4). Emerging oligotrophic conditions as a result of low BDOC concentration and/or presence of refractory carbon sources is further linked to an increased transformation of biodegradable TOrCs (e.g. gemfibrozil) during MAR (Maeng et al., 2012b; Rauch-Williams et al., 2010).

Gaining evidence about the trophic strategy (oligotrophy vs. copiotrophy) of soil organisms by use of information derived from bacterial genomes regarding carbon utilization such as transporter diversity and substrate specificity was proposed by Trivedi et al. (2013). Lauro et al. (2009) were able to predict the trophic lifestyle of organisms in the marine environment by use of specific characteristics prevailing in the genome of oligotrophs or copiotrophs, respectively. They used the marine model organisms *P. angustum* S14 (copiotroph) and *S. alaskensis* RB2256 (oligotroph) to identify genomic features characteristic for copio-/ and oligotrophs and established a model to predict the trophic strategy based on genome and metagenome data. Thereby, concentration of nutrients in terms of growth characteristics of the model oligotroph *S. alaskensis* ranged within

nanomolar dimensions (Lauro et al., 2009). However, this concentration refers to nutrients in total and does not contain more specific information about the organic carbon content.

As prevailing carbon conditions – oligotroph vs. copiotroph environments - play a crucial role in the transformation of TOrCs during MAR, it would be of great benefit to predict these conditions by use of genomic markers. To the best of our knowledge, characterizing carbon conditions present in engineered filtration systems using features of bacterial genomes have so far not been subject of current studies yet. Hence, the transfer of the approach from Lauro et al. (2009) on MAR systems will be promising in characterizing ambient boundary conditions at MAR sites, even though their approach was established in the marine environment.

3 Research significance, objectives, and hypotheses

3.1. Objectives and hypotheses

Due to their incomplete removal in conventional WWTPs, TOrCs can be detected in surface water, groundwater and drinking water in a range of several nanogram to microgram per liter (Luo et al., 2014; Petrie et al., 2015). Many of these TOrCs occurring in the aquatic environment may have adverse effects on the environmental and human health (Li, 2014; Pal et al., 2014). Thus, an efficient removal of TOrCs in the environment is of great interest. Managed aquifer recharge (MAR) systems such as riverbank filtration or soil-aquifer treatment (Sprenger et al., 2017) are natural treatment systems with a high potential to efficiently remove biodegradable TOrCs (Regnery et al., 2017). It is assumed that the removal of TOrCs in MAR is mainly driven by biotransformation (Alidina et al., 2014a; Maeng et al., 2011a), while a co-metabolic mechanism has been proposed (Alidina et al., 2014a). An enhanced transformation for biodegradable TOrCs has been observed under oxic and carbon-limited conditions (Regnery et al., 2015b) especially, if the primary substrate is shaped by refractory substances such as humic acids (Alidina et al., 2014b). Based on these results, Regnery et al. (2016) introduced the sequential MAR technology (SMART) which consists of two infiltration steps with an intermediate aeration leading to proposed favorable oxic and carbon-limited conditions for improved TOrCs transformation. So far, determination of carbon-limited conditions is based on a differential measurement of the DOC concentration. Another possibility to asses prevailing carbon conditions relies on genomic markers which are characteristic for carbon-limited preferring (oligotrophic) / carbon-rich preferring (copiotrophic) organisms. The prediction of trophic strategies of organisms (oligotrophy/copiotrophy) by use of genomic features was previously achieved in the marine environment (Lauro et al., 2009).

This doctoral thesis targets the following objectives:

- **Objective I**
  Validate the **applicability of the SMART concept** considering the environmental and operational conditions of the case study Berlin.

- **Objective II**
  Determine the effect of biodegradable **dissolved organic carbon composition** as well as **concentration** on TOrCs removal.

- **Objective III**
  Characterize oxic and **carbon-limited conditions** using redox and bulk organic parameters and biomolecular methods.

The objectives were addressed by testing the following hypotheses:

- **Hypothesis I**
  SMART can result in improved removal of potentially health relevant TOrCs compared to currently practiced MAR systems in Berlin.

- **Hypothesis II**
  The fate of molecular components and characteristic functional groups of the primary substrate correlates with the degradation of structurally similar TOrCs.

- **Hypothesis III**
  The concentration of refractory carbon (like humic acids) controls TOrCs removal in MAR systems under oxic conditions.

- **Hypothesis IV**
  Trophic strategies of the microbial community in engineered filtration systems can be distinguished based on genomic features such as genome size and specific clusters of orthologous groups (COGs).

3.2. Structure of the dissertation

The structure of this dissertation project is illustrated in Figure 3-1.

In **chapter 4**, hypothesis I *"SMART can result in improved removal of potentially health relevant TOrCs compared to currently practiced MAR systems in Berlin"* was tested at laboratory-scale. A soil-column experiment consisted of four parallel set-ups, each comprised of two columns operated in series which were filled with sand of an artificial recharge facility in Berlin, Germany was performed. Between the sequential columns an intermediate treatment process occurred: no aeration (representing conventional bank filtration), aeration with air (SMART air), oxidation with pure oxygen (SMART O_2) or with ozone (SMART O_3). The aim was to test the influence of the different aeration and oxidation strategies on the performance regarding TOrCs transformation in comparison to a conventional operated BF (no aeration).

Hypothesis I was also addressed in **chapter 5** considering findings from an existing artificial recharge facility in Berlin, Germany. Thereby, the SMART approach was compared to a conventionally operated MAR (cMAR) in Berlin, Germany with respect to the transformation of TOrCs as a function of organic carbon and redox conditions. The scope of this study was to test the applicability of SMART under prevailing field conditions in Berlin.

Hypothesis II *"The fate of molecular components and characteristic functional groups of the primary substrate correlates with the degradation of structurally similar TOrCs*" is being discussed in **chapter 6**. This chapter targets the transformation of TOrCs in the presence of effluent organic matter as primary substrate. Detailed analyses of the organic matter composition were performed at different travel times in a laboratory-scale system mimicking SMART. The aim was to link changes of the organic matter composition with

the behavior of TOrCs throughout the system (i.e., easily degradable, redox sensitive, redox insensitive, persistent). In addition, the microbial community composition was characterized and further discussed with respect to the primary substrate composition, its changes during infiltration and moreover, the TOrCs transformation.

In **chapter 7**, the third hypothesis *"The concentration of refractory carbon (like humic acids) controls TOrCs removal in MAR systems under oxic conditions"* is assessed at laboratory-scale. The soil column set-up consisted of two parallel systems each fed with either drinking water or drinking water augmented with humic acids. TOrCs were spiked at environmental relevant concentrations. The scope of this study was to elucidate the transformation of TOrCs as a function of a highly refractory primary substrate at different concentrations.

Hypothesis 4 *"Trophic strategies of the microbial community in engineered filtration systems can be distinguished based on genomic features such as genome size and specific clusters of orthologous groups (COGs)"* is addressed in **chapter 8**. This study focusses on the trophic strategies of microbial communities within MAR under different organic carbon availability. The information of bacterial genomes was used to identify markers which are characteristic for bacteria settled in carbon-rich or carbon-limited environments. Based on these markers, a Bayesian network was established to predict the trophic strategy of a microbial community within MAR.

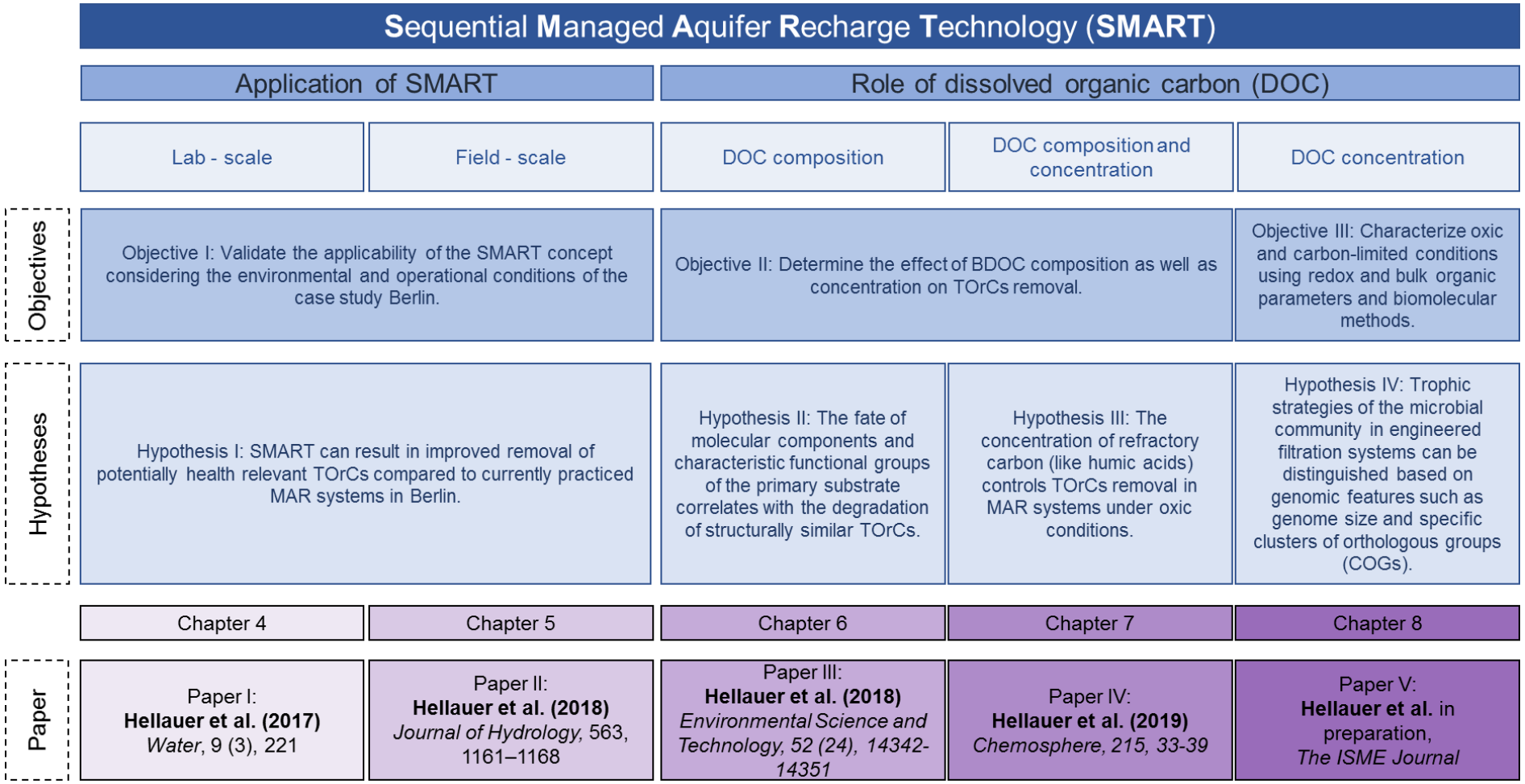

Figure 3-1: Overview of the structure of the dissertation.

4 Advancing sequential managed aquifer recharge technology (SMART) using different intermediate oxidation processes

This chapter has been previously published as follows[8]:

Hellauer, K., Mergel, D., Ruhl, A.S., Filter, J., Hübner, U., Jekel, M., Drewes, J.E., 2017. Advancing Sequential Managed Aquifer Recharge Technology (SMART) Using Different Intermediate Oxidation Processes. *Water* 9 (3), 221.

Abstract

Managed aquifer recharge (MAR) systems are an efficient barrier for many contaminants. The biotransformation of trace organic chemicals (TOrCs) strongly depends on the redox conditions as well as on the dissolved organic carbon availability. Oxic and oligotrophic conditions are favored for enhanced TOrCs removal which is obtained by combining two filtration systems with an intermediate aeration step. In this study, four parallel laboratory-scale soil column experiments using different intermittent aeration techniques were selected to further optimize TOrCs transformation during MAR: no aeration, aeration with air, pure oxygen and ozone. Rapid oxygen consumption, nitrate reduction and dissolution of manganese confirmed anoxic conditions within the first filtration step, mimicking traditional bank filtration. Aeration with air led to suboxic conditions, whereas oxidation by pure oxygen and ozone led to fully oxic conditions throughout the second system. The sequential system resulted in an equal or better transformation of most TOrCs compared to the single step bank filtration system. Despite the fast oxygen consumption, acesulfame, iopromide, iomeprol and valsartan were degraded within the first infiltration step. The compounds benzotriazole, diclofenac, 4-Formylaminoantipyrine, gabapentin, metoprolol, valsartan acid and venlafaxine revealed a significantly enhanced removal in the systems with intermittent oxidation compared to the conventional treatment without aeration. Further improvement of benzotriazole and gabapentin removal by using pure oxygen confirmed potential oxygen limitation in the second column after aeration with air. Ozonation resulted in an enhanced removal of persistent compounds (i.e., carbamazepine, candesartan, olmesartan) and further increased the attenuation of gabapentin, methylbenzotriazole, benzotriazole, and venlafaxine. Diatrizoic acid revealed little degradation in an ozone–MAR hybrid system.

[8]This study was performed to test Hypothesis I that SMART can result in improved removal of potentially health relevant TOrCs compared to currently practiced MAR systems in Berlin.

4.1. Introduction

The potential to cause adverse health effects by the presence of trace organic chemicals (TOrCs), such as pharmaceuticals, household chemicals, industrial chemicals, and pesticides, in the aqueous environment is increasingly recognized as a serious environmental issue (Li, 2014; Luo et al., 2014; Petrie et al., 2015; Schwarzenbach et al., 2006). Due to their insufficient degradation in conventional wastewater treatment plants, TOrCs can be detected in surface water, groundwater and drinking water in a concentration range of ng/L to µg/L (Benotti et al., 2009; Glassmeyer et al., 2005; Heberer, 2002; Kasprzyk-Hordern et al., 2008; Luo et al., 2014). Managed aquifer recharge (MAR) systems, such as riverbank filtration (RBF), soil aquifer treatment (SAT), or aquifer recharge and recovery (ARR) efficiently remove microbial contaminants, organic matter and TOrCs by adsorption, physicochemical filtration processes, as well as biological transformation while combining the advantages of low energy demand, little chemical input, and no generation of waste streams (Amy and Drewes, 2007; Hoppe-Jones et al., 2010; Missimer et al., 2011; Tufenkji et al., 2002). For a majority of TOrCs, biotransformation is the dominant removal mechanism (Alidina et al., 2014a). Previous studies have revealed that degradation of TOrC is more favorable under oxic and carbon depleted conditions represented by a low biodegradable dissolved organic carbon (BDOC) content (Grünheid et al., 2005; Hoppe-Jones et al., 2012; Li et al., 2013; Massmann et al., 2008a; Rauch-Williams et al., 2010; Regnery et al., 2015a). The coupling of two MAR systems with an intermediate aeration step, as established by the sequential managed aquifer recharge technology (SMART) (Regnery et al., 2016), was designed to provide these favorable conditions in the second infiltration system. In the first infiltration step of SMART (mimicking conventional riverbank filtration systems), easily biodegradable DOC is quickly consumed, usually resulting in complete oxygen depletion and prevailing anoxic conditions. After re-aeration of the extracted water, carbon-depleted and oxic conditions can be maintained in the subsequent subsurface filtration system. This approach was successfully demonstrated at the full-scale MAR facility Prairie Waters Project (Aurora, CO, USA) showing enhanced biodegradation of various TOrCs (e.g., caffeine, diclofenac, dilantin, gemfibrozil, meprobamate, and naproxen) compared to single-stage conventional riverbank filtration (Regnery et al., 2016).

However, some TOrCs such as the antiepileptic drugs carbamazepine and primidone are highly persistent to biodegradation under most conditions. For the removal of such compounds during SMART, an additional barrier would be needed. Ozonation is a well-established process for the removal of many TOrCs (Hollender et al., 2009; Huber et al., 2005). Since it provides additional dissolved oxygen and simultaneously increases the BDOC content, it was proposed as a suitable method in combination with subsequent groundwater infiltration (Hammes et al., 2006; Hübner et al., 2016; Kozyatnyk et al., 2013).

The aim of this study was to validate the SMART concept in a laboratory-scale soil column set-up fed with a blend of wastewater treatment plant effluent and Lake Tegel water. Furthermore, the removal of persistent TOrCs during SMART was enhanced by replacing aeration with oxidation by ozone. Therefore, four parallel soil column set-ups were established, each consisting of two columns and subject to different intermediate oxidation

techniques: no aeration (reference system), aeration with air, aeration with oxygen, and aeration with ozone.

4.2. Material and methods

4.2.1. Soil column experiments

The laboratory-scale soil column experiment consisted of four parallel systems. Each system was comprised of two columns (h = 1.00 m; ID = 0.14 m; sampling ports: 0.25, 0.50, 0.75 m), which were connected in series (Figure 4-1). The intermediate treatment differed by applying different oxidation techniques: no aeration (system BF), aeration with air (SMART air), aeration with pure oxygen (SMART O_2), or aeration/oxidation with ozone (0.6 ± 0.1 mg O_3/mg DOC, n = 12; SMART O_3). The columns were filled with sand which derived from recharge basin No. 3 at the full-scale Saatwinkel MAR facility, Berlin. Sand for the first column of all systems was taken from 0 to 100 cm depth. For the subsequent columns, the top 20 cm colmation layer was removed. The sand was sieved and homogenized to remove any constituents larger than 4 mm. After preconditioning for 10 months (40 days with tap water, 9 months with Lake Tegel water), experiments were conducted for five months with a mixture of Lake Tegel water and effluent from wastewater treatment plant (WWTP) Ruhleben in a ratio of 3:1 to simulate the worst case scenario for the influence of WWTP effluent. Lake water and secondary effluent were collected monthly and stored at room temperature (lake water) or at 11 °C (secondary effluent), respectively. The feed container was refilled weekly and stored at room temperature. The columns were operated top-down with a flow rate of 60 mL/h resulting in a hydraulic retention time (HRT) of approximately six days (based on preliminary experiments with the same column set-up). The influent was delivered using an 8-channel Ismatec pump (model 931, Ismatec, Wertheim, Germany) and Pharmed® Ismaprene tubings (Ismatec Tubing, Persistaltic, 2-Stop, Color: Purple/White; Kinesis, Langenfeld, Germany).

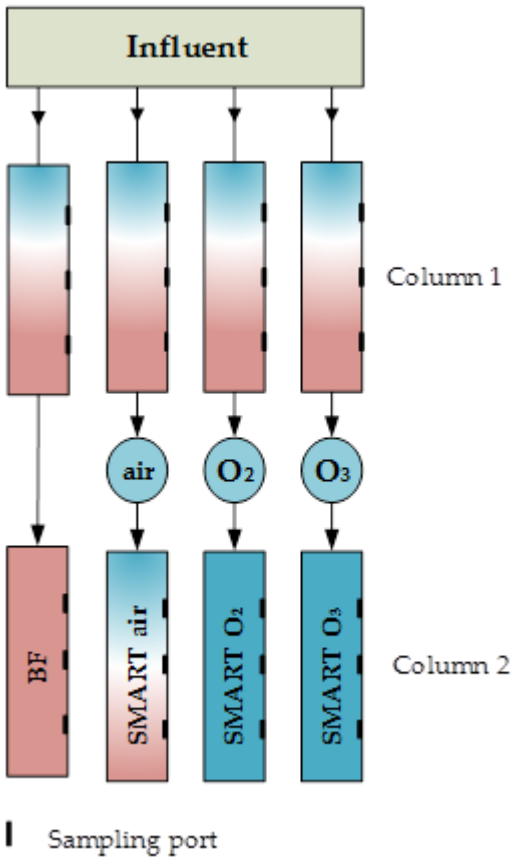

Figure 4-1: Conceptual design of the laboratory-scale soil column set-up (h = 1.00 m, ID = 0.14 m; HRT ≈ 6 days).

4.2.2. Aeration/Oxidation

Intermediate aeration of the SMART air system was achieved using an air stone diffuser in a small bubble column. Aerated water was delivered to the second column by gravity. Treatment with pure oxygen and ozone was conducted weekly in a 13 L-semi-batch stirred

tank reactor. Gaseous ozone was produced from pure oxygen using a Modular 8 HC generator (Wedeco, Herford, Germany). Ozone concentrations of applied and off-gas as well as gas flow rate were measured continuously using BMT 964 and BMT 961 TPC (BMT, Stahnsdorf, Germany) and 807 MFM O2 (Bürkert, Ingelfingen, Germany) probes, respectively. In order to set up a complete mass balance and calculate consumed ozone, all off-gas ozone was stripped with pure oxygen before sampling. For aeration with pure oxygen, the system was used without ozone production for ten minutes. The oxygen- or ozone-treated water was fed to the second columns from Plastigas® bags (Linde, Pullach, Germany) to prevent degassing with a slightly reduced flow rate of 58 mL/h.

4.2.3. Analytical methods

The samples from the in- and effluents of each column, as well as after the aeration with pure oxygen or the oxidation with ozone, respectively, were collected once a week with respect to the HRT. Additionally, in the second columns of the systems SMART air, SMART O_2 and SMART O_3, depth profile measurements were performed for the parameters dissolved oxygen, dissolved organic carbon (DOC), ultraviolet absorbance at 254 nm (UV_{254}), and TOrCs every second to third week. The dissolved oxygen was measured in situ by use of oxygen flow through cells (PreSens, Regensburg, Germany). All samples were filtered (cellulose nitrate, 0.45 µm; Sartorius, Göttingen, Germany) prior to all analyses except for iron and manganese, which were measured unfiltered. The nitrate, nitrite, and ammonia concentrations were determined using a flow injection analysis (FIASTAR 5000, Foss Tecator, Hamburg, Germany). Iron and manganese measurements were carried out using atom absorption spectrometry (Flame: 906AA, GBC-Scientific Equipment Pty Ltd., Hampshire, IL, USA; Graphit furnace: SpectrAA-400, Varian, Palo Alto, CA, USA). The DOC concentration was determined by a varioTOC Cube analyzer (Elementar, Langenselbold, Germany) and the UV_{254} was measured on a spectral photometer Lamda 12 (Perkin Elmer, Waltham, MA, USA). The specific UV absorbance (SUVA) was calculated as the ratio of the UV_{254} and the DOC concentration. The quantification of selected TOrCs was conducted by high performance liquid chromatography coupled with tandem mass spectrometry (HPLC–MS/MS) based on the method described by Zietzschmann et al. (2014). The compounds were chromatographically separated with a XSelect HSS T3 XP column (2.1 mm inner diameter, 50 mm length, 2.5 µm spherical silica particles as substrate, C18 phase, reversed-phase mode) that was protected with an XSelect HSS T3 VanGuard pre-column (2.1 mm inner diameter, 5 mm length, 2.5 µm particle size) and detected on a triple quadrupole with electro spray ionization (TSQ Vantage; Thermo Scientific, Waltham, MA, USA). Ultra-pure water mixed with 5 vol.-% methanol and 0.1 vol.-% formic acid and pure methanol were used as mobile phases at a volume flow of 500 µL/min using a linear gradient. All TOrCs, their limits of quantification (LOQ), fragments for quantification/qualification as well as internal standards used for quantification are listed in Table SI-4 1.

4.3. Results and discussion

4.3.1. Redox conditions

Relevant redox parameters in all systems are summarized in Table 4-1. The results of the first filtration step are given as mean value of all four columns. The oxygen concentration

in the influent with 7.7 ± 0.4 mg/L was almost saturated and completely consumed within the first 1.5 days of infiltration (Table 4-1, Figure 4-2a). Significant nitrate reduction (students *t*-test, paired, $\alpha < 0.05$), formation of nitrite, and dissolution of manganese from the soil confirm anoxic conditions in the first columns. These results are in line with previous research reporting mostly anoxic bank filtration conditions in Berlin with rapid oxygen consumption by a high content of organic material (Massmann et al., 2008b). The dissolution of manganese within the first filtration step slightly decreased during the experimental period, which may be explained by the decreasing availability of particulate organic carbon (POC) from the sand. The iron concentrations in the entire soil column system were not higher than 0.4 mg/L. In the second column of the reference system without aeration, an additional decrease of nitrate concentrations indicated prevailing anoxic conditions. Manganese was slightly removed, possibly due to oxygen intrusion resulting in Mn(II) oxidation and precipitation between the columns. After aeration with air, dissolved oxygen was quickly consumed again in the second column (Figure 4-2b). Subsequent column passage in this column can be described as suboxic, which is characterized by a dissolved oxygen concentration of less than 1.0 mg/L, but no significant consumption of alternative electron acceptors (Regnery et al., 2015b). Only aeration with pure oxygen and treatment by ozone, both leading to high oversaturation of dissolved oxygen, resulted in fully oxic conditions throughout the second columns (Table 4-1). In all intermediate aeration/oxidation processes, manganese (II) was oxidized and deposited on the top of the columns as a dark layer, which was removed manually every three to four months. NH_4^+-N concentrations were not higher than 0.03 ± 0.02 mg/L in all systems ($n \geq 14$).

Table 4-1: Dissolved organic carbon (DOC) concentration and redox parameters measured in the system influents and effluents as well as after the aeration with air, pure oxygen or ozone respectively.

Para-Meter	Influent $n \geq 17$	Column 1 $n \geq 64$	After Aeration $n \geq 16$		BF $n \geq 15$	Smart Air $n \geq 15$	Smart O_2 $n \geq 14$	Smart O_3 $n \geq 15$
			Air	O_2 and O_3				
DOC (mg/L)	8.2 ± 0.6	6.6 ± 0.7	-	6.3 ± 0.5 *	6.5 ± 0.6	5.8 ± 0.4	5.2 ± 0.5	4.4 ± 0.4
O_2 (mg/L)	7.74 ± 0.43	0.02 ± 0.09	7.14 ± 0.45	22.01 ± 5.76	0.03 ± 0.08	0.04 ± 0.10	14.32 ± 4.50	16.12 ± 2.08
NO_3-N (mg/L)	4.8 ± 0.8	3.8 ± 0.7	-	3.8 ± 0.7	3.5 ± 0.8	3.7 ± 0.7	3.9 ± 0.6	4.0 ± 0.7
NO_2-N (mg/L)	0.0 ± 0.0	0.3 ± 0.1	-	0.0 ± 0.0	0.2 ± 0.0	0.0 ± 0.0	0.0 ± 0.0	0.0 ± 0.0
Fe (mg/L)	0.2 ± 0.1	0.1 ± 0.1	-	-	0.1 ± 0.1	0.1 ± 0.1	0.1 ± 0.1	0.1 ± 0.1
Mn (mg/L)	0.1 ± 0.1	1.1 ± 0.4	-	-	0.6 ± 0.2	0.1 ± 0.1	0.0 ± 0.0	0.0 ± 0.0
Prevailing Redox Conditions		anoxic			anoxic	anoxic–suboxic	oxic	oxic

Note: *DOC concentration after ozonation.

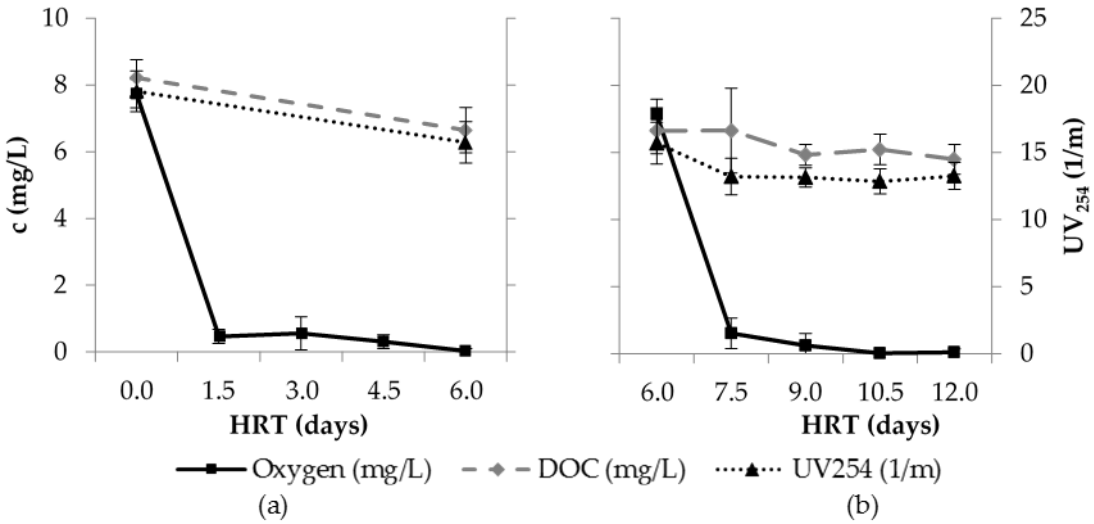

Figure 4-2: DOC, oxygen and UV_{254} absorbance (a) in the first column as an average from four different systems and (b) in the second filtration step after aeration with air (*n* ≥ 5).

4.3.2. Removal of bulk organic parameters

DOC and oxygen concentrations as well as the UV_{254} values within the first infiltration (a) and in the column after aeration with air (b) are shown in Figure 4-2. Results after aeration with pure oxygen and ozone are given in Figure SI-4 1 in the supplementary material. In the first filtration step, oxygen was completely consumed after 1.5 days of infiltration and 1.6 ± 0.5 mg/L DOC (19%) were attenuated (Figure 4-2a). After the aeration with air, the oxygen concentration increased up to 7.1 ± 0.5 mg/L, but was also degraded within the first couple of days (Figure 4-2b). The DOC degradation of 0.8 ± 0.5 mg/L (10%) was significantly higher as compared to the system BF. The UV_{254} decreased from 15.7 ± 1.6 to 13.2 ± 1.0 m^{-1} after aeration (Figure 4-2b). The SUVA did not significantly change after aeration with air between column influent and effluent (SUVA = 2.3 ± 0.2 L/(m·mg)).

A mass balance of dissolved oxygen and inorganic compounds (1.0 mg NO_2^- - N ≙ 1.14 mg O_2; 1.0 mg Mn^{2+} ≙ 0.29 mg O_2) resulted in oxygen consumption of approximately 6.6 mg/L by organic compounds. Since the observed DOC removal is too low (0.8 ± 0.5 mg/L) to account for this oxygen consumption, it is hypothesized that transformation of particular organic carbon (POC) present within the sand column might have contributed to the overall oxygen consumption. Similar results indicating that the targeted oligotrophic conditions were not fully established after aeration were also obtained from other columns (first filtration step, systems SMART O_2 and SMART O_3).

The aeration with oxygen provided oxic conditions throughout the system (Table 4-1) and improved the DOC removal as well as the UV_{254} reduction compared to aeration with air (Figure 4-3). These results confirm the limitation of DOC degradation in the aerated system due to a limited availability of dissolved oxygen.

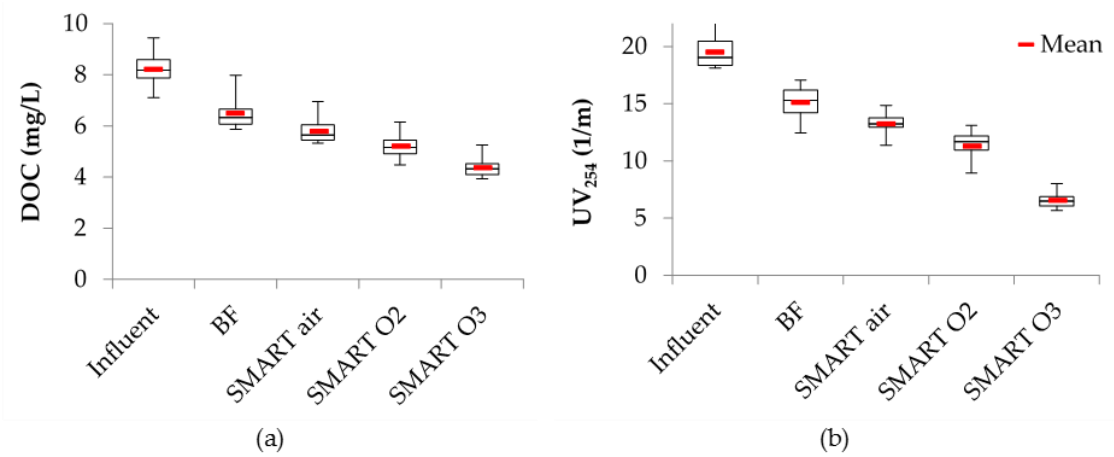

Figure 4-3: DOC concentrations (a) and UV_{254} absorbance values (b) of the influent and the effluents of all four systems: Bank filtration (BF), sequential managed aquifer recharge technology (SMART) air, SMART O_2, SMART O_3 ($n \geq 16$). Whiskers indicate maximum and minimum values.

Ozonation of the effluent from the first column resulted also in oxic conditions throughout the subsequent column system (Table 4-1). During ozonation, DOC and UV_{254} decreased from 6.6 ± 0.7 to 6.3 ± 0.5 mg/L and from 15.7 ± 1.6 to 9.5 ± 0.9 m^{-1}, respectively. Ozonation also further enhanced the DOC degradation by 24%, likely due to the formation of biodegradable compounds during oxidation reactions with ozone (Hammes et al., 2006). However, in our experiments, elevated ozone dosages were needed due to the consumption of reduced inorganic compounds such as nitrite and manganese. For planning of full-scale operation, the effects of these reduced compounds regarding oxidation demand need to be considered.

4.3.3. Transformation of trace organic chemicals as a function of different oxidation techniques

TOrCs are discussed in the following section regarding their degradation efficiencies in different filtration systems as a function of the aeration technique applied. The influent concentrations, the limits of quantification (LOQ) as well as the second-order rate constants for the reactions of the compounds with ozone or ·OH-radicals, respectively (k_{O3} and k_{OH}) of all quantified TOrCs are given in Table SI-4 1. The results of the TOrCs which could be detected after the first filtration step are shown in Figure 4-4. Furthermore, the transformation of these compounds as a function of the HRT in the second systems after aeration with air, pure oxygen or ozone, respectively, are given in Figure SI-4 2 in the supplementary material.

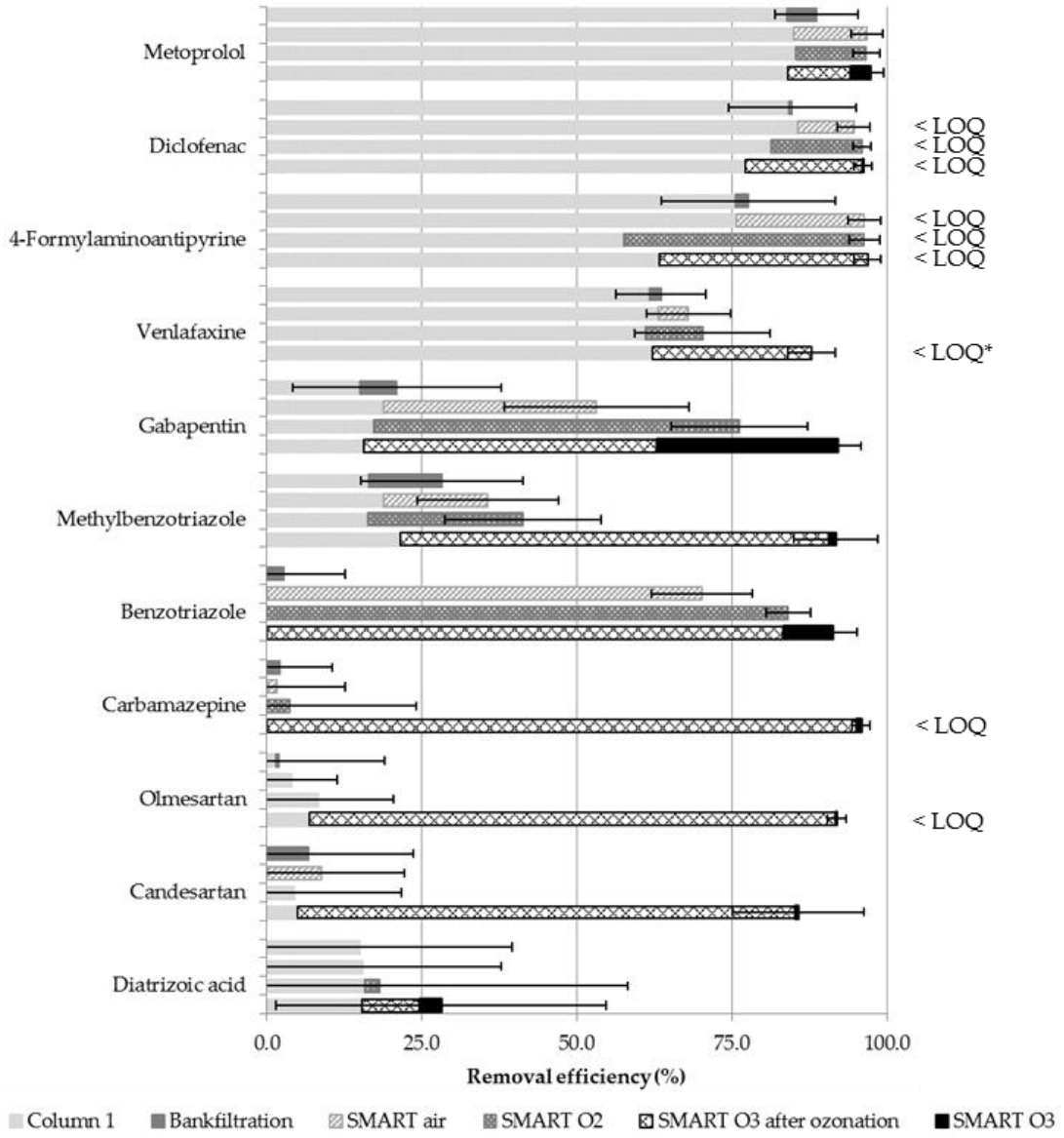

Figure 4-4: Removal efficiency (%) of all quantified trace organic chemicals (TOrCs) which were not degraded below the limits of quantification (LOQ) in the first column ($n \geq 8$). (* Venlafaxine was degraded below LOQ during ozonation whereas an increase of the concentration up to 65 ± 13 ng/L in the following filtration step was observed.)

4.3.3.1. Consistency and reproducibility of observed degradation

The influent concentrations of all quantified TOrCs decreased during the experimental period. This may be explained due to decreasing TOrCs concentrations in the Lake Tegel, Berlin, since the effluent from the WWTP Schönerlinde, Berlin, was only partly discharged into local channel flowing to Lake Tegel during the experiments. Detailed results from measurements of the antibiotic sulfamethoxazole shown in Figure 4-5 revealed an increased compound removal by time, likely indicating the adaptation of bacteria for sulfamethoxazole biodegradation. After three months, the effluent concentration of the SMART air system was below the LOQ (50 ng/L) with one exception (c = 108 ng/L). These results are in line with previous findings reported by Baumgarten et al. (2011), who

observed a long adaption time of more than two years for an efficient degradation of sulfamethoxazole (60% under oxic conditions, no degradation under anaerobic conditions). In contrast to experiments from Baumgarten et al. (2011), columns were filled with sand from the infiltration basin and operated at higher temperatures, which might have shortened the need for an extended adaptation period. The observed increase through the column passage in the first weeks could be caused by analytical inaccuracies, but also formation of sulfamethoxazole from conjugated metabolites (e.g., N^4-acetylsulfamethoxazole) as previously reported from WWTPs might play a role (Göbel et al., 2005; Polesel et al., 2016). Similar to sulfamethoxazole, gabapentin showed a slightly increasing transformation in the SMART air system during the experimental period.

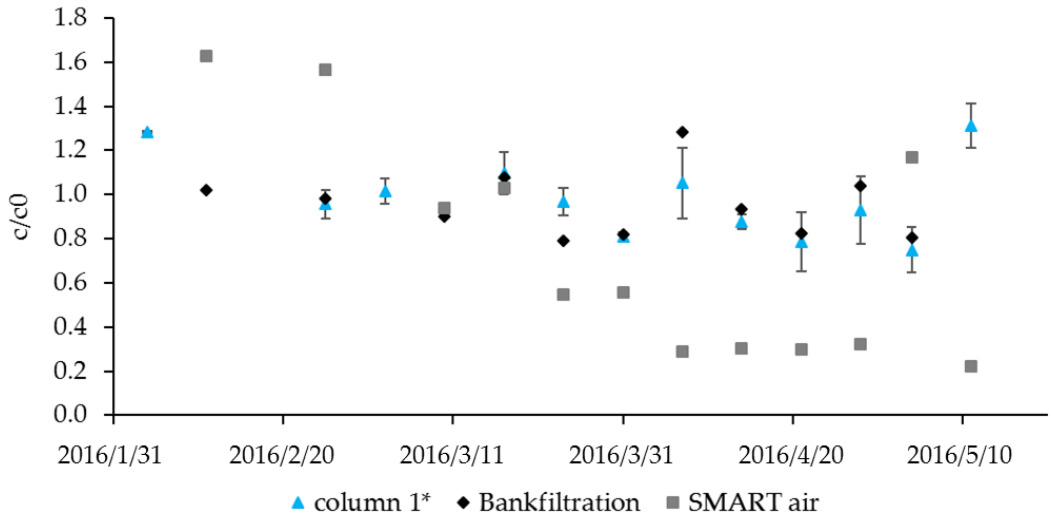

Figure 4-5: Improved removal efficiency of sulfamethoxazole in the SMART air system; * mean value of first column effluents, *n* = 2.

Transformation of diclofenac was already observed in the first filtration step and increased during the period of adaption up to a removal below the LOQ (100 ng/L) at the end of the experiment. The transformation of the other targeted TOrCs was consistent during the experiment despite decreasing influent concentrations. Results from the different column systems are summarized as average removal with standard deviation in Figure 4-4.

4.3.3.2. Compound removal during anoxic infiltration

The compounds acesulfame, iomeprol, iopromide, and valsartan were transformed to concentrations below the LOQ in the first filtration step (Table SI-4 1). It has to be noted that the influent concentrations were close to or even partly below the LOQ for acesulfame and valsartan, respectively. While rapid degradation of iomeprol and iopromid is known from bank filtration and groundwater recharge sites (Grünheid et al., 2005; Kormos et al., 2011; Wiese et al., 2011), efficient removal of acesulfame and valsartan was not expected. Acesulfame has been reported as a rather persistent compound and was even proposed as a conservative wastewater marker (Buerge et al., 2009; Scheurer et al., 2011; Wolf et al., 2012). However, Zucker et al. (2015) also revealed efficient degradation of acesulfame under certain (mostly oxic) conditions. For valsartan, ubiquitous occurrence in the aquatic environment as well as low to moderate biodegradation has been reported (Kasprzyk-

Hordern et al., 2008; Nödler et al., 2014). Similar to acesulfame, valsartan has been proposed as a wastewater marker in the environment (Nödler et al., 2016). To the best of our knowledge, this study reports for the first time, efficient elimination of this compound in MAR systems. Good removal (>70%) in the reference system under anoxic conditions was also observed for diclofenac, 4-Formylaminoantipyrine, and metoprolol. For these compounds, degradation mainly occurred in the first column, indicating more efficient removal during initial infiltration characterized by high microbial activity.

4.3.3.3. TOrC removal during SMART

The systems SMART air and SMART O_2 performed equal or better than the reference system for most compounds. Especially the removal of diclofenac, 4-Formylaminoantipyrine, benzotriazole, gabapentin, venlafaxine and metoprolol was significantly enhanced using the sequential approach (students *t*-test, paired, $\alpha < 0.05$). Further improvement of benzotriazole and gabapentin removal by using pure oxygen confirmed potential oxygen limitation in the second column after aeration with air. However, for efficient removal of most compounds, the establishment of fully oxic conditions throughout infiltration was obviously not needed, indicating a limited benefit from using pure oxygen for intermediate aeration.

4-Formylaminoantipyrine as a human metabolite of phenazone-type pharmaceuticals (Massmann et al., 2008a) was removed by 76% in the first column of the reference system with no significant increase with ongoing filtration under anoxic conditions (students *t*-test, paired, $\alpha = 0.18$). All SMART systems exhibited an efficient degradation of 4-Formylaminoantipyrine below the LOQ (100 ng/L) which implies a removal of >96%. These results confirm previous results suggesting a degradation of 4-Formylaminoantipyrine under oxic conditions of 94% (Wiese et al., 2011).

The removal of diclofenac in the system BF did not increase significantly compared to the first filtration step (students *t* -test, paired, $\alpha = 0.37$), whereas in the SMART air and SMART O_2 system a significantly enhanced and consistent transformation was observed (students *t*-test, paired, $\alpha < 0.05$). In SMART air, the concentration dropped below the LOQ (100 ng/L) with two exceptions. In the SMART O_2 system, the concentration consistently decreased below the LOQ. Wiese et al. (2011) confirmed degradation under oxic conditions for diclofenac of >90%, whereas Rauch-Williams et al. (2010) reported a faster removal under anoxic conditions. Our findings are in accordance to Regnery et al. (2016), who proposed no complete removal of diclofenac during a short riverbank filtration but a rapid transformation in the second filtration step after reaeration.

Previous studies reported different behaviors of benzotriazole biodegradation during MAR ranging from highly persistent to microbial processes (Breedveld et al., 2003) over preferred biodegradation under oxic conditions to biodegradation even under anoxic conditions with biodegradation half-lives of 29 ± 2 days (Alotaibi et al., 2015; Liu et al., 2011). However, our results confirm biodegradation under oxic conditions whereas no removal was achieved under anoxic conditions (Figure 4-4).

Biotransformation is the most likely degradation mechanism in wastewater treatment plants for metoprolol compared to sorption as shown by Maurer et al. (2007). Different

studies revealed an efficient removal of metoprolol in MAR or slow sand filters, respectively (Hübner et al., 2012; Maeng et al., 2011b; Nödler et al., 2013). Here, metoprolol was degraded by 84% in the first filtration step and overall by 89% in the reference system not employing an intermediate treatment. Aeration increased elimination up to 97% independently of the type of aeration technique employed.

Previous studies argue that gabapentin is persistent during SAT simulated in laboratory-scale soil column set-ups (Onesios and Bouwer, 2012). While the removals of gabapentin in the reference system (21%) support these findings (Figure 4-4), the removal efficiency of gabapentin under oxic conditions was significantly enhanced (53% in SMART air; 76% in SMART O_2). As shown in Figure 4-6, gabapentin was only eliminated within the first 1.5 days after aeration with air, which corresponds to the fast oxygen consumption in the SMART air system. The fully oxic SMART O_2 led to a continuous gabapentin degradation, which remained constant after 4.5 days post aeration. These results support the argument that gabapentin is very redox sensitive and could be degraded >53% under oxic conditions. However, it remains unclear, why initial removal after aeration with air was faster than in the fully oxic system.

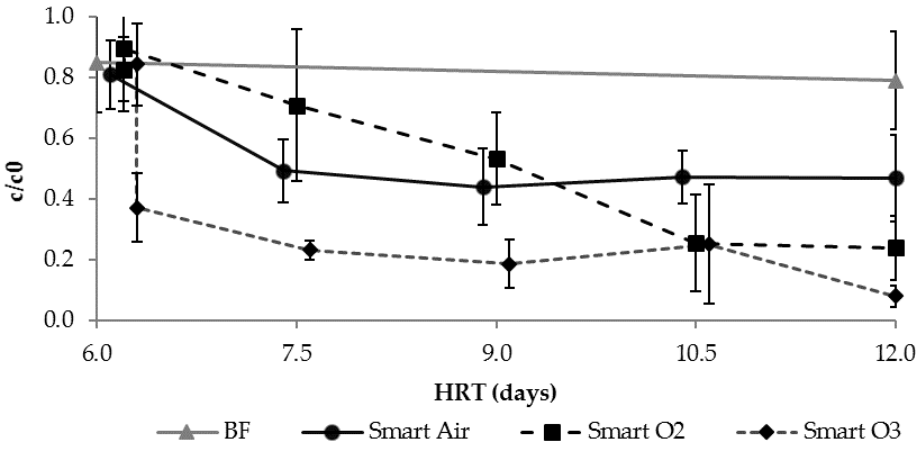

Figure 4-6: Degradation of gabapentin in the second filtration step of all four systems: BF, SMART air, SMART O_2 and SMART O_3 ($n \geq 2$).

Despite improved performance, removal of several compounds, such as benzotriazole, methylbenzotriazole, venlafaxine and sulfamethoxazole is still not effective and necessitates further improvement. In addition, compounds persistent to biodegradation such as carbamazepine, candesartan, olmesartan, and diatrizoic acid are not removed by SMART.

4.3.3.4. Application of ozone for intermediate aeration and oxidation

All TOrCs that were present after the first column infiltration were subject to oxidative transformation using ozonation. The removal efficiency of single substances depends on their reactivity with ozone. In previous research, compounds were separated into fast reacting compounds with apparent second order rate constants of $k_{O3} > 10^4\ M^{-1}\cdot s^{-1}$ (pH = 7), moderately ($10^2\ M^{-1}\cdot s^{-1} < k_{O3} < 10^4\ M^{-1}\cdot s^{-1}$; pH = 7), and slowly reacting compounds ($k_{O3} < 10^2\ M^{-1}\cdot s^{-1}$) (Hollender et al., 2009; Hübner et al., 2012). The rate constants of all quantified compounds are summarized in Table SI-4 1. Removal of fast

reacting TOrCs is dominated by direct reaction with ozone leading to a complete transformation of the parent compound at typically applied ozone dosages. In this study, the fast reacting compounds diclofenac, sulfamethoxazole, carbamazepine and venlafaxine were mainly removed below the limit of quantification although specific ozone consumption was relatively low (0.6 ± 0.1 mg O_3/mg DOC, n = 12). Despite removal below LOQ during ozonation, the compound venlafaxine was consistently detected in the effluent of the subsequent column at concentrations of 65 ± 13 ng/L. A reverse reaction from ozonation transformation products can be assumed as being the reason for this increase. The major transformation product from the reaction with ozone is venlafaxine N-oxide (Lester et al., 2013). Although a reduction seems unlikely under oxic conditions, a similar pathway has been reported for other N-oxides (Iobbi-Nivol et al., 1996; Maeda et al., 2014). More research is certainly needed to better understand these processes.

Moderately reacting compounds are oxidized by both, ozone and OH-radicals which are formed from ozone reactions with the water matrix (Buffle and von Gunten, 2006). Benzotriazole and methylbenzotriazole were removed by approximately 80% during ozonation within this study. Removal of these compounds could be easily enhanced by increasing ozone dosages to compensate high oxygen consumption by nitrite and Mn(II). Average concentrations of 0.2 mg/L NO_2^--N and 1.0 mg/L Mn(II) consume 0.7 and 0.9 mg/L ozone, respectively, since they are completely oxidized during ozonation due to high second-order rate constants with ozone ($k_{O3}(NO_2^-)$ = 3.7 x 10^5 $M^{-1}{\cdot}s^{-1}$; k_{O3}(Mn(II)) = 1.5 x 10^3 $M^{-1}{\cdot}s^{-1}$ (von Gunten, 2003a)).

Due to the formation of OH-radicals from the reactions of ozone in natural waters, also compounds, which are not reactive to ozone can be oxidized during ozonation. However, removal of these TOrCs is usually incomplete and variable depending on compound's reactivity with OH-radicals. In this study, gabapentin was removed by approximately 50% during ozonation. Together with improved biodegradation due to intermediate aeration, this compound could be eliminated close to the LOQ (50 ng/L) by the combination of sequential managed aquifer recharge with intermediate ozonation.

In contrast, the second-order rate constant for the reaction of diatrizoic acid with OH-radicals is comparatively low resulting in limited removal of 9% by ozonation (Real et al., 2009). Since this compound is also not efficiently biodegraded in soil columns, overall removal was below 30% in all investigated hybrid systems. These results demonstrate that some compounds can even persist during combined ozonation and biological treatment processes. This has previously also been observed for other TOrCs such as primidone (Hübner et al., 2012).

To the best of our knowledge, less is known about the rate constants of candesartan and olmesartan. It is assumed, that candesartan is a moderately reacting compound since its removal of 80% is similar to benzotriazole, whereas a fast removal of olmesartan below the LOQ (500 ng/L) was observed. The rapid degradation of olmesartan by ozone could probably be explained by the electron rich olefin group of the imidazole side chain.

It is well understood that ozonation does not result in mineralization of TOrCs but leads to a formation of transformation products. The potential removal of these products in biological treatment processes was reviewed by Hübner et al. (2015) and is not part of this

study. As a short summary, reactions of ozone with olefinic groups and electron-rich aromatic moieties mostly involve the cleavage of double bonds and aromatic rings resulting in better biodegradable products. In contrast, transformation of amines and sulfur-containing chemicals might also form highly persistent products. Further investigations are needed to analyze the relevance of transformation products in combined ozonation and MAR systems.

4.3.3.5. Formation and fate of the transformation product valsartan acid

During oxidative and biological treatment, compounds are often not mineralized but just transformed. Valsartan acid is a known transformation product from biodegradation of different sartanes such as valsartan, irbesartan, candesartan, and olmesartan (Letzel et al., 2015). In Figure 4-7a, changes of molar concentrations of valsartan, olmesartan, candesartan, and valsartan acid in the first filtration step are illustrated. Effluent concentrations of each compound of the first filtration step are summarized as mean values. Valsartan was transformed immediately below the LOQ of 100 ng/L in the first columns, whereas candesartan and olmesartan were persistent (also in the second columns of the systems BF, SMART air and SMART O_2, Figure SI-4 2). Although the decrease of valsartan came along with an increase of valsartan acid, formation of valsartan acid cannot be solely attributed to transformation of valsartan. It is suggested that degradation of other compounds such as irbesartan, which was not analyzed, might have contributed to valsartan acid formation (Letzel et al., 2015). In the second infiltration step, valsartan acid is efficiently attenuated in all systems with aeration (SMART air: 95%, SMART O_2/O_3: >99%), whereas it remained constant in the anoxic reference system (Figure 4-7b). These results are in accordance to Nödler et al. (2013), who proposed poor removal of valsartan acid during bank filtration. Oxic conditions seem to be favored for a sufficient biodegradation of valsartan acid.

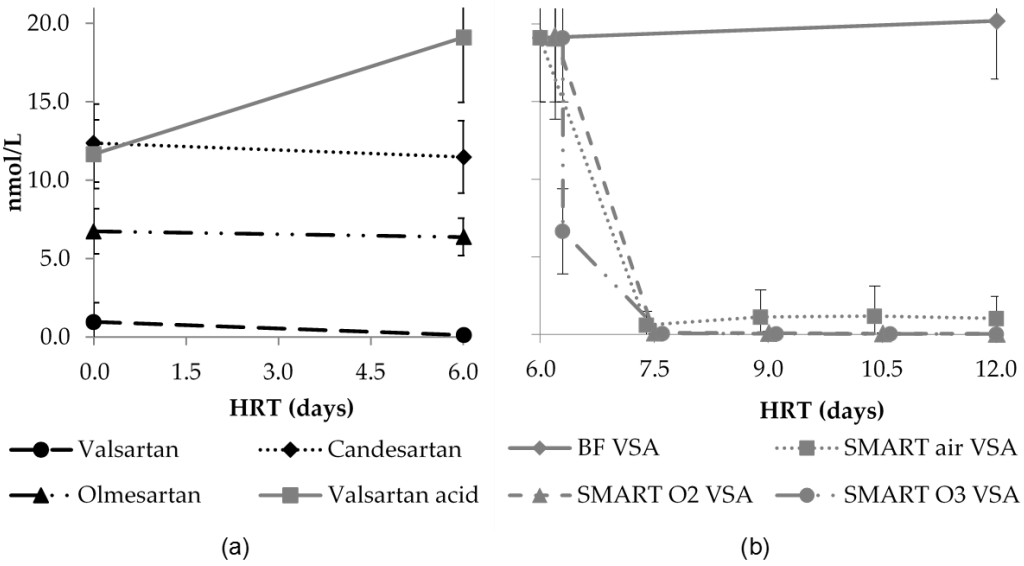

Figure 4-7: The formation of valsartan acid (VSA) in the first filtration step (grey line, a) and the transformation of valsartan, candesartan and olmesartan (black lines, a). Valsartan acid was degraded in the second filtration step after aeration with air, oxygen or ozonation (b) *n* ≥ 4.

4.4. Conclusions

The performance of the SMART concept as a combination of two MAR systems with an intermediate aeration step was compared to a conventional MAR system such as riverbank filtration. Different oxidants were tested between both filtration steps (i.e., air, pure oxygen, ozone) and investigated regarding the removal efficiency of select TOrCs. Rapid oxygen consumption, nitrate reduction and dissolution of manganese confirmed anoxic conditions within the first filtration step. Aeration with air did not result in sufficient oxygen concentrations to establish oxic conditions throughout the second column, resulting in oxygen limitation for DOC degradation in comparison to fully oxic column after aeration with pure oxygen. Ozonation increased the biodegradability of DOC, enhancing overall removal to 47%.

Most TOrCs were equally or better degraded in sequential systems with intermediate aeration compared to the single step bank filtration system. The compounds acesulfam, iomeprol, iopromide, and valsartan were degraded within the first infiltration step despite the fast oxygen consumption and prevailing anoxic conditions. Intermediate aeration resulted in the significantly enhanced removal of diclofenac, 4-Formylaminoantipyrine, metoprolol, gabapentin, venlafaxine, valsartan acid and benzotriazole. Among them, degradation of the compounds gabapentin and benzotriazole was still limited in the partly suboxic system after aeration and could be further enhanced under fully oxic conditions. Intermediate ozonation led to a significant degradation of the biological persistent compounds carbamazepine, candesartan, and olmesartan. Additionally, the attenuation of gabapentin, methylbenzotriazole, benzotriazole and venlafaxine was further increased. However, results also demonstrated that a few compounds (i.e., diatrizoic acid) are not efficiently removed in an ozone–MAR hybrid system.

Acknowledgements

The Berliner Wasserbetriebe (BWB) are gratefully acknowledged for financial support of this study. This publication was supported by the German Research Foundation (DFG) and the Technical University of Munich (TUM) in the framework of the Open Access Publishing Program.

Conflicts of Interest

The authors declare no conflict of interest. The founding sponsors had no role in the design of the study; in the collection, analyses, or interpretation of data; in the writing of the manuscript, and in the decision to publish the results.

Based on results of this study, hypothesis I that SMART can result in improved removal of potentially health relevant TOrCs compared to currently practiced MAR systems in Berlin could be confirmed.

5 Establishing sequential managed aquifer recharge technology (SMART) for enhanced removal of trace organic chemicals: Experiences from field studies in Berlin, Germany

This chapter has been previously published as follows[9]:

Hellauer, K., Karakurt, S., Sperlich, A., Burke, V., Massmann, G., Hübner, U., Drewes, J.E., 2018. Establishing sequential managed aquifer recharge technology (SMART) for enhanced removal of trace organic chemicals: Experiences from field studies in Berlin, Germany. *Journal of Hydrology* 563, 1161–1168.

Abstract

Despite the efficient removal of many contaminants including pathogens and trace organic chemicals (TOrCs) during managed aquifer recharge (MAR), fate and transport of TOrCs in the subsurface might not always occur under conditions that favor effective biotransformation resulting in a contamination risk where water is recovered for drinking water production. A promising technology that can lead to improved removal of TOrCs is the sequential MAR technology (SMART), which combines two infiltration steps with an intermediate aeration to establish more favorable oxic and carbon-limited conditions resulting in enhanced TOrCs transformation. The aim of this study was to test the performance of the SMART concept under field conditions in comparison to a conventional MAR using pond infiltration (cMAR) operated in Berlin, Germany. Although oxic conditions were obtained at both field sites considering infiltration depth to 200 cm, redox conditions were more stable at the SMART facility fed with bank filtrate. In addition, carbon-limited conditions were solely observed during SMART. Chemicals known to persist during MAR, including candesartan, carbamazepine, dihydroxydihydrocarbamazepine, olmesartan, oxypurinol, phenylethylmalonamide, primidone, and tolyltriazole exhibited a refractory behavior at both field sites, whereas valsartan acid, metformin, and gabapentin-lactam were removed by more than 85% during 200 cm of infiltration. 4-Formylaminoantipyrine, acesulfame, benzotriazole, and gabapentin exhibited a significantly enhanced transformation during SMART compared to the cMAR site. These results confirm that SMART can result in controlled oxic and carbon-depleted subsurface conditions during MAR facilitating an improved transformation of moderately degradable TOrCs by natural treatment processes.

[9] This study was conducted to test Hypothesis I that SMART can result in improved removal of potentially health relevant TOrCs compared to currently practiced MAR systems in Berlin.

5.1. Introduction

More than 70% of the drinking water for the city of Berlin originate from bank filtration (BF) or artificial groundwater recharge by surface spreading using the city's surface water sources (Heberer and Adam, 2004). As one of these drinking water resources, Lake Tegel located in the northwestern part of Berlin is receiving water from the River Havel and the confluence of the Tegeler Fliess and the Nordgraben. The flow of the Nordgraben is strongly impacted (70–90%) by discharge of the wastewater treatment plant (WWTP) Schönerlinde, Berlin resulting in a contribution of 17–35% WWTP effluent in Lake Tegel, (Henzler et al., 2014; Schimmelpfennig et al., 2012). More details on site specific conditions can be found elsewhere (Schimmelpfennig et al., 2012). Several studies investigated the performance of recharge systems including BF or surface spreading at Lake Tegel regarding the attenuation of TOrCs (Grünheid et al., 2005; Hass et al., 2012; Heberer et al., 2004; Heberer and Adam, 2004; Maeng et al., 2010; Massmann et al., 2006; van Baar, 2015). Although natural processes provide an effective barrier for several contaminants including many TOrCs (Amy and Drewes, 2007; Hiscock and Grischek, 2002; Tufenkji et al., 2002), there remains a potential contamination risk for public drinking water supply from chemicals that persist during conventional managed aquifer recharge (MAR) (Hass et al., 2012; Heberer et al., 2004) and exceed human health threshold levels.

Biological transformation has been reported as one of the most important removal mechanisms for many TOrCs in MAR systems (Alidina et al., 2014a; Maeng et al., 2011b). Efficiency of biotransformation is affected by prevailing redox conditions (Burke et al., 2014) as well as the composition and concentration of the biodegradable dissolved organic carbon (BDOC) since they shape structure and functionality of the microbial community (Alidina et al., 2014b; Li et al., 2014a; Rauch-Williams et al., 2010). Previous studies by Regnery et al. (2015b) demonstrated a more efficient TOrCs transformation under oxic and carbon-limited conditions. Biomolecular studies revealed the establishment of a more diverse microbial community under these conditions, which is capable of transforming more refractory organic matter and xenobiotics (Li et al., 2014a).

Based on these findings, the concept of sequential managed aquifer recharge technology (SMART) was developed consisting of a short infiltration step (e.g. via BF) to remove easily degradable organic matter followed by an intermediate aeration and a second infiltration step to provide favorable oxic and carbon-limited conditions for an enhanced TOrCs removal (Regnery et al., 2016). The establishment of these conditions has been documented at the full-scale MAR facility Prairie Waters Project in Aurora (Colorado, USA) resulting in enhanced transformation of biodegradable TOrCs (Regnery et al., 2016).

Previous laboratory-scale soil column experiments showed high potential of the SMART concept to enhance the removal of several compounds compared to current operation of MAR systems for Berlin (Hellauer et al., 2017). The objective of this study was to establish, validate and potentially improve the SMART concept for Berlin's drinking water production under field conditions. SMART was tested by modifying an existing infiltration basin of a recharge facility located on an island within Lake Tegel that was fed with bank filtrate from nearby drinking water production wells. Performance was compared by monitoring water

quality changes at a conventionally operated MAR site practicing pond infiltration using water from Lake Tegel directly.

5.2. Material and methods

5.2.1. Field sites

Both investigated field sites, the conventional MAR site using pond infiltration (cMAR) and SMART facility using aerated Lake Tegel bank filtrate for groundwater recharge, were located at Lake Tegel, Berlin, Germany (Figure 5-1). Performance of the cMAR facility was monitored at the Saatwinkel recharge basin #3, representing a total surface area of approximately 8900 m² (Figure 5-1, lower right). The operation of the basin was shut down in April 2014 and restarted in April 2016 prior to conducting this study. The basin was fed with Lake Tegel water without any pretreatment. The surface spreading basin (Figure 5-1, lower right) was equipped with two nested groundwater samplers (MP1, MP2) including suction cups (SK 20, UMS, Germany) and oxygen sensors (Pst3, Presens, Germany) at three different depths (0.5 m, 1.0 m and 2.0 m) below ground surface (bgs). The oxygen sensors were constructed according to the description from Hecht and Kölling (2001). Samples were collected from observation wells TEG 367 (screening interval: 12–14 m bgs), TEG 368OP (screening interval: 12–14 m bgs), and TEG 369OP (screening interval: 10.2–12.2 m bgs) located in flow direction to production well #20 (screening interval: 20–34 m bgs). Travel times to observation wells TEG 367, 368OP and 369OP were estimated based on previous investigations at this field site (Massmann et al., 2006).

The SMART concept was tested at the recharge facility Baumwerder, using half of an existing surface spreading basin of approximately 700 m² (Figure 5-1, top right and Figure SI-5 1). During the operation of the basin, six BF production wells were constantly operated. Bank filtrate from wells #1, 2, 3 and 10 was pumped via a delivery pipe into the basin while wells #6 and 9 were operated to deliver water to the drinking water production facility. Re-aeration of the lake bank filtered water was achieved by routing the abstracted water over a heap of rocks into the surface spreading basin. The basin was also equipped with suction cups and oxygen sensors at three different depths (MP 1, MP 2; 0.5 m, 1.0 m, 2.0 m bgs). In addition, three shallow observation wells (OW 1 screening interval: 2.9–4.9 m bgs, OW 2 screening interval: 2.9–4.9 m bgs, OW 3 screening interval: 2.8–4.8 m bgs) were installed within the basin. Deeper observation wells were placed in flow direction towards production wells #1 and #10, respectively, including TEG 383 (screening interval: 3.8–7.8 m bgs) and TEG 384 (screening interval: 7.2–11.2 m bgs), TEG 385 (screening interval: 5.1–9.1 m bgs), and TEG 386 (screening interval: 9.2–13.2 m bgs). Travel times were estimated in a tracer test using sodium bromide as conservative tracer. To achieve an initial bromide concentration of 300 mg/L in the basin, 70 kg of sodium bromide were rapidly added to the basin by initially dissolving the sodium bromide in 200 L of bank filtrate and subsequently distributing this solution by spreading over the basin via a hose.

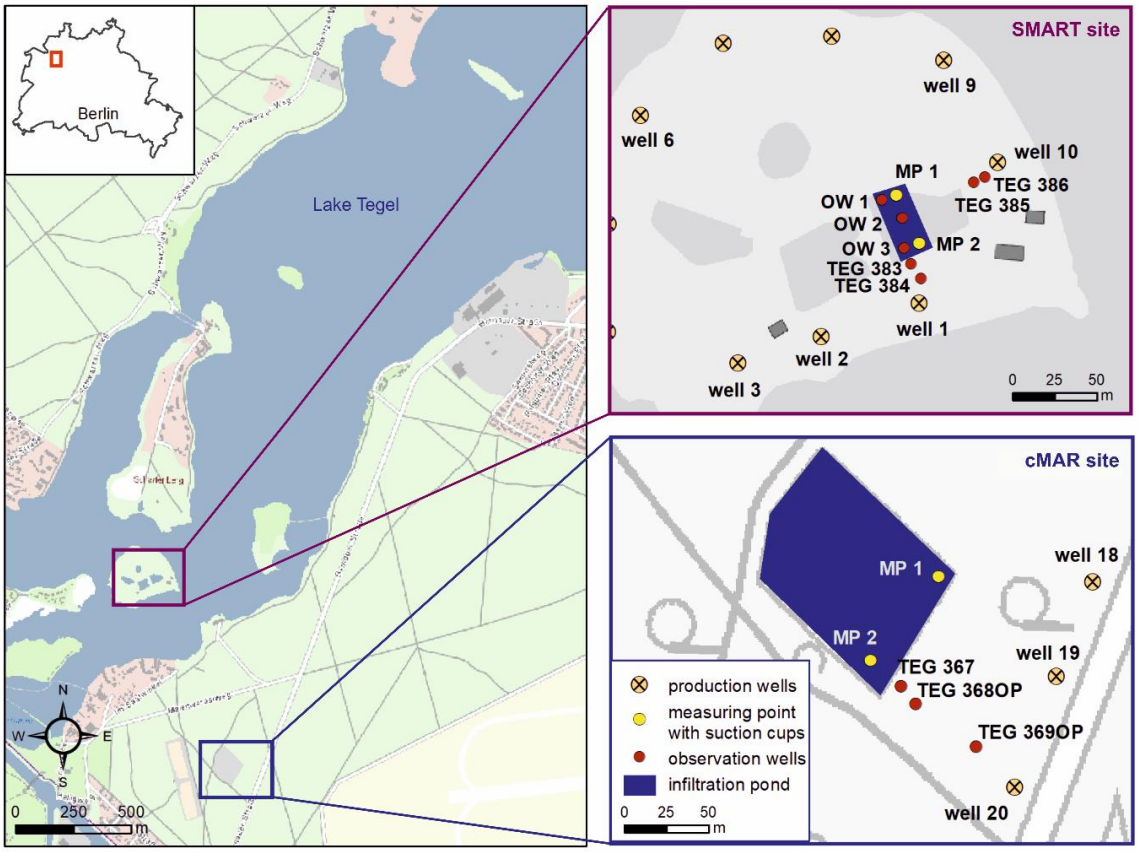

Figure 5-1: Location of the Lake Tegel, Berlin, Germany with the conventional MAR using pond infiltration site (cMAR site, lower right) and the SMART field site using lake bank filtrate for infiltration (top right) including measuring points (MP) with suction cups and dissolved oxygen sensors, observation wells (OW) and production wells.

5.2.2. Analytical methods

In order to record hydraulic heads in real time, each observation well was equipped with data loggers. Micro-Diver loggers (Schlumberger, The Netherlands) were installed into the observation wells TEG 367 and 368OP at the cMAR site and into the shallow observation wells (OW 1, OW 2, OW 3) at the SMART field site. Observation wells TEG 383-386 (SMART field site) were equipped with WPS 05 data logger with integrated GSM-module (Ackermann, Germany). One Baro-Diver (Schlumberger, The Netherlands) at the field site was installed for barometric compensation.

Dissolved oxygen (DO) concentrations in the recharge basin as well as at three different depths were determined by *in situ* PSt3 oxygen sensors (Presens, Germany), whereas the measurement in the observation wells was conducted using a handheld dissolved oxygen meter Oxi 330i (WTW, Germany). Ammonia was determined photometrically following DIN ISO 15923-1 (Gallery Plus, Thermo Scientific, USA). Nitrate was measured using ion chromatography (DIONEX ICS-1100, Thermo Scientific, USA) according to DIN EN ISO 10304-1 (D20). Iron and manganese were analyzed by an inductively coupled plasma – optical emission spectrometry (iCAP 6000 Series, Thermo Scientific, USA) based on DIN EN ISO 11885 (E22). Bulk organic carbon characterization was conducted

by dissolved organic carbon (DOC) (TOC-L, Shimadzu, Japan) and ultraviolet absorbance at 254 nm (UVA_{254}) (DR 5000, Hach, Lange, Germany) measurements according to DIN EN 1484 (H03) and DIN 38404-C03, respectively. TOrCs were quantified by liquid chromatography coupled with mass spectrometry, using either a tandem mass spectrometer (Xevo-TQ-S, Waters, USA) or a high resolution mass spectrometer ((Wode et al., 2012). Bromide was analyzed after filtration through 0.45 µm cellulose acetate filters (Sartorius Minisart®152) by ion chromatography (Basic IC plus, Metrohm, Germany) according to DIN EN ISO 14911.

5.3. Results and discussion

5.3.1. Site characterization

5.3.1.1. Feed water quality

Water quality and redox parameters as well as targeted TOrCs of both influent waters (cMAR site: Lake Tegel water; SMART field site: aerated lake bank filtrate) were recorded and are summarized in Table 5-1 and Table SI-5 1, respectively. In addition, the limit of quantification (LOQ) is given for all parameters. The average DO concentration in the water of Lake Tegel (10.6 ± 1.7 mg/L) was higher compared to the re-aerated bank filtrate feeding the recharge basin at the SMART field site (6.5 ± 1.1 mg/L). The DOC concentration of 4.7 ± 0.2 mg/L in the bank filtered water confirmed previous results reporting a residual non-degradable DOC of 4.7 mg/L at field conditions during bank filtration as well as pond infiltration in Berlin (Grünheid et al., 2005). Nitrate and ammonia concentrations were low in both waters, iron and manganese were slightly elevated in the bank filtered water suggesting prevalence of reduced (anoxic) conditions in the aquifer (Table 5-1).

Table 5-1: Redox and bulk organic parameters of the feed water at the cMAR site (Lake Tegel water) and the SMART site (aerated Lake Tegel bank filtrate); LOQ = limit of quantification.

	Redox parameters ($n \geq 11$)					Bulk organic parameters ($n \geq 21$)		
	O_2 [mg/L]	NO_3^--N [mg/L]	NH_4^+-N [mg/L]	Fe [mg/L]	Mn [mg/L]	DOC [mg/L]	UVA_{254} [m^{-1}]	SUVA [L/(mg·m)]
LOQ	0.015	0.05	0.04	0.03	0.01	0.5	0.5	-
cMAR site	10.6 ± 1.7	0.34 ± 0.20*	0.11 ± 0.05	0.05 ± 0.06	0.03 ± 0.04	7.3 ± 0.6	15.1 ± 1.0	2.1 ± 0.2
SMART site	6.5 ± 1.1	0.11 ± 0.06	0.08 ± 0.05	0.42 ± 0.32	0.26 ± 0.16	4.7 ± 0.2	11.3 ± 0.4	2.4 ± 0.1

* NO_3^--N concentration at the cMAR site was calculated from June 1, 2016 until the end of the experimental period due to strongly decreasing concentrations in the influent.

5.3.1.2. Tracer test

Based on the results of the tracer test performed at the SMART field site, travel times of ~0.09 days for 50 cm, ~0.15 days for 100 cm, and ~0.17 days for 200 cm of infiltration were determined for suction samplers at MP 1. A travel time of approximately 11 days was

determined to observation well TEG 386. No tracer was detected at observation wells TEG 383, TEG 384 and TEG 385. In addition, only very little bromide concentration was measured at MP 2. Based on these results, further discussions will be limited to results obtained from MP 1 and well TEG 386. A detailed description of the tracer test is provided in the Supplementary information.

Since no tracer test was performed at the cMAR site, the travel times to the suction samplers were estimated by the porosity of the soil within the basin (~41%) and the median of the infiltration rate (1.68 m/d) as approximately 0.12, 0.25 and 0.49 days to depths of 50, 100 and 200 cm, respectively. Due to spatially variable infiltration across the basins at both field sites and variable infiltration rates during the course of the study, the obtained residence times should be considered as approximate values. Travel times to the observation wells at the cMAR site (~3 days for TEG 367, ~7 days for TEG 368OP, ~25 days for TEG 369OP) were previously reported by Massmann et al. (2006).

5.3.1.3. Hydraulic conditions

The groundwater level at the cMAR site increased and reached steady-state conditions after approximately two months as shown in Figure 5-2a. A failure in the pumping devices resulted in a sudden depletion of water level in the basin and a decline of the infiltration rate for a few days after approximately three months. As illustrated in Figure 5-2a, the groundwater level below the basin as well as the infiltration rate decreased with ongoing operation time resulting in the necessity to remove the clogging layer in the recharge basin after approximately 5.5 months. These results are in line with Greskowiak et al. (2005) who proposed different hydraulic stages during conventional artificial recharge: In the beginning, the water saturation increases until the establishment of fully saturated conditions, followed by a decreasing infiltration rate due to the formation of a clogging layer resulting in unsaturated conditions underneath the basin and a decline in the groundwater level. At the final stage, no additional recharge can occur, which requires the removal of the clogging layer to restore infiltration.

In contrast to the cMAR site, clogging was not an issue at the SMART site during the experimental period of approximately nine months. The groundwater level underneath (OW 1, 2 and 3) and downstream of the basin (TEG 386) slightly increased during the first six months followed by a more dominant rise. Approximately seven months after initial operation, the groundwater level at TEG 386 remained at steady state until the end of the experimental period (Figure 5-2b). Also recharge volume to the basin at the SMART site, which was increased after approximately two months of operation to obtain a water level of at least 30 cm within the basin, remained nearly constant afterwards (Figure 5-2b). The reduced clogging compared to cMAR may be the result of a much lower content of particles, microorganisms and colloids in the lake bank filtrate, which are major factors causing clogging (Hiscock and Grischek, 2002). However, long-term effects due to precipitated iron or particular organic matter from algae growth resulting in the formation of a clogging layer were not taken into account yet and need to be addressed in further studies.

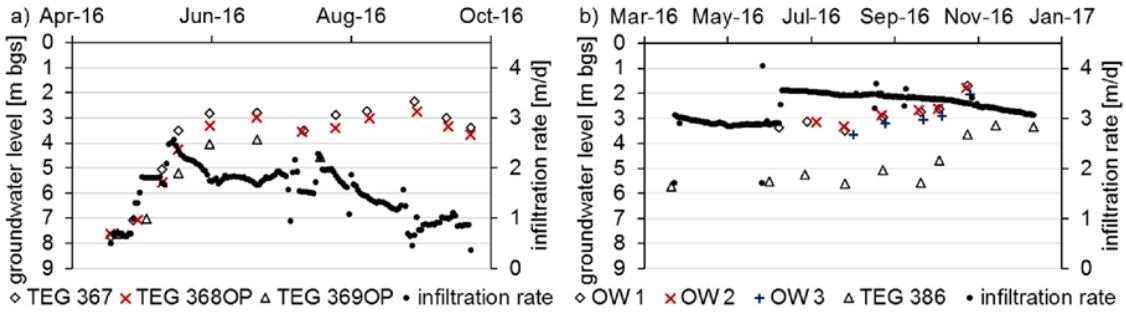

Figure 5-2: Infiltration rates and groundwater levels in the observation wells during the course of the study at (a) the cMAR site and (b) the SMART site.

5.3.2. Removal of bulk organic carbon

Measurements at the cMAR site revealed a continuously improved DOC removal during the start-up period (~6 weeks) and constant concentrations in the shallow groundwater were achieved until the end of the sampling campaign (Figure 5-3a). After a travel time of 0.49 days (200 cm of infiltration), an average of 2.1 ± 0.5 mg/L DOC were removed. The UVA_{254} values showed a similar trend resulting in a constant SUVA value throughout the first 200 cm of infiltration (2.1 ± 0.1 L/(mg·m)) indicating an equal utilization of aromatic and aliphatic organic compounds (Figure SI-5 4). Stable DOC concentrations of 4.6–5.2 mg/L were observed in the observation wells TEG 367, 368OP and 369OP, whereas the UVA_{254} values increased during longer travel time suggesting presence of a higher content of aromatic fractions within the organic matter in the deeper aquifer (SUVA [L/(mg·m)]: TEG 367/TEG 368OP = 2.3 ± 0.1; TEG 369OP = 2.6 ± 0.1). It can be hypothesized that this increase originates from mixing with older groundwater. However, the sampling campaign took approximately five months and therefore, the monitoring wells may not have been completely flashed with filtrate of the basin. Only 0.2 ± 0.2 mg/L DOC were removed during a travel time of 0.17 days (200 cm of infiltration) at the SMART site confirming the refractory character of the DOC in the bank filtrate of Lake Tegel (Figure 5-3b and Figure SI-5 4).

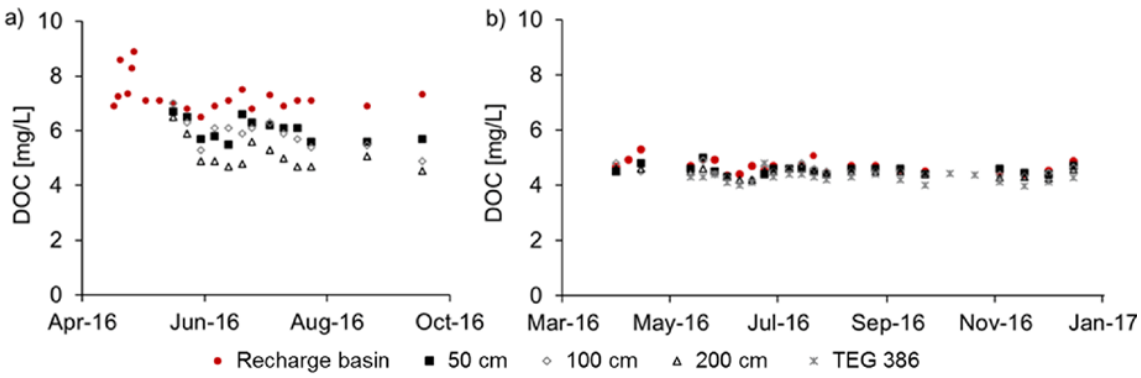

Figure 5-3: DOC concentrations in the recharge basins and groundwater during the course of the study at (a) the cMAR site and (b) the SMART site.

5.3.3. Redox conditions

At the cMAR site, the DO concentration dropped faster with depth compared to the SMART site, which is likely due to the presence of a higher amount of easily degradable DOC in the water of Lake Tegel (Figure 5-4). After a start-up of approximately 6 weeks the infiltration zone to a depth of 100 cm bgs (travel time: 0.25 days) was characterized by predominantly oxic redox conditions (DO >2 mg/L) whereas until a depth of 200 cm (travel time: 0.49 days) the DO concentration continued to decrease (DO = 1.4 ± 2.3 mg/L). Nevertheless, the DO values were highly variable during the infiltration at the cMAR site (Figure 5-4a). This may also be caused by instable operation (e.g. a pump failure resulted in decreased infiltration and oxygen intrusion into the subsurface). Suboxic redox conditions were observed in monitoring well TEG 367 characterized by low DO concentration (<1 mg/L) as well as a slight decrease of nitrate-N of 0.31 ± 0.03 mg/L (Figure SI-5 5). Despite the low DO concentrations at monitoring wells TEG 368OP and TEG 369OP, no additional nitrate reduction occurred confirming the refractory character of the DOC in the deeper aquifer. However, the nitrate concentration increased and exhibited the highest concentration in monitoring well TEG 369OP, which again may have resulted from mixing of younger with older groundwater in the well (Figure SI-5 5).

As illustrated in Figure 5-4b, the DO concentrations at the SMART site declined at infiltration depths of 50, 100 and 200 cm after an adaptation time of approximately 8 weeks, whereas the DO concentration measured in monitoring well TEG 386 remained constant at 0.4 ± 0.2 mg/L after 2.5 months. Oxic redox conditions (DO >2.5 mg/L) until a depth of 200 cm bgs (travel time: 0.17 days) were confirmed since no alternative electron acceptors such as nitrate, iron or manganese were consumed. However, after a travel time of approximately 11 days at monitoring well TEG 386, suboxic redox conditions (DO <1 mg/L) occurred (Figure SI-5 5). The presence of particular organic carbon (POC) in the deeper aquifer may have resulted in further oxygen depletion. Lower nitrate concentration at monitoring well TEG 386 compared to the suction sampler at 200 cm depth (ΔNO_3^--N = 0.15 ± 0.08 mg/L; Figure SI-5 5) confirms prevailing suboxic conditions based on the definition of distinct redox conditions by Regnery et al. (2015b). After travel to a depth of 50 cm bgs, iron and manganese concentrations were mostly below the LOQ at both field sites due to oxidation to (Fe(III)) and (Mn(IV)) during oxic infiltration, followed by precipitation and filtration in the top layer of the basin.

To sum up, oxic conditions during 200 cm bgs of infiltration were obtained at both field sites, cMAR (travel time: 0.49 days) and SMART (travel time: 0.17 days), whereas the DO concentrations at the SMART site were more stable compared to the cMAR site. Due to the relatively high content of easily degradable DOC in the Lake Tegel water, carbon-limited conditions (ΔDOC <1.0 mg/L) solely prevailed at the SMART site. Thus, favorable oxic and carbon-limited conditions for an enhanced TOrCs transformation were exclusively present at the SMART site.

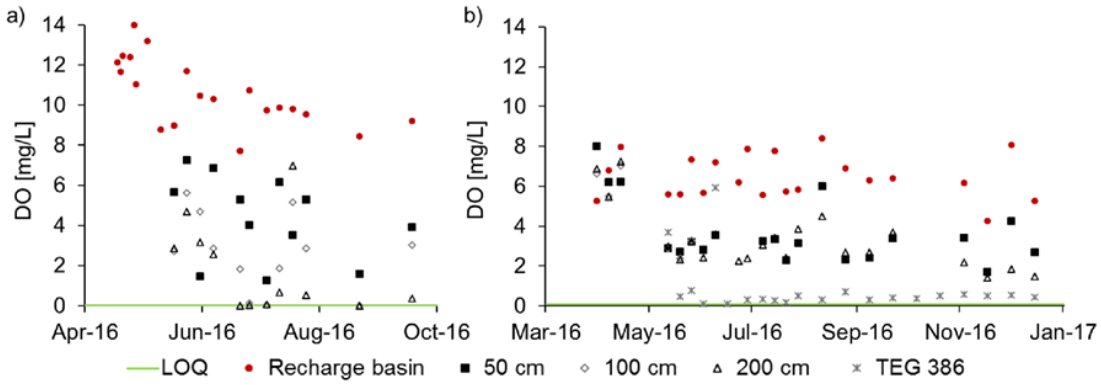

Figure 5-4: DO concentrations in the recharge basins and groundwater during the course of the study at (a) the cMAR site and (b) the SMART site.

5.3.4. Transformation of trace organic chemicals

5.3.4.1. Adaptation period

Out of the 22 analyzed compounds, 15 TOrCs were constantly detected above their LOQ in both feed waters (Table SI-5 1). Similar to the removal of bulk organic carbon and the observed depletion of DO, an adaptation phase resulting in steady improvement in removal of TOrC was observed in both systems. The adaptation for biotransformation was highly compound specific with acesulfame and metformin exhibiting the longest period of 2.5–3 months at the SMART site. Time resolved measurements of individual compounds in the infiltration basin and corresponding suction samplers at 50, 100 and 200 cm are shown in Figure SI-5 6 for the cMAR site and Figure SI-5 7 for the SMART site. A vertical line in the graphs indicates the assumed start of stable TOrCs concentration without further adaptation of microbial transformation after a travel time of 0.49 days at the cMAR site and 0.17 days at the SMART site, respectively. Following evaluation of removal rates is based on measurements after this date.

5.3.4.2. First-order removal rate constants

For a quantitative assessment of TOrC removal and to enable comparison with previous studies, first-order rate constants ƛ [d^{-1}] and half-lives were determined for the removal of individual TOrCs based on the estimated and determined travel times to a depth of 200 cm bgs at the cMAR and SMART sites (Table 5-2, Figure SI-5 8 and Figure SI-5 9). In addition, the R^2 value for the fit of the first-order decay model as well as the percentage removal at a depth of 200 cm bgs are given in Table 5-2. In accordance to Regnery et al. (2015b), the first-order decay model was considered acceptable for R^2 values larger than 0.63. Furthermore, first-order rate constants for compounds with <10% transformation were set to ƛ <0.01 d^{-1}.

Table 5-2: First-order removal rate constants ƛ [d^{-1}], half-lives $t_{1/2}$ [h], and percentage removal after 200 cm of infiltration of all quantified TOrCs at both field sites.

	cMAR site ($n \geq 6$)				SMART site ($n \geq 13$)			
TOrCs	ƛ [d^{-1}]	R^2	$t_{1/2}$ [h]	Removal [%]	ƛ [d^{-1}]	R^2	$t_{1/2}$ [h]	Removal [%]
Persistent behavior at both field sites								
Candesartan	<0.01	-	-	<10	<0.01	-	-	<10
Carbamazepine	<0.01	-	-	<10	<0.01	-	-	<10
Dihydroxydihydro-carbamazepine	<0.01	-	-	<10	<0.01	-	-	<10
Olmesartan	<0.01	-	-	<10	<0.01	-	-	<10
Oxypurinol	<0.01	-	-	<10	<0.01	-	-	<10
Phenylethyl-malonamide	<0.01	-	-	<10	<0.01	-	-	<10
Poor removal at either the cMAR or SMART site								
Primidone	1.24 ± 0.20	0.842	13.4	39 ± 35	<0.01	-	-	<10
Tolyltriazole	<0.01	-	-	<10	0.56 ± 0.05	0.937	29.6	10 ± 17
Efficient removal at both field sites								
Gabapentin-lactam	4.46 ± 0.43	0.980	3.7	89 ± 7	14.06 ± 1.23	0.990	1.2	94 ± 2
Metformin	3.03 ± 0.49	0.946	5.5	87 ± 4	6.90 ± 3.10	0.650	2.4	93 ± 5
Valsartan acid	4.64 ± 0.62	0.964	3.6	92 ± 7	11.53 ± 2.04	0.948	1.4	95 ± 4
Significantly better removal at the SMART site compared to the cMAR site								
Acesulfame	<0.01	-	-	<10	8.79 ± 3.36	0.754	1.9	93 ± 2
Benzotriazole	<0.01	-	-	<10	10.96 ± 0.49	0.996	1.5	83 ± 6
4-FAA	1.49 ± 0.30	0.880	11.2	62 ± 14	12.12 ± 1.76	0.959	1.4	78 ± 6
Gabapentin	0.36 ± 0.08	0.822	46.9	17 ± 10	4.94 ± 0.59	0.939	3.4	58 ± 13

Among the 15 compounds detected in feed waters, six TOrCs (i.e., candesartan, carbamazepine, dihydroxydihydrocarbamazepine olmesartan, oxypurinol, phenylethylmalonamide) exhibited a persistent behavior at both field sites with observed removal of less than 10% (ƛ <0.01 d^{-1}) after subsurface travel to a depth of 200 cm bgs. In addition, two compounds (primidone, tolyltriazole) were poorly removed (<50%) at both the cMAR or SMART sites. Persistent behavior in groundwater recharge systems under different environmental conditions is well documented for carbamazepine, primidone, phenylethylmalonamide, and oxypurinol (Drewes et al., 2003; Funke et al., 2015; Hass et al., 2012; Heberer et al., 2004; Massmann et al., 2006). In this study, primidone exhibited a removal up to 40% (200 cm infiltration) at the cMAR site, but initial concentrations close to the detection limit may also have caused some analytical inaccuracies. The persistent behavior of candesartan and olmesartan confirms previous laboratory-scale experiments mimicking a conventional bank filtration and SMART conditions (Hellauer et al., 2017). Reemtsma et al. (2010) reported inefficient removal of 4-Methylbenzotriazole during bank filtration in Berlin after a travel time of 120 days whereas 5-Methylbenzotriazole was sufficiently removed. Since both tolyltriazole isomers were not differentiated in this study, the observed removal of approximately 10% at the SMART site might be caused by specific transformation of the better degradable compound 5-Methylbenzotriazole.

Gabapentin-lactam, metformin and valsartan acid were transformed by more than 85% after travel to 200 cm bgs at both sites (travel time cMAR: 0.49 days; SMART: 0.17 days) with removal of gabapentin-lactam and metformin mostly below the LOQ (gabapentin-lactam: 0.01 µg/L; metformin: 0.02 µg/L). For all of these three compounds, the first-order

rate constants were at least twice as high in SMART compared to the conventional cMAR indicating a more efficient removal under stable oxic and carbon-limited conditions. The enhanced removal of valsartan acid in the SMART system confirms previous observations from laboratory-scale soil column experiments (Hellauer et al., 2017). Poor removal of valsartan acid under anoxic conditions was also observed during full-scale bank filtration (Nödler et al., 2013; van Baar, 2015). However, the fact that valsartan acid was also removed to concentrations close to the LOQ at the cMAR site, indicates better supply of DO in cMAR systems compared to conventionally operated bank filtration. Scheurer et al. (2012) reported an efficient degradation of metformin at trace concentrations during riverbank filtration or surface spreading from three full-scale waterworks in Germany. These results are in line with the efficient transformation of metformin below the LOQ in this study.

Based on a student *t*-test (unpaired, two sided), the removal of 4-Formylaminoantipyrine (4-FAA; $\alpha = 0.031$), acesulfame, benzotriazole, and gabapentin ($\alpha < 0.001$) was significantly enhanced during SMART compared to conventional cMAR. These results confirm data from preceding column experiments showing similar benefit of SMART operation for the compounds 4-FAA, benzotriazole and gabapentin (Hellauer et al., 2017). Efficient removal of 4-FAA was also observed in recharge systems using surface spreading (Massmann et al., 2006) and bank filtration (van Baar, 2015).

The most pronounced effects linked to stable oxic and carbon-limited conditions at the SMART site ($\lambda > 8\ d^{-1}$) were observed for the transformation of acesulfame and benzotriazole, both showing persistent behavior during conventional cMAR ($\lambda < 0.01\ d^{-1}$). While our previous column studies confirm highly redox sensitive transformation of benzotriazole (Hellauer et al., 2017), other studies also reported partial removal during bank filtration at Lake Tegel (Reemtsma et al., 2010). The high persistence of the artificial sweetener acesulfame at the cMAR site contradicts efficient degradation to concentrations below LOQ during initial, mostly anoxic infiltration in column experiments (Hellauer et al., 2017). These results, however, are in line with data from literature ranging from recalcitrant during soil-aquifer treatment with a residence time of more than 1.5 years (Scheurer et al., 2009) to rapid degradation in oxic and anoxic (denitrifying) activated sludge systems (Castronovo et al., 2017).

To further elucidate the efficiency of the SMART system regarding the transformation of moderately degradable TOrCs, determined first-order removal rate constants for acesulfame, benzotriazole, 4-FAA and tolyltriazole were compared with literature data in Figure 5-5. Burke et al. (2014) estimated first-order removal rate constants in laboratory-scale soil column experiments consisting of an undisturbed core from a riverbank filtration site at Lake Wannsee, Berlin, Germany at two different temperatures to simulate winter and summer conditions (6.5°C: oxic/penoxic; 19.7°C: oxic/penoxic/suboxic). Thereby, penoxic conditions referred to nearly oxic conditions as previously defined by Stuyfzand (1993). Regnery et al. (2015b) determined first-order removal rate constants for several TOrCs including acesulfame in controlled laboratory-scale soil column experiments under oxic and carbon-limited conditions. Removal rates reported by Burke et al. (2014) and Regnery et al. (2015b) confirm the observed high persistence of acesulfame, benzotriazole and tolyltriazole in conventional cMAR (Figure 5-5). Also removal rates for 4-FAA well

agree with literature data. However, data from Burke et al. (2014) indicate that improved removal of these substances is possible under specific conditions. Highest removal rates for all compounds except tolyltriazole, however, were observed with the SMART concept at fully oxic and carbon-limited conditions demonstrating the high potential of the sequential approach for biodegradation of moderately degradable TOrCs.

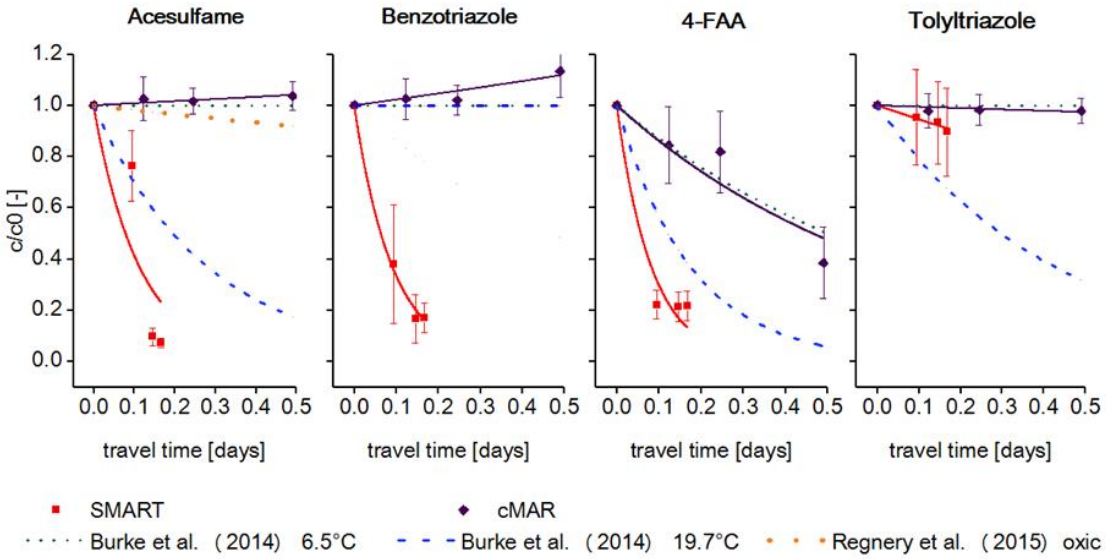

Figure 5-5: Comparison of first-order removal rate constants from the cMAR site and the SMART site with literature data (*n* ≥ 6).

5.3.4.3. TOrCs detected in groundwater monitoring wells

Concentrations of TOrCs in the groundwater monitoring wells are exemplarily shown for benzotriazole and metformin in Figure 5-6. Both compounds exhibited elevated concentrations in the monitoring wells compared to results from suction samplers. Also valsartan acid and primidone as well as the persistent TOrCs candesartan, carbamazepine, olmesartan, oxypurinol, and tolyltriazole were detected at higher concentrations in the observation wells at the cMAR site. Since TOrCs concentrations in the lake were continuously decreasing in the last months prior to experiments, mixing with older bank filtrate might have caused these effects.

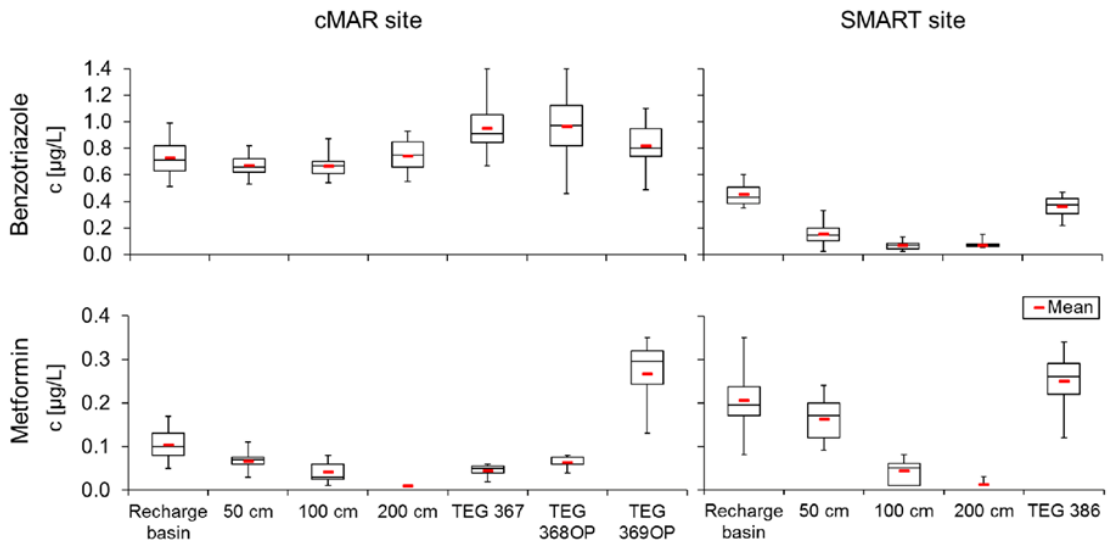

Figure 5-6: Removal of benzotriazole and metformin concentrations under adapted conditions at the cMAR site (left) and SMART site (right). Whiskers indicate the maximum and minimum concentrations observed and the horizontal line represents the median concentration (*n* ≥ 4).

5.4. Conclusions

The results of this study demonstrate the applicability of the SMART concept to enhance removal of trace organic chemicals under field-scale conditions. Re-aeration and subsequent infiltration of bank filtrate resulted in the constant establishment of oxic and carbon-limited conditions throughout 200 cm of infiltration in the shallow aquifer. Also, infiltration of lake water during conventional MAR using pond infiltration occurred at mainly oxic conditions, but availability of DO was less stable. In addition, availability of BDOC in the Lake Tegel water, which was removed by 2.1 ± 0.5 mg/L within 0.49 days (200 cm bgs) of infiltration, did not allow for establishment of favored carbon-limited conditions. Compared to conventional MAR using pond infiltration, the SMART concept performed equal or better regarding the removal of all biodegradable TOrCs. The compounds acesulfame and benzotriazole were removed by more than 80% at the SMART site after 0.17 days (200 cm bgs) of infiltration, whereas both compounds persisted in the conventional MAR system. In addition, the first-order removal rates of acesulfame, benzotriazole and 4-FAA at the SMART site were higher compared to reported values from literature emphasizing the potential to improve the transformation of moderately degradable TOrCs by optimizing prevailing conditions in natural treatment processes. However, further research is needed to prove long-term performance of trace organic chemical removal as well as infiltration rates at the SMART site. Due to precipitated iron, infiltration rates are expected to decrease over time. Accordingly, frequencies of cleaning and removal of the clogging layer need to be properly managed.

Acknowledgements

We would like to thank the Berliner Wasserbetriebe (BWB) and the German Federal Ministry for Research and Education (BMBF, grant number: 02WAV1404) for funding this study. We gratefully thank all involved persons, especially Dr. Uwe Dünnbier (BWB) for the analytical support, Dr. Sebastian Schimmelpfennig (BWB) for the operational support, implementation of the observation wells and organization of the tracer test as well as Dr. Hella Schwarzmüller (Kompetenzzentrum Wasser, Berlin) for the sampling of the observation wells. We also thank Claas Henning Lünsdorf, Leon Diehl, Annalena Schoppe and Birte Moser (Carl von Ossietzky University), Dr. Benjamin Gilfedder and Christian Jost (University of Bayreuth) for their help during the intensive tracer test sampling campaign and Fabian Thalmann (University of Applied Sciences Nordhausen), Mareike Harder, Maresa Kempin (Technical University of Berlin) and Jörn Frankenstein (BWB) for their help during operation and sampling at both field sites.

Hypothesis I that SMART can result in improved removal of potentially health relevant TOrCs compared to currently practiced MAR systems in Berlin could be confirmed.

6 Microbiome-triggered transformations of trace organic chemicals in the presence of effluent organic matter in managed aquifer recharge (MAR) systems

This chapter[10] is reprinted with permission from

Hellauer, K., Uhl, J., Lucio, M., Schmitt-Kopplin, P., Wibberg, D., Hübner, U., Drewes, J.E., 2018. Microbiome-Triggered Transformations of Trace Organic Chemicals in the Presence of Effluent Organic Matter in Managed Aquifer Recharge (MAR) Systems. *Environmental Science & Technology* 52 (24), 14342–14351.

Abstract

It is widely assumed that biodegradation of trace organic chemicals (TOrCs) in managed aquifer recharge (MAR) systems occurs via a cometabolic transformation with dissolved organic carbon serving as primary substrate. Hence, the composition facilitating bioavailability of the organic matter seems to have a great impact on TOrCs transformation in MAR systems. The aim of this study was to elucidate the character of effluent organic matter present in the feedwater of a simulated sequential MAR system throughout the infiltration by use of FT-ICR-MS analyses as well as spectroscopic methods. Furthermore, compositional changes were correlated with TOrCs targeted throughout the system as well as the abundance of different microbial phyla. On the basis of their behavior throughout the infiltration system in which different redox and substrate conditions prevailed, TOrCs were classified in four groups: easily degradable, redox insensitive, redox sensitive, and persistent. Masses correlating with persistent TOrCs were mainly comprised of CHNO-containing molecules but also of CHO which are known as carboxyl-rich alicyclic molecules, while CHOS and CHNOS can be neglected. Easily degradable TOrCs could be associated with CHNO-, CHO- and CHOS-containing compounds. However, a shift of molecular compounds to mostly CHOS was observed for redox-insensitive TOrCs. Three hundred thirty eight masses correlated with removal of redox-sensitive TOrCs, but no distinct clustering was identified.

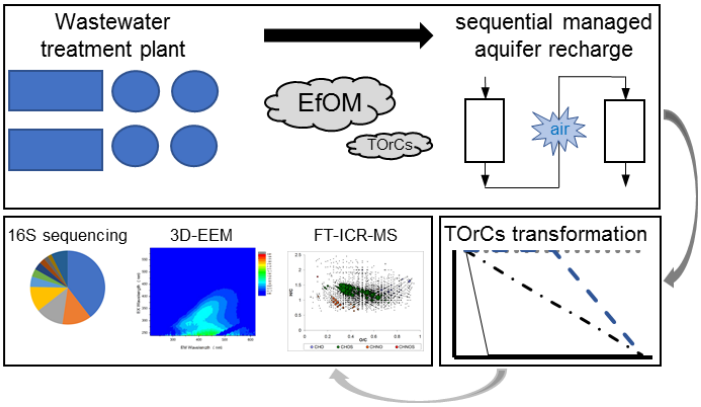

[10] This study was performed to test Hypothesis II that the fate of molecular components and characteristic functional groups of the primary substrate correlates with the degradation of structurally similar TOrCs.

6.1. Introduction

Trace organic chemicals (TOrCs) usually occur in wastewater treatment plants (WWTP) effluents as well as in the aquatic environment in a concentration range of nanograms to micrograms per liter (ng-µg/L), whereas the concentration of the dissolved organic carbon (DOC) is orders of magnitude higher, typically at several milligrams per liter (mg/L) (Grünheid et al., 2005; Hellauer et al., 2018a; Müller et al., 2017; Rauch-Williams et al., 2010). It is widely assumed that ambient concentrations of TOrCs are not sufficient to support microbial growth (Tran et al., 2013). Thus, additional organic matter or DOC is needed as a primary growth substrate (Tran et al., 2013). This transformation of rarely available substrates without any direct benefit to bacteria in the presence of growth-supporting substrates is known as cometabolism (Dalton et al., 1982). Recent studies indicated that the removal of TOrCs in the natural environment or engineered biological treatment systems commonly follows such cometabolic mechanisms (Alidina et al., 2014a; Tang et al., 2017). A key parameter for cometabolic transformation of TOrCs is the availability of biodegradable DOC (BDOC) as primary substrate, with respect to both its quality and its quantity (Alidina et al., 2014b; Rauch-Williams et al., 2010). Previous studies revealed that both the composition and the concentration of BDOC affect the total amount of biomass and the structure of the microbial community (Li et al., 2012; Li et al., 2013; Rauch-Williams and Drewes, 2006) as well as their functionality (Drewes et al., 2014) and, therefore, TOrCs removal (Alidina et al., 2014b). It is well established that the transformation of TOrCs is enhanced under carbon-limited conditions (Drewes et al., 2014; Hellauer et al., 2018a; Regnery et al., 2015b). Primary substrate comprised of refractory organic compounds, such as humic acid like organic matter, led to an increased TOrCs removal compared to systems using a high fraction of easily degradable compounds like peptone/yeast (Alidina et al., 2014b; Drewes et al., 2014). However, it still remains unclear which functional characteristics of the natural organic matter serving as primary substrate determine the efficacy of TOrCs biotransformation. To unravel the composition of the dissolved organic matter (DOM), several analytical tools were previously applied (Leenheer et al., 2000; Minor et al., 2014). DOM can be separated based on operationally defined polarity gradients using XAD-resins fractionation or according to its size using size-exclusion chromatography (Drewes et al., 2006; Drewes and Croue, 2002). Furthermore, spectroscopic methods like UV absorbance at 254 nm (UVA_{254}) and 3D fluorescence (3D EEM) were widely used (Baghoth et al., 2011; Li et al., 2014b; Murphy et al., 2010). However, applied alone these approaches have the disadvantage of deciphering only chromophoric DOM (Minor et al., 2014). In addition, analytical tools allowing for the assignment of functional groups, compound classes, and molecular formulas were commonly applied (Minor et al., 2014). This includes Fourier transform infrared (FT-IR) and nuclear magnetic resonance (NMR) spectroscopy (Drewes et al., 2006; Drewes and Croue, 2002; Minor et al., 2014) as well as more recently Fourier transform ion cyclotron resonance mass spectrometry (FT-ICR-MS) (Gonsior et al., 2011; Lavonen et al., 2015; Minor et al., 2014). Because of its high resolution and mass accuracy, FT-ICR-MS has a great capability to unravel the molecular complexity of DOM and is suitable for assigning molecular formulas for complex structures (Hertkorn et al., 2007; Stenson et al., 2003).

The aim of this study was to decipher the composition of effluent organic matter (EfOM) potentially serving as primary substrate in a simulated sequential managed aquifer recharge (MAR) system using FT-ICR-MS and spectroscopic methods and to correlate potential changes throughout the infiltration with the transformation of selected TOrCs as well as the abundance of microbial phyla. The sequential MAR technology (SMART) is defined as a combination of two infiltration steps in series with an intermediate aeration step to establish highly controlled oxic and carbon-limited conditions in the second infiltration system which are favorable for the removal of many TOrCs (Regnery et al., 2016).

6.2. Material and methods

6.2.1. Laboratory-scale column experiment

The laboratory-scale column experiment consisted of two sequential infiltration systems operated in downward flow direction under fully saturated conditions (Figure 6-1) for a period of approximately 8 months. Tertiary-treated effluent of the WWTP in Garching, Germany, was continuously fed into the first column. The influent to the system was stored at ~4°C and filled up twice a week without an additional spike of TOrCs due to their immediate presence in the tertiary-treated wastewater. Prior to sampling within this study, the column system was continuously operated with tertiary-treated WWTP effluent for more than 6 months. Both systems were connected with an intermediate aeration step using pressurized air to simulate SMART and therefore providing a series of different redox conditions and substrate availability. The columns of the first infiltration system (B01, B02; height (*h*) 50 cm, inner diameter (i.d.) 14 cm) were filled with technical sand (grain size ranged from 0.2 to 1.0 mm; Euroquarz GmbH, Germany) and the columns of the second infiltration system (b1-b4; *h* 30 cm, i.d. 9 cm) with aquifer material (d_{50} = 0.8 mm, f_{oc} = 0.003%), which was taken from from previous column experiments that were continuously operated for more than 5 years (Rauch-Williams et al., 2010; Regnery et al., 2015b). Flow rates of 60 (B01, B02) and 30 mL/h (b1-b4) resulted in a hydraulic retention time (HRT) of 2.1 or 0.9 days/column, respectively, an overall HRT of 7.8 days. The HRT was determined based on the C-peak method (Schudel et al., 2002) using the conservative tracer potassium bromide (data not shown). Columns were composed of poly(methyl methacrylate) and could be opened on top for soil sampling. All columns were equipped with oxygen sensor spots (SP-PSt3, PreSens, Germany) for noninvasive oxygen measurements along the length of the columns. Water samples to characterize the bulk organic carbon (DOC; UVA_{254}, 3D-EEM, FT-ICR-MS) and prevailing redox conditions (dissolved oxygen (DO); ammonium- and nitrate-nitrogen) as well as for quantifying TOrCs were taken (bi)weekly in the influent (0.0 days) and in the effluent of each column with respect to the HRT (2.1, 4.2, 5.1, 6.0, 6.9, and 7.8 days).

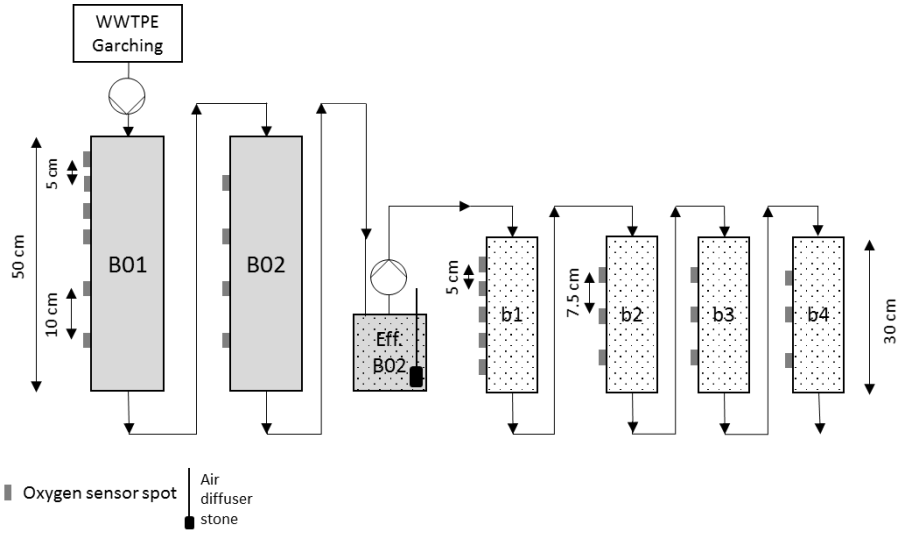

Figure 6-1: Laboratory-scale column experiment consisting of two infiltration steps (system 1, gray, columns B01, B02; system 2, patterned, columns b1-b4) operated in series with an intermediate aeration (Eff. B02, gray patterned). System was fed with effluent of the WWTP Garching, Germany (WWTPE), with a flow rate of 60 (system 1) and 30 mL/h (system 2).

6.2.2. Analytics

6.2.2.1. Sampling

Soil samples for 16S rRNA amplicon sequencing were collected once, approximately 1.5 months after the initial start of the experiment, from the top of each column. Water samples for bulk organic carbon and redox characterization as well as for TOrCs quantification were collected in 200 mL amber bottles and filtered through 0.45 µm with cellulose-nitrate filters (Sartorius AG, Germany). To characterize the EfOM, > 50 mL of sample was filtered (Whatman GF/F filter, Germany) followed by acidification to pH 2 using hydrochloric acid (32%, Merck KGaA, Germany) and stored at 4 °C pending further analysis.

6.2.2.2. DNA extraction and 16S rRNA amplicon sequencing

DNA was extracted in triplicate by use of the PowerSoil DNA Isolation Kit (MO BIO Laboratories, USA) according to the manufacturer's guidelines with the following exceptions: (i) 1.0 g of soil was used as starting material, (ii) a FastPrep-24 cell disrupter (MP Biomedicals, USA) was used at 6 m/s for 40 s for disruption of the cells. The eluted DNA was pooled prior to downstream analyses. To increase the purity of each DNA extract, the Genomic DNA Clean & Concentrator Kit (Zymo Research Europe, Germany) was used with an input of 100 µL of sample and 200 µL of binding buffer. Illumina library preparation was operated following the 16S Metagenomic Library Preparation workflow (15044223 Rev. B; Illumina, USA) targeting the V3 and V4 regions using a Nextera XT Index Kit (Illumina, USA) for indexing as previously described by Engel et al. (2018). Flash v.1.2.11 (Magoč and Salzberg, 2011) was used to merge MiSeq forward and reverse paired end reads with a maximum overlap of 300 bp. All merged reads were combined to a single file and further processed using USEARCH v9.2.61 (Edgar, 2010) as provided in the supporting information (SI Chapter 6: Microbiome-triggered transformations of trace organic chemicals in the presence of effluent organic matter in managed aquifer recharge

(MAR) systems). Taxonomy assignment of identified operational taxonomic units (OTUs) was obtained by use of Ribosomal Database Project (RDP) classifier (Wang et al., 2007).

6.2.2.3. Bulk organic carbon and redox parameters

For the DOC analysis, samples were acidified with hydrochloric acid to a pH of 2 and stored at 4 °C prior to the measurement in triplicate using a Vario TOC CUBE analyzer (Elementar, Germany). UVA_{254} was photometrically determined in duplicate using a BioSpec UV-1601 (Shimadzu Europa GmbH, Germany). As the ratio of UVA_{254} and the DOC the specific UV absorbance ($SUVA_{254}$) was calculated which could be used as a parameter representing the aromatic content of the DOC (Weishaar et al., 2003). To avoid quenching effects of the fluorescence signal, all samples with a DOC > 2 mg/L were diluted to 2 mg/L with ultrapure water prior to 3D fluorescence spectroscopy (Stahlschmidt et al., 2016) using a Aqualog fluorescence spectrometer (Horiba Scientific, USA). More information about the 3D fluorescence spectroscopy measurements are provided in the SI. The dissolved oxygen (DO) concentration was monitored with the Fibox 4.0 (PreSens, Germany) by use of the oxygen sensor spots within the columns as well as flow-through cells (FTC-PSt3, PreSens, Germany) in the influent and the effluents of each column (detection limit = 0.015 mg/L). Hach cuvette tests LCK304 (0.015–2.0 mg/L NH_4^+-N) and LCK340 (5–35 mg/L NO_3^--N) (HACH Lange GmbH, Germany) were used to determine the concentration of ammonium- and nitrate-nitrogen, respectively.

6.2.2.4. TOrCs quantification

Liquid chromatography coupled with tandem mass spectrometry (LC-MS/MS) was used to quantify TOrCs (Müller et al., 2017). Measurements were performed in positive electrospray ionization mode. All investigated TOrCs and their corresponding limits of quantification (LOQ) are listed in Table 6-1. If a measured TOrC concentration was lower than the stated LOQ, the detected value was set as one-half of the LOQ for further calculations.

6.2.2.5. FT-ICR-MS analysis

Prior to FT-ICR-MS, a solid-phase extraction (SPE) was performed as previously described by Dittmar et al. (2008). Therefore, 50 mL of each sample was extracted with 5 mL of methanol (LC-MS ChromasolV, Sigma-Aldrich, Germany) using PPL cartridges (Bond Elut PPL, 1 g, 3 mL; Agilent, USA) followed by a dilution of 1:50 (v/v %) with methanol. The analysis was conducted on a solariX FT-ICR-MS (Bruker Daltonik GmbH, Germany) equipped with a 12 T superconducting magnet (Magnex Scientific Inc., GB) and an APOLLO II electrospray ionization (ESI) source (Bruker Daltonik GmbH, Germany) in the negative ionization mode. Further information about mass spectra acquisition is provided in the SI. To elucidate masses, which were assigned to molecular formulas based on the elements ^{1}H, ^{12}C, ^{16}O, ^{14}N, and ^{34}S, van Krevelen diagrams (Kim et al., 2003) are used representing masses by means of their hydrogen to carbon (H/C) and oxygen to carbon (O/C) ratios. Molecules comprised of the elements H, C, and O are referred to as CHO in the following. The same counts for CHNO, CHOS, as well as CHNOS.

6.2.3. Statistical analyses

6.2.3.1. Parallel factor analysis (PARAFAC)

PARAFAC is a statistical method, which is often applied to identify and quantify components of 3D fluorescence spectroscopy data (Murphy et al., 2013). Therefore, normalized 3D-EEM data were exported with adjusted excitation wavelengths of 239-599 nm from the Aqualog software and further processed using the SOLO software (Eigenvector Research Inc., USA) (Stahlschmidt et al., 2016). Details of the PARAFAC analysis are given in the SI.

6.2.3.2. Multivariate analyses

Multiple coinertia analysis (MCIA) as well as orthogonal partial least-squares (OPLS) regression were used in order to describe the correlation between the masses extracted by use of FT-ICR-MS, the microbiome in terms of OTUs identified by applying 16S rRNA amplicon sequencing, and in the case of OPLS metadata (Table SI-6 2). For the correlation of masses (and metadata) with the microbiome, the OTUs from the top of the first column (B01) were assigned to the system′s influent B0 and OTUs from the top of each of the following columns (B02, b1-b4) were equalized to the effluent of its previous column (B01, B02-b3). Since no distinct differences in microbial community diversity in deeper sediments were observed (Li et al., 2013), OTUs from the top of column b4 were not only accorded to effluent b3 but also to the final effluent of the system. Prior to analyses, all data (masses, microbiome, and metadata) were stored in one matrix and a unit variance (UV) scaling was applied. The MCIA was calculated with the purpose of integrating the two different data sets: masses and OTUs. Therefore, the MixOmics package (RStudio Version 1.0.136, 2009-2016; RStudio, Inc, USA) was used. In order to describe the relation that links the metadata to the masses together with the OTUs an OPLS was calculated in SIMCA (Version 13.0.3.0; Umetrics, Umeå, Sweden). Therefore, a logarithmic transformation was applied, and the final model was built only with the significant metadata ($p < 0.05$). The model's goodness of fit was tested by the p values calculated with the CV-ANOVA (Cross Validation ANOVA). The procedure to select masses and OTUs, which were most relevant to describe the experimental design, followed the method previously described in Adrian et al. (2017).

6.3. Results and discussion

6.3.1. Long-term column characterization of column systems

6.3.1.1. Bulk organic and redox parameters

The initial DOC concentration of 7.6 ± 1.9 mg/L was reduced to 4.6 ± 0.9 mg/L within the first 4.2 days of infiltration with the majority of removal occurring within the first column (Figure 6-2). After reaeration, the DOC was further depleted in the second infiltration system resulting in a final concentration of 3.6 ± 0.6 mg/L after 7.8 days. A significant increase of $SUVA_{254}$ in the first system (student′s t-test, two-tailed, paired, $\alpha < 0.05$) indicates a preferred removal of easily degradable aliphatic structures changing the character of the DOC to more aromatic. No significant change in $SUVA_{254}$ was observed

after reaeration (Figure 6-2). Results of UVA_{254} measurements are presented in Figure SI-6 1.

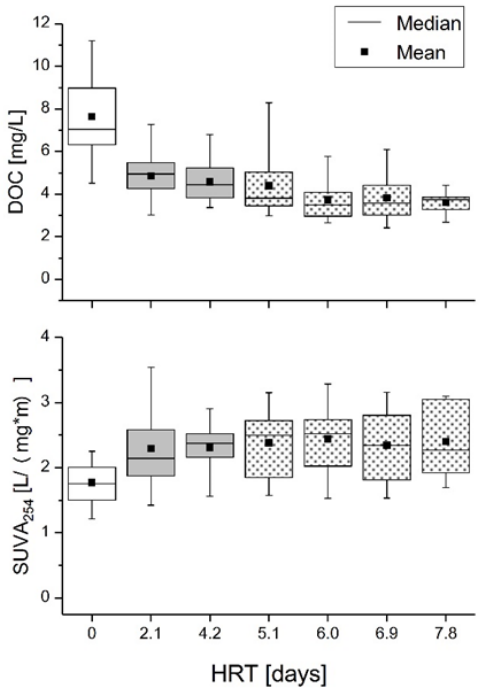

Figure 6-2: DOC concentration ($n \geq 12$) and $SUVA_{254}$ ($n \geq 11$) throughout the system with respect to the HRT. Box represents the 25–75 percentiles; whiskers indicate the maximum and minimum values.

On the basis of the 3D fluorescence measurements and the subsequent PARAFAC analysis, two characteristic components were identified (Figure SI-6 2). The accuracy of the PARAFAC model was confirmed by (i) a core consistency of 100%, (ii) 98% total variance explained, and (iii) 99% as a result of the split half analysis. The first component had a maximum fluorescence intensity at 239/451 nm ($\lambda_{Ex}/\lambda_{Em}$) and the second component at 239/376 nm, respectively. On the basis of previously published studies, Chen et al. (2003) classified five characteristic regions for organic compounds. Following this approach, component 1 was assigned to region III, fulvic acid-like substances, and component 2 to region II, aromatic protein II (tryptophan-like substances). The intensity of these two components decreased throughout the infiltration, while a strong decline was observed in the first column. This is in accordance to the removal of DOC and the reduction of UVA_{254}, which were also mainly removed or rather declined during the first 2 days. After reaeration, a further decrease of both components was detected in the second infiltration system showing a similar trend as the UVA_{254} measurements (cf. Figure SI-6 1 and Figure SI-6 3). Due to the high amount of easily degradable DOC in the influent, the oxygen ($DO_{Influent}$ = 5.9 ± 1.0 mg/L) was rapidly consumed during subsurface treatment (Figure SI-6 4). In addition, NO_3^--N concentration decreased insignificantly from 13.3 ± 2.4 mg/L to 12.0 ± 2.2 mg/L, indicating the prevalence of suboxic to anoxic conditions within 4.2 days of infiltration. An electron balance assuming an average oxidation number of zero for organic carbon resulted in a consumption of 2.2 mg/L DOC from influent oxygen (2.7 mg O_2/mg C). A decrease of NO_3^--N by 0.7 mg/L could be further explained due to the oxidation of 0.8 mg/L DOC to CO_2 (0.9 mg N/mg C), which confirms prevailing anoxic conditions in the first infiltration system. After reaeration, the DO immediately decreased within the first centimeters of infiltration which could not solely be explained by residues of easily degradable DOC in the influent to the second system. Therefore, redox conditions changed from oxic (DO (5.1 days) = 1.1 ± 1.3 mg/L) to suboxic defined by DO < 1.0 mg/L and ΔNO_3^--N < 0.5 mg/L (Regnery et al., 2015b). Ammonium (NH_4^+-$N_{Influent}$ = 0.10 ± 0.12 mg/L) was removed mainly below the LOQ (0.015 mg/L) after the first 2 days of infiltration (data not shown).

6.3.1.2. Trace organic chemicals

TOrCs were classified into four groups based on their behavior throughout the system (Table 6-1), namely (i) persistent compounds exhibiting less than 10% removal throughout the system, (ii) easily degradable compounds being removed below LOQ within 4.2 days, even under anoxic redox conditions, (iii) redox-insensitive compounds exhibiting removal in both systems before and after aeration, and (iv) redox-sensitive compounds being persistent in the first infiltration system (4.2 days) but efficiently transformed after reaeration. Relative removal of all targeted TOrCs throughout the system are given in Figure SI-6 5. Since limited contribution of sorption has been reported previously for similar column systems after long-term operation by Alidina et al. (2014b), biotransformation can be assumed as major mechanism for TOrCs removal in this study.

Table 6-1: List of TOrCs investigated during this study ($n \geq 7$)

TOrCs	LOQ [ng/L][a]	molecular formula	log *P* (log *D* pH 7.4)[d]	c_0 [ng/L]	removal [%] 4.2 days	removal [%] 7.8 days
persistent (≤10% after 7.8 days)						
carbamazepine	10; 5	$C_{15}H_{12}N_2O$	2.77 (2.77)	393 ± 98	<10	<10
primidone	25; 25	$C_{12}H_{14}N_2O_2$	1.12 (1.12)	72 ± 26	<10	<10
easily degradable (removal below LOQ within 4.2 days)						
citalopram[b]	5; 5	$C_{20}H_{21}FN_2O$	3.76 (1.41)	154 ± 48	>98	-
redox-insensitive (continuous removal within 7.8 days)						
climbazole[c]	5; 5	$C_{15}H_{17}ClN_2O_2$	4.34 (4.30)	111 ± 35	78 ± 21	>98
metoprolol[c]	2.5; 2.5	$C_{15}H_{25}NO_3$	1.76 (-0.47)	309 ± 104	80 ± 16	>99
diclofenac	25; 5	$C_{14}H_{11}Cl_2NO_2$	4.26 (1.10)	1326 ± 534	47 ± 19	94 ± 5
gabapentin	10; 2.5	$C_9H_{17}NO_2$	-1.27 (-1.27)	2246 ± 727	58 ± 15	92 ± 4
sotalol[c]	5; 5	$C_{12}H_{20}N_2O_3S$	-0.40 (-2.12)	41 ± 41	65 ± 46	>95
sulfamethoxazole	10; 5	$C_{10}H_{11}N_3O_3S$	0.79 (0.00)	131 ± 72	29 ± 41	55 ± 36
redox-sensitive (persistent in first infiltration system, removal after reaeration)						
benzotriazole	50; 50	$C_6H_5N_3$	1.30 (1.28)	4302 ± 1187	<10	35 ± 33
tramadol	5; 5	$C_{16}H_{25}NO_2$	2.45 (0.62)	265 ± 66	<10	71 ± 17
venlafaxine[c]	2.5; 2.5	$C_{17}H_{27}NO_2$	2.74 (1.22)	343 ± 74	<10	>99

[a]The LOQ was adjusted during the experimental period: the first number gives the LOQ of the first 5 months, the second number of the last 2 months of operation. [b]Removed <LOQ after 2.1 days of infiltration for most samples. [c]Removed <LOQ after 7.8 days of infiltration for most samples. [d]Calculated by use of Chemicalize (https://chemicalize.com/; accessed on 13.10.2018) developed by ChemAxon (http://www.chemaxon.com).

The persistent behavior of carbamazepine and primidone in MAR systems is well documented from field- as well as laboratory-scale investigations (Clara et al., 2004; Hass et al., 2012; Hellauer et al., 2017; Hellauer et al., 2018a). Removal up to 70% of citalopram in a carbon-rich environment has recently been shown from batch experiments using activated sludge (Beretsou et al., 2016). Climbazole as well as metoprolol were removed >75% even under anoxic redox conditions within 4.2 days of infiltration. A removal of >75% (HRT ≈ 12 days) under anoxic redox conditions for metoprolol was also observed in laboratory-scale column experiments (Hellauer et al., 2017). Muntau et al. (2017) reported a removal below the LOQ (5 ng/L) via soil-aquifer treatment (HRT < 1 day) for climbazole, confirming the results of this study. Diclofenac, gabapentin, and sotalol were removed <70% in the first but >90% in total after 7.8 days of infiltration. However, for sotalol 7 out of 22 measured influent concentrations were below the LOQ, and therefore, due to the low influent concentrations, further discussions about its removal efficiency are not expedient. Diclofenac is known to be biodegradable in MAR systems and particularly under oxic and

carbon-limited conditions (Hellauer et al., 2017; Regnery et al., 2015b; Regnery et al., 2016). In addition, a significantly enhanced transformation using the SMART approach in comparison to a conventional MAR treatment was previously reported for gabapentin (Hellauer et al., 2018a). In the case of the antibiotic drug sulfamethoxazole, moderate to poor transformations of approximately 30% were detected after 4.2 days and approximately 55% after 7.8 days of infiltration. In the literature, several studies focusing on sulfamethoxazole and its behavior in MAR systems are reporting ranges of biotransformation from partially and slowly removable during bank filtration and artificial recharge (Grünheid et al., 2005) to resistant to microbial biotransformation in a pilot-scale riverbank filtration system (Benotti et al., 2012). Three out of 12 investigated TOrCs, namely, benzotriazole, tramadol, and venlafaxine, persisted in the first infiltration system under mostly anoxic redox conditions but were transformed throughout the system at approximately 35% (benzotriazole), 70% (tramadol), and below the LOQ (venlafaxine) after reaeration with air under prevailing oxic to suboxic redox conditions. The high redox sensitivity and favored degradation under carbon-limited conditions were previously reported for benzotriazole (Hellauer et al., 2017; Hellauer et al., 2018a; Müller et al., 2017). However, removal up to 35% is not very efficient, and therefore, it is postulated that oxic to suboxic redox conditions are not sufficient. Tramadol was not degraded in the first 0.9 days after reaeration; however, interestingly, a steady transformation up to approximately 70% could be detected from 5.1 to 7.8 days of infiltration. It seems that the HRT had a significant influence on tramadol removal as it was previously shown to be persistent in a single stage as well as a sequential biofiltration system with an empty bed contact time of 290 to 2090 min (Müller et al., 2017). A transformation of >99% after reaeration was observed for venlafaxine emphasizing the benefit of predominant oxic and carbon-limited conditions for its removal. Previous results on venlafaxine degradation varied from persistent behavior in a single stage as well as sequential biofiltration (Müller et al., 2017) to degradation of >50% even under anoxic redox conditions (Hellauer et al., 2017). However, removal seemed most efficient under oxic conditions (Hellauer et al., 2017).

6.3.2. Microbial community structure

The microbiome was elucidated throughout the system based on 16S rRNA amplicon sequencing resulting in a median sequencing depth of approximately 60 000 reads. On the basis of this analysis, the most dominant phyla were *Proteobacteria* (40-48%), *Planctomycetes* (5–13%), *Acidobacteria* (12–22%), and *Bacteroidetes* (1-11%) (Figure SI-6 6). This is confirming previous studies reporting that these organisms are, among others, highly abundant in soil (Janssen, 2006). *Proteobacteria* were detected in all depths with the strongest contribution to the overall microbial community structure. Whereas in the top of the first column *α-* and *γ-Proteobacteria* dominated, after 6 days of infiltration *β-Proteobacteria* mainly occurred. *Planctomycetes* as well as *Bacteroidetes* were also enriched in the shallow sediments, and in contrast, *Acidobacteria* and *Nitrospirae* primarily prevailed in the second system characterized by carbon-limited (ΔDOC = 1.1 ± 1.2 mg/L) and oxic (DO > 1 mg/L) to suboxic (DO < 1 mg/L; ΔNO_3^--N < 0.5 mg/L) conditions. This characterization focused at the phyla and class level in order to provide a general overview of the microbial community structure in MAR systems.

6.3.3. Characterization of effluent organic matter (EfOM)

On the basis of the (-)ESI FT-ICR-MS measurements, masses were mainly detected up to 600 *m/z* with a resolution of >450 000 at 320 *m/z*. The EfOM was characterized by more than 1000 CHNO-containing molecules and a lower number (n = 572) of masses assigned to CHOS molecular composition with approximately 20 high-intensity signals (Figure 6-3). The high number of nitrogen-containing compounds could be linked to the peak of protein-like substances identified by the 3D fluorescence measurements (Figure SI-6 2), which are known to be specific for EfOM in comparison to natural organic matter (NOM) (Drewes et al., 2006; Nam and Amy, 2008). CHNO-containing molecules assigned to proteins and lignin-like substances from WWTP effluents have been identified previously (Maizel and Remucal, 2017). However, based on compound classes and their location within van Krevelen plots (Sleighter and Hatcher, 2007) the most intense signals of CHNO-containing molecules were in the area of lignin-like substances, and only a few masses were detected in the area of proteins. Molecules containing a sulfur atom (CHOS) were previously shown to be dominant in EfOM, which could partly be attributed to NOM reaction products of sulforeduction and substances from anthropogenic origin like anionic surfactants such as linear alkyl benzenesulfonates and their transformation products (Gonsior et al., 2011; Tseng et al., 2013). Well-known surfactants, which may be present in water and wastewater (Gonsior et al., 2011; Terrabase Inc.), are plotted in Figure SI-6 7, and those which were detected in the EfOM of this study are highlighted. The most detected masses in EfOM could be assigned to transformation products of surfactants pointing to a highly efficient removal of surfactants in the WWTP Garching. Throughout the infiltration, the relative abundance of masses assigned to CHO-containing molecules increased and a decrease of molecules comprised of CHNOS was observed (Figure SI-6 8 and Figure SI-6 9). However, even if shifts regarding the number of molecular formulas comprised of different elements were observed, the general pattern of elemental compositions elucidated from van Krevelen plots did not clearly change, showing that only a small fraction of the EfOM was affected by the process.

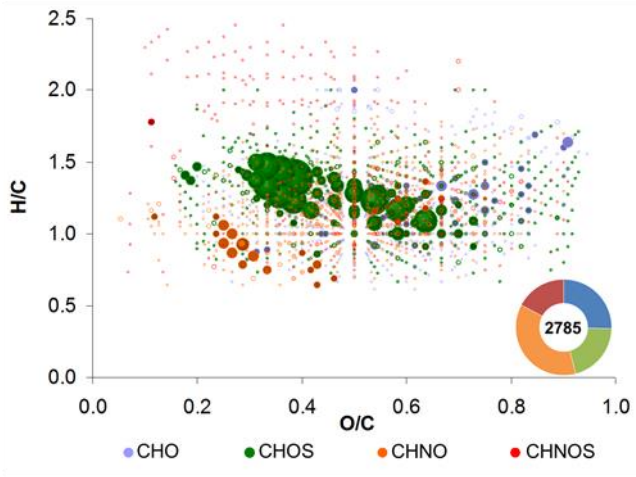

Figure 6-3: Van Krevelen plot of the effluent organic matter (EfOM) measured in column feedwater showing the H/C and O/C ratios of each mass assigned to a specific elemental composition (CHO, CHNO, CHOS, CHNOS). Bubble sizes depict the absolute intensity of each mass.

6.3.4. Fate of the EfOM and correlation with microbial community

6.3.4.1. Multiple coinertia analysis (MCIA)

To elucidate the coinertia between two data sets, masses assigned using FT-ICR-MS and OTUs identified via 16S rRNA amplicon sequencing, a MCIA was performed. Thereby, the influence of the organic matter on the microbial community composition at the phyla level could be revealed. A distinct separation between the influent and the first and the second infiltration system was shown by a clear clustering of masses and OTUs (Figure 6-4). Masses which could be detected throughout the system or even increased in the second infiltration system are further assigned as persistent (Figure SI-6 10, persistent). More than 50% of these persistent masses were composed of CHO-containing molecules, followed by CHNO (34%) and only some CHOS and CHNOS compounds. CHO- and CHNO-containing molecules seem to be more resistant against microbial degradation than molecules containing sulfur atoms. On the basis of the van Krevelen diagram of such persistent CHO-containing molecules, compounds could be designated as carboxyl-rich alicyclic molecules (CRAM), which are known as highly abundant and refractory dissolved organic matter (Hertkorn et al., 2006). Furthermore, the regions in van Krevelen diagrams in which persistent CHO- and CHNO-containing molecules were observed are characteristic for lignin- and tannin-like substances (Sleighter and Hatcher, 2007). Some of the high-intensity CHOS peaks could be assigned to biodegradation intermediates of dialkylltetralin sulfonates, and additionally, persistent compounds comprised of C, H, O, and S were also located in the region of lignins. These refractory substances have previously been found in soils and sediments (Derenne and Largeau, 2001) but also in WWTP effluents (Mesfioui et al., 2012). Hence, the persistent backbone after natural treatment seems to share similarities with organic matter found in the environment regarding elemental compositions which confirms results of a study previously performed by Drewes et al. (2006). Masses which were generally detected in the influent but with less intense signals in different effluents throughout the system (Figure 6-4, Influent B0; Figure SI-6 10:, easily degradable to redox insensitive) were characterized by a large proportion of sulfur-containing molecules (CHOS). Three of the most intense signals (H/C ≈ 0.3-0.4) were derived from sulfophenyl carboxylate compounds, also known as degradation products of linear alkylbenzenesulfonates (Riu et al., 1999). CHNO and CHO appeared similarly abundant, while the most intense signals of CHNO were obtained in the region of lignin-like substances, but CHO in the area of proteins and cellulose. Masses of the third group representing molecules, which had the highest intensities in the effluents of columns B01 and B02 coupled with efficient removal in the second system were strongly dominated by sulfur-containing compounds (Figure 6-4, B01, B02; Figure SI-6 10, redox sensitive). The relative contribution of CHNO remained constant in comparison to easily degradable and redox-insensitive compounds, CHNOS slightly increased, but the number of CHO became negligible. Hence, we assume compounds comprised of C, H, and O do not respond to changing redox conditions, whereby CHOS-containing molecules seemed to be sensitive with respect to oxygen availability in MAR systems.

Microbial taxa such as *Acidobacteria, Proteobacteria (α-, ß-, γ-Proteobacteria), Planctomycetes,* and *Verrucomicrobia* were dominant (relative abundance > 1%) in all three groups obtained by elaborating MCIA (Figure 6-4). This suggests that these phyla

do not essentially need specific growth substrates in MAR as they grow with any carbon source as primary substrate available within the system. *Bacteroidetes*, *Chloroflexi*, but also *Candidatus Saccharibacteria* and *candidate division WPS-1* were primarily correlated with masses showing an immediate removal in the first infiltration system which may indicate that those bacterial phyla prefer easily degradable organic matter as growth substrate. *Firmicutes* had a relative abundance of >1% within the cluster of persistent masses or those which have an increased intensity in the second system, but they were less abundant (<1%) in the other two groups (easily degradable/redox insensitive and redox sensitive). Thus, the majority of species belonging to *Firmicutes* seem to preferentially settle in MAR systems if the organic matter is characterized by a high refractory content.

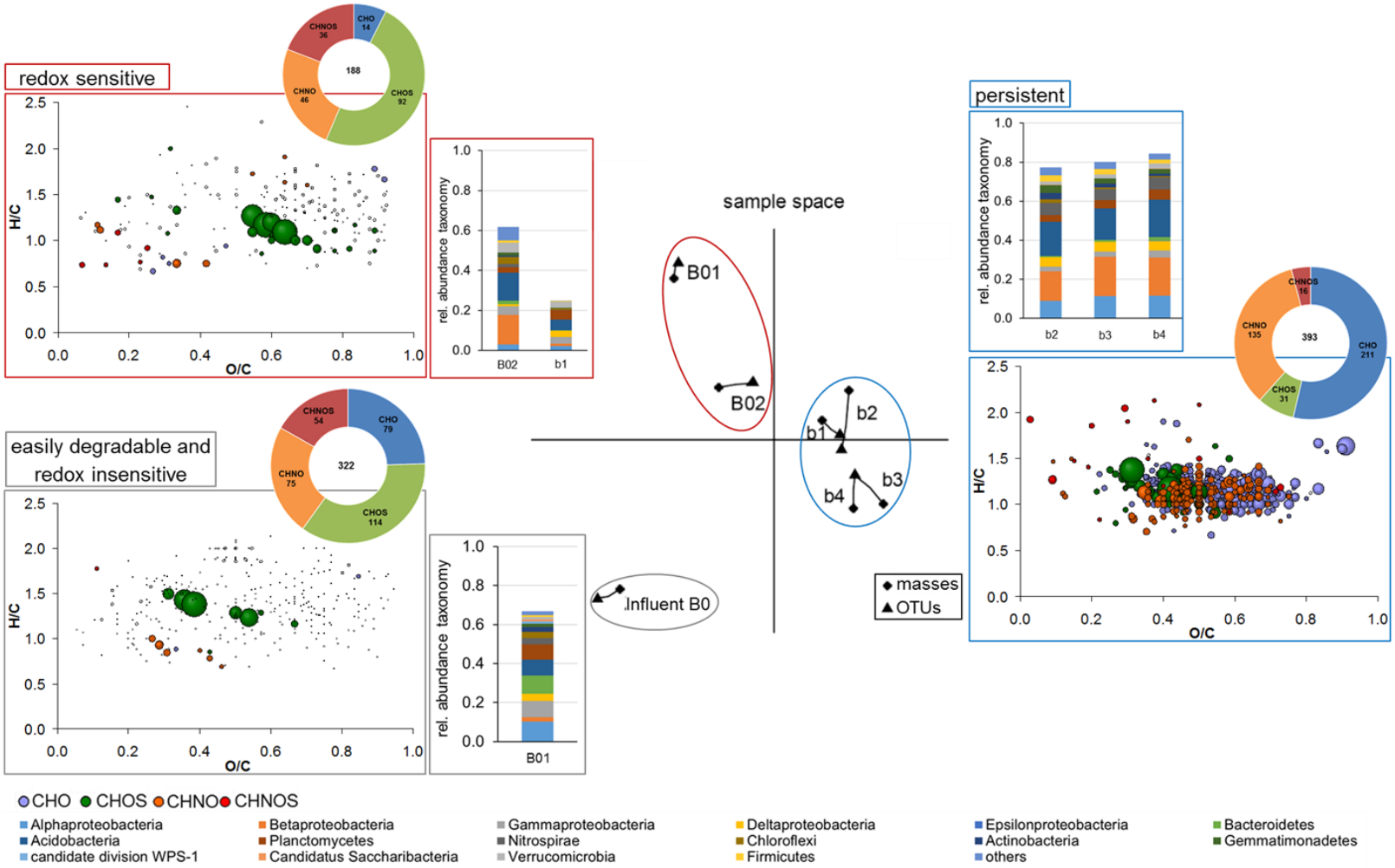

Figure 6-4: On the basis of multiple coinertia analysis three distinct clusters of masses (diamonds) and OTUs (triangles) were identified according to the influent (Influent B0) and the first (B01, B02) and the second (b1-b4) infiltration system. Corresponding OTUs (B01–b4) and masses are connected by a line, whose length is proportional to the divergence between the data from the same sample. Van Krevelen diagrams, absolute numbers of masses and their elemental compositions, as well as taxonomy assignments representative for each cluster are shown. Total number of masses are given within each circle; abundance of microbial phyla or classes are shown as relative values.

6.3.4.2. Orthogonal partial least-squares analysis (OPLS)

As a cometabolic transformation of TOrCs in MAR systems is widely assumed (Alidina et al., 2014a), a correlation between masses assigned by use of FT-ICR-MS and detected TOrCs may be evident. The establishment of the microbial community on phyla level at different depths based on receiving feedwater should be elucidated. In addition, the microbiome which could be involved in the transformation processes of the primary substrate and therefore the TOrCs had to be considered. Hence, an OPLS was performed to emphasize masses as well as OTUs, which correlate with targeted TOrCs. Bulk organic parameters (DOC, UVA_{254}) as well as redox parameters (DO, NO_3^- -N) were also included in the model. However, NO_3^--N will not be considered in further discussions as its actual concentration will be biased especially after reaeration. As shown in Figure 6-5, masses and OTUs were successfully clustered with respect to the four distinct groups: easily degradable, redox-insensitive, redox-sensitive, and persistent compounds (Table 6-1), which indicates there is a relation between the behavior of TOrCs in MAR and primary substrate. The persistent compounds primidone and carbamazepine strongly correlated with masses dominated by CHNO- and CHO-containing molecules, while CHOS and CHNOS ones can be neglected (Figure SI-6 11). In accordance to results obtained by applying MCIA, CHO- and CHNO-containing molecules could be assigned to refractory dissolved organic matter such as CRAM (Derenne and Largeau, 2001; Hertkorn et al., 2006; Mesfioui et al., 2012). It could be assumed that TOrCs correlating with such refractory organic matter may also be incorporated in the environmental organic backbone. With respect to the easily degradable TOrC citalopram, relative abundances of CHO and CHOS were approximately 30%, while CHNO-containing molecules were most frequently detected (38%; Figure 6-5). For CHO, the most intense signals were observed from oxidized compounds (O/C > 0.5) within a H/C range of 1.0-1.5. In the case of CHNO, signals with O/C < 0.4 and H/C 0.75–1 but also with O/C > 0.5 and H/C 1.0-1.5 were detected. Single highly intense CHOS signals could be assigned to sulfophenyl carboxylates and intermediates of dialkylltetralin sulfonates. The largest group of TOrCs was those showing a redox-independent behavior, namely, transformation throughout the system under anoxic as well as oxic to suboxic redox conditions (Table 6-1, Figure SI-6 5). From easily degradable to redox-insensitive compounds a shift from approximately 30% to approximately 50% regarding the relative abundance of CHOS was observed. In contrast, the number of CHO- and CHNO-containing molecules decreased from approximately 30-40% (easily degradable) to approximately 20% (redox insensitive). While CHO-containing molecules were mainly characterized by most intense signals in the area of O/C > 0.5 and H/C > 1.0, CHNO exhibited intensive signals in the range of O/C < 0.5 and H/C < 1.0. The fourth group of major interest within this study contained the TOrCs benzotriazole, tramadol, and venlafaxine due to their redox-sensitive behavior (Table 6-1). There are 338 masses in total which could be unambiguously assigned to molecular formulas containing C, H, O, and/or N and/or S following this trend. In this group, molecules comprised of CHO were less abundant (17%); CHOS and CHNOS occurred to approximately 25% each. CHNO-containing molecules were the most abundant group with more than 30%. In all four molecular groups, no distinct clustering was obtained in the van Krevelen plots; they were all detected in a range of O/C 0.2–1.0 and H/C of 0.5-2.0.

Microbial phyla imply highly diverse characteristics regarding metabolic functions as they are comprised of a variety of species having specialized strategies to utilize growth substrate. In accordance to the results observed by the use of MCIA, the microbiome which seems to not prefer a specific growth substrate was mainly comprised of *α-Proteobacteria*, *Acidobacteria*, and *Planctomycetes* (relative abundance > 1% at all four groups; Figure 6-5*)*. *Firmicutes* and *Gemmatimonadetes* could be correlated with persistent masses having a relative abundance of >1% but <1% in correlation with easily degradable, redox-insensitive, or redox-sensitive compounds. A higher abundance of *Firmicutes* in simulated MAR receiving primary substrate mainly shaped by refractory humic acid in comparison to easily degradable peptone/yeast has previously been reported (Li et al., 2014a). A relative abundance of >1% in correlation with easily degradable and redox-insensitive masses, TOrCs as well as the DOC and UVA_{254} but also with redox-sensitive masses, TOrCs and DO was observed for *Bacteroidetes* (Figure 6-5). As this phylum was also correlated to easily degradable masses using MCIA it may be suggested that *Bacteroidetes* remarkably contribute to degradation of organic matter and, therefore, cometabolic transformation of TOrCs. Similar results were observed by Li et al. (2013), who proposed a link between *Bacteroidetes* abundance and BDOC reduction. Microbial phyla with an abundance of >1% solely correlated to either easily degradable, redox-insensitive or redox-sensitive compounds could not be identified. However, based on phylum level, it will not be possible to derive a deeper understanding of metabolic pathways and their associated metabolites. Nevertheless, a correlation between compounds comprised of CHOS with easily degradable and redox-insensitive masses was figured out, while persistent organic matter mainly correlated with highly refractory CRAM. To further elucidate the correlation between TOrCs transformation and the composition of organic matter, NMR analysis would be expedient to emphasize not only compound classes but also functional groups which correlate between organic matter and TOrCs.

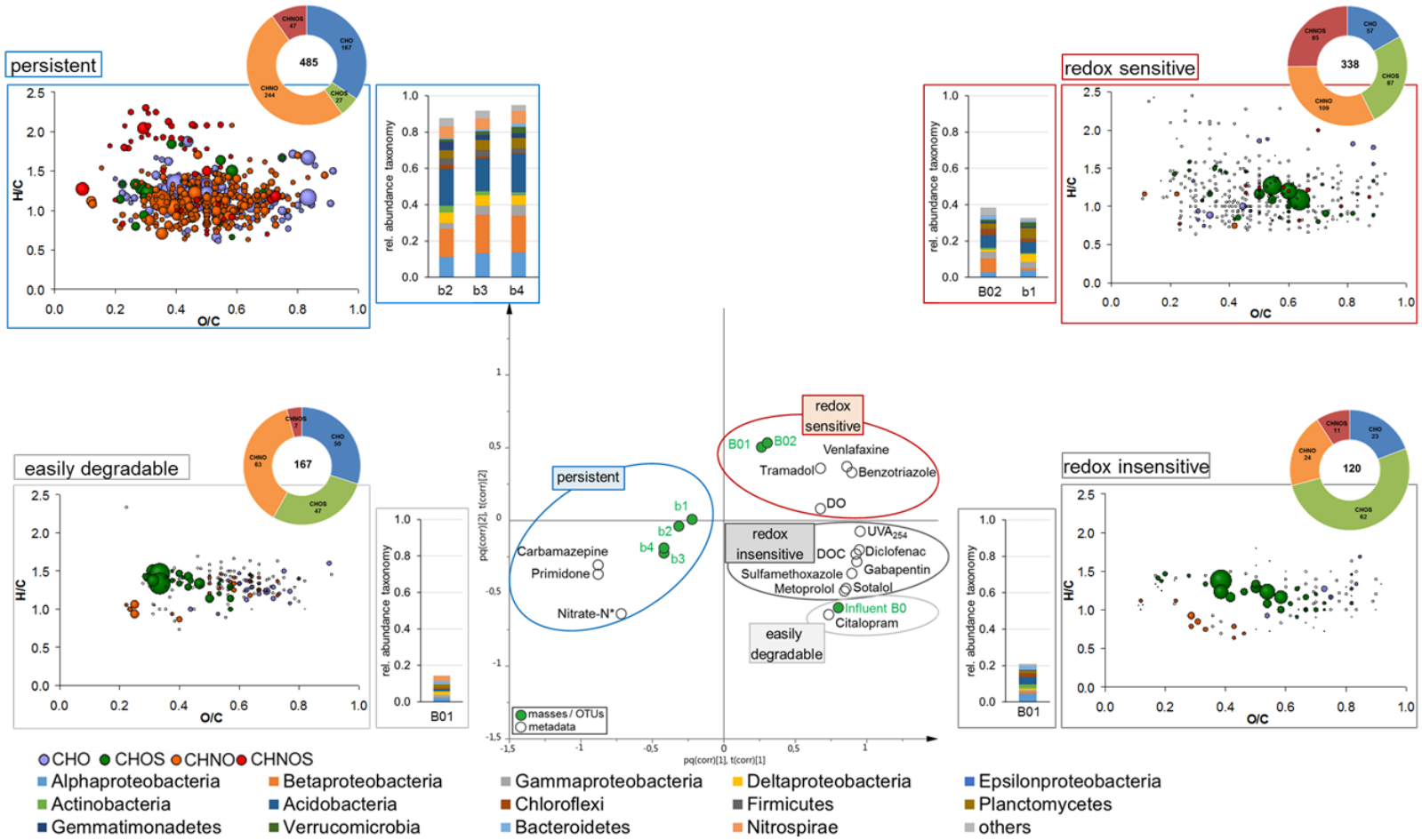

Figure 6-5: On the basis of orthogonal partial least-squares (OPLS) regression clusters of masses and OTUs were identified according to the four categories of TOrCs and their behavior in MAR systems: (i) persistent, (ii) easily degradable, (iii) redox insensitive, (iv) redox sensitive. Van Krevelen diagrams, absolute numbers of masses and their elemental compositions, as well as taxonomy assignments representative for each cluster are shown. Total number of masses are given within each circle; abundance of microbial phyla or classes, respectively, are shown as relative values; consider that the microbiome of column B01 corresponds to the influent B0 and each column (B02-b4) to the effluent of the previous column (B01-b3). OPLS model gave the following values for the goodness of its fit and the goodness of the prediction: R^2Y(cum) = 0.9 and Q^2(cum) = 0.9. (*) Not considered for further discussions.

Acknowledgements

This study was funded by the German Federal Ministry for Research and Education as part of the TrinkWave project (BMBF, grant no. 02WAV1404). We thank all involved colleagues from the Chair of Urban Water Systems Engineering for their technical and analytical support, especially Hubert Moosrainer, Nicole Zollbrecht, Myriam Reif, Ursula Wallentits, Heidrun Mayrhofer, Wolfgang Schröder, and Johann Müller as well as our graduate students Nathalie Vas, Franka Busch, and Michael Osina. The bioinformatics support of the BMBF-funded project 'Bielefeld-Gießen Center for Microbial Bioinformatics–BiGi (Grant no. 031A533)' within the German Network for Bioinformatics Infrastructure (de.NBI) is gratefully acknowledged.

Notes

The authors declare no competing financial interest.

Based on the results of this study, Hypothesis II that the fate of molecular components and characteristic functional groups of the primary substrate correlates with the degradation of structurally similar TOrCs cannot be confirmed. Even though no correlation between functional groups of the primary substrate and the structure TOrCs could be revealed as the analytical tools used in this study are not appropriate to do so, compound classes could be assigned to different classes of TOrCs. This represents a first step towards a more detailed analyses of primary substrate and TOrCs and their role during MAR.

7 Biotransformation of trace organic chemicals in the presence of highly refractory dissolved organic carbon

This chapter has previously been published as follows[11]:

Hellauer, K., Martínez Mayerlen, S., Drewes, J.E., Hübner, U., 2019. Biotransformation of trace organic chemicals in the presence of highly refractory dissolved organic carbon. *Chemosphere* 215, 33–39.

Abstract

Previous studies demonstrated that the transformation of trace organic chemicals (TOrCs) in managed aquifer recharge (MAR) systems is favored under carbon-limited and oxic redox conditions especially, if the dissolved organic carbon (DOC) serving as primary substrate has a refractory character. Since co-metabolism is suggested to be the dominant removal mechanism, it is hypothesized that TOrCs transformation is controlled by the concentration of the refractory carbon under oxic redox conditions. A laboratory-scale soil column experiment mimicking MAR was established to investigate the influence of two different concentrations of highly refractory carbon sources on TOrCs transformation, namely drinking water (DW) and drinking water augmented with humic acid (DW + HA). Oxic redox conditions and carbon-limitation were present in both systems (ΔDOC_{DW+HA} ≈ 0.6-0.7 mg/L; ΔDOC_{DW} ≈ 0.1 mg/L). Of the 12 TOrCs investigated seven exhibited moderate to efficient transformation in both systems with only one compound (diclofenac) showing significantly enhanced (co-metabolic) biotransformation by adding humic acids as primary growth substrate. It is postulated that transformation of some TOrCs is characterized by metabolic degradation under starving conditions (ΔDOC ≤ 0.1 mg/L). By comparing the transformation efficiency of selected TOrCs with previous studies operated under carbon-limited and oxic conditions, an inconsistent behavior of some compounds was observed. These results demonstrate that key factors triggering the transformation of TOrCs are still poorly understood and thus, further investigations regarding the biodegradation pathways of TOrCs, upregulation of key enzymes by the microbial community but also more detailed analysis of the composition of the biodegradable DOC are needed.

[11] This study was performed to test Hypothesis III that the concentration of refractory carbon (like humic acids) controls TOrCs removal in MAR systems under oxic conditions.

7.1. Introduction

Managed aquifer recharge (MAR) systems, such as river and lake bank filtration and groundwater recharge by surface spreading are natural water treatment systems providing an effective barrier for many contaminants like e.g., turbidity, pathogens, dissolved organic carbon, taste and odor compounds (Grünheid et al., 2005; Maeng et al., 2012a; Regnery et al., 2017). Also a high efficiency for attenuation of many trace organic chemicals (TOrCs) by sorption and biodegradation is well documented in the peer-reviewed literature (Grünheid et al., 2005; Maeng et al., 2011a; Regnery et al., 2015a). However, some compounds are not sufficiently removed in MAR systems even after hydraulic retention times of weeks to months. Several studies report that for instance the corrosion inhibitor benzotriazole or the artificial sweetener acesulfame can still be detected in MAR filtrate at concentrations of a few hundred nanograms to several micrograms per liter (Reemtsma et al., 2010; Scheurer et al., 2009), despite their general susceptibility to microbial degradation (Alotaibi et al., 2015; Castronovo et al., 2017). These findings point to the importance of predominant boundary conditions for efficient TOrC transformation during MAR. With a few exceptions, degradation of most compounds is favored under oxic redox conditions (dissolved oxygen concentration > 1 mg/L) (Massmann et al., 2008a; Regnery et al., 2015b). In addition, Li et al. (2013) showed that the composition of the microbial community could be significantly influenced by the availability of biodegradable dissolved organic carbon (BDOC). Whereas biomass positively correlated with the availability of BDOC, the diversity of the microbial community increased with decreasing BDOC concentrations. Active establishment of carbon-limited and oxic condition in lab- and full-scale applications resulted in improved transformation in particular of TOrCs commonly characterized as moderately or poorly degradable (Hellauer et al., 2017; Hellauer et al., 2018a; Müller et al., 2017; Regnery et al., 2016). In addition to the absolute concentration of the primary substrate, its composition seems to have a significant impact on the efficiency of TOrCs transformations in MAR systems. A study by Li et al. (2014a) revealed that the metabolic potential of the microbial community to degrade xenobiotic compounds is enhanced if the BDOC has a refractory character and is present at low concentrations. In laboratory-scale experiments, an equal or more efficient transformation of several biodegradable TOrCs investigated in the presence of hydrophobic acids in comparison to other investigated feed water matrices (i.e., effluent organic matter which is known as organic matter derived from wastewater treatment plant discharges, hydrophilic carbon and colloidal organic carbon) was reported by Rauch-Williams et al. (2010). Alidina et al. (2014b) observed enhanced removal for several TOrCs in columns fed with low BDOC concentrations primarily comprised of humic acid (HA) compared to those comprised of easily degradable organic carbon sources (peptone/yeast). The authors assumed co-metabolic transformation of TOrCs that was triggered by increased concentration of HAs as growth substrate for bacteria. However, simultaneously diminished availability of easily degradable substrates in their experiments might also have stimulated utilization of alternative growth substrates by bacteria as suggested by Egli (2010).

Based on the assumption of a pre-dominantly co-metabolic biotransformation of TOrCs, we hypothesize that the concentration of refractory carbon (like humic acids) controls TOrCs transformation in MAR systems under oxic conditions. In previous column batch

tests with feed water recirculation, D'Alessio et al. (2015) did not observe a distinct trend regarding enhanced removal of biodegradable TOrCs with increased concentrations of HA added to surface water (initial TOC: ≈ 3; ≈ 10; ≈ 20 mg/L). However, in that study TOrCs were spiked at relatively high concentrations of 50 µg/L which might have induced metabolic adaptation as suggested previously for other compounds like sulfamethoxazole (Baumgarten et al., 2011). Tang et al. (2017) investigated the degradation of spiked pharmaceuticals (initial concentrations: 1.2–14.6 µg/L) in laboratory-scale moving bed biofilm reactors (MBBRs) at four different levels of HA mixed with secondary treated wastewater (initial DOC [mg/L]: 4.4 (0 mg/L HA); 11 (25 mg/L HA); 13 (37.5 mg/L HA), and 30 (100 mg/L HA)). The degradation rate constants for ten of the 13 investigated biodegradable TOrCs were enhanced with an increasing amount of HA indicating that the presence of complex substrate might stimulate degradation via a co-metabolic-like mechanism (Tang et al., 2017).

In contrast to previous studies, long-term column experiments were conducted in this study under carbon-limited conditions (ΔDOC ≤ 0.7 mg/L) with TOrCs spiked at environmentally relevant concentrations of approximately 400 ng/L each with the objective to elucidate the impact of refractory organic carbon as primary growth substrate on (co-metabolic) TOrC biotransformation. Columns were fed with a low-carbon drinking water feed matrix with and without an additional spike of HA. In addition, TOrC biotransformation was compared to results from other systems operated at comparable conditions.

7.2. Material and methods

7.2.1. Laboratory-scale column experiment

The experimental system consisted of two parallel set-ups each comprised of a pre-treatment step and the main experiment in duplicate columns (Figure 7-1). Unchlorinated drinking water (DW, Figure 7-1a) and drinking water containing humic acid (DW + HA, Figure 7-1b) were pre-treated in columns (HRT = 2.1 days) to remove easily degradable DOC prior to infiltration into the main columns. The HA solution was prepared weekly by dissolving 500 mg HA sodium salt 70% (CAS-No. 68131-04-4; Carl Roth, Germany) in 10 L drinking water followed by filtration through a paper filter (MN 651 ¼ 320 mm; Macherey-Nagel GmbH & Co. KG, Germany) and stored at room temperature. The top layer of the pre-treatment column operated with HA dissolved in drinking water was periodically removed to discard residual particulate matter from HA solution. HA content after paper filtration was not measured but effluent DOC from pre-treatment columns was continuously monitored (Table 7-2). After pre-treatment, effluents were reaerated with compressed air and spiked with a mix of several TOrCs (~12 µg/L) at a ratio of 1:30 to establish a final concentration of 300–500 ng/L in the influents of the DW and DW + HA columns. The main experimental set-up consisted of two soil columns filled with aquifer material (height = 30 cm; inner diameter = 9 cm), which were operated in top-down mode under fully saturated flow conditions. The hydraulic retention time (HRT) of 0.9 days at a flow rate of 30 mL/h was determined in a tracer test using potassium bromide following the c-peak method (Schudel et al., 2002).

In the conditioning phase, both column systems (DW and DW + HA) were operated with drinking water without any HA nor TOrCs spiked for approximately one year. Five months

prior to the start of the experiment, TOrCs were spiked into the main columns (operated with DW) for three months. Feeding with HA solution and spiking of the final TOrCs mixture (Table 7-1) was initiated 2 and 1.5 months prior to the start of the experiment.

Water samples for bulk organic carbon (DOC, ultraviolet absorbance at 254 nm (UVA_{254}), color), nitrogen species (i.e., nitrate, nitrite, and ammonium), as well as for TOrCs quantification were collected biweekly from the in- and effluent of each column over a period of five months. Based on a HRT of 0.9 days, the effluent was taken approximately one day after influent sampling. In addition, dissolved oxygen (DO) concentrations were monitored using a fiber optic based system (Fibox 4.0, PreSens, Germany) in column influents (at the top of the columns, PSt3 oxygen sensor constructed as described by Hecht and Kölling (2001)), as well as in flow-through cells (FTC-PSt3; PreSens, Germany) in the effluent of each column.

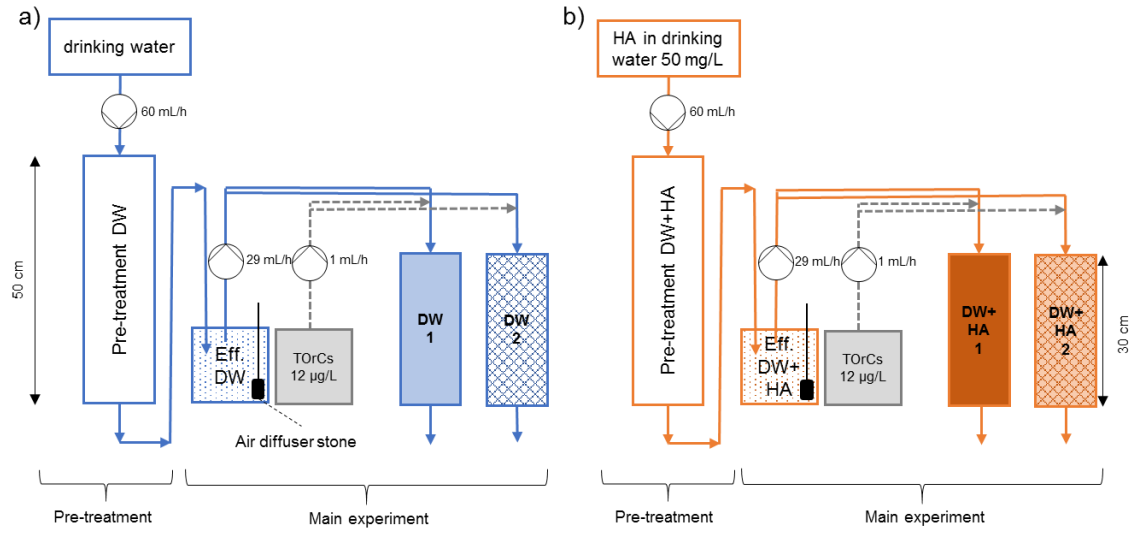

Figure 7-1: Laboratory-scale column experiment consisting of two parallel set-ups (pre-treatment and main experiment) fed with a) drinking water (DW) and b) humic acid solution spiked to drinking water (DW + HA). Columns DW and DW + HA were operated in duplicate (columns 1 and 2).

7.2.2. Analytics

Prior to the analyses, samples were filtrated using cellulose-nitrate filters with 0.45 µm pore size (Sartorius AG, Germany). The DOC analysis was performed on a Vario TOC cube TOC analyzer (Elementar GmbH, Germany) with a detection limit of 0.5 mg/L after sample acidification to a pH of 2. UVA_{254} and color (436 nm) were measured using a DR 6000 UV/vis Spectrophotometer (HACH, Germany). The specific UV absorbance at 254 nm ($SUVA_{254}$) was calculated as the ratio of UVA_{254} and DOC as an indicator for the aromatic carbon content (Weishaar et al., 2003). 3D-fluorescence spectroscopy was performed to further elucidate the character of the DOC using an Aqualog® fluorescence spectrometer (Horiba Scientific, USA). The following settings were chosen: i) integration time 1 s, ii) excitation increment 3 nm, iii) emission increment 1.64 nm, iv) Excitation-wavelength 230-599 nm, v) emission wavelength 212-621 nm, and vi) medium charge coupled device (CCD). Each blank subtracted 3D-Excitation-Emission-matrix (3D-EEM)

was further corrected (inner filter algorithm, first and second order Rayleigh masking) and normalized to Raman units (R.U.). The concentrations of nitrate (NO_3^--N), nitrite (NO_2^--N), and ammonium (NH_4^+-N) were determined using cuvette tests (HACH, Germany) with a detection range of 0.23–13.5 mg/L (Test LCK 339, NO_3^--N), 0.015–0.6 mg/L (Test LCK 341, NO_2^--N), and 0.015–2 mg/L (Test LCK 304, NH_4^+-N), respectively. The final measurements were performed with a DR 6000 UV/vis Spectrophotometer (HACH, Germany).

TOrCs were quantified using liquid chromatography coupled with tandem mass spectrometry (LC-MS/MS) based on a method previously published by Müller et al. (2017). In this study, measurements were performed in positive electrospray ionization mode only. The influent concentrations of all investigated TOrCs (mean concentration of all four columns) and their corresponding limits of quantification (LOQ) are listed in Table 7-1. If detected concentrations of TOrCs were < LOQ, values were set as LOQ/2 for further calculations. As the caffeine concentration already decreased in the influent stock solution during the experimental period, results for this chemical analysis are not included. Differences between column duplicates receiving the same feed water were characterized based on a student's *t*-test, two-tailed, paired ($\alpha < 0.01$). Differences between columns fed with different influents were only assigned as significant if both columns of DW were significantly different from both DW + HA columns (Student's *t*-test, two-tailed, unpaired, $\alpha < 0.01$).

Table 7-1: Influent concentrations and LOQ of all targeted TOrCs (*n* = 39).

Compound	LOQ [ng/L]	Influent concentration [ng/L]
Atenolol	10	487 ± 92
Benzotriazole	50	299 ± 122
Caffeine	10	< LOQ
Carbamazepine	5	433 ± 48
Diclofenac	5	375 ± 57
Gabapentin	2.5	420 ± 51
Iopromide	50	463 ± 66
Metoprolol	2.5	387 ± 52
Phenazone	10	542 ± 96
Phenytoin	5	459 ± 62
Primidone	25	461 ± 56
Sulfamethoxazole	5	419 ± 50
Venlafaxine	2.5	581 ± 73

7.3. Results and discussion

7.3.1. Bulk organic carbon and redox characteristics

Influent and effluent concentrations of bulk organic carbon and redox parameters for the column experiments are listed in Table 7-2. The influent concentrations from columns receiving the same feed water are shown as average values. Significant differences in effluents from duplicate columns were solely observed in columns fed with DW + HA for the parameters DOC, UVA_{254} and color at 436 nm.

The influent DOC concentration of the DW + HA columns (3.13 ± 0.62 mg/L) was in the same range as previously reported for river bank filtrate (Regnery et al., 2016), whereas

the DOC of the DW columns influent (0.71 ± 0.16 mg/L) was much lower (Table 7-2). In the DW columns, measured ΔDOC of ≈ 0.1 mg/L confirmed the presence of a very low amount of biodegradable organic carbon compared to slightly higher removal observed in the DW + HA columns (ΔDOC ≈ 0.6–0.7 mg/L). Relatively low $SUVA_{254}$ values indicate a less aromatic character of the DW organic matter (1.07 ± 0.41 L/(mg·m)) compared to the DW + HA feed water (7.18 ± 0.91 L/(mg·m)), even though its character was highly refractory according to the slight DOC removal and insignificant changes of UVA_{254} and color during travel through the DW columns (Table 7-2). An average UVA_{254} value of 22 1/m in influent samples of the DW + HA columns confirmed the prevalence of aromatic substances. No significant change of $SUVA_{254}$ was observed throughout the filtration in DW + HA columns 1 and 2. Therefore, it may be assumed that the microbial community is capable of transforming highly refractory DOC under prevailing carbon-limited conditions.

Table 7-2: Bulk organic and redox parameters of influents and effluents of columns DW and DW + HA. Influent values are given as mean ± standard deviation of both parallel columns receiving the same feed water (*n* ≥ 6), effluent values are shown for each column (*n* ≥ 3).

Parameter	DW			DW + HA		
	Influent	Effluent		Influent	Effluent	
		DW 1	DW 2		DW + HA 1	DW + HA 2
DOC [mg/L]	0.71 ± 0.16	0.65 ± 0.25	0.58 ± 0.09	3.13 ± 0.62	2.54 ± 0.35	2.39 ± 0.28
ΔDOC [mg/L]		0.11 ± 0.29	0.09 ± 0.13		0.62 ± 0.58	0.71 ± 0.49
UVA_{254} [1/m]	0.74 ± 0.24	0.81 ± 0.19	0.72 ± 0.17	22.05 ± 2.82	17.97 ± 2.29	17.07 ± 2.19
$Color_{436}$[1/m]	0.01 ± 0 02	0.01 ± 0 02	0.01 ± 0 02	2.44 ± 0.38	1.75 ± 0.30	1.64 ± 0.29
$SUVA_{254}$ [L/(mg·m)]	1.07 ± 0.41	1.35 ± 0.43	1.26 ± 0.32	7.18 ± 0.91	7.14 ± 0.68	7.16 ± 0.55
DO [mg/L]	7.56 ± 0.53	7.17 ± 0.70	7.22 ± 0.76	7.23 ± 0.59	6.02 ± 0.80	5.77 ± 0.87
ΔDO [mg/L]		0.42 ± 0.27	0.30 ± 0.31		1.21 ± 0.49	1.46 ± 0.44
NO_3^--N [mg/L]*	< LOQ	< LOQ	< LOQ	0.27 ± 0.01	0.24 ± 0.01	0.23 ± 0.01
NO_2^--N [mg/L]**	< LOQ	< LOQ	< LOQ	0.018 ± 0.003	0.017 ± 0.003	< LOQ

*LOQ (NO_3^--N) = 0.23 mg/L; **LOQ (NO_2^--N) = 0.015 mg/L

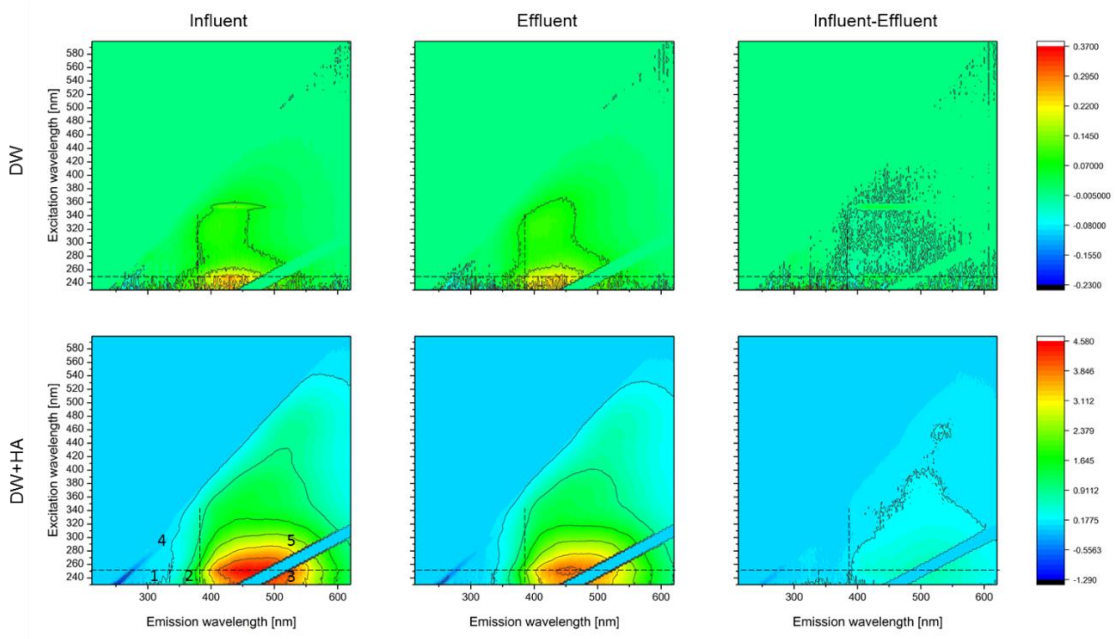

Figure 7-2: 3D-EEM of an influent and effluent sample from columns DW- (top) and DW + HA- (bottom) as well as the difference between the influent and effluent. Dashed lines indicate five characteristic regions previously summarized by Chen et al. (2003): 1) aromatic protein I; 2) aromatic protein II; 3) fulvic acid-like; 4) microbial by-product-like; 5) humic acid-like. Note the different intensity scales of DW (-0.2300–0.3700) and DW + HA (-1.290 - 4.580).

Based on 3D-fluorescence spectroscopy, the composition of the primary substrate was further investigated. As representatively shown in Figure 7-2 for one column of each duplicate experiment, the DW + HA influent and effluent was mainly characterized by humic and fulvic-acid like substances, while the DW influent and effluent showed much lower intensity in the area of fulvic acid-like compounds and only a slight signal from humic acid-like substances. Calculation of intensity differences between influent and effluent (Figure 7-2, right) confirmed, that no distinct changes in the DOC composition occurred throughout the infiltration in DW columns. Also changes of fluorescence signals from different compounds in DW + HA columns were limited despite higher DOC removal of 0.6–0.7 mg/L.

In the DW columns, only a slight DO consumption of 0.3–0.4 mg/L was observed during column passage, which confirms the observed small DOC removal (Table 7-2). As a consequence of a more substantial DOC mineralization, more oxygen was consumed in the DW + HA columns ($\Delta DO \approx 1.2–1.5$ mg/L). Based on DO measurements in all four columns, oxic redox conditions prevailed with stable nitrate concentrations and no formation of nitrite. Ammonium levels were below the LOQ (NH_4^+-N < 0.015 mg/L) in all samples.

7.3.2. Transformation of TOrCs as a function of different refractory biodegradable DOC concentrations under oxic conditions

The compounds carbamazepine, primidone, phenytoin, and phenazone persisted in all four columns even under carbon-limited and oxic redox conditions (Figure 7-3). While this

persistent behavior of carbamazepine, primidone and phenytoin was expected based on previous observations (Bertelkamp et al., 2014; Clara et al., 2004; Hass et al., 2012; Hoppe-Jones et al., 2010), the refractory character of phenazone was not expected. Previous studies using slow sand filtration reported phenazone removal below the LOQ (Hübner et al., 2012) and elimination by 66% in a full-scale riverbank filtration facility in Berlin, Germany under pre-dominantly oxic redox conditions (Massmann et al., 2008a). Even in biologically-active drinking water filters efficient removal of 90% has been reported indicating good biodegradability under oxic and carbon-limited conditions (Reddersen et al., 2002). In contrast, no biodegradation of phenazone was observed during a laboratory-scale MBBR study (Tang et al., 2017).

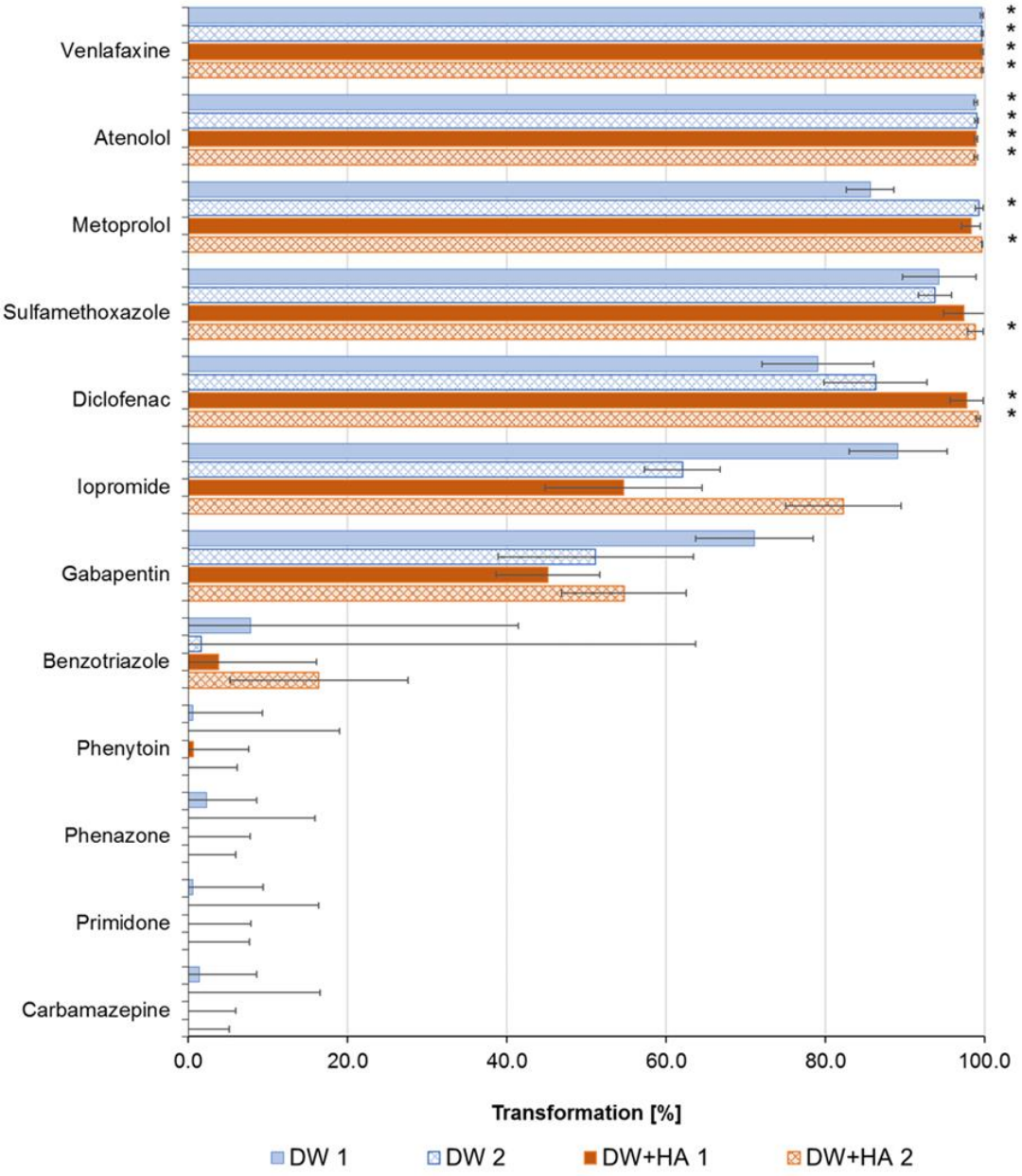

Figure 7-3: Transformation of targeted TOrCs in different columns under oxic redox conditions in the presence/absence of humic acid ($n \geq 9$). * removed below limit of quantification (LOQ) in most samples. Error bars indicate standard deviation.

In general, the observed effects in the presence of humic acid on the transformation of biodegradable TOrCs were very limited. Diclofenac was the only compound, which was significantly better transformed in the DW + HA columns in comparison to the columns receiving just drinking water. In case of DW + HA columns 1 and 2, the transformation was mainly below the LOQ resulting in a percentage removal of ≥ 98%, whereas a transformation of 79 ± 7% and 86 ± 6% was detected for DW columns 1 and 2, respectively. However, the differences between DW column 1 and 2 were also classified as significant. In addition, transformation of metoprolol, gabapentin and iopromide exhibited significant differences between duplicates receiving the same feed water (DW and DW + HA), which was also observed for benzotriazole in columns fed with DW + HA suggesting possible variability of results from individual columns. The compounds atenolol and venlafaxine were transformed below the LOQ for most samples, independent of feed water matrix applied. Also sulfamethoxazole exhibited very efficient degradation with a mean transformation of > 90% in all four columns.

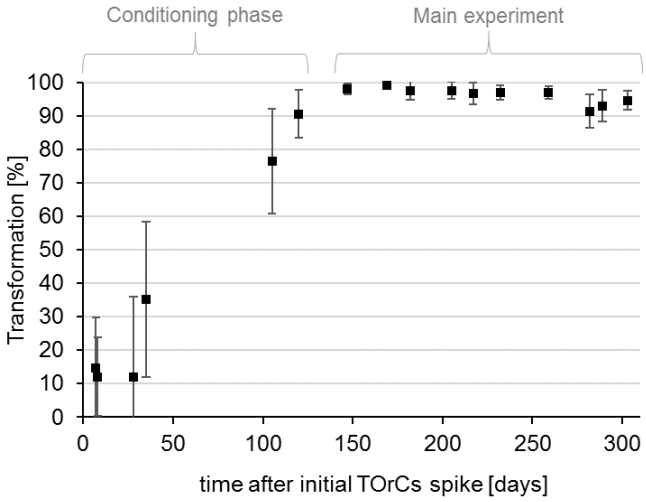

Figure 7-4: Increased transformation of sulfamethoxazole from the conditioning phase until the end of the experiment (*n* = 3-4). Values of all four columns were averaged, error bars indicate standard deviation.

Based on these results, the hypothesis of co-metabolic TOrC biotransformation triggered by an elevated presence of HA-like organic matter could not be confirmed. Even though the concentration of the ΔDOC of both investigated primary substrates was enhanced by HA addition ($\Delta DOC_{DW} \approx 0.1$ mg/L; $\Delta DOC_{DW+HA} \approx 0.6$-$0.7$ mg/L; Table 7-2), this enhancement did not result in a significantly better transformation of the targeted TOrCs. The limited effect of HA addition on compound transformation might suggest that microbial communities under very low-carbon substrate conditions are capable for metabolic degradation of some TOrCs. This assumption is further supported by an observed adaption to sulfamethoxazole in the maturation period prior to the experiment which resulted in a gradual increase of compound transformation (Figure 7-4), as previously reported by Baumgarten et al. (2011). In contrast, Alidina et al. (2014a) observed no adaption of the microbial community to sulfamethoxazole in columns fed with HA solution. Findings by Alidina et al. (2014a) are in accordance with the results of our study as no adaption to all other targeted compounds was observed. However, a significantly

increased transformation was obtained in columns fed with peptone/yeast after an adaption to sulfamethoxazole of more than 300 days in comparison to non-exposed columns (Alidina et al., 2014a).

In contrast to results observed within this study, Tang et al. (2017) observed enhanced degradation for many investigated compounds spiked at concentrations > 1 µg/L towards higher HA concentrations, including the compounds iopromide, atenolol and metoprolol, which were also measured in this study. Different results indicate that metabolic capabilities of a microbial community are a factor of environmental conditions. While bacteria seem to develop strategies to metabolize some TOrCs at starving conditions (ΔDOC in DW of ≈ 100 µg/L), which might also involve mixed substrate growth as described previously (Egli, 2010), co-metabolic degradation might be the dominant process in systems with higher amount of biodegradable organic carbon. It can be expected that these effects are also very site and compound specific. Further research is needed to elucidate drivers for metabolic and co-metabolic transformation of TOrCs in natural and engineered systems.

7.3.3. Comparison of TOrCs transformation under oxic and carbon-limited conditions

Experiments were conducted to mimic oxic and carbon-limited conditions which have been demonstrated to be favorable for an enhanced TOrCs transformation (Müller et al., 2017; Regnery et al., 2015b; Regnery et al., 2016). Despite the establishment of these optimized conditions, several known biodegradable compounds exhibited no (phenazone), poor (benzotriazole), and moderate removal (iopromide, gabapentin), while others were quickly or almost completely removed (venlafaxine). To illustrate inconsistencies of the removal of individual compounds with results from other systems, transformation efficiencies of five readily (diclofenac, venlafaxine, metoprolol), moderately (gabapentin), and poorly (benzotriazole) degraded compounds (compare Figure 7-3 for transformation in this study) have been compared to results from other studies performed under oxic and carbon-limited conditions such as Müller et al. (2017) (investigating sequential biofiltration) and Hellauer et al. (2017; 2018a) investigating sequential managed aquifer recharge technology (SMART) at lab- and field-scale (Figure 7-5). The concepts of sequential biofiltration and SMART are explained elsewhere (Müller et al., 2017; Regnery et al., 2016). The influent concentration of targeted TOrCs as well as relevant operational, redox and bulk organic parameters are listed in Table 7-3 for the different systems. In all investigated systems despite sequential biofiltration and lab-scale SMART, carbon-limited (ΔDOC < 1 mg/L) and oxic redox conditions prevailed (Table 7-3). In particular, redox conditions in sequential biofiltration were characterized as suboxic (ΔDO < 1 mg/L, ΔNO_3^--N < 0.5 mg/L (Regnery et al., 2015b)) in deeper filter depths (Müller et al., 2017) and carbon-limitation in lab-scale SMART was not observed (Hellauer et al., 2017).

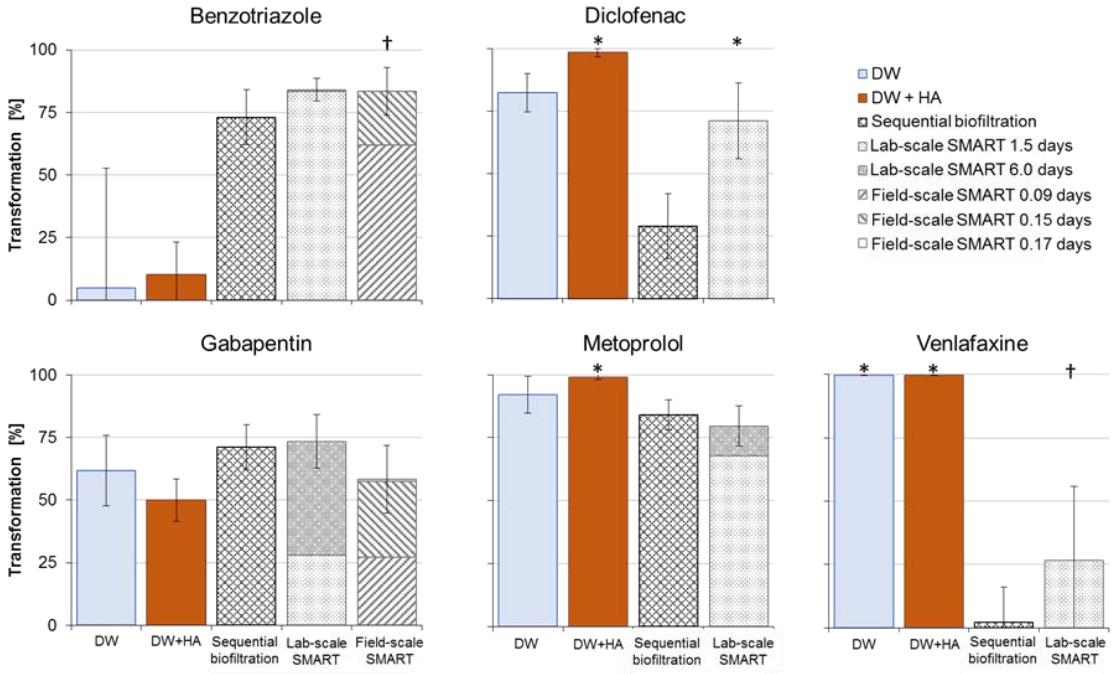

Figure 7-5: Transformation of selected TOrCs in biological treatment systems operating under carbon-limited and oxic (suboxic) redox conditions (Hellauer et al., 2018a; Hellauer et al., 2017; Müller et al., 2017); Stacked bars represent additive removal at different HRT; Error bars indicate standard deviation. $n \geq 4$. * mainly removed < LOQ; † no further transformation observed with longer HRT.

Table 7-3: Bulk organic carbon and redox conditions as well as TOrCs influent concentration of different systems.

Parameter	System				
	DW	DW + HA	Field-scale SMART (Hellauer et al., 2018a)	Lab-scale SMART O_2* (Hellauer et al., 2017)	Sequential biofiltration (Müller et al., 2017)
estimated maturation time to TOrCs	≈ 5 months		≈ 5 months	≈ 10 months	≈ 10 months
HRT [days]	0.9	0.9	0.09 0.15 0.17	1.5 6.0	0.6
ΔDOC [mg/L] ($n \geq 6$)	0.1 ± 0.2	0.7 ± 0.5	0.1 ± 0.2 0.0 ± 0.2 0.1 ± 0.1	n.a. 2.0 ± 1.7	1.2 ± 0.8
ΔDO [mg/L] ($n \geq 3$)	0.4 ± 0.3	1.3 ± 0.5	3.2 ± 0.7 0.1 ± 0.2 0.0 ± 0.1	7.9 ± 8.9 3.5 ± 3.7	7.2 ± 1.6
$DO_{Effluent}$ [mg/L] ($n \geq 3$)	7.2 ± 0.7	5.9 ± 0.8	2.8 ± 0.8	14.3 ± 4.5	0.7 ± 1.4**
Influent concentration TOrCs [ng/L]					
Benzotriazole ($n \geq 5$)	309 ± 170	288 ± 47	456 ± 78	2,716 ± 484	2,951 ± 424
Gabapentin ($n \geq 5$)	420 ± 59	419 ± 45	291 ± 52	441 ± 103	792 ± 167
Diclofenac ($n \geq 4$)	384 ± 62	367 ± 51	n.a.	239 ± 179	1061 ± 362
Metoprolol ($n \geq 5$)	386 ± 56	388 ± 49	n.a.	52 ± 39	189 ± 36
Venlafaxine ($n \geq 5$)	587 ± 80	575 ± 66	n.a.	81 ± 14	314 ± 36

*reaeration with pure oxygen.
**suboxic redox conditions prevailed in the deeper zones of sequential biofiltration system (Müller et al., 2017).
n.a. not available.

The transformation of the moderately degradable compound gabapentin under oxic conditions was consistent in all systems studied. Also metoprolol exhibited similar transformation with slightly better degradation in experiments from this study (>90%) compared to SMART (≈ 80%) and sequential biofiltration (≈ 84%). Diclofenac was efficiently degraded in different subsurface treatment systems (with slightly less efficient transformation in DW columns) while only a 29% transformation was observed during sequential biofiltration. It was previously assumed that diclofenac is degraded only under strictly oxic conditions if a sufficient retention time is maintained (Müller et al., 2017).

Venlafaxine persisted sequential biofiltration and was transformed by less than 30% in SMART. However, in DW and DW + HA columns the transformation reached concentration levels of less than the LOQ. To the best of our knowledge, this is the first time that such an efficient transformation of venlafaxine was reported in biological treatment systems confirming the high capability of carbon-limiting biological systems to remove xenobiotic compounds at low concentrations. On the other hand, benzotriazole was successfully transformed in SMART and sequential biofiltration, whereas only a poor transformation was observed in DW and DW + HA columns of this study. Also the compounds phenazone and iopromide, which were not monitored or were below LOQ in influent of SMART and sequential biofiltration but efficiently removed in other oxic systems (Grünheid et al., 2005; Reddersen et al., 2002), were not or only moderately biotransformed during this study.

The different transformation efficiencies indicate variations of enzymatic capabilities between different systems despite similar redox conditions and availability of biodegradable organic carbon. According to pathway prediction based on the Eawag Biocatalysis/Biodegradation Database (Gao et al., 2010) initial microbial attack of compounds showing good degradability in DW and DW + HA columns (gabapentin, metoprolol, venlafaxine) most likely occurs via e.g. oxidative N-deamination (EAWAG-BBD biotransformation rule: #bt0063). Especially enzymes for dealkylation and deamination of the tertiary amine of venlafaxine do not seem to be abundant in all systems under oxic and carbon-limited conditions. In contrast, dioxygenation of aromatics with subsequent oxidation to catechol derivates (*vic*-unsubstituted aromatics: #bt0005, e.g. benzotriazole; mono-substituted aromatics: #bt0353, e.g. phenazone) as well as the primary reaction of the biodegradation pathway known for iopromide (oxidation of a primary alcohol to an aldehyde, #bt0001; Schulz et al. (2008)) seem to be less efficient in DW and DW + HA columns. Proposed transformation of diclofenac by EAWAG-BBD follows an attack of an oxygenase resulting in the formation of 2,3-Dihydroxyphenylacetic acid by release of 2,6-Dichloroaniline (#bt0065), which occurs in all investigated systems given sufficient hydraulic retention time. However, further research is needed to confirm hypothesized pathways and identify relevant enzymes.

In summary, determining factors for the biotransformation of TOrCs in biofiltration treatment systems are still not fully understood. While there is a growing evidence for an enhanced transformation of many TOrCs under oxic and carbon-limited conditions, some TOrCs exhibited an inconsistent transformation pattern during these conditions. To better understand metabolic and co-metabolic degradation of TOrCs, it is important to further investigate the transformation pathways of TOrCs and associated enzymes in biofiltration

systems as well as the structure and functionality of the microbial community. Furthermore, a more detailed characterization of the composition of the primary substrate using advanced techniques such as Fourier transform ion cyclotron resonance mass spectrometry (FT-ICR-MS) and its influence on TOrCs transformation is subject to ongoing research to elucidate the impact of BDOC as primary substrate for co-metabolic TOrC transformation.

7.4. Conclusion

Carbon-limited and oxic conditions are favorable for the transformation of many TOrCs in biofiltration systems such as managed aquifer recharge (MAR). While previous studies indicate that the transformation efficiency can be influenced by shaping the organic matter composition towards more refractory humic acids (Alidina et al., 2014b) or by addition of humic acids (Tang et al., 2017), a benefit of adding humic acid solution could not be confirmed under carbon-limited conditions evaluated in this study. Although spiking of HA in drinking water resulted in significantly enhanced feed DOC concentrations and DOC removal ($\Delta DOC_{DW+HA} \approx 0.6\text{-}0.7$ mg/L compared to $\Delta DOC_{DW} \approx 0.1$ mg/L), only one compound (diclofenac) exhibited significantly enhanced biotransformation. Given the limited impact of availability of humic acid as primary substrate we assume metabolic transformation for the other 6 out of 12 investigated TOrCs, which were moderately to well removed at applied starving conditions ($\Delta DOC \leq 0.1$ mg/L). A comparison of the transformation of selected TOrCs with results from other systems operated under carbon-limited and oxic (partly suboxic) conditions revealed an inconsistent behavior of some compounds. For instance, venlafaxine was transformed below the LOQ in the DW and DW + HA systems but was rather persistent in other systems, while benzotriazole exhibited poor transformation in DW + HA and DW column systems but was well removed in SMART and sequential biofiltration. These results indicate that there is still a lack of knowledge regarding the determining factors triggering the transformation of TOrCs in biofiltration and MAR systems and therefore, fundamental studies investigating the upregulation of key enzymes by the microbial community by means of metatranscriptome analysis are essential to better understand principles of metabolic and co-metabolic TOrC degradation. Also more detailed analysis of the composition of the biodegradable DOC might help to understand its influence on TOrCs transformation under carbon-limited conditions.

Conflicts of interest

The authors declare no competing financial interest.

Acknowledgements

This study was funded by the German Federal Ministry for Research and Education (BMBF) as part of the TrinkWave Research Project under grant number 02WAV1404. We would like to thank staff members of the Chair of Urban Water Systems Engineering for their technical and analytical support, especially Hubert Moosrainer, Nicole Zollbrecht, Myriam Reif, Wolfgang Schröder and Johann Müller.

Based on the results observed within this study, Hypothesis III that the concentration of refractory carbon (like humic acids) controls TOrCs removal in MAR systems under oxic conditions must be rejected.

8 Genomic Bayesian networks identify trophic strategies in microbiomes of managed aquifer recharge (MAR) systems

This paper is in preparation for submission to the journal *The ISME Journal* as follows[12]:

Hellauer, K., Michel, P., Holland, S.I., Hübner, U., Drewes, J.E., Lauro, F.M., Manefield, M.J., in preparation. Genomic Bayesian networks identify trophic strategies in microbiomes of managed aquifer recharge (MAR) systems. *The ISME Journal*.

[12] This study was performed to test Hypothesis IV that trophic strategies of the microbial community in engineered filtration systems can be distinguished based on genomic features such as genome size and specific clusters of orthologous groups (COGs).

8.1. Introduction

Microorganisms exhibit distinct trophic strategies depending on their habitat. Some organisms do preferentially grow under limited nutrient conditions, so called oligotrophs, and others demand environments which are rich in nutrients, also known as copiotrophs (Poindexter, 1981). In general, copiotrophs have been associated with a *r*-strategy population growth, high growth rate, a strong fluctuation in population size depending on the amount of available nutrients and a poor ability to cope with stressful conditions. Conversely, oligotrophs are characterized by a *K*-strategy growth, low maximum growth rate, a more or less constant population size over time and they may remain viable even under environmental stress (Fierer et al., 2007; Lauro et al., 2009). In addition, Lever et al. (2015) reviewed, that the size of the cell of copiotrophic organisms decreases in case of starvation, while no or only limited change in cell size will be observed for oligotrophs. Differences in the genome size have also been observed between oligotrophs (smaller genome) and copiotrophs (large genome) (Lauro et al., 2009) which may be explained by the 'streamlining theory' describing the reduction of the size but also complexity of the cell to achieve an efficient uptake of available resources (Giovannoni et al., 2014).

Based on a study from Ishida et al. (1989) amongst others, Schut et al. (1997) reviewed that oligotrophic organisms may be distinguished in obligate oligotrophs which are not capable to grow in rich media, and facultative oligotrophs, which are able to grow in poor as well as in rich media. In addition, Fierer et al. (2007) studied the general trophic characteristics of the bacterial phyla *Acidobacteria*, *Bacteroidetes*, *Firmicutes*, *Actinobacteria*, *α-Proteobacteria* and *β-Proteobacteria* in soil from various ecosystems. Thereby, *Acidobacteria* were mainly present in soil with less nutrients (oligotrophs), whereas *β-Proteobacteria* and *Bacteroidetes* could be referred to copiotroph organisms. Though, neither *Firmicutes* and *Actinobacteria*, *nor α-Proteobacteria* could distinctly be related to copio- or oligotrophs. Nevertheless, considering organisms not at phyla but at genus or species levels, trophic strategies may become more clear and could be clustered as either copio- or oligotroph (Fierer et al., 2007).

Lauro et al. (2009) reported, that the traits defining the trophic strategy of an organism have a genetic basis and therefore, the information contained in a bacterial genome can be used to infer its trophic life style. Whilst Lauro et al. (2009) established this approach in the marine environment, it is of interest, whether this concept of genomic markers characteristic for copio- and oligotroph environments could be transferred to other microbiological habitats.

In managed aquifer recharge (MAR) systems, oligotrophic, particularly carbon-limited, conditions are favored for the transformation of many trace organic chemicals (TOrCs) like pharmaceuticals, pesticides or industrial chemicals (Hellauer et al., 2018a; Regnery et al., 2015b). So far, carbon-limitation is defined as a biodegradable dissolved organic carbon concentration (ΔDOC) of less than 1 mg/L (Hoppe-Jones et al., 2012; Regnery et al., 2016). Thereby, ΔDOC is determined by a differential measurement of the DOC concentration in the influent and after a distinct time of infiltration. Organisms which are expected to be dominant under such advantageous carbon-limited conditions can be assigned to oligotrophs. Therefore, it may be suitable to use the genomic information of

the prevailing microbial community in MAR systems, to confirm favorable oligotrophic, carbon-limited conditions.

Based on the approach proposed by Lauro et al. (2009), it was hypothesized that trophic strategies of the microbial community in MAR systems can be distinguished based on genomic features such as genome size and specific clusters of orthologous groups (COGs). To test this hypothesis, organisms which preferentially grow under carbon-limited (oligotroph) or carbon-rich (copiotroph) conditions, respectively, had to be identified. Based on characterized genomic markers in combination with a metagenomic dataset a Bayesian network analysis was performed followed by a sensitivity analysis to establish those markers with the strongest forecasting power.

8.2. Materials and methods

8.2.1. Bacterial genomes

To select for genomic markers characteristic for carbon-rich (further referred to copiotroph) or carbon-limited (further referred to oligotroph) environments, organisms which preferentially grow under these conditions had to be identified. To do so, a growth experiment was performed, followed by a phylogenetic assignment of identified species to elucidate closest relatives. Finally, bacterial genomes were analyzed.

8.2.1.1. Growth experiment

Organisms from copio- and oligotroph environments prevailing in simulated MAR systems were isolated. A detailed description about the laboratory-scale column experiments from which the soil was taken is given elsewhere (Hellauer et al., 2018b; Hellauer et al., 2019). In brief, three soil column set-ups mimicking a MAR system, were fed with either wastewater treatment plant effluent (WWTPE), biofiltered drinking water (DW), or biofiltered drinking water enriched with humic acid solution (DW+HA). The system fed with WWTPE consisted of six soil columns in series in which a reaeration step of the filtered WWTPE was performed prior to the third column. Soil samples extracted from the column directly receiving WWTPE was used to identify copiotrophs and will be called WWTPE in the following. Columns receiving filtrate of the WWTPE (third column of the WWTPE system), DW or DW+HA, respectively, reflect oligotrophic environments and are labeled WF, DW and DW+HA, respectively. Feed water for all columns was saturated with dissolved oxygen. Carbon-limitation is defined as ΔDOC of less than 1 mg/L (Hoppe-Jones et al., 2012), whilst ΔDOC >1 mg/L will be defined as carbon-rich. As the DOC was the only nutrient source which has been quantified in the studies by Hellauer et al. (2018b) and Hellauer et al. (2019), the trophic strategy of the organisms - oligotrophy and copiotrophy - will be referred to as carbon-limited and carbon-rich prevailing conditions, respectively.

One gram of soil sample was rinsed in 800 µL 1 x PBS buffer three times with in-between centrifugation (500 rpm, 30 sec). Cells immobilized on the soil particles were detached by vortexing the soil sample vigorously in specific medium or 1 x PBS buffer (see Table SI-8 1, Table SI-8 2) followed by centrifugation (500 rpm, 30 sec). 100 µL of cell suspension was spread on agar-plates prepared with R2A agar (Difco™ R2A agar, BD, Germany), R2A 1:10 and medium based on influents to the columns WWTPE, WF, DW and DW+HA,

and inoculated for several days (Table SI-8 1, Table SI-8 2). Colonies were randomly picked and cultivated for a second time prior to subsequent analyses.

8.2.1.2. Polymerase chain reaction (PCR) and sanger sequencing

To identify the species of selected colonies that grew from soil characterized by copiotrophic (WWTPE) and oligotrophic (WF, DW, DW+HA) conditions, a colony polymerase chain reaction (PCR) selecting for the 16S gene was performed, followed by sanger sequencing.

The colony PCR was performed after the second cultivation step with the primers 27f_BamHI (5' – ATA TGG ATC CAG AGT TTG ATC CTG GCT CAG – 3') and 1492r_XhoI (5'– ATA TCT CGA GTA CGG YTA CCT TGT TAC GAC TT – 3') (universal primers 27f and 1492r according to Lane (1991)). A total volume of 25 µL was used containing 1 µL reverse and forward primer (Eurofins MWG Operon, Ebersberg, Germany) at a concentration of 5 pmol, 1 µL dimethylsulfoxide (DMSO; Cas-Nr.: 67-68-5; SERVA Electrophoresis GmbH, Heidelberg, Germany), 9.5 µL nuclease free water and 12.5 µL GoTaq® G2 HotStart Master Mix (Promega, Mannheim, Germany). The following program was used for amplification in a Thermocycler primus 96 (PEQLAB, Erlangen, Germany): denaturation at 95 °C for 2 min, followed by ten cycles of denaturation at 95 °C, 30 sec; annealing at 60 °C, 30 sec; elongation at 72°C, 1 min and further 20 cycles of denaturation at 95 °C, 30 sec; annealing at 55 °C, 30 sec; elongation at 72°C, 1 min. Finally, elongation at 72 °C for 5 min was done. At least three putative different organisms of each plate were sent for sanger sequencing with 27f primer (Lane, 1991) (Eurofins MWG Operon, Ebersberg, Germany).

8.2.1.3. Phylogenetic assignment

A nucleotide blast (Altschul et al., 1990) was performed for sequence alignments of each isolated organism. Out of 213 picked and 153 successfully sequenced colonies, copiotrophic and oligotrophic organisms were selected based on distinct criteria like the origin of the organism (growth from soil characterized by oligo- or copiotrophic conditions) but also the ability of the organisms to grow on agar plates rich in carbon (R2A plate) or with less available carbon (WF/WWTPE/DW/DW+HA/R2A 1:10 plate) (Table 8-1).

To determine the closest relative of each isolated organism, a phylogenetic tree was generated including all available type-strains of each specie as reference using MEGA7 (Kumar et al., 2016), whereby bootstrap analysis (1000 replicates) was performed to ensure statistical confidence. The phylogenetic tree was assembled based on the best-fit model identified for each sequence (Table SI-8 3) after sequence alignment using MUSCLE (Edgar, 2004) and trimming.

Table 8-1: Characteristics to identify copiotrophic and oligotrophic organisms based on growth experiment. WWTPE: wastewater treatment plant effluent; WF: effluent of columns receiving WWTPE; DW: drinking water; DW+HA: drinking water augmented with humic acids. Numbers in parenthesis indicate species count based on picked colonies.

Copiotrophs	Oligotrophs
• Growth from soil characterized by copiotrophic conditions* (≥ 3) • Weak/no growth from soil characterized by oligotrophic conditions** (≤ 1) • Growth on R2A plate (≥ 1) • Weak/no growth on WF/WWTPE/DW/DW+HA plates (≤ 2)	• Growth from soil characterized by oligotrophic conditions** (≥ 3) • Weak/no growth from soil characterized by copiotrophic conditions* (≤ 1) • Growth on WF/WWTPE/DW/DW+HA/R2A 1:10 plate (≥ 1) • Weak/no growth on R2A plates (≤ 2)

* columns fed with wastewater treatment plant effluent (WWTPE)
** columns fed with biofiltrated wastewater treatment plant effluent (WF), drinking water (DW) or drinking water augmented with HA (DW+HA)

8.2.2. Identification of genomic markers

To identify specific genomic markers which are characteristic for organisms preferentially growing under copiotrophic or oligotrophic conditions, available genomes of closest sequenced relatives were downloaded from the National Center for Biotechnology Information Reference Sequence Database (NCBI RefSeq; O'Leary et al. (2016)) for further analyses. The quality of each genome was assessed using checkM v1.0.9 (Parks et al., 2015) and only those genomes with a completeness of at least 95 % and less than 3 % contamination were taken into account in the following. If more than one assembly was available for the identified specie that genome was taken which was elucidated based on the workflow shown in Figure SI-8 1. The absolute number of nucleotides was recorded and the number of 16S rRNA copy numbers was determined by use of rnammer 1.2 (Lagesen et al., 2007). Furthermore, PSORTb v.3.0 (Yu et al., 2010) was used to predict subcellular localization of proteins. A protein blast of each open reading frame (ORF) against the clusters of orthologous groups (COG) database (Tatusov, 2000) was performed as previously described in Lauro et al. (2009). By use of STAMP v2.1.3 (Parks et al., 2014), statistically significant differences between individual COG categories were assessed using the following settings: i) statistical test: White`s non-parametric t-test (White et al., 2009), ii) type: one-sided; iii) CI-method: DP: bootstrap (0.95); bootstrapping: 1000 replicates, iv) p-value filter: 0.05000, and v) multiple test correction: Storey FDR (Storey and Tibshirani, 2003). Differences for all other potential genomic markers (genome size, rRNA operon number, protein localization and COG category) were elucidated by applying a student`s *t*-test, one tailed, unpaired with $\alpha < 0.05$.

8.2.3. Metagenomic dataset

The metagenomic dataset used in this study originates from a field experiment at the Taif River, Taif, Saudia Arabia, previously published by Li et al. (2016a). In brief, eight river sediment samples were collected from cross sections (CS) in different depth (5, 25, 50 cm), up- (CS1, CS2) and downstream (CS3, CS4) of a wastewater treatment plant

discharge to the Taif River. The samples upstream of the discharge as well as downstream in greater depth (CS1-5, CS2-5, CS3-50, CS4-50) as well as outside of the riverbed (CS1-C) were referred to as oligotrophic, carbon-limited environments. The samples downstream of the discharge in the shallow sediments were characterized as copiotrophic, carbon-rich environments (CS3-5, CS4-5, CS4-25). Detailed information about the metagenome sequencing and analyses is provided in Li et al. (2016a). COG categories as well as individual COG categories of the metagenomic dataset were elucidated in the same way as described for bacterial genomes in section 8.2.2.

8.2.4. Bayesian network analysis

The challenging tasks dealing with genomic data originates from the high number of feature space (genomic markers) compared to a very limited number of samples. Therefore, this research investigated a methodology to reduce dimensionalities and features space and applied this to Bayes network theory. Although there are some limitations, Bayesian network models are known as a category of graphical probabilistic models which can deal with small data sets (Bookholt et al., 2014).

As described by Zhou (2011), the following advantages can be associated with graphical models:

- simple and intuitive interpretation of the structures of probabilistic models.
- usage to design and motivate new models.
- additional insights into the properties of the model, including the conditional independence properties.
- models can be expressed in terms of graphical manipulations, in which the underlying mathematical expressions are carried along implicitly.

With those capabilities, graphical models such as Bayesian networks appear to be a highly valuable concept for model development in the field of genome classification.

Based on significantly different markers for carbon-limited and carbon-rich preferring organisms of the bacterial genomes as well as information regarding the COG categories and individual COGs of metagenomes, a Bayesian network analysis was performed. To do so, data of genomic and metagenomics data was combined and split into a training and test dataset. The required model workflow is shown in Figure 8-1.

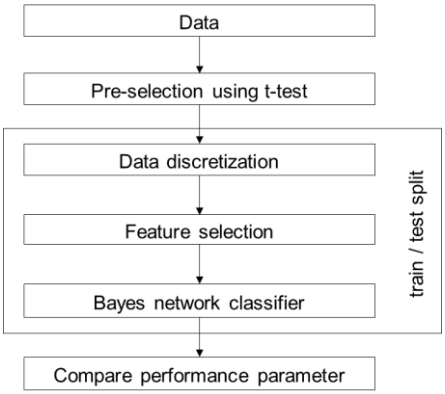

Figure 8-1: Workflow to generate a Bayesian network model.

Central aspects in this workflow are the discretization, feature selection and classifier step. Therefore, some more details are presented next on those components in the workflow.

Discretization of numeric data: The overall target of the final model is to predict the trophic states carbon-rich (copiotrophic) and carbon-limited (oligotrophic). This represents a classification task and in order to reduce the complexity respectively dimensionality of each feature a discretization approach is used. In detail, an equal distance discretization for 2 states (binary features) is applied to all features Although, information loss is inherently connected with this method, it is a well known method and commonly used for Bayesian networks as for example in Friedman and Goldszmidt (1996).

Features selection: Due to the high number of available genomic markers a correlation based attribute selection method has been applied to the data to reduce the feature space (Hall et al., 2009).

Bayes Network classifier: Bayesian network classifiers consist of a network structure and this research focused on three different strategies to derive them. Conditional independence is a central requirement to learn Bayes network. Here the chosen learning algorithms cover different interpretation of conditional independence. All classifiers are part of the Weka software tool set and can be reviewed in the software documentation (Bouckaert, 2004):

- **CI search algorithm:** The CI-search algorithm class supports Bayes net structure search algorithms that are based on conditional independence test (as opposed to for example score based of cross validation based search algorithms).
- **ICS search algorithm:** This Bayes Network learning algorithm uses conditional independence tests to find a skeleton, finds V-nodes and applies a set of rules to find the directions of the remaining arrows.
- **Tree Augmented Naïve Bayes (TAN) algorithm:** This Bayes Network learning algorithm determines the maximum weight spanning tree and returns a Naïve Bayes network augmented with a tree. Conditional independence is here assumed as given.

To assess the performance of the model, the indicators i) *AUC* (Provost and Domingos, 2003) and related parameter AUROC (Fawcett, 2004), ii) *Recall* (Witten et al., 2016) *and iii) Kappa statistic* (Witten et al., 2016) were used . Michel et al. (in preparation) provides more in depth explanation on this performance indicator set for classification.

8.2.5. Validation

To further test if the developed approach is suitable to predict trophic strategies of microbial communities in engineered filtration systems, the proposed model which consisted of genomic markers of the bacterial genomes as well as the metagenomic dataset from a field experiment in Saudi Arabia (Li et al., 2016a) was applied to the test dataset.

8.3. Results

8.3.1. Identification of carbon-rich and carbon-limited preferring organisms

Cultivation and subsequent sanger sequencing resulted in a total of 32 different species out of 153 successfully sequenced colonies. All detected organisms and their abundance are provided in the supplementary information (Table SI-8 4). *Pseudomonas* and *Flavobacterium* were identified as carbon-rich preferring organisms (copiotrophs), whereas *Brevundimonas*, *Caulobacter*, *Cupriavidus*, *Microbacterium*, *Nocardia*, *Rheinheimera*, *Sphingopyxis* and *Tsukamurella* were classified as carbon-limited preferring species (oligotrophs) based on criteria given in Table 8-1. After phylogenetic assignment of each sequence against available type strains, closest relatives were identified (Table SI-8 3) and genomes were downloaded. In case of *Rheinheimera*, no genomes of any close relative species were available and therefore, this species was not included in the analysis. For all other species, at least one high-quality genome (completeness > 95%, contamination < 3%) was available to identify genomic markers. All identified species including their Accession number, date of download from RefSeq, as well as quality metrics are given in Table 8-2

Table 8-2: Bacterial genomes used for identification of genomic markers, RefSeq Accession nr., date of download as well as the quality hits based on checkM v1.0.9 (Parks et al., 2015) are given.

	Species	Accession Nr.	date of download	checkM – completeness [%]	checkM – contamination [%]
oligotrophs	*Brevundimonas nasdae* TPW30	GCF_000813765	11.10.2017	99.68	0.81
	Brevundimonas vesicularis FDAARGOS_289	GCF_002208825	11.10.2017	99.68	1.03
	Caulobacter segnis ATCC 21756	GCF_000092285	11.10.2017	99.68	0.49
	Caulobacter vibrioides T5M6	GCF_001449105	11.10.2017	99.68	0.65
	Cupriavidus oxalaticus NBRC 13593	GCF_001592245	11.10.2017	99.94	0.03
	Microbacterium maritypicum MF109	GCF_000455825	11.10.2017	98.74	0.51
	Microbacterium oxydans Moxy_1 (Isolate)	GCF_900095745	11.10.2017	100.00	0.00
	Nocardia asteroides NBRC 15531	GCF_000308355	11.10.2017	99.37	2.11
	Sphingopyxis alaskensis RB2256	GCF_000013985	11.10.2017	99.98	0.00
	Sphingopyxis bauzanensis DSM 22271	GCF_002205675	11.10.2017	99.30	1.73
	Sphingopyxis flava R11H	GCF_900168005	24.05.2018	99.30	2.21
	Sphingopyxis indica DS 15	GCF_900188185	24.05.2018	99.98	0.68
	Tsukamurella pulmonis DSM44 142	GCF_001575205	14.05.2018	99.94	0.52
	Tsukamurella pseudospumae JCM 13375	GCF_900103175	16.05.2018	100.00	0.98
copiotrophs	*Flavobacterium saliperosum* CGMCC 1.3801 (CFB group bacteria)	GCF_900100625	02.05.2018	99.65	0.06
	Flavobacterium limnosediminis JC2902 (CFB group bacteria)	GCF_000498535	02.05.2018	99.65	0.50
	Flavobacterium cauense R2A-7 (CFB group bacteria)	GCF_000498475	11.10.2017	99.65	0.00
	Pseudomonas stutzeri 28a24	GCF_000590475	11.10.2017	99.80	0.14
	Pseudomonas vranovensis DSM 16006	GCF_000425805	11.10.2017	100.00	0.75
	Pseudomonas cichorii JBC1	GCF_000517305	02.05.2018	100.00	0.43
	Pseudomonas plecoglossicida NyZ12	GCF_000831585	02.05.2018	99.87	2.19
	Pseudomonas trivialis IHBB745	GCF_001186335	02.05.2018	99.66	0.23
	Pseudomonas lurida MYb11	GCF_002966835	02.05.2018	99.59	0.41
	Pseudomonas paralactis DSM 29164	GCF_001439735	02.05.2018	99.80	0.40

8.3.2. Characterization of genomic markers

Genomic markers which are significantly different between copiotrophs and oligotrophs are listed in Table 8-3 (individual COG categories are shown in Table SI-8 5). Even though no significant difference between the genome size of copio-/oligotrophs was observed, this information was included in the list as it has previously been shown that oligotrophic organisms have a smaller genome as copiotrophs (Lauro et al., 2009). Oligotrophs were characterized by only a few rRNA operon copy numbers, whereby copiotrophs exhibit several. It was further observed that proteins localized on the cell wall are characteristic for oligotrophs as well as genes involved in the biosynthesis, transport and catabolism of secondary metabolites (COG category Q), lipid transport and metabolism (COG category I) but also in general functions (COG category R). On the other hand, a higher number of proteins localized in the outer membrane and periplasm is typical of copiotrophs and

additionally, genes involved in coenzyme transport and metabolism (COG category H) and signal transduction mechanisms (COG category T) are more dominant. A total number of 167 significantly different individual COG categories were elucidated (Table SI-8 5) with 143 more abundant for oligotrophs and 24 more dominant with copiotrophs. Most of the individual COGs belong to the COG categories associated with metabolism (C, I) and information storage and processing (K, L) but also with unknown or general predicted functions (S, R). Thereby, the individual COGs associated to these COG categories are mainly higher in oligotrophs which is, in case of COG categories I and R in accordance to the observations made regarding the significant different COG categories (Table 8-3). However, individual COG categories associated with inorganic ion transport and metabolism (COG category P) were more dominant in copiotrophs.

Table 8-3: Genome characteristics enabling differentiation between copiotrophs and oligotrophs including general parameters, protein localization and COG categories.

parameter	copiotroph (median)	oligotroph (median)	total median	p-value
general				
Genome size (bp)[a, b]	large (5'841'910)	small (4'206'652)	4'693'491	0.1818[b]
rRNA operon numbers[a]	many (3)	few (1)	1	0.0198
Protein localization				
Cellwall[c]	low (0.00 %)	high (0.00 %)	0.00 %	0.0397
Outer Membrane[a]	high (2.60 %)	low (2.35 %)	2.50 %	0.0382
Periplasmic[a]	high (2.98 %)	low (1.94 %)	2.21 %	0.0327
COG category				
H (Coenzyme transport and metabolism)	high (4.38 %)	low (4.04 %)	4.20 %	0.0358
T (Signal transduction mechanisms)[a]	high (10.12 %)	low (5.95 %)	6.63 %	0.0122
Q (secondary metabolite biosynthesis, transport and catabolism)[a]	low (3.53 %)	high (3.96 %)	3.62 %	0.0152
I (lipid transport and metabolism)[a]	low (4.24 %)	high (7.01 %)	4.96 %	0.0002
R (General functional prediction only)	low (9.74 %)	high (11.06 %)	10.72 %	0.0000

[a]in accordance to Lauro et al. (2009)
[b]not significantly different
[c]five out of 14 carbon-limited organisms had proteins localized on the cellwall, zero out of ten in case of carbon-rich organisms.

In addition to the information about the relative abundance of the identified genomic markers of the bacterial genomes (Table 8-3, Table SI-8 5), the relative abundance of the identified genomic markers regarding COG categories and individual COGs of the metagenomic data were elucidated. As shown in Table 8-4, the COG categories H, Q and R behave similarly for genomes and metagenomes. On the contrary, COG category T is low and COG category I is high for copiotrophs derived from metagenomes while the opposite applies to bacterial genomes (Table 8-3, Table 8-4). With respect to the individual COG categories, 53 out of 167 exhibit the same trend regarding the abundance for copio-/oligotrophic samples (Table SI-8 5).

Table 8-4: Relative abundance of COG categories of metagenomes.

COG category	copiotroph (median)	oligotroph (median)	total median
H (Coenzyme transport and metabolism)	high (4.19%)	low (4.10%)	4.11%
T (Signal transduction mechanisms)	low (6.21%)	high (7.19%)	6.94%
Q (Secondary metabolites biosynthesis, transport and catabolism)	low (3.67%)	high (4.02%)	3.87%
I (Lipid transport and metabolism)	high (5.31%)	low (4.63%)	4.76%
R (General function prediction only)	low (9.77%)	high (10.92%)	10.78%

8.3.3. Bayesian network analysis

The (individual) COG categories which are significantly different between copiotrophs and oligotrophs (Table 8-3, Table SI-8 5) were used in combination with data derived from metagenomes (Table 8-4, Table SI-8 5) to establish a Bayesian model. Thereby, data were randomly split into training and test data sets (c.f. Figure 8-1). Three structure learning strategies were applied to generate a Bayesian model: i) CI search algorithm, ii) ICS search algorithm, and iii) TAN algorithm. All three strategies resulted in a valid model (Table 8-5) composed of the same markers. However, due to the less promising performance of ICS in comparison to CI and TAN algorithm (Table 8-5), ICS search algorithm will be excluded for further application within this study. The network as well as the sensitivity analysis of the ICS search algorithm is provided in the SI (Figure SI-8 2, Table SI-8 6).

Table 8-5: Performance indicators of three tested strategies.

	Validation (stdev)		
Network / Parameter	CI network	ICSS network	TAN network
Recall	0.92 (0.15)	0.87 (0.20)	0.95 (0.13)
AUROC	0.99 (0.04)	0.95 (0.14)	0.98 (0.08)
Kappa	0.82 (0.33)	0.71 (0.42)	0.89 (0.27)

The successfully established models derived from the TAN and CI search algorithms are comprised of two COG categories and nine individual COGs which are listed in Table 8-6. The sensitivity of these eleven genomic markers is similar between the TAN and the CI search algorithm and the models derived from both networks are not significantly different. The use of either TAN or CI search algorithm depends on the conditional independency of the COG categories. If a conditional independency between COG categories used as genomic markers can be expected to be unlikely, the TAN algorithm would be used rather than the CI search algorithm. In summary, valid Bayesian models to predict prevailing trophic strategies could be generated on the basis of genomic markers derived from bacterial genomes by use of a combination of a genomic and metagenomic dataset. The TAN network graph of the genomic markers for predicting the trophic strategies oligotrophy and copiotrophy are shown in Figure 8-2, the CI search network graphs are represented in Figure 8-3.

Table 8-6: Sensitivity analysis of TAN and CI network.

		Mutual Info	Percent	Variance of Belief
TAN network	Class*	0.97602	100	0.2417355
	COG_category_R	0.50768	52	0.1478387
	COG0491	0.48439	49.6	0.1454875
	COG0596	0.35909	36.8	0.1036073
	COG0640	0.34746	35.6	0.1011201
	COG4941	0.28654	29.4	0.0898298
	COG1595	0.28639	29.3	0.0897850
	COG_category_Q	0.27509	28.2	0.0790371
	COG1028	0.23333	23.9	0.0739349
	COG0265	0.22879	23.4	0.0637869
	COG0761	0.18799	19.3	0.0601541
	COG1062	0.14498	14.9	0.0468853
CI Network	Class*	0.97602	100	0.2417355
	COG_category_R	0.58497	59.9	0.1653122
	COG0491	0.54822	56.2	0.1616355
	COG0640	0.39826	40.8	0.1125167
	COG0596	0.39826	40.8	0.1125166
	COG4941	0.33636	34.5	0.1021312
	COG1595	0.33636	34.5	0.1021312
	COG_category_Q	0.30585	31.3	0.0857929
	COG1028	0.27755	28.4	0.0850520
	COG0265	9.22879	23.4	0.0637869
	COG0761	0.22400	23	0.0692650
	COG1062	0.17501	17.9	0.0546508

*class refers to the trophic strategies copiotrophy and oligotrophy.

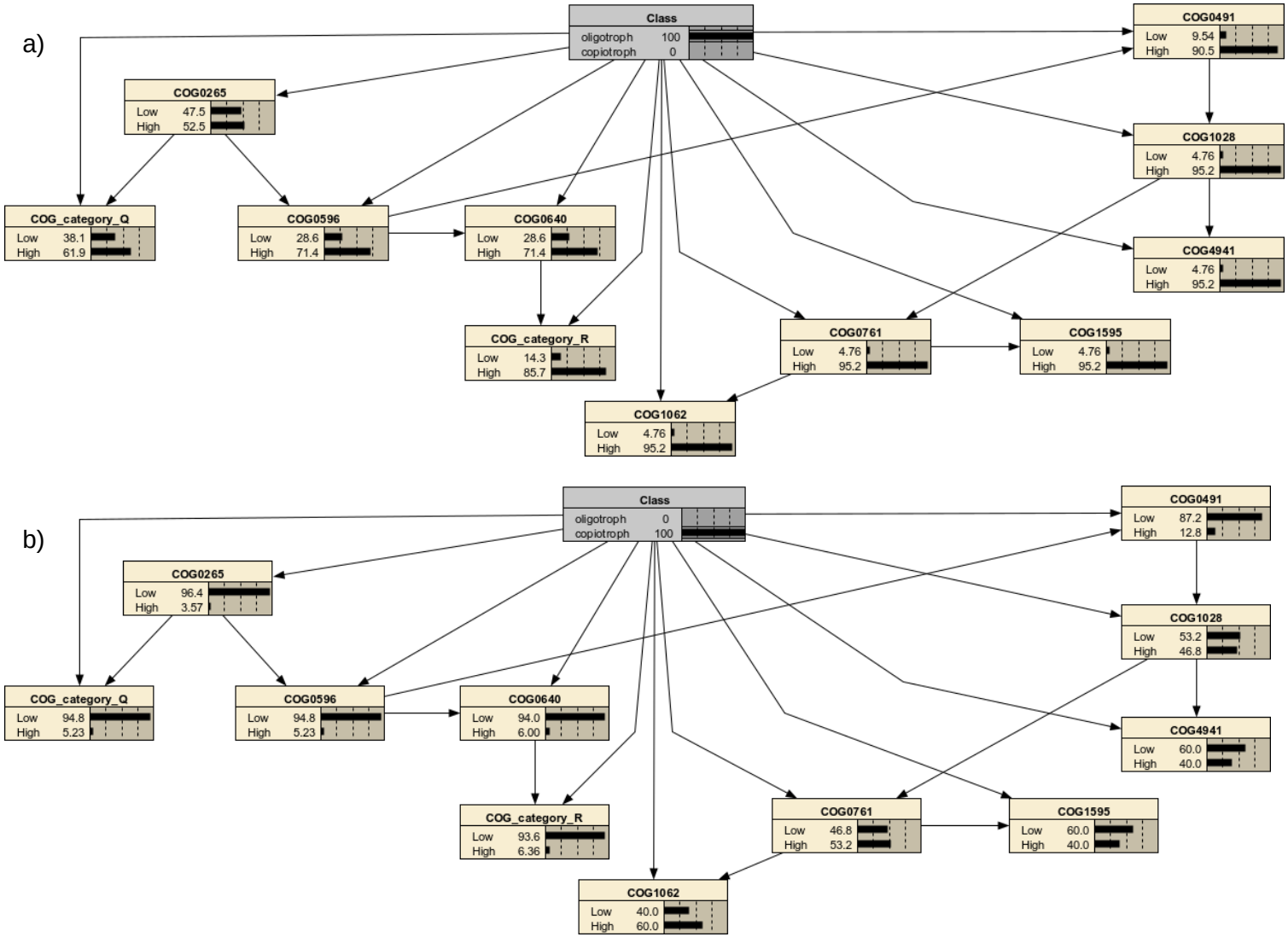

Figure 8-2: TAN network graph for the prediction of the trophic strategies a) oligotrophy and b) copiotrophy.

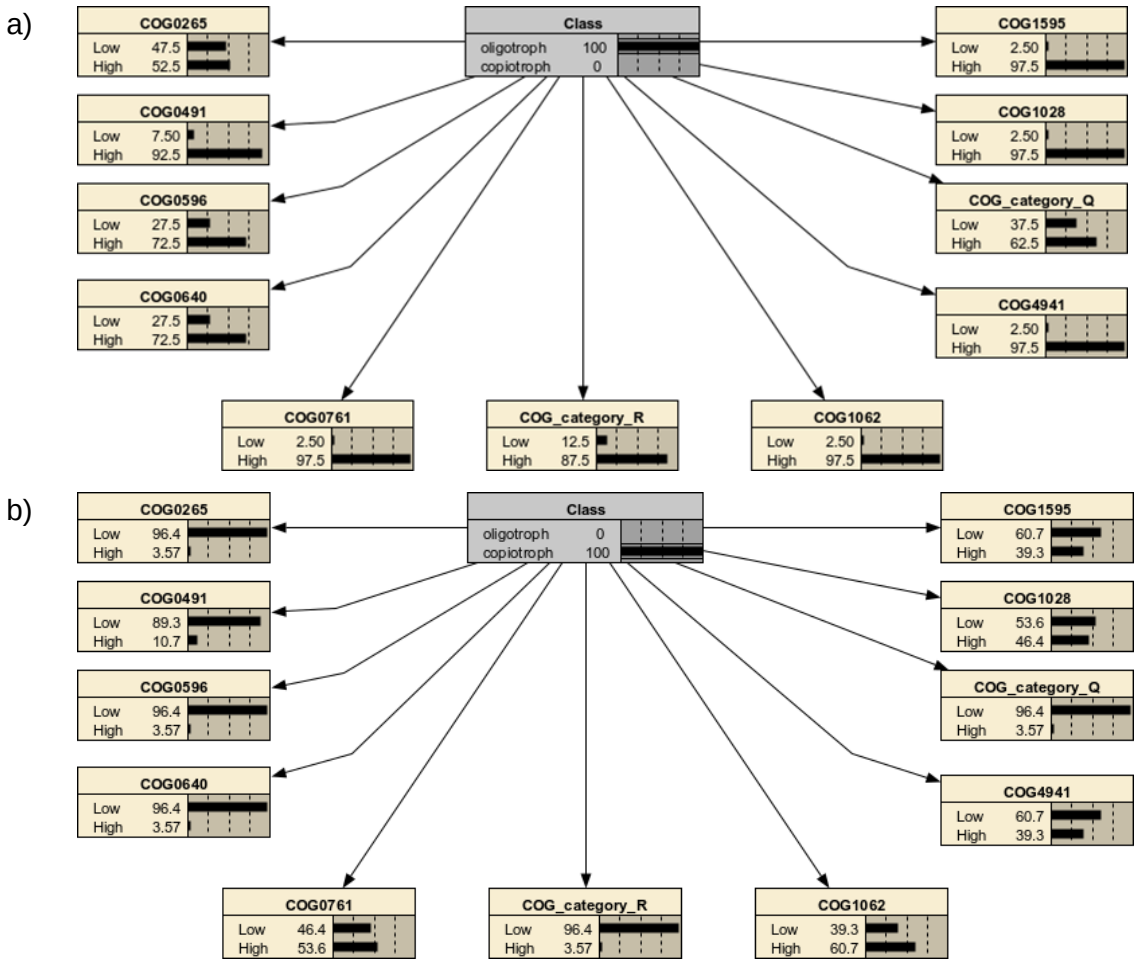

Figure 8-3: CI network for the prediction of the trophic strategies a) oligotrophy and b) copiotrophy.

8.4. Discussion

Bacteria from a model MAR system that grow preferentially under carbon-rich conditions (*Flavobacterium*, *Pseudomonas*) or under carbon limitation (*Brevundimonas*, *Caulobacter*, *Cupriavidus*, *Microbacterium*, *Nocardia*, *Sphingopyxis* and *Tsukamurella)*, were identified based on cultivation on agar plates. With respect to the principle of facultative vs. obligate oligotrophs, organisms identified as carbon-limited preferring species may be assigned as facultative rather than obligate oligotrophs (Koch, 2001; Schut et al., 1997). Furthermore, most organisms may not be seen as strict oligotrophs/copiotrophs due to their wide range of physiological capabilities (Ho et al., 2017). Nevertheless, based on the plate counts a distinct categorization regarding carbon availability could be made resulting in two groups of organisms enabling identification of genomic markers representative for prevailing carbon conditions.

It is well established that the rRNA operon copy number of microorganisms serves as a surrogate for their ability to utilize nutrients available in the environment (Klappenbach et al., 2000; Roller et al., 2016). In accordance to Lauro et al. (2009), significantly higher rRNA operon numbers were observed for copiotrophs in comparison to oligotrophs (Table 8-3). Even though the difference in genome size was not significant, a general trend showing larger genomes for copiotrophs and smaller genomes for oligotrophs was obtained which is in line with recent studies indicating that small genomes could be advantageous for living in oligotrophic environments such as oceans (Swan et al., 2013). Furthermore, proteins localized in the outer membrane and periplasm are more abundant in carbon-rich preferring organisms as previously shown for copio- and oligotrophic organisms in the marine environment (Lauro et al., 2009). The significantly higher content of proteins localized in the cell wall of carbon-limited preferring organisms may be biased due to the fact that Gram positive bacteria (*Nocardia*, *Microbacterium*, *Tsukamurella*) were assigned to carbon-limited preferring organisms within this study. Similar to copiotrophic organisms in the marine environment (Lauro et al., 2009) and bacteria found in Mediterranean semiarid soils characterized by high soil DOC (Bastida et al., 2016), carbon-rich preferring species in simulated MAR systems have a higher abundance of genes encoding proteins which could be assigned to signal transduction mechanisms (COG category T). In addition, proteins involved in coenzyme transport and metabolism (COG category H) were enriched in copiotrophs. Oligotrophs were enriched in COGs for lipid transport and metabolism (COG category I) as well as secondary metabolites biosynthesis, transport and catabolism (COG category Q), which confirms findings previously made in the marine environment (Lauro et al., 2009) including among others Cytochrome P450 (COG2124). A probable contribution of Cytochrome P450 on the transformation of TOrCs in MAR systems was previously proposed by Li et al. (2014a), who observed a higher abundance of genes encoding for Cytochrome P450 under carbon-limited, highly refractory carbon conditions. These results may further support the assumption that oligotrophic conditions are favored for an enhanced TOrCs removal.

Based on identified genomic markers, Bayesian models could be generated. The models were trained and tested by a combination and random split of genome and metagenome data resulting in a set of eleven genomic features. Even though, all these markers are more abundant in the bacterial genome of oligotrophs compared to copiotrophs (Table 8-3,

Table SI-8 5), the genomic features are able to predict prevailing carbon-rich (copiotrophic) as well as carbon-limited (oligotrophic) conditions within a network as a function of their individual abundance. This could be explained due to the fact how the dataset was discretized and hence, the combination of COG categories with their abundance within a network lead to a statistically proposed probability of prevailing copiotrophic or oligotrophic conditions. Due to the fact, that the genomic marker COG0761 behaved differently in the metagenome dataset (high for copiotroph, low for oligotroph; Table SI-8 5) in comparison to the bacterial genomes (low for copiotroph, high for oligotroph; Table SI-8 5), its influence on the prediction of copiotrophic conditions is limited for both models (TAN and CI search algorithm) as could be seen in Figure 8-2b and Figure 8-3b. However, to obtain more robust models the use of larger datasets in future studies is highly recommended.

8.5. Conclusion

Genomic markers identified from bacterial genomes in combination with a metagenomic dataset were used to predict prevailing trophic strategies of microbial communities in MAR systems. A workflow to identify trophic strategies of the abundant taxa of the microbial community in MAR systems was developed based on genomic features such as genome size and specific clusters of orthologous groups (COGs). Remarkably, in contrast to marine environments, genome size was not a suitable marker for predicting prevailing carbon conditions in engineered filtration systems. The approach established within this study will provide a suitable concept to predict favorable oligotrophic conditions for an enhanced transformation of TOrCs during MAR using metagenomic data. Nevertheless, it is strongly suggested to use larger datasets for the establishment of more robust models.

Acknowledgements

This study was funded by the German Federal Ministry for Research and Education as part of the TrinkWave project (BMBF, grant number: 02WAV1404). We would like to thank all involved colleagues from the School of Civil and Environmental Engineering and School of Chemical Engineering (University of New South Wales) as well as from the Chair of Urban Water Systems Engineering (Technical University of Munich) for their technical and analytical support, especially Dr. Bastian Herzog, Hubert Moosrainer, Nicole Zollbrecht, Myriam Reif, Ursula Wallentits, Heidrun Mayrhofer and Sara Mayerlen. Furthermore, we want to gratefully acknowledge Dr. Dong Li for providing continuous feedback regarding the metagenomic data and Dr. Christian Wurzbacher for proofreading the manuscript. We also would like to thank the German Academic Exchange Service (DAAD) for the financial support for Karin Hellauer during her stay at the University of New South Wales, Australia and TUM's International Program to support Mike Manefield with an August-Wilhelm Scheer Visiting Professorship.

Competing Interests

The authors declare no competing financial interest.

Based on the results of this study, Hypothesis IV that trophic strategies of the microbial community in engineered filtration systems can be distinguished based on genomic features such as genome size and specific clusters of orthologous groups (COGs) could only partly be confirmed. In general, the outcome emphasizes the usage of genomic markers (COG categories and individual COG categories) to predict the trophic strategy of the prevailing microbiome in MAR systems. However, the proposed applicability of the genome size as possible marker must be rejected.

9 Discussion and outlook

Throughout this dissertation project, a broad spectrum of approaches, methods, analyses and concepts from various disciplines were applied to further investigate the underlying biotransformation mechanisms of the SMART concept under conditions prevailing in the case study Berlin and to assess the influence of BDOC on the transformation of TOrCs during MAR.

Firstly, the application of SMART was tested considering environmental and operational conditions in Berlin (**chapters 4** and **5**) with the focus on

- a conceptual design of the laboratory-scale and field experiments;
- the procedural implementation of SMART;
- investigating transformations of TOrCs as a function of different intermediate aeration techniques (**chapter 4**) as well as with respect to differences between SMART and conventional MAR during full-scale investigations (**chapter 5**).

The second approach targeted the hypothesis that the fate of molecular components and characteristic functional groups of the primary substrate correlates with the degradation of structurally similar TOrCs (**chapter 6**). Thereby, the aim was

- to perform a detailed analyses of the composition of the DOC using advanced analytical tools, including (-)ESI FT-ICR-MS in combination with other spectroscopic methods (3D-fluorescence; UVA_{254}, SUVA);
- to derive a correlation of characteristics of the organic matter composition with TOrCs during SMART to identify potentially common properties of DOC and TOrCs;
- and to elucidate the microbial community structure as a function of the composition of the DOC and linking microbial phyla distributions to observed transformation of TOrCs during SMART.

A further task during this dissertation project was to test the hypothesis that the concentration of refractory carbon (like humic acids) controls TOrCs removal in MAR systems under oxic conditions (**chapter 7**). The key aspects were to

- monitor DOC composition using 3D-fluorescence spectroscopy in addition to DOC, UVA_{254} and color (436 nm) measurements;
- determine the TOrCs transformation as a function of highly refractory primary substrate applied at different concentrations;
- compare the efficiency of TOrCs transformation under oxic and carbon-limited conditions considering findings from various studies (laboratory-scale SMART using oxygen as intermediate oxidant (**chapter 4**), field-scale SMART (**chapter 5**), sequential biofiltration (Müller et al., 2017), this study (**chapter 7**));
- highlight possible degradation pathways using the Eawag-BBD Pathway Prediction System (Gao et al., 2010).

The fourth main emphasis relied on the concept of oligotrophy and copiotrophy as trophic strategies of microbial communities testing the hypothesis that “trophic strategies of the microbial community in engineered filtration systems can be distinguished based on genomic features such as genome size and specific clusters of orthologous groups (COGs)”. To do so,

- a growth experiment was performed to determine carbon-rich and /-limited preferring organisms based on soil of column studies investigated in **chapters 6** and **7**;
- bacterial genomes were analyzed to emphasize characteristics for either carbon-rich or /-limited preferring organisms;
- Bayesian network analyses were carried out by use of identified genomic markers to establish a model which could generally be applied using (meta)genomic data to elucidate prevailing carbon conditions within MAR systems.

In the following sections the main outcomes of this dissertation project will be discussed with respect to the latest literature. Strengths and weaknesses of applied approaches, methods and strategies will be highlighted and recommendation for future studies will be provided.

9.1. Sequential managed aquifer recharge as promising tool for improved water quality

9.1.1. Transformation of TOrCs under oxic and carbon-limited conditions

In **chapters 4** and **5** the hypothesis “SMART can result in improved removal of potentially health relevant TOrCs compared to currently practiced MAR systems in Berlin” was tested at laboratory- and field-scale. During the laboratory-scale experiment (**chapter 4**) favorable oxic conditions could not be established in the SMART air system as oxygen was rapidly consumed after reaeration resulting in suboxic to anoxic redox conditions. Oxic redox conditions solely prevailed after treatment with pure oxygen or oxidation with ozone, respectively. A strong DOC depletion (> 1 mg/L) was observed in SMART air and SMART O_2 indicating an insufficient DOC removal in the first infiltration step. Hence, carbon-limited conditions were not present, which may be explained by the presence of particulate organic carbon (POC) in the soil of the first column. Infiltration through sediments rich in organic carbon (e.g. POC) leads to a high oxygen consumption and could further hamper DOC removal (Filter et al., 2017). At the field sites, favorable carbon-limited and oxic conditions prevailed at the SMART facility in comparison to cMAR (**chapter 5**). Even though the water was reaerated by directing the bank filtrate over a heap of rocks prior to infiltration, it was not fully saturated with dissolved oxygen (DO = 6.5 ± 1.1 mg/L). Furthermore, the consumed oxygen could not be correlated with the slight degradation of DOC of the carbon-depleted bank filtrate (ΔDOC_{200cm} = 0.2 ± 0.2 mg/L) which could rather be a result of POC originating from for instance leaves of adjacent trees present at the basin (Bayarsaikhan et al., 2018; Filter et al., 2017).

Even though favorable conditions were not fully present in SMART air and SMART O_2, the transformation of TOrCs was similar or even better in comparison to the BF system (see

chapter 4.3.3). Under carbon-limited and oxic conditions at the SMART field site, removal rates of all biodegradable TOrCs were higher at the SMART field site as at cMAR site (Figure 9-1). Especially removal of compounds like 4-FAA, gabapentin and benzotriazole was significantly increased in SMART at lab- and field-scale compared to BF/cMAR. To conclude, both experiments (laboratory- and field-scale) indicated a successful applicability of SMART under field conditions in Berlin confirming the proposed hypothesis. It could be emphasized that oxic redox conditions as well as a limited availability of easily degradable organic carbon enhance the attenuation of biodegradable TOrCs. However, several aspects have to be considered prior to final implementation which will be discussed in section 9.1.2.

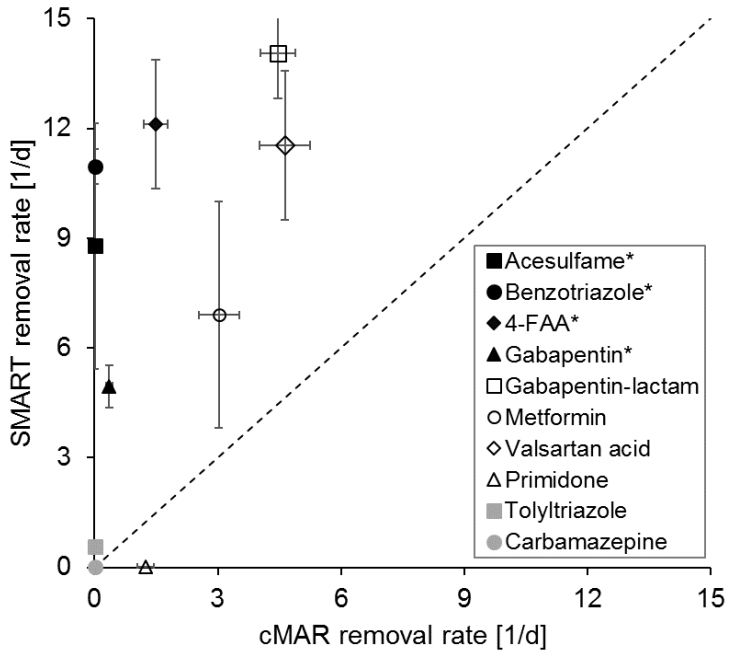

Figure 9-1: Comparison of first order removal rate derived from SMART and cMAR. Error bars indicate standard deviation; *significantly better transformed during SMART. Data derived from Hellauer et al. (2018a) (chapter 5).

The transformation of TOrCs in simulated SMART systems was also part of studies discussed in **chapters 6** and **7**. For many compounds during these studies, the transformation was sufficient at the established oxic and carbon-limited conditions. A summary of targeted TOrCs throughout this dissertation project is given in Table 9-1.

Table 9-1: Removal of all targeted TOrCs throughout this dissertation project.

	Chapter 4 Hellauer et al. (2017)	**Chapter 5** Hellauer et al. (2018a)	**Chapter 6** Hellauer et al. (2018b)	**Chapter 7*** Hellauer et al. (2019)
Prevailing conditions / **Compound**	BF: anoxic, not carbon-limited SMART air: suboxic, partly carbon-limited SMART O_2 and O_3: oxic, partly carbon-limited	cMAR: suboxic, not carbon-limited SMART: oxic, carbon-limited	Suboxic to anoxic; partly carbon-limited	Oxic; carbon-limited
Removal independent of prevailing redox conditions				
Efficient degradation during MAR (BF, cMAR) and SMART				
Atenolol	n.a.	n.a.	n.a.	> LOQ
Citalopram	n.a.	n.a.	MAR	n.a.
Gabapentin-lactam	n.a.	MAR	n.a.	n.a.
Iomeprol	MAR	n.a.	n.a.	n.a.
Iopromide	MAR	n.a.	n.a.	> 45%
Metformin	n.a.	MAR	n.a.	n.a.
Valsartan	MAR	n.a.	n.a.	n.a.
Poor degradation or persistent behavior during MAR (BF, cMAR) and SMART				
Diatrizoic acid	persistent	n.a.	n.a.	n.a.
Dihydroxydihydro-carbamazepine	n.a.	persistent	n.a.	n.a.
Oxypurinol	n.a.	persistent	n.a.	n.a.
Phenytoin	n.a.	n.a.	n.a.	persistent
Phenazone	n.a.	n.a.	n.a.	persistent
Phenylethylmalonamide	n.a.	persistent	n.a.	n.a.
Primidone	n.a.	poorly	persistent	persistent
Carbamazepine	persistent	persistent	persistent	persistent
Olmesartan	persistent	persistent	n.a.	n.a.
Candesartan	persistent	persistent	n.a.	n.a.
Tolyltriazole	MAR†	poorly	n.a.	n.a.
Removal dependent of prevailing redox conditions (significantly enhanced removal during SMART)				
Valsartan acid	SMART	MAR	n.a.	n.a.
Climbazole	n.a.	n.a.	SMART	n.a.
Acesulfame	MAR	SMART	n.a.	n.a.
4-FAA	SMART	SMART	n.a.	n.a.
Diclofenac	SMART	n.a.	SMART	> 75%
Gabapentin	SMART	SMART	SMART	> 45%
Metoprolol	SMART	n.a.	SMART	> 75%
Sotalol	n.a.	n.a.	SMART	n.a.
Sulfamethoxazole	-	n.a.	MAR	> 75%
Tramadol	n.a.	n.a.	SMART	n.a.
Venlafaxine	SMART	n.a.	SMART	> LOQ
Benzotriazole	SMART	SMART	SMART	poorly

n.a. not evaluated
MAR: removal observed even under conventional MAR treatment (BF, cMAR).
SMART: removal significantly enhanced after reaeration.
-: no statement possible due to incomplete adaptation.
* no comparison between SMART and MAR possible; removal efficiencies described in percentage removal or removal below LOQ (< LOQ). See **chapter 7** for more detailed information.
† 5-Methyl-1H-benzotriazole

At a first glance, many similarities regarding TOrCs transformation between the different studied systems appear. For instance, the persistent compounds carbamazepine and primidone were not or only poorly removed during MAR or SMART, respectively, which is in accordance to earlier studies reported in the literature (Burke et al., 2017; Clara et al., 2004; Hass et al., 2012). Also 4-FAA which is known to be biodegradable to a certain extent under oxic redox conditions (Burke et al., 2017; Massmann et al., 2008a) showed equal removal in systems studied within this dissertation project (c.f. **chapters 4** and **5**). In addition, gabapentin exhibited removal of > 45% under mainly oxic and carbon-limited conditions in all systems (**chapters 4** to **7**). This is in accordance to a recently published study by Henning et al. (2018) who observed an efficient gabapentin removal in bench-scale experiments under aerobic conditions but no significant attenuation under anaerobic conditions as well as to results reported by Schaper et al. (2018), who pointed out that gabapentin could be removed in the hyporheic zone under oxic/suboxic but not under anoxic redox conditions. This indicates the high redox sensitivity of gabapentin during MAR.

It also seems very likely that diclofenac generally responses to oxic and carbon-limited conditions as in all studied systems an efficient removal was observed. This confirms a previous study by Regnery et al. (2015b), who observed a complete attenuation of diclofenac under oxic and carbon-limited conditions. However, Müller et al. (2017) recently reported a diclofenac elimination of only 29% during sequential biofiltration characterized by carbon-limited and oxic to suboxic conditions. A similar phenomenon was observed for venlafaxine which could be removed below the LOQ in columns fed with DW or DW+HA (**chapter 7**). However, in laboratory-scale SMART O_2, a removal of < 30% after reaeration was reported (**chapter 4**) and in case of sequential biofiltration, venlafaxine persisted (Müller et al., 2017). On the contrary, a poor removal of benzotriazole under oxic and carbon-limited conditions was observed (**chapter 7**) while an efficient transformation of > 70% was monitored in SMART O_2 (**chapter 4**), field-scale SMART (**chapter 5**) as well as sequential biofiltration (Müller et al., 2017). Schaper et al. (2018) could measure a benzotriazole removal of approximately 50% during infiltration through the hyporheic zone, while the attenuation was significant under oxic/suboxic conditions. Further, the compound phenazone persisted under oxic and carbon-limited conditions (**chapter 7**) even if oxic redox conditions were described as favorable for the attenuation of phenazone (Burke et al., 2017; Massmann et al., 2008a).

Even though the boundary conditions (prevailing redox and carbon conditions) seem to be similar, significantly different behavior of several TOrCs could be observed. The reason may be found in the composition of the feed water. However, the sequential biofiltration system (Müller et al., 2017) as well as the SMART system used in **chapter 6** were fed with the same feed water quality (tertiary treated WWTP effluent, Garching, Germany) which weakens this assumption. Nevertheless, minor compositional differences regarding the DOC may have a dominant effect on TOrCs behavior. This highlights the great importance of further studying DOC composition in more detail. Different HRT may be another possibility but this seems also unlikely, as the sequential biofiltration system (Müller et al., 2017) performed better with respect to benzotriazole transformation in comparison with DW and DW+HA columns even at shorter travel times (**chapter 7**). The reason for the different behavior of TOrCs even under similar redox and carbon conditions might be the

biotransformation pathways of TOrCs and enzymes involved therein. By use of the Eawag Biocatalysis/Biodegradation Database (Gao et al., 2010) most likely pathways of each TOrC could be predicted. Many of the TOrCs which exhibited removal in most of the studied systems (e.g., gabapentin, metoprolol, tramadol and venlafaxine) follow the pathway rule #bt0063 which describes the oxidative elimination of an R residue from an amine like dealkylation or deamination, while different pathways were assigned to diclofenac (#bt0065) or benzotriazole (#bt0005). Systems may harbor a different microbial community structure which may further result in a different functionality. The microbial community structure can be assessed using 16S rRNA amplicon sequencing (Engel et al., 2018; Li et al., 2012; Li et al., 2013) and the functionality via metagenomics (Drewes et al., 2014; Li et al., 2014a) and/or metatranscriptomics (Yu et al., 2012). Metagenome analyses are applied to gain information about all genes present in the studied sample, while it is not possible to asses if the genes are active or not. Therefore, metatranscriptome analyses can be applied which allow a better understanding of the transcriptional activity of the prevailing microbiome (Hassa et al., 2018; Simon and Daniel, 2011). Both techniques, metagenome and metatranscriptome analyses will be helpful to further elucidate differences in biodegradation of selected TOrCs even under similar redox and carbon conditions.

9.1.2. Recommendations and improvements for future SMART applications

As discussed in detail in **chapter 7**, oxic redox conditions are a crucial factor with respect to TOrCs transformation during MAR. This has additionally been shown in the studies performed within this dissertation project (c.f. **chapters 4**, **5**, **6** and **7** as well as **9.1.1**). Therefore, the establishment of oxic redox conditions in the influent as well as in the subsurface of the second infiltration step must essentially be achieved. This could be managed by improving the aeration practice to provide a fine distribution of the water for highly oxygen saturation prior to infiltration instead of a single water flow over a heap of rocks. Techniques such as aeration towers, cascade aeration or diffuser plates may be suitable. Moreover, an oversaturation of the influent water with oxygen by using e.g. hydrogen peroxide could be a possible option. Another possibility would be to cover the infiltration basin to avoid an accumulation of leaves and further, to avoid algae growth due to intense sunlight which results in additional oxygen consumption.

A further aspect which has to be considered is that aeration of the influent water may result in clogging due to precipitation of iron (Fe^{3+}) or manganese (Mn^{4+}) which further leads to decreasing infiltration rates (Sharma and Amy, 2010). However, this will only be the case if the preliminary first infiltration step, e.g. RBF was operated under anoxic conditions and iron as well as manganese prevailing in soil of the infiltration zone which will result in a dissolution of iron and manganese. Therefore, iron but also manganese concentrations in the bank filtrate should be monitored prior to infiltration. As shown in **chapter 4**, oxidized manganese after aeration/oxidation deposited on the top of the second infiltration system which necessitates removal of the top layer approximately every third month. Clogging may not only be caused by iron and manganese oxides/hydroxides, but also by particles or the prevailing biofilm (Bouwer, 2002; Hiscock and Grischek, 2002). Results of **chapter 5** revealed less clogging or rather slower establishment of the clogging layer at the SMART field site in comparison to cMAR. Overall, information about long-term performance of

SMART with respect to clogging is still missing. As clogging is very site specific, it needs to be considered individually for each study site based on boundary conditions like iron concentration of the bank filtrate used for subsequent infiltration.

So far, surface spreading techniques require a large physical footprint. For instance, one basin of the cMAR site in Berlin has a size of approximately 8,900 m² with a median infiltration rate of 1.68 m/d (Hellauer et al., 2018a, **chapter 5**). The infiltration rate and thus, the required area strongly depends on the permeability of the sediment. In the beginning of a recharge cycle the infiltration rate is mainly driven by a vertical flow due to gravity as the zone below the pond is unsaturated. With ongoing operation of the basin, the water level below the pond rises and gets hydraulically connected with the water in the basin. Hence, the infiltration rate is determined through the horizontal groundwater flow. The infiltration rate is going to decrease when a clogging layer within the basin starts to develop due to the precipitation of iron(III), manganese(IV) or calcium carbonate, algae growth, settlement of particles or establishment of a biofilm and biomass. This results in an establishment of an unsaturated zone below the infiltration pond leading to a hydraulic disconnection between the pond and the groundwater. Hence, an abrasion of the clogging layer is essential to provide sufficient infiltration (Bouwer, 2002; Greskowiak et al., 2005; Hiscock and Grischek, 2002). If it would be possible to minimize size requirements by improving the infiltration into the aquifer, MAR may be applied more often especially in urban areas where space is limited. This could be achieved for instance by vadose zone infiltration through infiltration trenches. Thereby, water is lead through a trench of approximately 5 m depths and variable lengths providing a large infiltration area. They are filled with gravel allowing for an efficient infiltration with reduced HRT due to the high permeability of the filling material. In addition, trenches could be covered to avoid intrusion of surrounding materials and to merge with the ambient landscape. Nonetheless, one disadvantage of this technology is the impossibility to backwash and clean the trench in case of clogging (Bouwer, 2002). However, this problem could be minimized by operating the SMART approach where infiltration trenches are used as second infiltration step after e.g. RBF due to the elimination of factors causing clogging (e.g. particles, biomass) during the first infiltration. However, if the first infiltration step is operated under anoxic conditions efficient treatment is needed to remove reduced compounds like iron or manganese. Another scenario would be to apply SMART using two infiltration trenches which has the advantage of minimizing the required infiltration area. Thereby, both infiltration trenches can be covered resulting in the elimination of many clogging issues. Nevertheless, the infiltration through the subsurface has to result in required water quality standards (Regnery et al., 2017) and especially in Germany, where often no additional water disinfection is applied it is highly recommended to guarantee an HRT of at least 50 days. More research is required especially with the focus on pathogen elimination during reduced infiltration times.

A combination of ozonation with subsequent MAR is promising due to efficient transformation of biological persistent TOrCs and enhanced DOC removal which has previously been shown by e.g. Lakretz et al. (2017). This was also observed within this dissertation project when ozone was applied as intermediate oxidant in the laboratory-scale experiment (**chapter 4**). An increased DOC removal in SMART O_3 was observed which is more likely an effect of the formation of biodegradable compounds after ozonation

(Kozyatnyk et al., 2013). In addition, the performance of SMART could be increased as compounds like carbamazepine which persist biodegradation were sufficiently removed and moreover, the transformation of compounds e.g. gabapentin or benzotriazole which were significantly better transformed in SMART air and O_2 in comparison to BF could be further enhanced in the following infiltration. However, the fate of bromate formed during ozonation of bromide containing waters has to be considered as concentrations might exceed the limit of 10 µg/L given by the European Drinking Water Directive (European Commission, 1998) as shown by Hübner et al. (2016). During biological treatment like subsequent SAT, bromate removal is solely efficient under anoxic but not under oxic conditions (Hübner et al., 2016; Wang et al., 2018). Furthermore, concentrations of reduced inorganic residues (e.g. NO_2^-, Mn(II), Fe(II)) have to be kept as low as possible as they may outcompete oxidation of TOrCs by ozone due to their high reaction rate constants and additionally, behavior of transformation products formed during ozonation have to be considered (c.f. section 2.4).

9.2. DOC composition and TOrCs transformation

As discussed in section 2.2.2, a co-metabolic transformation of TOrCs in MAR systems is widely assumed due to their low concentration in comparison to DOC. Therefore, the BDOC as primary substrate plays a major role as it is responsible for the expression of required enzymes for TOrCs transformation (Tran et al., 2013).

9.2.1. Linkage between molecular components, microbial community and TOrCs

Based on the assumption of a co-metabolic TOrCs transformation, we hypothesized that the fate of molecular components and characteristic functional groups of the primary substrate correlates with the degradation of structurally similar TOrCs (**chapter 6**).

Persistent TOrCs like carbamazepine and primidone could be associated with highly refractory carboxylic-rich alicyclic moieties (CRAM; Hertkorn et al. (2006)). As CRAM was detected in deep ocean organic matter, it is assumed that a similar refractory organic backbone is omnipresent in the environment. This assumption was confirmed by a study from Zark and Dittmar (2018), who observed not distinguishable DOM components in marine as well as freshwater environments. More than 50% of all masses assigned to TOrCs exhibiting a continuous degradation throughout the system belonged to sulfur containing molecules. Thus, CHOS containing molecules have a higher tendency to get biodegraded as e.g. CHO containing compounds. We were further able to link microbial phyla and masses to clusters of TOrCs. It has to be considered that discussions on phyla level should be complemented in future studies with investigations regarding the presence and activity of enzymes which could potentially be involved in TOrCs transformation. A first insight into coupling the microbiome and TOrCs was provided and could be used as starting point for future investigations. However, a link of functional groups with structurally similar TOrCs could not be derived. Hence, the hypothesis could not be confirmed by using FT-ICR-MS in combination with 3D-fluorescence, UVA_{254} and SUVA. It is highly recommended for future studies with the intention to elucidate structure of complex material such as organic matter, to combine FT-ICR-MS with NMR. This combination has previously been highlighted for such purpose (Hertkorn et al., 2013) and is commonly

applied to elucidate organic matter characteristics in the environment (Dvorski et al., 2016; Hertkorn et al., 2016; Li et al., 2016c). Furthermore, it would be suggested to use a less complex water matrix to reduce the high load of signals in the FT-ICR-MS spectrum. For instance, columns used in **chapter 7**, fed with DW and DW+HA would be appropriate not only because of the feed water composition, but also because of the prevailing stable carbon-limited (ΔDOC ≤ 0.7 mg/L) and oxic (DO concentration > 1 mg/L) conditions. It would be more adequate to solely get samples from the in- and effluent of columns DW and DW+HA for three to four times instead of sampling water from different depths throughout a travel time of approximately eight days as done so far. This will result in a statistically more robust dataset and may allow the assessment of metabolic pathways based on identified metabolites via FT-ICR-MS in combination with NMR and prevailing microbial species.

9.2.2. Co-metabolic vs metabolic TOrCs transformation

The influence of DOC composition on TOrCs transformation in MAR was also the scope of the study discussed in **chapter 7** in which the hypothesis "The concentration of refractory carbon (like humic acids) controls TOrCs removal in MAR systems under oxic conditions" was tested. Columns fed with DW had a very low BDOC concentration of ≤ 0.1 mg/L, columns fed with DW+HA had a slightly higher BDOC concentration (≤ 0.7 mg/L). Surprisingly, no reliable significant difference in TOrCs transformation was observed between systems DW and DW+HA, hence the proposed hypothesis was rejected (c.f. section 7.3.2). Tang et al. (2017) observed an enhanced transformation of many biodegradable TOrCs after increasing the HA content in bench-scale MBBR which supports the hypothesis of a co-metabolic process. However, in our study, even under extremely low BDOC concentrations (≤ 0.1 mg/L) sufficient transformation of seven out of 12 targeted TOrCs was observed. This suggests that under very low carbon conditions, the microbial community can use TOrCs as sole carbon source. Therefore, metabolism seems to be a possible process for TOrCs transformation during MAR which may be based on the ability of the microbiome prevailing in carbon-depleted environments to metabolize a broader consortium of available substrate as previously proposed by Egli (2010).

Tran et al. (2013) summarized in their review that metabolic as well as co-metabolic biotransformation occur in natural as well as engineered treatment systems. They further stated that metabolic biodegradation of TOrCs is solely assigned to heterotrophic bacteria and fungi while co-metabolism was also observed by autotrophic organisms. TOrCs may be degraded via metabolism as well as co-metabolism, e.g. sulfamethoxazole, as reviewed by Wang and Wang (2018). In addition, naproxen was degraded in culture experiments by *Stenotrophomonas maltophilia* KB2 metabolically up to 28% while adding glucose as carbon source, removal strongly increases (78%) indicating a co-metabolic process. Using phenol as additional carbon source, naproxen was degraded by 40% (Wojcieszyńska et al., 2014). Furthermore, a metabolic degradation of diclofenac by *Labrys portucalensis* F11 reached 70%, while a complete attenuation was obtained via co-metabolism after continuously feeding acetate as further carbon source (Moreira et al., 2018). Also Bessa et al. (2017) observed an enhanced transformation of diclofenac in batch-scale experiments using *Brevibacterium* sp. D4 by periodically adding acetate in comparison to use diclofenac as sole carbon source. However, in all these studies the

concentration of targeted TOrCs exceeded environmentally relevant concentrations. Additionally, the experiments were performed in defined media containing a distinct carbon source while DOC in general provides a diverse mixture of organic compounds. The study presented within this dissertation project (**chapter 7**) highlights the possibility of metabolic TOrCs transformation at concentrations of several hundred nanogram per liter in the presence of barely available (≤ 0.1 mg/L), complex organic substrate.

However, it still remains unclear when the shift from co-metabolic to metabolic transformation occurs or if it is more likely a continuous process shifting from co-metabolic to metabolic and vice versa. To better understand these processes, the transformation pathways of TOrCs during MAR have to be elucidated and furthermore, enzymes which are involved in their degradation have to be determined. This could be achieved by spiking a single compound in columns DW and DW+HA and targeting its transformation as well as transformation products in combination with metatranscriptomic analyses. Furthermore, the initial concentration of a spiked TOrC which exhibited poor removal so far could be varied to assess whether an increased availability could result in a metabolic transformation due to the upregulation of necessary enzymes.

9.3. Identification of favorable carbon-limited (oligotrophic) conditions using genomic markers

Lauro et al. (2009) established the approach of assigning the trophic strategy of an organism based on genomic markers in the marine environment. Trophic strategies of microbial communities as a result of the availability of nutrients are of great interest in engineered filtration system, because of nutrient depleted, more generally spoken carbon-depleted conditions lead to an enhanced transformation of TOrCs (c.f. **chapter 5**). It was hypothesized that trophic strategies of the microbial community in engineered filtration systems can be distinguished based on genomic features such as genome size and specific clusters of orthologous groups (COGs). Within this dissertation project, the successful adaptation of the concept proposed by Lauro et al. (2009) was emphasized (**chapter 8**) which could be used at MAR and SMART field sites to monitor prevailing carbon conditions. The approach presented herein based on the establishment of a Bayesian model by use of a set of genomic markers characteristic for carbon-rich or -limited preferring organisms. Hence, the hypothesis could be confirmed with respect to COG categories, while the genome size was not part of the model.

For future applications, several recommendations should be taken into account and a few improvements in the general experimental set-up have to be considered. During this study, a conservative cultivation experiment was performed to select for carbon-rich and carbon-limited preferring organisms. However, this technique may select for facultative oligotrophs rather than obligate oligotrophs (Koch, 2001; Schut et al., 1997). Hence, cultivation techniques based on the principle of dilution (Button et al. (1993), Senechkin et al. (2010)) are highly recommended for a more precise selection and to reduce the number of facultative oligotrophs. To dedicate genomic markers, bacterial genomes of closest relatives of isolated organisms identified via a phylogenetic tree were used. Even though these organisms share many similarities, a bias will be given. The organism identified during growth experiment may have developed individual strategies to survive in the given

environment where it was isolated from. Thus, sequencing individual genomes and further using this information for identifying genomic markers will be a possible improvement in comparison to use genomes of closest relatives. To provide an overview of prevailing microbial organisms in the environment, 16S rRNA amplicon sequencing should be performed. Organisms isolated via cultivation techniques could be compared with the overall microbial community to assess if the majority of cultivated organisms is similar to the abundance of species assigned via 16S rRNA amplicon sequencing. Although, differences will be observed between cultivated and sequenced organisms as 16S rRNA amplicon sequencing will assess even non-culturable species, information derived from 16S rRNA amplicon sequencing may be helpful to get a better understanding of prevailing microbial community under distinct boundary conditions. However, even though several aspects could be improved, a first insight in applying genomic markers to identify prevailing carbon conditions in engineered MAR systems could be provided.

9.4. Outlook

Throughout this dissertation project it was shown that SMART is a reliable and promising natural-based treatment technique for improved water quality (chapters **4** to **7**). To allow a wide application of SMART, additional research needs be considered in the future. Regarding process engineering, the implementation of infiltration trenches for reduced area requirements instead of infiltration ponds must be addressed and, furthermore, SMART has to be optimized with respect to the precipitation of reduced species after reaeration. Another aspect could be to apply in situ aeration instead of pumping the water up, reaerate externally followed by second infiltration. This would result firstly in reduced costs due to the absence of energy consumption for pumping and secondly, the SMART concept could be scaled down into a single infiltration system instead of two combined MAR systems. However, a homogenous contribution of the induced gas bubbles has to be guaranteed to allow a steady flow of the water throughout the system. The equal flow in terms of controlled hydraulic conditions are essential and must be addressed in future studies.

Prevailing carbon and redox conditions in MAR systems are mainly characterized by applying DOC and UV absorbance as well as dissolved oxygen and terminal electron acceptors (nitrate, nitrite, iron, manganese) measurements. In future applications, the characterization should be extended to use of 3D fluorescence measurements in combination with PARAFAC to elucidate components present in the water and how do they behave throughout infiltration. As proposed in **chapter 8** genomic markers may additionally be suitable to predict prevailing carbon conditions. As the microbiome plays a crucial role for the improvement of the water quality within MAR, its characterization is essential. Therefore, besides the biomass and microbial community structure its functionality by performing metagenome and metatranscriptome analyses would be beneficial.

To derive a deeper understanding of the processes involved in the TOrCs transformation during MAR, several aspects should be considered in the future. On the one hand, investigating the biotransformation pathways of selected TOrCs would be of great interest. This could help to decipher the enzymes involved in the attenuation of TOrCs and to

emphasize the reactions catalyzed by those. This information in addition to the knowledge about the metabolic potential of the microbiome derived from metagenome and metatranscriptome analyses may shed some light on underlying processes (co-metabolic versus metabolic) for the transformation of TOrCs during MAR. On the other hand, studies dealing with the influence of DOC composition on TOrCs transformation are important. FT-ICR-MS in combination with NMR analyses would allow for structural elucidation of the organic matter which could further be used to highlight correlations between structural properties of the organic carbon and biotransformed TOrCs. Detailed compositional analyses of the organic matter could be coupled with metagenome and metatranscriptome analyses to derive information on metabolic pathways for instance via accessing the KEGG (Kyoto Encyclopedia of Genes and Genomes) database (Kanehisa, 2000).

References

Adrian, M., Lucio, M., Roullier-Gall, C., Héloir, M.-C., Trouvelot, S., Daire, X., Kanawati, B., Lemaître-Guillier, C., Poinssot, B., Gougeon, R., Schmitt-Kopplin, P., 2017. Metabolic Fingerprint of PS3-Induced Resistance of Grapevine Leaves against Plasmopara viticola Revealed Differences in Elicitor-Triggered Defenses. *Frontiers in plant science* 8, 101. doi:10.3389/fpls.2017.00101.

Alidina, M., Li, D., Drewes, J.E., 2014a. Investigating the role for adaptation of the microbial community to transform trace organic chemicals during managed aquifer recharge. *Water Research* 56, 172–180. doi:10.1016/j.watres.2014.02.046.

Alidina, M., Li, D., Ouf, M., Drewes, J.E., 2014b. Role of primary substrate composition and concentration on attenuation of trace organic chemicals in managed aquifer recharge systems. *Journal of Environmental Management* 144, 58–66. doi:10.1016/j.jenvman.2014.04.032.

Alidina, M., Shewchuk, J., Drewes, J.E., 2015. Effect of temperature on removal of trace organic chemicals in managed aquifer recharge systems. *Chemosphere* 122, 23–31. doi:10.1016/j.chemosphere.2014.10.064.

Alotaibi, M.D., Patterson, B.M., McKinley, A.J., Reeder, A.Y., Furness, A.J., Donn, M.J., 2015. Fate of benzotriazole and 5-methylbenzotriazole in recycled water recharged into an anaerobic aquifer: column studies. *Water Research* 70, 184–195. doi:10.1016/j.watres.2014.11.040.

Altschul, S.F., Gish, W., Miller, W., Myers, E.W., Lipman, D.J., 1990. Basic local alignment search tool. *Journal of Molecular Biology* 215 (3), 403–410. doi:10.1016/S0022-2836(05)80360-2.

Amy, G., Drewes, J., 2007. Soil Aquifer Treatment (SAT) as a Natural and Sustainable Wastewater Reclamation/Reuse Technology: Fate of Wastewater Effluent Organic Matter (EfOM) and Trace Organic Compounds. *Environmental Monitoring and Assessment* 129 (1-3), 19–26. doi:10.1007/s10661-006-9421-4.

Archer, E., Petrie, B., Kasprzyk-Hordern, B., Wolfaardt, G.M., 2017. The fate of pharmaceuticals and personal care products (PPCPs), endocrine disrupting contaminants (EDCs), metabolites and illicit drugs in a WWTW and environmental waters. *Chemosphere* 174, 437–446. doi:10.1016/j.chemosphere.2017.01.101.

Arp, D.J., Yeager, C.M., Hyman, M.R., 2001. Molecular and cellular fundamentals of aerobic cometabolism of trichloroethylene. *Biodegradation* 12 (2), 81–103. doi:10.1023/A:1012089908518.

Baghoth, S.A., Sharma, S.K., Amy, G.L., 2011. Tracking natural organic matter (NOM) in a drinking water treatment plant using fluorescence excitation-emission matrices and PARAFAC. *Water Research* 45 (2), 797–809. doi:10.1016/j.watres.2010.09.005.

Bastida, F., Torres, I.F., Moreno, J.L., Baldrian, P., Ondoño, S., Ruiz-Navarro, A., Hernández, T., Richnow, H.H., Starke, R., García, C., Jehmlich, N., 2016. The active microbial diversity drives ecosystem multifunctionality and is physiologically related to carbon availability in Mediterranean semi-arid soils. *Molecular ecology* 25 (18), 4660–4673. doi:10.1111/mec.13783.

Baumgarten, B., Jährig, J., Reemtsma, T., Jekel, M., 2011. Long term laboratory column experiments to simulate bank filtration: factors controlling removal of

sulfamethoxazole. *Water Research* 45 (1), 211–220. doi:10.1016/j.watres.2010.08.034.

Bayarsaikhan, U., Filter, J., Gernert, U., Jekel, M., Ruhl, A.S., 2018. Fate of leaf litter deposits and impacts on oxygen availability in bank filtration column studies. *Environmental Research* 164, 495–500. doi:10.1016/j.envres.2018.03.033.

Benotti, M.J., Song, R., Wilson, D., Snyder, S.A., 2012. Removal of pharmaceuticals and endocrine disrupting compounds through pilot- and full-scale riverbank filtration. *Water Science & Technology: Water Supply* 12 (1), 11. doi:10.2166/ws.2011.068.

Benotti, M.J., Trenholm, R.A., Vanderford, B.J., Holady, J.C., Stanford, B.D., Snyder, S.A., 2009. Pharmaceuticals and Endocrine Disrupting Compounds in U.S. Drinking Water. *Environmental Science & Technology* 43 (3), 597–603. doi:10.1021/es801845a.

Beretsou, V.G., Psoma, A.K., Gago-Ferrero, P., Aalizadeh, R., Fenner, K., Thomaidis, N.S., 2016. Identification of biotransformation products of citalopram formed in activated sludge. *Water Research* 103, 205–214. doi:10.1016/j.watres.2016.07.029.

Bergheim, M., Gieré, R., Kümmerer, K., 2012. Biodegradability and ecotoxicitiy of tramadol, ranitidine, and their photoderivatives in the aquatic environment. *Environmental Science and Pollution Research International* 19 (1), 72–85. doi:10.1007/s11356-011-0536-y.

Bertelkamp, C., Reungoat, J., Cornelissen, E.R., Singhal, N., Reynisson, J., Cabo, A.J., van der Hoek, J.P., Verliefde, A.R.D., 2014. Sorption and biodegradation of organic micropollutants during river bank filtration: a laboratory column study. *Water Research* 52, 231–241. doi:10.1016/j.watres.2013.10.068.

Bertelkamp, C., van der Hoek, J.P., Schoutteten, K., Hulpiau, L., Vanhaecke, L., Vanden Bussche, J., Cabo, A.J., Callewaert, C., Boon, N., Löwenberg, J., Singhal, N., Verliefde, A.R.D., 2016. The effect of feed water dissolved organic carbon concentration and composition on organic micropollutant removal and microbial diversity in soil columns simulating river bank filtration. *Chemosphere* 144, 932–939. doi:10.1016/j.chemosphere.2015.09.017.

Bessa, V.S., Moreira, I.S., Tiritan, M.E., Castro, P.M.L., 2017. Enrichment of bacterial strains for the biodegradation of diclofenac and carbamazepine from activated sludge. *International Biodeterioration & Biodegradation* 120, 135–142. doi:10.1016/j.ibiod.2017.02.008.

Bookholt, F.D., Stuurman, P., Hanea, A.M., 2014. Practical Guidelines for Learning Bayesian Networks from Small Data Sets. *Open Access Library Journal* 01 (03), 1–13. doi:10.4236/oalib.1100481.

Bouckaert, R.R., 2004. Bayesian network classifiers in Weka. (Working paper series. University of Waikato, Department of Computer Science. No. 14/2004). Hamilton, New Zealand: University of Waikato.

Bouwer, H., 2002. Artificial recharge of groundwater: Hydrogeology and engineering. *Hydrogeology Journal* 10 (1), 121–142. doi:10.1007/s10040-001-0182-4.

Bragança, I., Danko, A.S., Pacheco, J., Frascari, D., Delerue-Matos, C., Domingues, V.F., 2016. Cometabolic Degradation of Anti-Inflammatory and Analgesic Pharmaceuticals by a Pentane Enrichment Culture. *Water, Air, & Soil Pollution* 227 (7). doi:10.1007/s11270-016-2933-9.

Breedveld, G.D., Roseth, R., Sparrevik, M., Hartnig, T., Hem, L.J., 2003. Persistence of the De-Icing Additive Benzotriazole at an Abandoned Airport. *Water, Air, and Soil Pollution: Focus* 3 (3), 91–101. doi:10.1023/A:1023961213839.

Brezina, E., Prasse, C., Meyer, J., Mückter, H., Ternes, T.A., 2017. Investigation and risk evaluation of the occurrence of carbamazepine, oxcarbazepine, their human metabolites and transformation products in the urban water cycle. *Environmental Pollution* 225, 261–269. doi:10.1016/j.envpol.2016.10.106.

Buerge, I.J., Buser, H.-R., Kahle, M., Müller, M.D., Poiger, T., 2009. Ubiquitous Occurrence of the Artificial Sweetener Acesulfame in the Aquatic Environment: An Ideal Chemical Marker of Domestic Wastewater in Groundwater. *Environmental Science & Technology* 43 (12), 4381–4385. doi:10.1021/es900126x.

Buffle, M.-O., von Gunten, U., 2006. Phenols and Amine Induced HO • Generation During the Initial Phase of Natural Water Ozonation. *Environmental Science & Technology* 40 (9), 3057–3063. doi:10.1021/es052020c.

Burke, V., Greskowiak, J., Asmuß, T., Bremermann, R., Taute, T., Massmann, G., 2014. Temperature dependent redox zonation and attenuation of wastewater-derived organic micropollutants in the hyporheic zone. *Science of The Total Environment* 482-483, 53–61. doi:10.1016/j.scitotenv.2014.02.098.

Burke, V., Greskowiak, J., Grünenbaum, N., Massmann, G., 2017. Redox and Temperature Dependent Attenuation of Twenty Organic Micropollutants - A Systematic Column Study. *Water Environment Research* 89 (2), 155–167. doi:10.2175/106143016X14609975746000.

Burke, V., Treumann, S., Duennbier, U., Greskowiak, J., Massmann, G., 2013. Sorption behavior of 20 wastewater originated micropollutants in groundwater--column experiments with pharmaceutical residues and industrial agents. *Journal of Contaminant Hydrology* 154, 29–41. doi:10.1016/j.jconhyd.2013.08.001.

Button, D.K., Schut, F., Quang, P., Martin, R., Robertson, B.R., 1993. Viability and isolation of marine bacteria by dilution culture: Theory, procedures, and initial results. *Applied and Environmental Microbiology* 59 (3), 881–891.

Carvajal, G., Branch, A., Michel, P., Sisson, S.A., Roser, D.J., Drewes, J.E., Khan, S.J., 2017. Robust evaluation of performance monitoring options for ozone disinfection in water recycling using Bayesian analysis. *Water Research* 124, 605–617. doi:10.1016/j.watres.2017.07.079.

Castronovo, S., Wick, A., Scheurer, M., Nödler, K., Schulz, M., Ternes, T.A., 2017. Biodegradation of the artificial sweetener acesulfame in biological wastewater treatment and sandfilters. *Water Research* 110, 342–353. doi:10.1016/j.watres.2016.11.041.

Chen, W., Westerhoff, P., Leenheer, J.A., Booksh, K., 2003. Fluorescence Excitation−Emission Matrix Regional Integration to Quantify Spectra for Dissolved Organic Matter. *Environmental Science & Technology* 37 (24), 5701–5710. doi:10.1021/es034354c.

Clara, M., Kreuzinger, N., Strenn, B., Gans, O., Kroiss, H., 2005. The solids retention time-a suitable design parameter to evaluate the capacity of wastewater treatment plants to remove micropollutants. *Water Research* 39 (1), 97–106. doi:10.1016/j.watres.2004.08.036.

Clara, M., Strenn, B., Kreuzinger, N., 2004. Carbamazepine as a possible anthropogenic marker in the aquatic environment: investigations on the behaviour of Carbamazepine in wastewater treatment and during groundwater infiltration. *Water Research* 38 (4), 947–954. doi:10.1016/j.watres.2003.10.058.

Cleuvers, M., 2003. Aquatic ecotoxicity of pharmaceuticals including the assessment of combination effects. *Toxicology Letters* 142 (3), 185–194. doi:10.1016/S0378-4274(03)00068-7.

D'Alessio, M., Yoneyama, B., Ray, C., 2015. Fate of selected pharmaceutically active compounds during simulated riverbank filtration. *Science of The Total Environment* 505, 615–622. doi:10.1016/j.scitotenv.2014.10.032.

Dalton, H., Stirling, D.I., Quayle, J.R., 1982. Co-Metabolism [and Discussion]. *Philosophical Transactions of the Royal Society B: Biological Sciences* 297 (1088), 481–496. doi:10.1098/rstb.1982.0056.

Derenne, S., Largeau, C., 2001. A Review of Some Important Families of Refractory Macromolecules: Composition, Origin, and Fate in Soils and Sediments. *Soil Science* 166 (11), 833–847. doi:10.1097/00010694-200111000-00008.

Dillon, P., 2005. Future management of aquifer recharge. *Hydrogeology Journal* 13 (1), 313–316. doi:10.1007/s10040-004-0413-6.

Dillon, P., Toze, S., Page, D., Vanderzalm, J., Bekele, E., Sidhu, J., Rinck-Pfeiffer, S., 2010. Managed aquifer recharge: rediscovering nature as a leading edge technology. *Water Science & Technology* 62 (10), 2338–2345. doi:10.2166/wst.2010.444.

Dittmar, T., Koch, B., Hertkorn, N., Kattner, G., 2008. A simple and efficient method for the solid-phase extraction of dissolved organic matter (SPE-DOM) from seawater. *Limnology and Oceanography: Methods* 6 (6), 230–235. doi:10.4319/lom.2008.6.230.

Drewes, J.E., et al., 2018. Dynamik der Klarwasseranteile in Oberflächengewässern und mögliche Herausforderungen für die Trinkwassergewinnung in Deutschland. <https://www.umweltbundesamt.de/sites/default/files/medien/421/publikationen/2018_08_02_factsheet_abschluss_klarwasseranteile_final_1.pdf> (retrieved 01.09.18).

Drewes, J.E., Croue, J.-P., 2002. New approaches for structural characterization of organic matter in drinking water and wastewater effluents. *Water Science & Technology: Water Supply* 2 (2), 1–10.

Drewes, J.E., Heberer, T., Rauch, T., Reddersen, K., 2003. Fate of Pharmaceuticals During Ground Water Recharge. *Ground Water Monitoring & Remediation* 23 (3), 64–72. doi:10.1111/j.1745-6592.2003.tb00684.x.

Drewes, J.E., Li, D., Regnery, J., Alidina, M., Wing, A., Hoppe-Jones, C., 2014. Tuning the performance of a natural treatment process using metagenomics for improved trace organic chemical attenuation. *Water Science & Technology* 69 (3), 628. doi:10.2166/wst.2013.750.

Drewes, J.E., Quanrud, D.M., Amy, G.L., Westerhoff, P.K., 2006. Character of Organic Matter in Soil-Aquifer Treatment Systems. *Journal of Environmental Engineering* 132 (11), 1447–1458. doi:10.1061/(ASCE)0733-9372(2006)132:11(1447).

Dvorski, S.E.-M., Gonsior, M., Hertkorn, N., Uhl, J., Müller, H., Griebler, C., Schmitt-Kopplin, P., 2016. Geochemistry of Dissolved Organic Matter in a Spatially Highly Resolved Groundwater Petroleum Hydrocarbon Plume Cross-Section. *Environmental Science & Technology* 50 (11), 5536–5546. doi:10.1021/acs.est.6b00849.

Edgar, R.C., 2004. MUSCLE: Multiple sequence alignment with high accuracy and high throughput. *Nucleic Acids Research* 32 (5), 1792–1797. doi:10.1093/nar/gkh340.

Edgar, R.C., 2010. Search and clustering orders of magnitude faster than BLAST. *Bioinformatics* 26 (19), 2460–2461. doi:10.1093/bioinformatics/btq461.

Egli, T., 2010. How to live at very low substrate concentration. *Water Research* 44 (17), 4826–4837. doi:10.1016/j.watres.2010.07.023.

Ellis, L.B.M., Gao, J., Fenner, K., Wackett, L.P., 2008. The University of Minnesota pathway prediction system: Predicting metabolic logic. *Nucleic Acids Research* 36 (Web Server issue), W427-32. doi:10.1093/nar/gkn315.

Engel, K., Sauer, J., Jünemann, S., Winkler, A., Wibberg, D., Kalinowski, J., Tauch, A., Caspers, B.A., 2018. Individual- and Species-Specific Skin Microbiomes in Three Different Estrildid Finch Species Revealed by 16S Amplicon Sequencing. *Microbial Ecology* 76 (2), 518–529. doi:10.1007/s00248-017-1130-8.

European Commission, 1998. Council Directive 98/83/EC of 3 November 1998 on the quality of water intended for human consumption. Official Journal of the European Communities, L330, 32–54. <http://data.europa.eu/eli/dir/1998/83/oj>.

Fawcett, T., 2004. ROC Graphs: Notes and Practical Considerations for Researchers. *Machine Learning* 31, 1–38.

Fierer, N., Bradford, M.A., Jackson, R.B., 2007. Toward an Ecological Classification of Soil Bacteria. *Ecology* 88 (6), 1354–1364. doi:10.1890/05-1839.

Filter, J., Jekel, M., Ruhl, A.S., 2017. Impacts of Accumulated Particulate Organic Matter on Oxygen Consumption and Organic Micro-Pollutant Elimination in Bank Filtration and Soil Aquifer Treatment. *Water* 9 (5), 349. doi:10.3390/w9050349.

Friedman, N., Goldszmidt, M., 1996. Discretizing Continuous Attributes While Learning Bayesian Networks, in: In Proc. ICML. Morgan Kaufmann, pp. 157–165.

Funke, J., Prasse, C., Lütke Eversloh, C., Ternes, T.A., 2015. Oxypurinol - A novel marker for wastewater contamination of the aquatic environment. *Water Research* 74, 257–265. doi:10.1016/j.watres.2015.02.007.

Gao, J., Ellis, L.B.M., Wackett, L.P., 2010. The University of Minnesota Biocatalysis/Biodegradation Database: Improving public access. *Nucleic Acids Research* 38 (Database issue), D488-91. doi:10.1093/nar/gkp771.

Gavrilescu, M., Demnerová, K., Aamand, J., Agathos, S., Fava, F., 2015. Emerging pollutants in the environment: Present and future challenges in biomonitoring, ecological risks and bioremediation. *New Biotechnology* 32 (1), 147–156. doi:10.1016/j.nbt.2014.01.001.

Giovannoni, S.J., Cameron Thrash, J., Temperton, B., 2014. Implications of streamlining theory for microbial ecology. *The ISME Journal* 8 (8), 1553–1565. doi:10.1038/ismej.2014.60.

Glassmeyer, S.T., Furlong, E.T., Kolpin, D.W., Cahill, J.D., Zaugg, S.D., Werner, S.L., Meyer, M.T., Kryak, D.D., 2005. Transport of Chemical and Microbial Compounds from Known Wastewater Discharges: Potential for Use as Indicators of Human Fecal Contamination. *Environmental Science & Technology* 39 (14), 5157–5169. doi:10.1021/es048120k.

Göbel, A., Thomsen, A., McArdell, C.S., Joss, A., Giger, W., 2005. Occurrence and Sorption Behavior of Sulfonamides, Macrolides, and Trimethoprim in Activated

Sludge Treatment. *Environmental Science & Technology* 39 (11), 3981–3989. doi:10.1021/es048550a.

Golan-Rozen, N., Chefetz, B., Ben-Ari, J., Geva, J., Hadar, Y., 2011. Transformation of the recalcitrant pharmaceutical compound carbamazepine by Pleurotus ostreatus: Role of cytochrome P450 monooxygenase and manganese peroxidase. *Environmental Science & Technology* 45 (16), 6800–6805. doi:10.1021/es200298t.

Gonsior, M., Zwartjes, M., Cooper, W.J., Song, W., Ishida, K.P., Tseng, L.Y., Jeung, M.K., Rosso, D., Hertkorn, N., Schmitt-Kopplin, P., 2011. Molecular characterization of effluent organic matter identified by ultrahigh resolution mass spectrometry. *Water Research* 45 (9), 2943–2953. doi:10.1016/j.watres.2011.03.016.

Grenni, P., Ancona, V., Barra Caracciolo, A., 2018. Ecological effects of antibiotics on natural ecosystems: A review. *Microchemical Journal* 136, 25–39. doi:10.1016/j.microc.2017.02.006.

Greskowiak, J., Prommer, H., Massmann, G., Johnston, C.D., Nützmann, G., Pekdeger, A., 2005. The impact of variably saturated conditions on hydrogeochemical changes during artificial recharge of groundwater. *Applied Geochemistry* 20 (7), 1409–1426. doi:10.1016/j.apgeochem.2005.03.002.

Greskowiak, J., Prommer, H., Massmann, G., Nützmann, G., 2006. Modeling Seasonal Redox Dynamics and the Corresponding Fate of the Pharmaceutical Residue Phenazone During Artificial Recharge of Groundwater. *Environmental Science & Technology* 40 (21), 6615–6621. doi:10.1021/es052506t.

Gross-Wittke, A., Gunkel, G., Hoffmann, A., 2010. Temperature effects on bank filtration: Redox conditions and physical-chemical parameters of pore water at Lake Tegel, Berlin, Germany. *Journal of Water and Climate Change* 1 (1), 55–66. doi:10.2166/wcc.2010.005.

Grünheid, S., Amy, G., Jekel, M., 2005. Removal of bulk dissolved organic carbon (DOC) and trace organic compounds by bank filtration and artificial recharge. *Water Research* 39 (14), 3219–3228. doi:10.1016/j.watres.2005.05.030.

Grünheid, S., Hübner, U., Jekel, M., 2008. Impact of temperature on biodegradation of bulk and trace organics during soil passage in an indirect reuse system. *Water Science & Technology* 57 (7), 987–994. doi:10.2166/wst.2008.207.

Hall, M., Frank, E., Holmes, G., Pfahringer, B., Reutemann, P., Witten, I.H., 2009. The WEKA data mining software. *ACM SIGKDD Explorations Newsletter* 11 (1), 10–18. doi:10.1145/1656274.1656278.

Hamann, E., Stuyfzand, P.J., Greskowiak, J., Timmer, H., Massmann, G., 2016. The fate of organic micropollutants during long-term/long-distance river bank filtration. *Science of The Total Environment* 545-546, 629–640. doi:10.1016/j.scitotenv.2015.12.057.

Hammes, F., Salhi, E., Köster, O., Kaiser, H.-P., Egli, T., von Gunten, U., 2006. Mechanistic and kinetic evaluation of organic disinfection by-product and assimilable organic carbon (AOC) formation during the ozonation of drinking water. *Water Research* 40 (12), 2275–2286. doi:10.1016/j.watres.2006.04.029.

Hass, U., Dünnbier, U., Massmann, G., 2012. Occurrence and distribution of psychoactive compounds and their metabolites in the urban water cycle of Berlin (Germany). *Water Research* 46 (18), 6013–6022. doi:10.1016/j.watres.2012.08.025.

Hassa, J., Maus, I., Off, S., Pühler, A., Scherer, P., Klocke, M., Schlüter, A., 2018. Metagenome, metatranscriptome, and metaproteome approaches unraveled

compositions and functional relationships of microbial communities residing in biogas plants. *Applied Microbiology and Biotechnology* 102 (12), 5045–5063. doi:10.1007/s00253-018-8976-7.

Heberer, T., 2002. Tracking persistent pharmaceutical residues from municipal sewage to drinking water. *Journal of Hydrology* 266 (3-4), 175–189. doi:10.1016/S0022-1694(02)00165-8.

Heberer, T., Adam, M., 2004. Transport and Attenuation of Pharmaceutical Residues During Artificial Groundwater Replenishment. *Environmental Chemistry* 1 (1), 22. doi:10.1071/EN04008.

Heberer, T., Massmann, G., Fanck, B., Taute, T., Dünnbier, U., 2008. Behaviour and redox sensitivity of antimicrobial residues during bank filtration. *Chemosphere* 73 (4), 451–460. doi:10.1016/j.chemosphere.2008.06.056.

Heberer, T., Mechlinski, A., Fanck, B., Knappe, A., Massmann, G., Pekdeger, A., Fritz, B., 2004. Field Studies on the Fate and Transport of Pharmaceutical Residues in Bank Filtration. *Ground Water Monitoring & Remediation* 24 (2), 70–77. doi:10.1111/j.1745-6592.2004.tb00714.x.

Hecht, H., Kölling, M., 2001. A low-cost optode-array measuring system based on 1 mm plastic optical fibers — new technique for in situ detection and quantification of pyrite weathering processes. *Sensors and Actuators B: Chemical* 81 (1), 76–82. doi:10.1016/S0925-4005(01)00934-0.

Hellauer, K., Karakurt, S., Sperlich, A., Burke, V., Massmann, G., Hübner, U., Drewes, J.E., 2018a. Establishing sequential managed aquifer recharge technology (SMART) for enhanced removal of trace organic chemicals: Experiences from field studies in Berlin, Germany. *Journal of Hydrology* 563, 1161–1168. doi:10.1016/j.jhydrol.2017.09.044.

Hellauer, K., Martínez Mayerlen, S., Drewes, J.E., Hübner, U., 2019. Biotransformation of trace organic chemicals in the presence of highly refractory dissolved organic carbon. *Chemosphere* 215, 33–39. doi:10.1016/j.chemosphere.2018.09.166.

Hellauer, K., Mergel, D., Ruhl, A.S., Filter, J., Hübner, U., Jekel, M., Drewes, J.E., 2017. Advancing Sequential Managed Aquifer Recharge Technology (SMART) Using Different Intermediate Oxidation Processes. *Water* 9 (3), 221. doi:10.3390/w9030221.

Hellauer, K., Uhl, J., Lucio, M., Schmitt-Kopplin, P., Wibberg, D., Hübner, U., Drewes, J.E., 2018b. Microbiome-Triggered Transformations of Trace Organic Chemicals in the Presence of Effluent Organic Matter in Managed Aquifer Recharge (MAR) Systems. *Environmental Science & Technology* 52 (24), 14342–14351. doi:10.1021/acs.est.8b04559.

Henning, N., Kunkel, U., Wick, A., Ternes, T.A., 2018. Biotransformation of gabapentin in surface water matrices under different redox conditions and the occurrence of one major TP in the aquatic environment. *Water research* 137, 290–300. doi:10.1016/j.watres.2018.01.027.

Henzler, A.F., Greskowiak, J., Massmann, G., 2014. Modeling the fate of organic micropollutants during river bank filtration (Berlin, Germany). *Journal of Contaminant Hydrology* 156, 78–92. doi:10.1016/j.jconhyd.2013.10.005.

Henzler, A.F., Greskowiak, J., Massmann, G., 2016. Seasonality of temperatures and redox zonations during bank filtration – A modeling approach. *Journal of Hydrology* 535, 282–292. doi:10.1016/j.jhydrol.2016.01.044.

Hertkorn, N., Benner, R., Frommberger, M., Schmitt-Kopplin, P., Witt, M., Kaiser, K., Kettrup, A., Hedges, J.I., 2006. Characterization of a major refractory component of marine dissolved organic matter. *Geochimica et Cosmochimica Acta* 70 (12), 2990–3010. doi:10.1016/j.gca.2006.03.021.

Hertkorn, N., Frommberger, M., Witt, M., Koch, B.P., Schmitt-Kopplin, P., Perdue, E.M., 2008. Natural organic matter and the event horizon of mass spectrometry. *Analytical Chemistry* 80 (23), 8908–8919. doi:10.1021/ac800464g.

Hertkorn, N., Harir, M., Cawley, K.M., Schmitt-Kopplin, P., Jaffé, R., 2016. Molecular characterization of dissolved organic matter from subtropical wetlands: A comparative study through the analysis of optical properties, NMR and FTICR/MS. *Biogeosciences* 13 (8), 2257–2277. doi:10.5194/bg-13-2257-2016.

Hertkorn, N., Harir, M., Koch, B.P., Michalke, B., Schmitt-Kopplin, P., 2013. High-field NMR spectroscopy and FTICR mass spectrometry: Powerful discovery tools for the molecular level characterization of marine dissolved organic matter. *Biogeosciences* 10 (3), 1583–1624. doi:10.5194/bg-10-1583-2013.

Hertkorn, N., Ruecker, C., Meringer, M., Gugisch, R., Frommberger, M., Perdue, E.M., Witt, M., Schmitt-Kopplin, P., 2007. High-precision frequency measurements: indispensable tools at the core of the molecular-level analysis of complex systems. *Analytical and Bioanalytical Chemistry* 389 (5), 1311–1327. doi:10.1007/s00216-007-1577-4.

Hiscock, K.M., Grischek, T., 2002. Attenuation of groundwater pollution by bank filtration. *Journal of Hydrology* 266 (3-4), 139–144. doi:10.1016/S0022-1694(02)00158-0.

Ho, A., Di Lonardo, D.P., Bodelier, P.L.E., 2017. Revisiting life strategy concepts in environmental microbial ecology. *FEMS Microbiology Ecology* 93 (3). doi:10.1093/femsec/fix006.

Hollender, J., Zimmermann, S.G., Koepke, S., Krauss, M., McArdell, C.S., Ort, C., Singer, H., von Gunten, U., Siegrist, H., 2009. Elimination of organic micropollutants in a municipal wastewater treatment plant upgraded with a full-scale post-ozonation followed by sand filtration. *Environmental Science & Technology* 43 (20), 7862–7869. doi:10.1021/es9014629.

Hoppe-Jones, C., Dickenson, E.R.V., Drewes, J.E., 2012. The role of microbial adaptation and biodegradable dissolved organic carbon on the attenuation of trace organic chemicals during groundwater recharge. *Science of The Total Environment* 437, 137–144. doi:10.1016/j.scitotenv.2012.08.009.

Hoppe-Jones, C., Oldham, G., Drewes, J.E., 2010. Attenuation of total organic carbon and unregulated trace organic chemicals in U.S. riverbank filtration systems. *Water Research* 44 (15), 4643–4659. doi:10.1016/j.watres.2010.06.022.

Huber, M.M., Canonica, S., Park, G.-Y., von Gunten, U., 2003. Oxidation of Pharmaceuticals during Ozonation and Advanced Oxidation Processes. *Environmental Science & Technology* 37 (5), 1016–1024. doi:10.1021/es025896h.

Huber, M.M., Göbel, A., Joss, A., Hermann, N., Löffler, D., McArdell, C.S., Ried, A., Siegrist, H., Ternes, T.A., von Gunten, U., 2005. Oxidation of Pharmaceuticals during Ozonation of Municipal Wastewater Effluents: A Pilot Study. *Environmental Science & Technology* 39 (11), 4290–4299.

Huber, M.M., Ternes, T.A., Gunten, U. von, 2004. Removal of Estrogenic Activity and Formation of Oxidation Products during Ozonation of 17α-Ethinylestradiol. *Environmental Science & Technology* 38 (19), 5177–5186. doi:10.1021/es035205x.

Hübner, U., Kuhnt, S., Jekel, M., Drewes, J.E., 2016. Fate of bulk organic carbon and bromate during indirect water reuse involving ozone and subsequent aquifer recharge. *Journal of Water Reuse and Desalination* 6 (3), 413–420. doi:10.2166/wrd.2015.222.

Hübner, U., Miehe, U., Jekel, M., 2012. Optimized removal of dissolved organic carbon and trace organic contaminants during combined ozonation and artificial groundwater recharge. *Water Research* 46 (18), 6059–6068. doi:10.1016/j.watres.2012.09.001.

Hübner, U., Seiwert, B., Reemtsma, T., Jekel, M., 2014. Ozonation products of carbamazepine and their removal from secondary effluents by soil aquifer treatment--indications from column experiments. *Water Research* 49, 34–43. doi:10.1016/j.watres.2013.11.016.

Hübner, U., von Gunten, U., Jekel, M., 2015. Evaluation of the persistence of transformation products from ozonation of trace organic compounds - A critical review. *Water Research* 68, 150–170. doi:10.1016/j.watres.2014.09.051.

Iobbi-Nivol, C., Pommier, J., Simala-Grant, J., Méjean, V., Giordano, G., 1996. High substrate specificity and induction characteristics of trimethylamine-N-oxide reductase of Escherichia coli. *Biochimica et Biophysica Acta (BBA) - Protein Structure and Molecular Enzymology* 1294 (1), 77–82. doi:10.1016/0167-4838(95)00271-5.

Ishida, Y., Fukami, K., Eguchi, M., Yoshinaga, I. (Eds.), 1989. Strategies for growth of oligotrophic bacteria in the pelagic environment. In: Hattori T, Ishida Y, Maruyama Y, Morita RY. (eds). Japan Scientific Societies Pr, Tokyo, 724 pp.

Janssen, P.H., 2006. Identifying the dominant soil bacterial taxa in libraries of 16S rRNA and 16S rRNA genes. *Applied and Environmental Microbiology* 72 (3), 1719–1728. doi:10.1128/AEM.72.3.1719-1728.2006.

Jekel, M., Dott, W., Bergmann, A., Dünnbier, U., Gnirß, R., Haist-Gulde, B., Hamscher, G., Letzel, M., Licha, T., Lyko, S., Miehe, U., Sacher, F., Scheurer, M., Schmidt, C.K., Reemtsma, T., Ruhl, A.S., 2015. Selection of organic process and source indicator substances for the anthropogenically influenced water cycle. *Chemosphere* 125, 155–167. doi:10.1016/j.chemosphere.2014.12.025.

Kahle, M., Buerge, I.J., Müller, M.D., Poiger, T., 2009. Hydrophilic anthropogenic markers for quantification of wastewater contamination in ground- and surface waters. *Environmental Toxicology and Chemistry* 28 (12), 2528–2536. doi:10.1897/08-606.1.

Kanehisa, M., 2000. KEGG: Kyoto Encyclopedia of Genes and Genomes. *Nucleic Acids Research* 28 (1), 27–30. doi:10.1093/nar/28.1.27.

Kasprzyk-Hordern, B., Dinsdale, R.M., Guwy, A.J., 2008. The occurrence of pharmaceuticals, personal care products, endocrine disruptors and illicit drugs in surface water in South Wales, UK. *Water Research* 42 (13), 3498–3518. doi:10.1016/j.watres.2008.04.026.

Kasprzyk-Hordern, B., Dinsdale, R.M., Guwy, A.J., 2009. The removal of pharmaceuticals, personal care products, endocrine disruptors and illicit drugs during

wastewater treatment and its impact on the quality of receiving waters. *Water Research* 43 (2), 363–380. doi:10.1016/j.watres.2008.10.047.

Kim, S., Kramer, R.W., Hatcher, P.G., 2003. Graphical Method for Analysis of Ultrahigh-Resolution Broadband Mass Spectra of Natural Organic Matter, the Van Krevelen Diagram. *Analytical Chemistry* 75 (20), 5336–5344. doi:10.1021/ac034415p.

Klappenbach, J.A., Dunbar, J.M., Schmidt, T.M., 2000. rRNA Operon Copy Number Reflects Ecological Strategies of Bacteria. *Applied and Environmental Microbiology* 66 (4), 1328–1333. doi:10.1128/AEM.66.4.1328-1333.2000.

Koch, A.L., 2001. Oligotrophs versus copiotrophs. *BioEssays : news and reviews in molecular, cellular and developmental biology* 23 (7), 657–661. doi:10.1002/bies.1091.

Korich, D.G., Mead, J.R., Madore, M.S., Sinclair, N.A., Sterling, C.R., 1990. Effects of ozone, chlorine dioxide, chlorine, and monochloramine on Cryptosporidium parvum oocyst viability. *Applied and Environmental Microbiology* 56 (5), 1423–1428.

Kormos, J.L., Schulz, M., Ternes, T.A., 2011. Occurrence of iodinated X-ray contrast media and their biotransformation products in the urban water cycle. *Environmental Science & Technology* 45 (20), 8723–8732. doi:10.1021/es2018187.

Kozyatnyk, I., Swietlik, J., Raczyk-Stanislawiak, U., Dabrowska, A., Klymenko, N., Nawrocki, J., 2013. Influence of oxidation on fulvic acids composition and biodegradability. *Chemosphere* 92 (10), 1335–1342. doi:10.1016/j.chemosphere.2013.05.046.

Kumar, S., Stecher, G., Tamura, K., 2016. MEGA7: Molecular Evolutionary Genetics Analysis Version 7.0 for Bigger Datasets. *Molecular biology and evolution* 33 (7), 1870–1874. doi:10.1093/molbev/msw054.

Lagesen, K., Hallin, P., Rødland, E.A., Staerfeldt, H.-H., Rognes, T., Ussery, D.W., 2007. RNAmmer: Consistent and rapid annotation of ribosomal RNA genes. *Nucleic Acids Research* 35 (9), 3100–3108. doi:10.1093/nar/gkm160.

Lajeunesse, A., Blais, M., Barbeau, B., Sauve, S., Gagnon, C., 2013. Ozone oxidation of antidepressants in wastewater -Treatment evaluation and characterization of new by-products by LC-QToFMS. *Chemistry Central journal* 7 (1), 15. doi:10.1186/1752-153X-7-15.

Lakretz, A., Mamane, H., Cikurel, H., Avisar, D., Gelman, E., Zucker, I., 2017. The Role of Soil Aquifer Treatment (SAT) for Effective Removal of Organic Matter, Trace Organic Compounds and Microorganisms from Secondary Effluents Pre-Treated by Ozone. *Ozone: Science & Engineering* 39 (5), 385–394. doi:10.1080/01919512.2017.1346465.

Lane, D., 1991. 16S/23S rRNA sequencing, In: Stackebrandt, E., Goodfellow, M. (Eds.), Nucleic Acid Techniques in Bacterial Systematics. Wiley, New York, USA, pp. 115–175.

Lapworth, D.J., Baran, N., Stuart, M.E., Ward, R.S., 2012. Emerging organic contaminants in groundwater: A review of sources, fate and occurrence. *Environmental Pollution* 163, 287–303. doi:10.1016/j.envpol.2011.12.034.

Lauro, F.M., McDougald, D., Thomas, T., Williams, T.J., Egan, S., Rice, S., DeMaere, M.Z., Ting, L., Ertan, H., Johnson, J., Ferriera, S., Lapidus, A., Anderson, I., Kyrpides, N., Munk, A.C., Detter, C., Han, C.S., Brown, M.V., Robb, F.T., Kjelleberg, S., Cavicchioli, R., 2009. The genomic basis of trophic strategy in marine bacteria.

Proceedings of the National Academy of Sciences 106 (37), 15527–15533. doi:10.1073/pnas.0903507106.

Lavonen, E.E., Kothawala, D.N., Tranvik, L.J., Gonsior, M., Schmitt-Kopplin, P., Köhler, S.J., 2015. Tracking changes in the optical properties and molecular composition of dissolved organic matter during drinking water production. *Water Research* 85, 286–294. doi:10.1016/j.watres.2015.08.024.

Leenheer, J.A., Croué, J.-P., 2003. Characterizing aquatic dissolved organic matter. *Environmental Science & Technology* 37 (1), 18A-26A.

Leenheer, J.A., Croué, J.-P., Benjamin, M., Korshin, G.V., Hwang, C.J., Bruchet, A., Aiken, G.R., 2000. Comprehensive Isolation of Natural Organic Matter from Water for Spectral Characterizations and Reactivity Testing: Barrett, S. E., Krasner, S. W., Amy, G. L., Eds; ACS Symposium Series 761. American Chemical Society: Washington, DC 2000, In: Barrett, S.E., Krasner, S.W., Amy, G.L. (Eds.), Natural organic matter and disinfection by-products. Characterization and control in drinking water : [Symposium sponsored by the Division of Environmental Chemistry at the 217th National Meeting of the American Chemical Society, Anaheim, CA, March 21-25, 1999], vol. 761. ACS, Washington, DC, pp. 68–83.

Lester, Y., Mamane, H., Zucker, I., Avisar, D., 2013. Treating wastewater from a pharmaceutical formulation facility by biological process and ozone. *Water Research* 47 (13), 4349–4356. doi:10.1016/j.watres.2013.04.059.

Letzel, T., Bayer, A., Schulz, W., Heermann, A., Lucke, T., Greco, G., Grosse, S., Schüssler, W., Sengl, M., Letzel, M., 2015. LC-MS screening techniques for wastewater analysis and analytical data handling strategies: Sartans and their transformation products as an example. *Chemosphere* 137, 198–206. doi:10.1016/j.chemosphere.2015.06.083.

Lever, M.A., Rogers, K.L., Lloyd, K.G., Overmann, J., Schink, B., Thauer, R.K., Hoehler, T.M., Jørgensen, B.B., 2015. Life under extreme energy limitation: A synthesis of laboratory- and field-based investigations. *FEMS Microbiology Reviews* 39 (5), 688–728. doi:10.1093/femsre/fuv020.

Li, D., Alidina, M., Drewes, J.E., 2014a. Role of primary substrate composition on microbial community structure and function and trace organic chemical attenuation in managed aquifer recharge systems. *Applied Microbiology and Biotechnology* 98 (12), 5747–5756. doi:10.1007/s00253-014-5677-8.

Li, D., Alidina, M., Ouf, M., Sharp, J.O., Saikaly, P., Drewes, J.E., 2013. Microbial community evolution during simulated managed aquifer recharge in response to different biodegradable dissolved organic carbon (BDOC) concentrations. *Water Research* 47 (7), 2421–2430. doi:10.1016/j.watres.2013.02.012.

Li, D., Sharp, J.O., Drewes, J.E., 2016a. Influence of Wastewater Discharge on the Metabolic Potential of the Microbial Community in River Sediments. *Microbial Ecology* 71 (1), 78–86. doi:10.1007/s00248-015-0680-x.

Li, D., Sharp, J.O., Saikaly, P.E., Ali, S., Alidina, M., Alarawi, M.S., Keller, S., Hoppe-Jones, C., Drewes, J.E., 2012. Dissolved Organic Carbon Influences Microbial Community Composition and Diversity in Managed Aquifer Recharge Systems. *Applied and Environmental Microbiology* 78 (19), 6819–6828. doi:10.1128/AEM.01223-12.

Li, S., Wang, S., Yan, W., 2016b. Biodegradation of Methyl tert-Butyl Ether by Co-Metabolism with a Pseudomonas sp. Strain. *International Journal of Environmental Research and Public Health* 13 (9), 883. doi:10.3390/ijerph13090883.

Li, W.C., 2014. Occurrence, sources, and fate of pharmaceuticals in aquatic environment and soil. *Environmental Pollution* 187, 193–201. doi:10.1016/j.envpol.2014.01.015.

Li, W.-T., Chen, S.-Y., Xu, Z.-X., Li, Y., Shuang, C.-D., Li, A.-M., 2014b. Characterization of dissolved organic matter in municipal wastewater using fluorescence PARAFAC analysis and chromatography multi-excitation/emission scan: A comparative study. *Environmental science & technology* 48 (5), 2603–2609. doi:10.1021/es404624q.

Li, Y., Harir, M., Lucio, M., Gonsior, M., Koch, B.P., Schmitt-Kopplin, P., Hertkorn, N., 2016c. Comprehensive structure-selective characterization of dissolved organic matter by reducing molecular complexity and increasing analytical dimensions. *Water Research* 106, 477–487. doi:10.1016/j.watres.2016.10.034.

Liu, Y.-S., Ying, G.-G., Shareef, A., Kookana, R.S., 2011. Biodegradation of three selected benzotriazoles under aerobic and anaerobic conditions. *Water Research* 45 (16), 5005–5014. doi:10.1016/j.watres.2011.07.001.

Luo, Y., Guo, W., Ngo, H.H., Nghiem, L.D., Hai, F.I., Zhang, J., Liang, S., Wang, X.C., 2014. A review on the occurrence of micropollutants in the aquatic environment and their fate and removal during wastewater treatment. *Science of The Total Environment* 473-474, 619–641. doi:10.1016/j.scitotenv.2013.12.065.

Maeda, S., Uchida, S., Kisaki, T., 2014. Microbial Degradation of Nicotine-N′-oxide I Degradation Products. *Agricultural and Biological Chemistry* 42 (8), 1455–1460. doi:10.1080/00021369.1978.10863187.

Maeng, S.K., Abel, C.D.T., Sharma, S.K., Park, N.S., Amy, G.L., 2012a. Removal of geosmin and 2-methylisoborneol during managed aquifer recharge: Batch and column studies. *Journal of Water Supply: Research and Technology—AQUA* 61 (4), 220. doi:10.2166/aqua.2012.096.

Maeng, S.K., Ameda, E., Sharma, S.K., Grützmacher, G., Amy, G.L., 2010. Organic micropollutant removal from wastewater effluent-impacted drinking water sources during bank filtration and artificial recharge. *Water Research* 44 (14), 4003–4014. doi:10.1016/j.watres.2010.03.035.

Maeng, S.K., Sharma, S.K., Abel, C.D.T., Magic-Knezev, A., Amy, G.L., 2011a. Role of biodegradation in the removal of pharmaceutically active compounds with different bulk organic matter characteristics through managed aquifer recharge: batch and column studies. *Water Research* 45 (16), 4722–4736. doi:10.1016/j.watres.2011.05.043.

Maeng, S.K., Sharma, S.K., Abel, C.D.T., Magic-Knezev, A., Song, K.-G., Amy, G.L., 2012b. Effects of effluent organic matter characteristics on the removal of bulk organic matter and selected pharmaceutically active compounds during managed aquifer recharge: Column study. *Journal of Contaminant Hydrology* 140-141, 139–149. doi:10.1016/j.jconhyd.2012.08.005.

Maeng, S.K., Sharma, S.K., Lekkerkerker-Teunissen, K., Amy, G.L., 2011b. Occurrence and fate of bulk organic matter and pharmaceutically active compounds in managed aquifer recharge: a review. *Water Research* 45 (10), 3015–3033. doi:10.1016/j.watres.2011.02.017.

Maeng, S.K., Sharma, S.K., Magic-Knezev, A., Amy, G., 2008. Fate of effluent organic matter (EfOM) and natural organic matter (NOM) through riverbank filtration. *Water Science & Technology* 57 (12), 1999–2007. doi:10.2166/wst.2008.613.

Magoč, T., Salzberg, S.L., 2011. FLASH: fast length adjustment of short reads to improve genome assemblies. *Bioinformatics* 27 (21), 2957–2963. doi:10.1093/bioinformatics/btr507.

Maizel, A.C., Remucal, C.K., 2017. The effect of advanced secondary municipal wastewater treatment on the molecular composition of dissolved organic matter. *Water Research* 122, 42–52. doi:10.1016/j.watres.2017.05.055.

Massmann, G., Dünnbier, U., Heberer, T., Taute, T., 2008a. Behaviour and redox sensitivity of pharmaceutical residues during bank filtration - Investigation of residues of phenazone-type analgesics. *Chemosphere* 71 (8), 1476–1485. doi:10.1016/j.chemosphere.2007.12.017.

Massmann, G., Greskowiak, J., Dünnbier, U., Zuehlke, S., Knappe, A., Pekdeger, A., 2006. The impact of variable temperatures on the redox conditions and the behaviour of pharmaceutical residues during artificial recharge. *Journal of Hydrology* 328 (1-2), 141–156. doi:10.1016/j.jhydrol.2005.12.009.

Massmann, G., Nogeitzig, A., Taute, T., Pekdeger, A., 2008b. Seasonal and spatial distribution of redox zones during lake bank filtration in Berlin, Germany. *Environmental Geology* 54 (1), 53–65. doi:10.1007/s00254-007-0792-9.

Maurer, M., Escher, B.I., Richle, P., Schaffner, C., Alder, A.C., 2007. Elimination of beta-blockers in sewage treatment plants. *Water Research* 41 (7), 1614–1622. doi:10.1016/j.watres.2007.01.004.

McDowell, D.C., Huber, M.M., Wagner, M., Gunten, U. von, Ternes, T.A., 2005. Ozonation of Carbamazepine in Drinking Water: Identification and Kinetic Study of Major Oxidation Products. *Environmental Science & Technology* 39 (20), 8014–8022. doi:10.1021/es050043l.

Mesfioui, R., Love, N.G., Bronk, D.A., Mulholland, M.R., Hatcher, P.G., 2012. Reactivity and chemical characterization of effluent organic nitrogen from wastewater treatment plants determined by Fourier transform ion cyclotron resonance mass spectrometry. *Water Research* 46 (3), 622–634. doi:10.1016/j.watres.2011.11.022.

Michel, P., Ortega, G., Miklos, D., Khan, S.J., Drewes, J.E., in preparation. Applying machine-learning algorithms using online process control data to predict scavenger occurrence in advanced oxidation processes.

Minor, E.C., Swenson, M.M., Mattson, B.M., Oyler, A.R., 2014. Structural characterization of dissolved organic matter: a review of current techniques for isolation and analysis. *Environmental Science. Processes & Impacts* 16 (9), 2064–2079. doi:10.1039/C4EM00062E.

Missimer, T.M., Drewes, J.E., Maliva, R.G., Amy, G., 2011. Aquifer Recharge and Recovery: Groundwater Recharge Systems for Treatment, Storage, and Water Reclamation. *Ground Water* 49 (6), 771. doi:10.1111/j.1745-6584.2011.00846.x.

Moreira, I.S., Bessa, V.S., Murgolo, S., Piccirillo, C., Mascolo, G., Castro, P.M.L., 2018. Biodegradation of Diclofenac by the bacterial strain Labrys portucalensis F11. *Ecotoxicology and Environmental Safety* 152, 104–113. doi:10.1016/j.ecoenv.2018.01.040.

Müller, J., Drewes, J.E., Hübner, U., 2017. Sequential biofiltration - A novel approach for enhanced biological removal of trace organic chemicals from wastewater treatment plant effluent. *Water Research* 127, 127–138. doi:10.1016/j.watres.2017.10.009.

Muntau, M., Schulz, M., Jewell, K.S., Hermes, N., Hübner, U., Ternes, T., Drewes, J.E., 2017. Evaluation of the short-term fate and transport of chemicals of emerging concern during soil-aquifer treatment using select transformation products as intrinsic redox-sensitive tracers. *Science of The Total Environment* 583, 10–18. doi:10.1016/j.scitotenv.2016.12.165.

Murphy, K.R., Butler, K.D., Spencer, R.G.M., Stedmon, C.A., Boehme, J.R., Aiken, G.R., 2010. Measurement of dissolved organic matter fluorescence in aquatic environments: an interlaboratory comparison. *Environmental Science & Technology* 44 (24), 9405–9412. doi:10.1021/es102362t.

Murphy, K.R., Stedmon, C.A., Graeber, D., Bro, R., 2013. Fluorescence spectroscopy and multi-way techniques. PARAFAC. *Analytical Methods* 5 (23), 6557. doi:10.1039/c3ay41160e.

Nam, S.-N., Amy, G., 2008. Differentiation of wastewater effluent organic matter (EfOM) from natural organic matter (NOM) using multiple analytical techniques. *Water Science & Technology* 57 (7), 1009–1015. doi:10.2166/wst.2008.165.

Nödler, K., Hillebrand, O., Idzik, K., Strathmann, M., Schiperski, F., Zirlewagen, J., Licha, T., 2013. Occurrence and fate of the angiotensin II receptor antagonist transformation product valsartan acid in the water cycle--a comparative study with selected beta-blockers and the persistent anthropogenic wastewater indicators carbamazepine and acesulfame. *Water Research* 47 (17), 6650–6659. doi:10.1016/j.watres.2013.08.034.

Nödler, K., Tsakiri, M., Aloupi, M., Gatidou, G., Stasinakis, A.S., Licha, T., 2016. Evaluation of polar organic micropollutants as indicators for wastewater-related coastal water quality impairment. *Environmental Pollution* 211, 282–290. doi:10.1016/j.envpol.2016.01.014.

Nödler, K., Tsakiri, M., Licha, T., 2014. The impact of different proportions of a treated effluent on the biotransformation of selected micro-contaminants in river water microcosms. *International Journal of Environmental Research and Public Health* 11 (10), 10390–10405. doi:10.3390/ijerph111010390.

O'Leary, N.A., Wright, M.W., Brister, J.R., Ciufo, S., Haddad, D., McVeigh, R., Rajput, B., Robbertse, B., Smith-White, B., Ako-Adjei, D., Astashyn, A., Badretdin, A., Bao, Y., Blinkova, O., Brover, V., Chetvernin, V., Choi, J., Cox, E., Ermolaeva, O., Farrell, C.M., Goldfarb, T., Gupta, T., Haft, D., Hatcher, E., Hlavina, W., Joardar, V.S., Kodali, V.K., Li, W., Maglott, D., Masterson, P., McGarvey, K.M., Murphy, M.R., O'Neill, K., Pujar, S., Rangwala, S.H., Rausch, D., Riddick, L.D., Schoch, C., Shkeda, A., Storz, S.S., Sun, H., Thibaud-Nissen, F., Tolstoy, I., Tully, R.E., Vatsan, A.R., Wallin, C., Webb, D., Wu, W., Landrum, M.J., Kimchi, A., Tatusova, T., DiCuccio, M., Kitts, P., Murphy, T.D., Pruitt, K.D., 2016. Reference sequence (RefSeq) database at NCBI: Current status, taxonomic expansion, and functional annotation. *Nucleic Acids Research* 44 (D1), D733-45. doi:10.1093/nar/gkv1189.

Onesios, K.M., Bouwer, E.J., 2012. Biological removal of pharmaceuticals and personal care products during laboratory soil aquifer treatment simulation with different primary substrate concentrations. *Water Research* 46 (7), 2365–2375. doi:10.1016/j.watres.2012.02.001.

Pal, A., He, Y., Jekel, M., Reinhard, M., Gin, K.Y.-H., 2014. Emerging contaminants of public health significance as water quality indicator compounds in the urban water cycle. *Environment international* 71, 46–62. doi:10.1016/j.envint.2014.05.025.

Parks, D.H., Imelfort, M., Skennerton, C.T., Hugenholtz, P., Tyson, G.W., 2015. CheckM: Assessing the quality of microbial genomes recovered from isolates, single cells, and metagenomes. *Genome Research* 25 (7), 1043–1055. doi:10.1101/gr.186072.114.

Parks, D.H., Tyson, G.W., Hugenholtz, P., Beiko, R.G., 2014. STAMP: Statistical analysis of taxonomic and functional profiles. *Bioinformatics* 30 (21), 3123–3124. doi:10.1093/bioinformatics/btu494.

Petrie, B., Barden, R., Kasprzyk-Hordern, B., 2015. A review on emerging contaminants in wastewaters and the environment: current knowledge, understudied areas and recommendations for future monitoring. *Water Research* 72, 3–27. doi:10.1016/j.watres.2014.08.053.

Poindexter, J.S., 1981. Oligotrophy, In: Alexander, M. (Ed.), Advances in Microbial Ecology, vol. 5. Springer US; Imprint; Springer, Boston, MA, pp. 63–89.

Polesel, F., Andersen, H.R., Trapp, S., Plosz, B.G., 2016. Removal of Antibiotics in Biological Wastewater Treatment Systems-A Critical Assessment Using the Activated Sludge Modeling Framework for Xenobiotics (ASM-X). *Environmental Science & Technology* 50 (19), 10316–10334. doi:10.1021/acs.est.6b01899.

Prior, J.E., Shokati, T., Christians, U., Gill, R.T., 2010. Identification and characterization of a bacterial cytochrome P450 for the metabolism of diclofenac. *Applied Microbiology and Biotechnology* 85 (3), 625–633. doi:10.1007/s00253-009-2135-0.

Provost, F., Domingos, P., 2003. Tree Induction for Probability-Based Ranking. *Machine Learning* 52 (3), 199–215. doi:10.1023/A:1024099825458.

Qiu, S., McComb, A.J., Bell, R.W., Davis, J.A., 2005. Response of soil microbial activity to temperature, moisture, and litter leaching on a wetland transect during seasonal refilling. *Wetlands Ecology and Management* 13 (1), 43–54. doi:10.1007/s11273-003-3054-y.

Rauch-Williams, T., Drewes, J.E., 2006. Using soil biomass as an indicator for the biological removal of effluent-derived organic carbon during soil infiltration. *Water Research* 40 (5), 961–968. doi:10.1016/j.watres.2006.01.007.

Rauch-Williams, T., Hoppe-Jones, C., Drewes, J.E., 2010. The role of organic matter in the removal of emerging trace organic chemicals during managed aquifer recharge. *Water Research* 44 (2), 449–460. doi:10.1016/j.watres.2009.08.027.

Ray, C., Grischek, T., Schubert, J., Wang, J.Z., Speth, T.F., 2002. A Perspective of Riverbank Filtration. *Journal - American Water Works Association* 94 (4), 149–160. doi:10.1002/j.1551-8833.2002.tb09459.x.

Real, F.J., Benitez, F.J., Acero, J.L., Sagasti, J.J.P., Casas, F., 2009. Kinetics of the Chemical Oxidation of the Pharmaceuticals Primidone, Ketoprofen, and Diatrizoate in Ultrapure and Natural Waters. *Industrial & Engineering Chemistry Research* 48 (7), 3380–3388. doi:10.1021/ie801762p.

Reddersen, K., Heberer, T., Dünnbier, U., 2002. Identification and significance of phenazone drugs and their metabolites in ground- and drinking water. *Chemosphere* 49 (6), 539–544. doi:10.1016/S0045-6535(02)00387-9.

Reemtsma, T., Berger, U., Arp, H.P.H., Gallard, H., Knepper, T.P., Neumann, M., Quintana, J.B., Voogt, P. de, 2016. Mind the Gap: Persistent and Mobile Organic

Compounds-Water Contaminants That Slip Through. *Environmental Science & Technology* 50 (19), 10308–10315. doi:10.1021/acs.est.6b03338.

Reemtsma, T., Miehe, U., Dünnbier, U., Jekel, M., 2010. Polar pollutants in municipal wastewater and the water cycle: occurrence and removal of benzotriazoles. *Water Research* 44 (2), 596–604. doi:10.1016/j.watres.2009.07.016.

Regnery, J., Barringer, J., Wing, A.D., Hoppe-Jones, C., Teerlink, J., Drewes, J.E., 2015a. Start-up performance of a full-scale riverbank filtration site regarding removal of DOC, nutrients, and trace organic chemicals. *Chemosphere* 127, 136–142. doi:10.1016/j.chemosphere.2014.12.076.

Regnery, J., Gerba, C.P., Dickenson, E.R.V., Drewes, J.E., 2017. The importance of key attenuation factors for microbial and chemical contaminants during managed aquifer recharge: A review. *Critical Reviews in Environmental Science and Technology* 47 (15), 1409–1452. doi:10.1080/10643389.2017.1369234.

Regnery, J., Wing, A.D., Alidina, M., Drewes, J.E., 2015b. Biotransformation of trace organic chemicals during groundwater recharge: How useful are first-order rate constants? *Journal of Contaminant Hydrology* 179, 65–75. doi:10.1016/j.jconhyd.2015.05.008.

Regnery, J., Wing, A.D., Kautz, J., Drewes, J.E., 2016. Introducing sequential managed aquifer recharge technology (SMART) – From laboratory to full-scale application. *Chemosphere* 154, 8–16. doi:10.1016/j.chemosphere.2016.03.097.

Riu, J., Gonzalez-Mazo, E., Gomez-Parra, A., Barceló, D., 1999. Determination of parts per trillion level of carboxylic degradation products of linear alkylbenzenesulfonates in coastal water by solid-phase extraction followed by liquid chromatography/ionspray/mass spectrometry using negative ion detection. *Chromatographia* 50 (5-6), 275–281. doi:10.1007/BF02490828.

Roller, B.R.K., Stoddard, S.F., Schmidt, T.M., 2016. Exploiting rRNA operon copy number to investigate bacterial reproductive strategies. *Nature Microbiology* 1 (11), 16160. doi:10.1038/nmicrobiol.2016.160.

Schaffer, M., Börnick, H., Nödler, K., Licha, T., Worch, E., 2012. Role of cation exchange processes on the sorption influenced transport of cationic β-blockers in aquifer sediments. *Water research* 46 (17), 5472–5482. doi:10.1016/j.watres.2012.07.013.

Schaper, J.L., Seher, W., Nützmann, G., Putschew, A., Jekel, M., Lewandowski, J., 2018. The fate of polar trace organic compounds in the hyporheic zone. *Water Research* 140, 158–166. doi:10.1016/j.watres.2018.04.040.

Scheurer, M., Brauch, H.-J., Lange, F.T., 2009. Analysis and occurrence of seven artificial sweeteners in German waste water and surface water and in soil aquifer treatment (SAT). *Analytical and Bioanalytical Chemistry* 394 (6), 1585–1594. doi:10.1007/s00216-009-2881-y.

Scheurer, M., Michel, A., Brauch, H.-J., Ruck, W., Sacher, F., 2012. Occurrence and fate of the antidiabetic drug metformin and its metabolite guanylurea in the environment and during drinking water treatment. *Water Research* 46 (15), 4790–4802. doi:10.1016/j.watres.2012.06.019.

Scheurer, M., Storck, F.R., Graf, C., Brauch, H.-J., Ruck, W., Lev, O., Lange, F.T., 2011. Correlation of six anthropogenic markers in wastewater, surface water, bank filtrate, and soil aquifer treatment. *Journal of Environmental Monitoring : JEM* 13 (4), 966–973. doi:10.1039/c0em00701c.

Schimmelpfennig, S., Kirillin, G., Engelhardt, C., Nützmann, G., Dünnbier, U., 2012. Seeking a compromise between pharmaceutical pollution and phosphorus load: Management strategies for Lake Tegel, Berlin. *Water Research* 46 (13), 4153–4163. doi:10.1016/j.watres.2012.05.024.

Schmitt-Kopplin, P., Gelencser, A., Dabek-Zlotorzynska, E., Kiss, G., Hertkorn, N., Harir, M., Hong, Y., Gebefugi, I., 2010. Analysis of the unresolved organic fraction in atmospheric aerosols with ultrahigh-resolution mass spectrometry and nuclear magnetic resonance spectroscopy: organosulfates as photochemical smog constituents. *Analytical Chemistry* 82 (19), 8017–8026. doi:10.1021/ac101444r.

Schudel, B., Biaggi, D., Dervey, T., Kozel, R., Müller, I., Ross, J.H., Schindler, U., 2002. Einsatz künstlicher Tracer in der Hydrogeologie - Praxishilfe. Berichte des BWG, Serie Geologie 3. Bundesamt für Wasser und Geologie BWG, Bern.

Schulz, M., Löffler, D., Wagner, M., Ternes, T.A., 2008. Transformation of the X-ray Contrast Medium Iopromide In Soil and Biological Wastewater Treatment. *Environmental Science & Technology* 42 (19), 7207–7217. doi:10.1021/es800789r.

Schut, F., Prins, R.A., Gottschal, J.C., 1997. Oligotrophy and pelagic marine bacteria: Facts and fiction. *Aquatic Microbial Ecology* 12 (2), 177–202. doi:10.3354/ame012177.

Schwarzenbach, R.P., Escher, B.I., Fenner, K., Hofstetter, T.B., Johnson, C.A., von Gunten, U., Wehrli, B., 2006. The Challenge of Micropollutants in Aquatic Systems. *Science* 313 (5790), 1072–1077. doi:10.1126/science.1127291.

Senechkin, I.V., Speksnijder, A.G.C.L., Semenov, A.M., van Bruggen, A.H.C., van Overbeek, L.S., 2010. Isolation and partial characterization of bacterial strains on low organic carbon medium from soils fertilized with different organic amendments. *Microbial Ecology* 60 (4), 829–839. doi:10.1007/s00248-010-9670-1.

Sharma, S.K., Amy, G., 2010. Natural Treatment Systems, In: Edzwald, J.K. (Ed.), Water quality & treatment. A handbook on drinking water, 6th ed. American Water Works Association and McGraw-Hill Inc., USA, pp. 1–33.

Simon, C., Daniel, R., 2011. Metagenomic analyses: Past and future trends. *Applied and Environmental Microbiology* 77 (4), 1153–1161. doi:10.1128/AEM.02345-10.

Sleighter, R.L., Hatcher, P.G., 2007. The application of electrospray ionization coupled to ultrahigh resolution mass spectrometry for the molecular characterization of natural organic matter. *Journal of mass spectrometry : JMS* 42 (5), 559–574. doi:10.1002/jms.1221.

Sontheimer, H., Heilker, E., Jekel, M.R., Nolte, H., Vollmer, F.H., 1978. The Mülheim Process. *Journal - American Water Works Association* 70 (7), 393–396. doi:10.1002/j.1551-8833.1978.tb04199.x.

Sprenger, C., Hartog, N., Hernández, M., Vilanova, E., Grützmacher, G., Scheibler, F., Hannappel, S., 2017. Inventory of managed aquifer recharge sites in Europe: Historical development, current situation and perspectives. *Hydrogeology Journal* 25 (6), 1909–1922. doi:10.1007/s10040-017-1554-8.

Stahlschmidt, M., Regnery, J., Campbell, A., Drewes, J.E., 2016. Application of 3D-fluorescence/PARAFAC to monitor the performance of managed aquifer recharge facilities. *Journal of Water Reuse and Desalination* 6 (2), 249-263. doi:10.2166/wrd.2015.220.

Stefan, C., Ansems, N., 2018. Web-based global inventory of managed aquifer recharge applications. *Sustainable Water Resources Management* 4 (2), 153–162. doi:10.1007/s40899-017-0212-6.

Stenson, A.C., Marshall, A.G., Cooper, W.T., 2003. Exact Masses and Chemical Formulas of Individual Suwannee River Fulvic Acids from Ultrahigh Resolution Electrospray Ionization Fourier Transform Ion Cyclotron Resonance Mass Spectra. *Analytical Chemistry* 75 (6), 1275–1284. doi:10.1021/ac026106p.

Storey, J.D., Tibshirani, R., 2003. Statistical significance for genomewide studies. *Proceedings of the National Academy of Sciences* 100 (16), 9440–9445. doi:10.1073/pnas.1530509100.

Stuart, M., Lapworth, D., Crane, E., Hart, A., 2012. Review of risk from potential emerging contaminants in UK groundwater. *Science of The Total Environment* 416, 1–21. doi:10.1016/j.scitotenv.2011.11.072.

Stuyfzand, P.J., 1993. Hydrochemistry and hydrology of the coastal dune area of the Western Netherlands. Dissertation. Vrije Universiteit, Amsterdam.

Suarez, S., Dodd, M.C., Omil, F., Gunten, U. von, 2007. Kinetics of triclosan oxidation by aqueous ozone and consequent loss of antibacterial activity: Relevance to municipal wastewater ozonation. *Water Research* 41 (12), 2481–2490. doi:10.1016/j.watres.2007.02.049.

Swan, B.K., Tupper, B., Sczyrba, A., Lauro, F.M., Martinez-Garcia, M., González, J.M., Luo, H., Wright, J.J., Landry, Z.C., Hanson, N.W., Thompson, B.P., Poulton, N.J., Schwientek, P., Acinas, S.G., Giovannoni, S.J., Moran, M.A., Hallam, S.J., Cavicchioli, R., Woyke, T., Stepanauskas, R., 2013. Prevalent genome streamlining and latitudinal divergence of planktonic bacteria in the surface ocean. *Proceedings of the National Academy of Sciences of the United States of America* 110 (28), 11463–11468. doi:10.1073/pnas.1304246110.

Tang, K., Escola Casas, M., Ooi, G.T.H., Kaarsholm, K.M.S., Bester, K., Andersen, H.R., 2017. Influence of humic acid addition on the degradation of pharmaceuticals by biofilms in effluent wastewater. *International journal of hygiene and environmental health* 220 (3), 604–610. doi:10.1016/j.ijheh.2017.01.003.

Tatusov, R.L., 2000. The COG database: A tool for genome-scale analysis of protein functions and evolution. *Nucleic Acids Research* 28 (1), 33–36. doi:10.1093/nar/28.1.33.

Ternes, T.A., Herrmann, N., Bonerz, M., Knacker, T., Siegrist, H., Joss, A., 2004. A rapid method to measure the solid-water distribution coefficient (Kd) for pharmaceuticals and musk fragrances in sewage sludge. *Water Research* 38 (19), 4075–4084. doi:10.1016/j.watres.2004.07.015.

Ternes, T.A., Meisenheimer, M., McDowell, D., Sacher, F., Brauch, H.-J., Haist-Gulde, B., Preuss, G., Wilme, U., Zulei-Seibert, N., 2002. Removal of Pharmaceuticals during Drinking Water Treatment. *Environmental Science & Technology* 36 (17), 3855–3863. doi:10.1021/es015757k.

Ternes, T.A., Stüber, J., Herrmann, N., McDowell, D., Ried, A., Kampmann, M., Teiser, B., 2003. Ozonation: A tool for removal of pharmaceuticals, contrast media and musk fragrances from wastewater? *Water Research* 37 (8), 1976–1982. doi:10.1016/S0043-1354(02)00570-5.

Terrabase Inc. Surfactants. <http://www.terrabase-inc.com/> (retrieved 29.06.18).

Tran, N.H., Urase, T., Ngo, H.H., Hu, J., Ong, S.L., 2013. Insight into metabolic and cometabolic activities of autotrophic and heterotrophic microorganisms in the biodegradation of emerging trace organic contaminants. *Bioresource Technology* 146, 721–731. doi:10.1016/j.biortech.2013.07.083.

Trivedi, P., Anderson, I.C., Singh, B.K., 2013. Microbial modulators of soil carbon storage: Integrating genomic and metabolic knowledge for global prediction. *Trends in microbiology* 21 (12), 641–651. doi:10.1016/j.tim.2013.09.005.

Tseng, L.Y., Gonsior, M., Schmitt-Kopplin, P., Cooper, W.J., Pitt, P., Rosso, D., 2013. Molecular characteristics and differences of effluent organic matter from parallel activated sludge and integrated fixed-film activated sludge (IFAS) processes. *Environmental Science & Technology* 47 (18), 10277–10284. doi:10.1021/es4002482.

Tufenkji, N., Ryan, J.N., Elimelech, M., 2002. The promise of bank filtration. *Environmental Science & Technology* 36 (21), 422A–428A.

Umweltbundesamt, 2003. Bewertung der Anwesenheit teil- oder nicht bewertbarer Stoffe im Trinkwasser aus gesundheitlicher Sicht: Empfehlung des Umweltbundesamtes nach Anhörung der Trinkwasserkommission beim Umweltbundesamt. *Bundesgesundheitsblatt - Gesundheitsforschung - Gesundheitsschutz* 46 (3), 249–251. doi:10.1007/s00103-002-0576-7.

Umweltbundesamt, 2018. Liste der nach GOW bewerteten Stoffe. <https://www.umweltbundesamt.de/sites/default/files/medien/374/dokumente/liste_der_nach_gow_bewerteten_stoffe_201802.pdf> (retrieved Februar 2018).

van Baar, P., 2015. Entwicklung und Anwendung von UHPLC-MS Verfahren für organische Spurenstoffe zur Bewertung der Sicherheit der Rohwasserressourcen der Wasserwerke der Stadt Berlin. Dissertation. Technische Universität Berlin, Berlin.

von Gunten, U., 2003a. Ozonation of drinking water: Part I. Oxidation kinetics and product formation. *Water Research* 37 (7), 1443–1467. doi:10.1016/S0043-1354(02)00457-8.

von Gunten, U., 2003b. Ozonation of drinking water: Part II. Disinfection and by-product formation in presence of bromide, iodide or chlorine. *Water Research* 37 (7), 1469–1487. doi:10.1016/S0043-1354(02)00458-X.

Wang, F., van Halem, D., Ding, L., Bai, Y., Lekkerkerker-Teunissen, K., van der Hoek, J.P., 2018. Effective removal of bromate in nitrate-reducing anoxic zones during managed aquifer recharge for drinking water treatment: Laboratory-scale simulations. *Water Research* 130, 88–97. doi:10.1016/j.watres.2017.11.052.

Wang, J., Wang, S., 2018. Microbial degradation of sulfamethoxazole in the environment. *Applied Microbiology and Biotechnology* 102 (8), 3573–3582. doi:10.1007/s00253-018-8845-4.

Wang, Q., Garrity, G.M., Tiedje, J.M., Cole, J.R., 2007. Naive Bayesian Classifier for Rapid Assignment of rRNA Sequences into the New Bacterial Taxonomy. *Applied and Environmental Microbiology* 73 (16), 5261–5267. doi:10.1128/AEM.00062-07.

Weishaar, J.L., Aiken, G.R., Bergamaschi, B.A., Fram, M.S., Fujii, R., Mopper, K., 2003. Evaluation of Specific Ultraviolet Absorbance as an Indicator of the Chemical Composition and Reactivity of Dissolved Organic Carbon. *Environmental Science & Technology* 37 (20), 4702–4708. doi:10.1021/es030360x.

White, J.R., Nagarajan, N., Pop, M., 2009. Statistical methods for detecting differentially abundant features in clinical metagenomic samples. *PLOS (computational biology)* 5 (4), e1000352. doi:10.1371/journal.pcbi.1000352.

Wiese, B., Massmann, G., Jekel, M., Heberer, T., Dünnbier, U., Orlikowski, D., Grützmacher, G., 2011. Removal kinetics of organic compounds and sum parameters under field conditions for managed aquifer recharge. *Water Research* 45 (16), 4939–4950. doi:10.1016/j.watres.2011.06.040.

Witten, I.H., et al., 2016. Data mining: Practical machine learning tools and techniques, Fourth edition ed. Morgan Kaufmann, Cambridge, MA, 11 pp.

Wode, F., Reilich, C., van Baar, P., Dünnbier, U., Jekel, M., Reemtsma, T., 2012. Multiresidue analytical method for the simultaneous determination of 72 micropollutants in aqueous samples with ultra high performance liquid chromatography-high resolution mass spectrometry. *Journal of Chromatography A* 1270, 118–126. doi:10.1016/j.chroma.2012.10.054.

Wojcieszyńska, D., Domaradzka, D., Hupert-Kocurek, K., Guzik, U., 2014. Bacterial degradation of naproxen--undisclosed pollutant in the environment. *Journal of Environmental Management* 145, 157–161. doi:10.1016/j.jenvman.2014.06.023.

Wolf, L., Zwiener, C., Zemann, M., 2012. Tracking artificial sweeteners and pharmaceuticals introduced into urban groundwater by leaking sewer networks. *Science of The Total Environment* 430, 8–19. doi:10.1016/j.scitotenv.2012.04.059.

Yu, K., Zhang, T., Liles, M.R., 2012. Metagenomic and Metatranscriptomic Analysis of Microbial Community Structure and Gene Expression of Activated Sludge. *PLoS ONE* 7 (5), e38183. doi:10.1371/journal.pone.0038183.

Yu, N.Y., Wagner, J.R., Laird, M.R., Melli, G., Rey, S., Lo, R., Dao, P., Sahinalp, S.C., Ester, M., Foster, L.J., Brinkman, F.S.L., 2010. PSORTb 3.0: Improved protein subcellular localization prediction with refined localization subcategories and predictive capabilities for all prokaryotes. *Bioinformatics* 26 (13), 1608–1615. doi:10.1093/bioinformatics/btq249.

Zark, M., Dittmar, T., 2018. Universal molecular structures in natural dissolved organic matter. *Nature Communications* 9 (1), 3178. doi:10.1038/s41467-018-05665-9.

Zhou, Y., 2011. Structure Learning of Probabilistic Graphical Models: A Comprehensive Survey. *CoRR* abs/1111.6925.

Zietzschmann, F., Worch, E., Altmann, J., Ruhl, A.S., Sperlich, A., Meinel, F., Jekel, M., 2014. Impact of EfOM size on competition in activated carbon adsorption of organic micro-pollutants from treated wastewater. *Water Research* 65, 297–306. doi:10.1016/j.watres.2014.07.043.

Zucker, I., Mamane, H., Cikurel, H., Jekel, M., Hübner, U., Avisar, D., 2015. A hybrid process of biofiltration of secondary effluent followed by ozonation and short soil aquifer treatment for water reuse. *Water Research* 84, 315–322. doi:10.1016/j.watres.2015.07.034.

Zwiener, C., Frimmel, F.H., 2004. LC-MS analysis in the aquatic environment and in water treatment technology--a critical review. Part II: Applications for emerging contaminants and related pollutants, microorganisms and humic acids. *Analytical and Bioanalytical Chemistry* 378 (4), 862–874. doi:10.1007/s00216-003-2412-1.

Appendix

SI Chapter 4: Advancing sequential managed aquifer recharge technology (SMART) using different intermediate oxidation processes

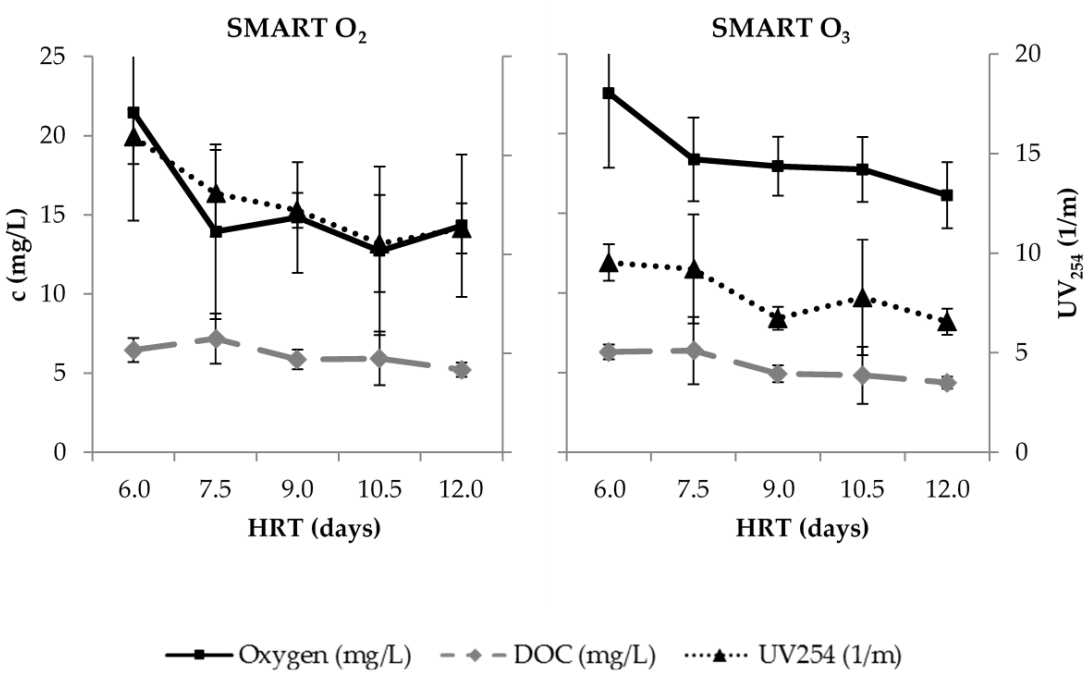

Figure SI-4 1: Profile data of the DO, DOC and UVA_{254} measurements of the systems SMART O_2 and SMART O_3 after aeration with pure oxygen or ozone, respectively ($n \geq 4$).

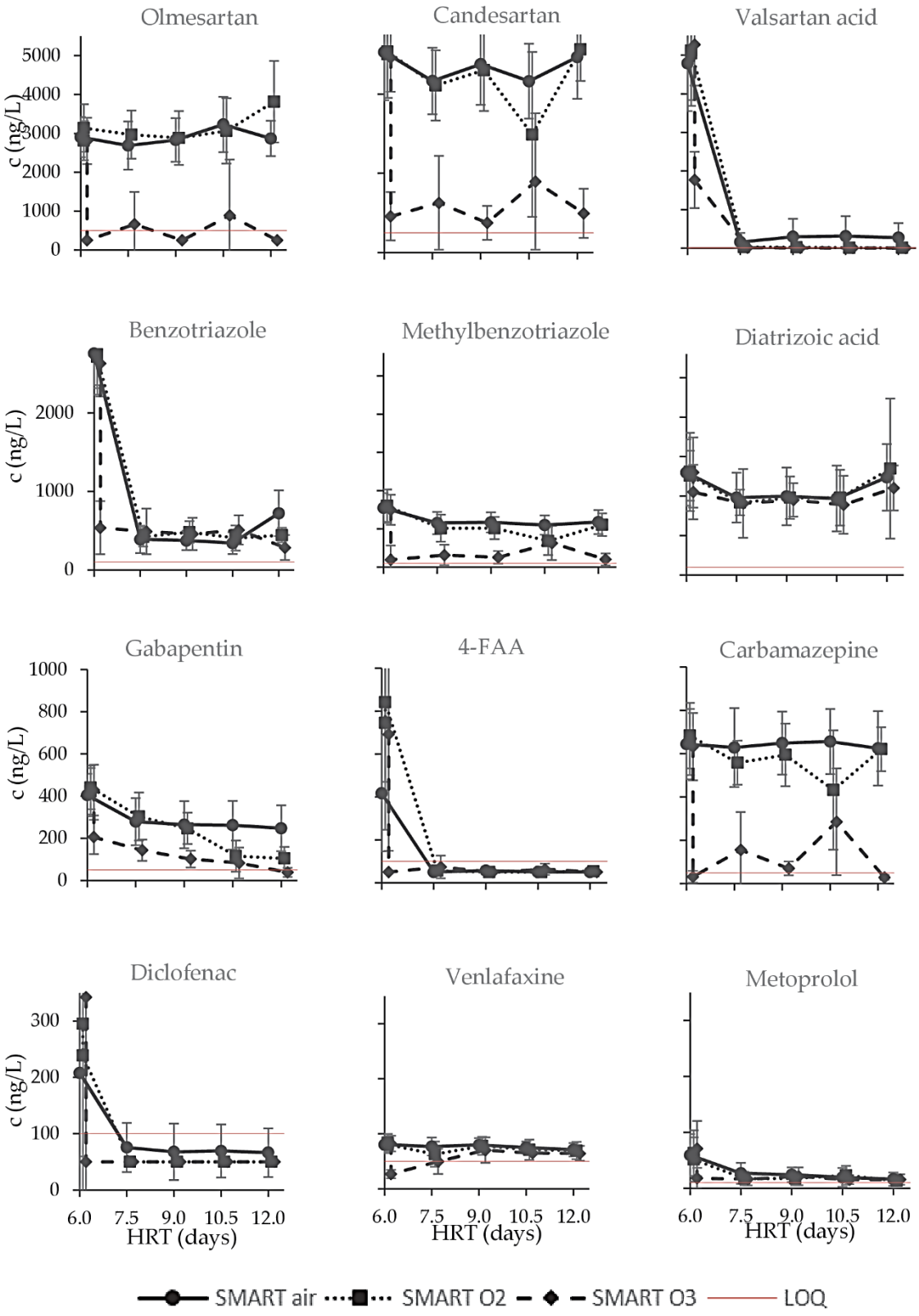

Figure SI-4 2: Profile data of the systems SMART air, SMART O_2 and SMART O_3 after aeration with air, pure oxygen or ozone, respectively, of all quantified TOrCs with effluent concentrations of the first filtration step > LOQ despite sulfamethoxazole. Values < LOQ are referred to LOQ/2.Results are shown as mean values with standard deviation as error bars (*n* ≥ 4).

Table SI-4 1: List of quantified TOrCs.

Compound	Molecular Formula	Influent Concentration (ng/L)	LOQ (ng/L)	$k_{O3}(M^{-1}s^{-1})$	$k_{OH}(M^{-1}s^{-1})$	Fragments Quantifier/ Qualifier (m/z)	Internal Standard
Acesulfame	$C_4H_5NO_4S$	556 ± 276	250	88 [1]	4.6 x 10^9 [1]	82.1/78.0	acesulfame-d4_86.1 / acesulfame-d4_78.0
Benzotriazole	$C_6H_5N_3$	2603 ± 472	100	2.4 x 10^2 [2]	7.6 x 10^9 [3]	65.0/92.0	benzotriazole-d4_69.1 / benzotriazole-d4_96.1
Candesartan	$C_{24}H_{20}N_6O_3$	5448 ± 1099	500	-	-	263/423	benzotriazole-d4_143.0 / benzotriazole-d4_320.0
Carbamazepine	$C_{15}H_{12}N_2O$	667 ± 191	50	~ 3 x 10^5 [4][a]	8.8 ± 1.2 x 10^9 [4][b]	194.1/179.1	carbamazepine-d8_202.1 / carbamazepine-d8_185.1
Diatrizoic acid*	$C_{11}H_9I_3N_2O_4$	1667 ± 911	100	0.05 ± 0.01 [5]	5.4 ± 0.3 x 10^8 [5]	361.0/233.0	iopromide-d3_575.8 / iopromide-d3_299.6
Diclofenac	$C_{14}H_{11}Cl_2NO_2$	1291 ± 444	100	~ 1 x 10^6 [4][a]	7.5 ± 1.5 x 10^9 [4][b]	214.0/179.0	diclofenac-d4_218.0 / diclofenac-d4_183.0
Gabapentin	$C_9H_{17}NO_2$	517 ± 125	50	2.2 x 10^2 [2]	9.1 x 10^9 [2]	137.1/154.1	gabapentin-d4_139.1 / gabapentin-d4_158.1
Iomeprol	$C_{17}H_{22}I_3N_3O_8$	1179 ± 414	100	similar to iopromide**	2.0 ± 0.1 x 10^9 [6]	531.9/404.9	iomeprol-d3_534.9 / iomeprol-d3_407.9
Iopromide	$C_{18}H_{24}I_3N_3O_8$	970 ± 489	10	< 0.8 [4][a]	3.3 ± 0.6 x 10^9 [4][b]	572.8/299.6	iopromide-d3_575.8 / iopromide-d3_299.6
Methylbenzotriazole	$C_7H_7N_3$	955 ± 250	50	4.0-4.9 x 10^2 [7]	-	77.0/79.1	5-methylbenzotriazole-d6_81.0 / 5-methylbenzotriazole-d6_85.0
Metoprolol	$C_{15}H_{25}NO_3$	450 ± 280	10	2.0 ± 0.6 x 10^3 [8]	7.3 ± 0.2 x 10^9 [8]	116.1/159.0	sulfamethoxazole-d4_160.0 / sulfamethoxazole-d4_112.0
Olmesartan	$C_{24}H_{26}N_6O_3$	3010 ± 641	500	-	-	207/429	5-methylbenzotriazole-d6_81.0 / 5-methylbenzotriazole-d6_85.0
Sulfamethoxazole	$C_{10}H_{11}N_3O_3S$	137 ± 54	50	~ 2.5 x 10^6 [4][a]	5.5 ± 0.7 x 10^9 [4][b]	156.0/108.0	sulfamethoxazole-d4_160.0 / sulfamethoxazole-d4_112.0
Valsartan	$C_{24}H_{29}N_5O_3$	422 ± 534	100	38 [2]	~10^{10} [2]	291.0/235.0	bezafibrate-d4_143.0 / bezafibrate-d4_320.0
Valsartan acid	$C_{14}H_{10}N_4O_2$	3103 ± 582	10	-	-	206/178	5-methylbenzotriazole-d6_81.0 / 5-methylbenzotriazole-d6_85.0
Venlafaxine	$C_{17}H_{27}NO_2$	234 ± 69	50	8.5 x 10^3 [2]	~10^{10} [2]	58.0/260.0	carbamazepine-d8_202.1 / carbamazepine-d8_185.1
4-Formylaminoantipyrine	$C_{12}H_{13}N_3O_2$	1656 ± 924	100	6.5 x 10^4 [9]	-	77.0/56.1	sulfamethoxazole-d4_160.0 / sulfamethoxazole-d4_112.0

[1] pH = 7, T = 20°C; [2] pH = 7, T = 22 ± 2°C; [3] pH = 5.8; [4][a] pH = 7, T = 20°C; [4][b] pH = 7, T = 25°C; [5] T = 20°C; [6] pH = 7.0 ± 0.1, T = 22 ± 1 ° C; [7] pH = 7; [8] pH = 7, 20 - 22°C; [9] pH = 7, 20 °C; *k_{O3} and k_{OH} refer to diatrizoate; ** both compounds have similar structures.

References

1. Kaiser, H.-P.; Köster, O.; Gresch, M.; Périsset, P.M.; Jäggi, P.; Salhi, E.; von Gunten, U. Process Control For Ozonation Systems: A Novel Real-Time Approach. Ozone Sci. Eng. 2013, 35, 168–185.

2. Lee, Y.; Kovalova, L.; McArdell, C.S.; von Gunten, U. Prediction of micropollutant elimination during ozonation of a hospital wastewater effluent. Water Res. 2014, 64, 134–148.

3. Naik, D.B.; Moorthy, P.N. Studies on the transient species formed in the pulse radiolysis of benzotriazole. Radiat. Phys. Chem. 1995, 46, 353–357.

4. Huber, M.M.; Canonica, S.; Park, G.-Y.; von Gunten, U. Oxidation of Pharmaceuticals during Ozonation and Advanced Oxidation Processes. Environ. Sci. Technol. 2003, 37, 1016–1024.

5. Real, F.J.; Benitez, F.J.; Acero, J.L.; Sagasti, J.J.P.; Casas, F. Kinetics of the Chemical Oxidation of the Pharmaceuticals Primidone, Ketoprofen, and Diatrizoate in Ultrapure and Natural Waters. Ind. Eng. Chem. Res. 2009, 48, 3380–3388.

6. Jeong, J.; Jung, J.; Cooper, W.J.; Song, W. Degradation mechanisms and kinetic studies for the treatment of X-ray contrast media compounds by advanced oxidation/reduction processes. Water Res. 2010, 44, 4391–4398.

7. Holger Lutze. Ozonung von Benzotriazolen. Bachelor Thesis, 2005.

8. Benner, J.; Salhi, E.; Ternes, T.; von Gunten, U. Ozonation of reverse osmosis concentrate: kinetics and efficiency of beta blocker oxidation. Water Res. 2008, 42, 3003–3012.

9. Favier, M.; Dewil, R.; van Eyck, K.; van Schepdael, A.; Cabooter, D. High-resolution MS and MS(n) investigation of ozone oxidation products from phenazone-type pharmaceuticals and metabolites. Chemosphere 2015, 136, 32–41.

SI Chapter 5: Establishing sequential managed aquifer recharge technology (SMART) for enhanced removal of trace organic chemicals: Experiences from field studies in Berlin, Germany

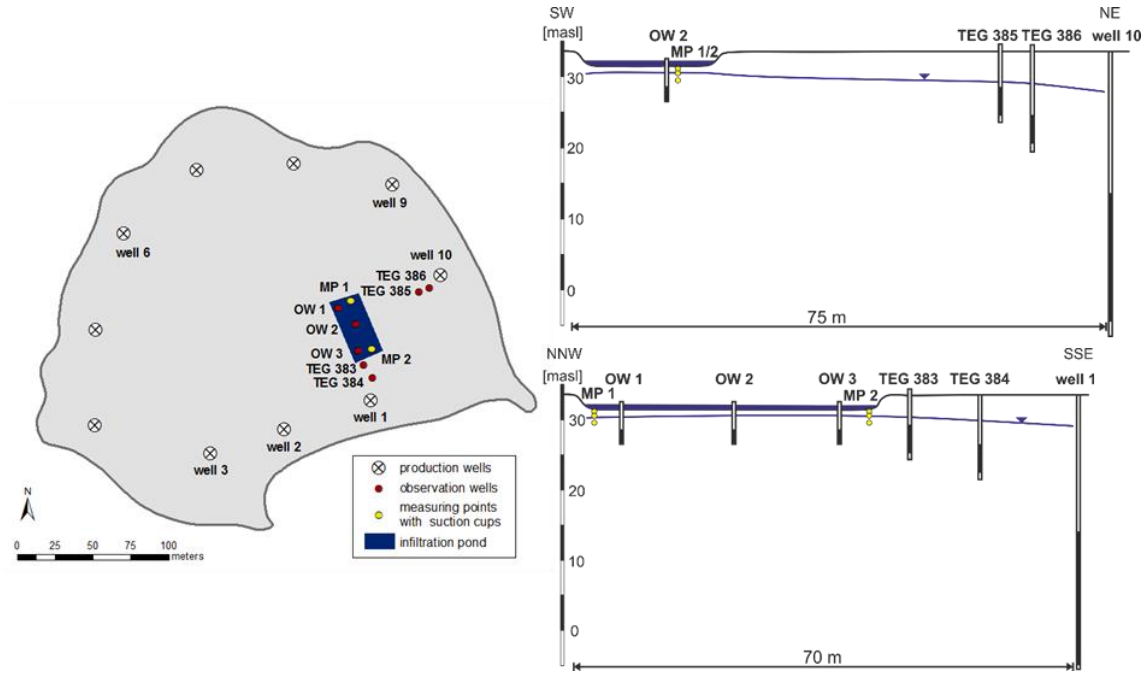

Figure SI-5 1: SMART field site at the recharge facility Baumwerder, located in Lake Tegel (Berlin, Germany) (left) and cross section of two installed transects at the infiltration basin (right).

Table SI-5 1: Influent concentrations of all quantified TOrCs at the cMAR site and SMART site during the experimental period. Mean values are given with standard deviation; concentrations measured below the limit of quantification (LOQ) were set as LOQ/2. (* excluded for further analysis)

		cMAR site (*n* ≥ 19)		SMART site (*n* ≥ 19)	
TOrCs	**LOQ [µg/L]**	**Mean [µg/L]**	**Median [µg/L]**	**Mean [µg/L]**	**Median [µg/L]**
4-FAA	0.020	0.33 ± 0.10	0.29	0.05 ± 0.01	0.05
Acesulfame	0.100	0.30 ± 0.03	0.30	0.78 ± 0.17	0.78
Benzotriazole	0.050	0.73 ± 0.14	0.71	0.46 ± 0.08	0.43
Bisoprolol*	0.025	< LOQ		< LOQ	
Caffeine*	0.100	< LOQ		< LOQ	
Candesartan	0.010	0.18 ± 0.04	0.17	0.14 ± 0.01	0.13
Carbamazepine	0.025	0.21 ± 0.07	0.19	0.30 ± 0.06	0.30
Diclofenac*	0.010	< LOQ		< LOQ	
Dihydroxydihydro-carbamazepine	0.020	0.17 ± 0.03	0.16	0.05 ± 0.01	0.05
Gabapentin	0.010	0.22 ± 0.06	0.21	0.29 ± 0.05	0.30
Gabapentin-	0.010	0.07 ± 0.01	0.07	0.12 ± 0.01	0.12
Metformin	0.020	0.10 ± 0.03	0.10	0.21 ± 0.07	0.20
Metoprolol*	0.030	0.06 ± 0.04	0.06	< LOQ	
Olmesartan	0.010	0.06 ± 0.03	0.05	0.11 ± 0.01	0.11
Oxypurinol	0.050	1.71 ± 0.34	1.70	1.93 ± 0.59	1.80
Phenylethylmalon-amide	0.010	0.03 ± 0.01	0.03	0.05 ± 0.01	0.05
Pregabalin*	0.010	0.03 ± 0.01	0.02	< LOQ	
Primidone	0.025	0.06 ± 0.02	0.06	0.06 ± 0.01	0.06
Sulfamethoxazole*	0.020	0.02 ± 0.01	0.02	< LOQ	
Tolyltriazole	0.025	0.21 ± 0.04	0.20	0.12 ± 0.03	0.12
Valsartan*	0.025	0.08 ± 0.05	0.08	< LOQ	
Valsartan acid	0.010	1.21 ± 0.20	1.20	0.59 ± 0.09	0.58

Tracer test

After applying and mixing of sodium bromide as conservative tracer to the recharge basin at the SMART field site, samples were taken from the basin water in the vicinity of the observation wells (SFW OW 1, SFW OW 2, SFW OW 3, Figure SI-5 2). A maximum bromide concentration of 441 mg/L was measured at the center of the basin (SFW OW 2). Next to OW 1, the bromide concentration was not higher than 147 mg/L, whereas only 37 mg/L were detected next to OW 3 (SFW OW 3). The very low bromide concentration at SFW OW 3 suggests that the added tracer was rapidly diluted by the influent entering the recharge basin at the location of OW 3. Based on the tracer test results, travel times of ~0.09 days for 50 cm, ~0.15 days for 100 cm, and ~0.17 days for 200 cm of infiltration were determined for suction samplers at MP 1 (Figure SI-5 3a). However, at MP 2 the detected tracer concentration was very low compared to MP 1 (< 1 mg/L vs. > 400 mg/L, Figure SI-5 3b), likely due to heterogeneous distribution of bromide in the recharge basin. The travel times to observation wells OW 1 – 3 screened > 2.8 m bgs were estimated as ~0.38 days (OW 1), ~0.30 days (OW 2), and ~0.39 days (OW 3), respectively (Figure SI-5 3c). Since OW 3 had a much lower bromide concentration (maximum: ~ 30 mg/L) compared to OW 1 and 2 (> 150 mg/L), these results support the dilution assumption leading to a weak detection of bromide near the influent as shown for MP 2. A travel time of approximately 11 days to observation well TEG 386 as well as travel times of 17 days and 18 days to wells #1 and #10, respectively, were determined from tracer breakthrough curves (Figure SI-5 3d). No increase of bromide was detected in observation wells TEG 383, TEG 384, and TEG 385. It is assumed that the infiltration path of the main water flow towards production wells #1 and #10 occurs at lower depth than the observation wells and therefore no detection of the tracer at the observation wells TEG 383-385 could be observed. Based on these results, further discussions will be limited to results obtained from MP 1 and well TEG 386. Monitoring wells OW 1-3 were not sampled regularly and only used to monitor the groundwater level below the basin.

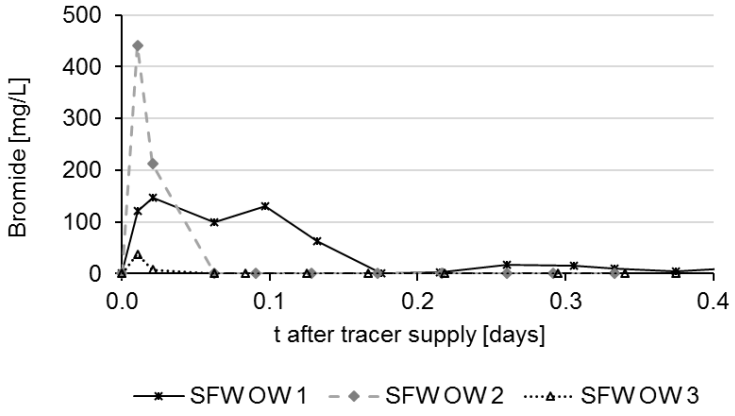

Figure SI-5 2: Tracer concentration in the surface water (SFW) applied to the recharge basin at the SMART field site in the vicinity of observation wells OW 1, 2 and 3.

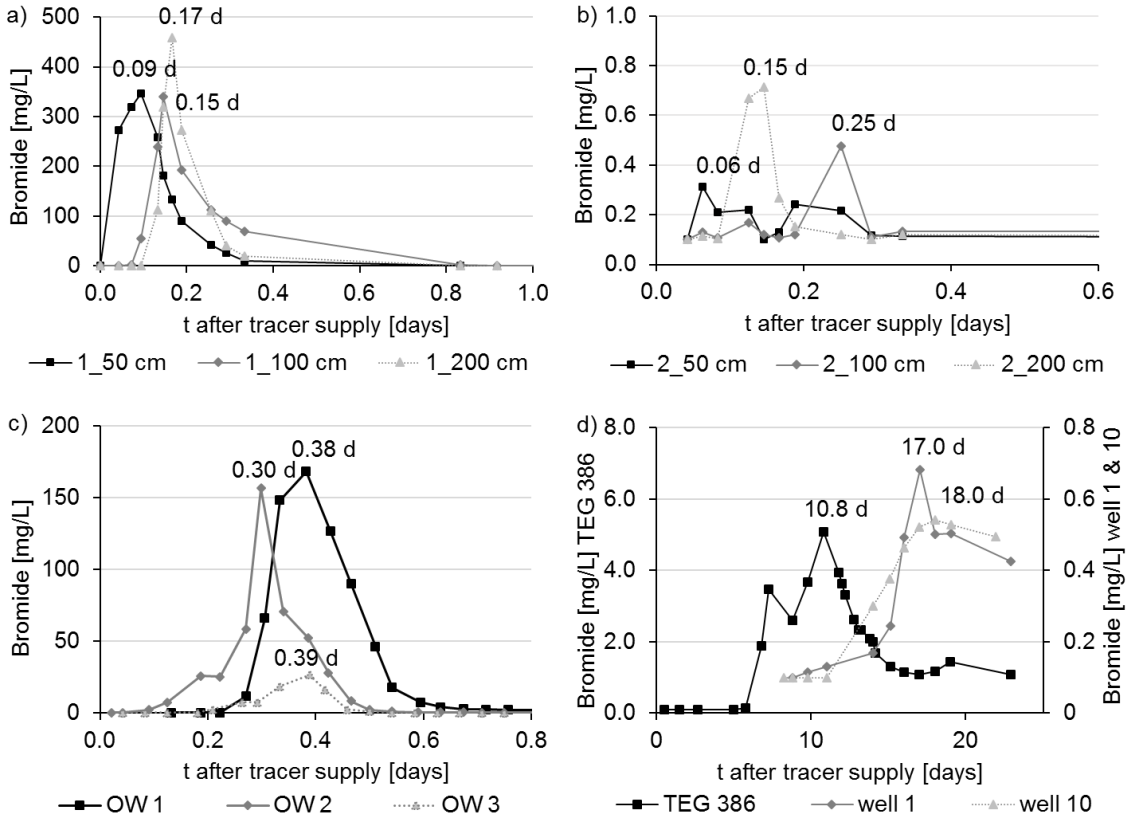

Figure SI-5 3: Results of the tracer test at the SMART field site (a) at measuring point 1 and (b) measuring point 2 in three different depths (50 cm, 100 cm, 200 cm), (c) observation wells within the basin (OW 1, 2 and 3) as well as (d) observation well TEG 386 and production wells 1 and 10.

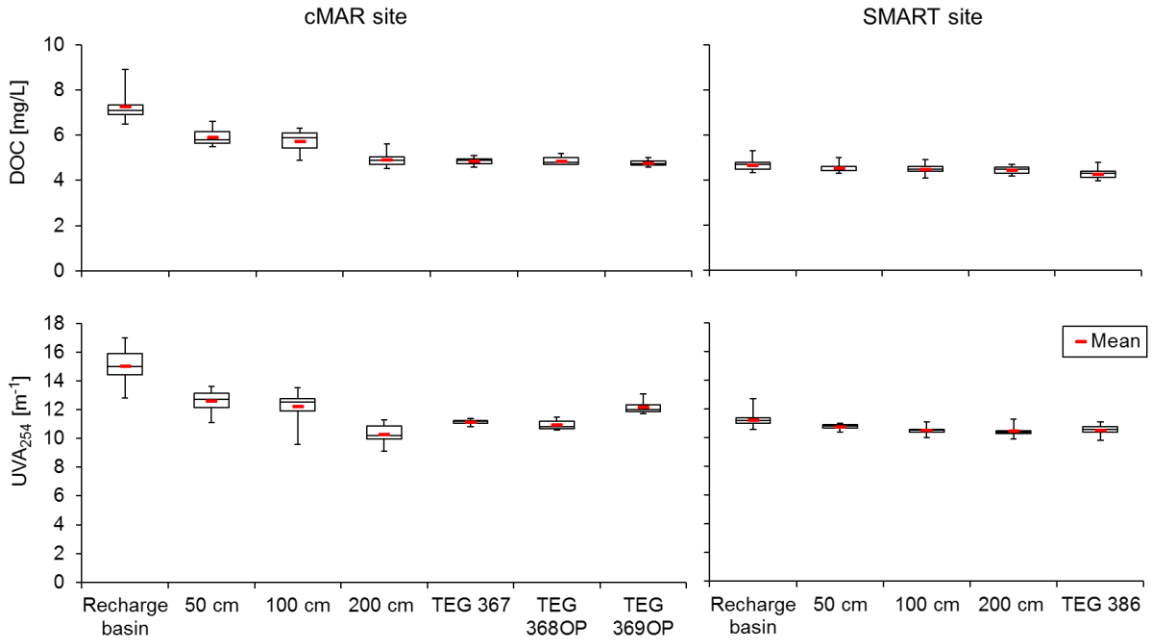

Figure SI-5 4: DOC concentration [mg/L] and UV absorbance at 254 nm [m^{-1}] after successful adaptation at the cMAR site (left; *n* ≥ 4) and SMART site (right, *n* ≥ 20) in different depths and the observation wells. Whiskers indicate the maximum and minimum values and the horizontal line represents the median.

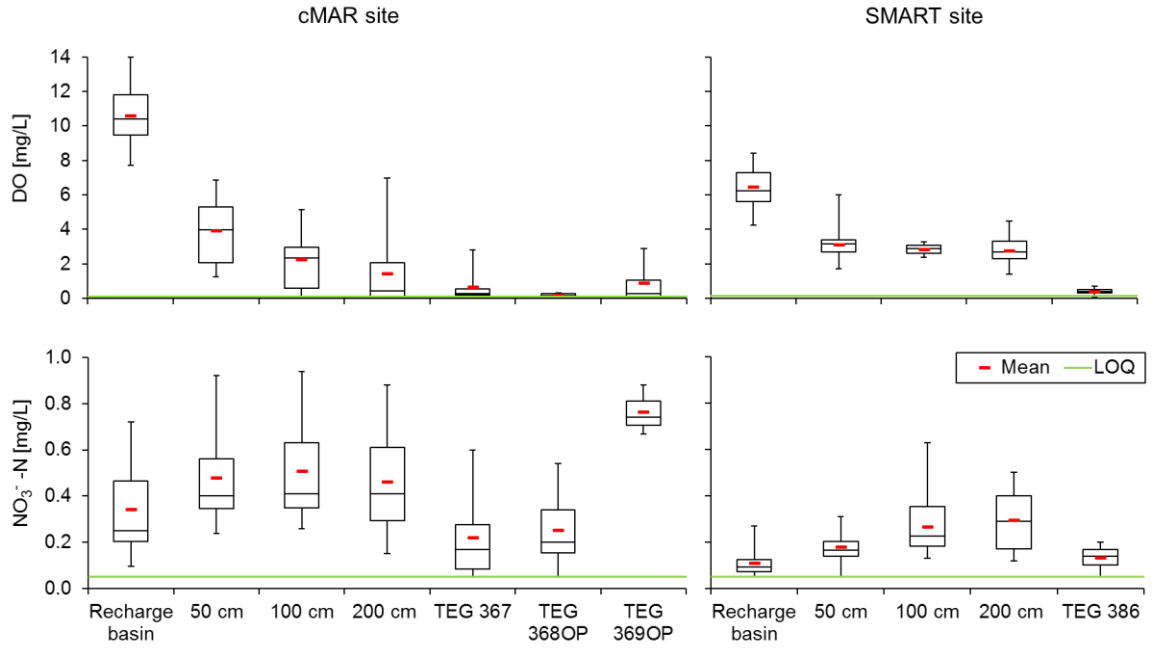

Figure SI-5 5: Dissolved oxygen and nitrate nitrogen concentration [mg/L] after successful adaptation at the cMAR site (left; *n* ≥ 3) and SMART site (right, *n* ≥ 3) in different depths and the observation wells. Whiskers indicate the maximum and minimum values and the horizontal line represents the median.

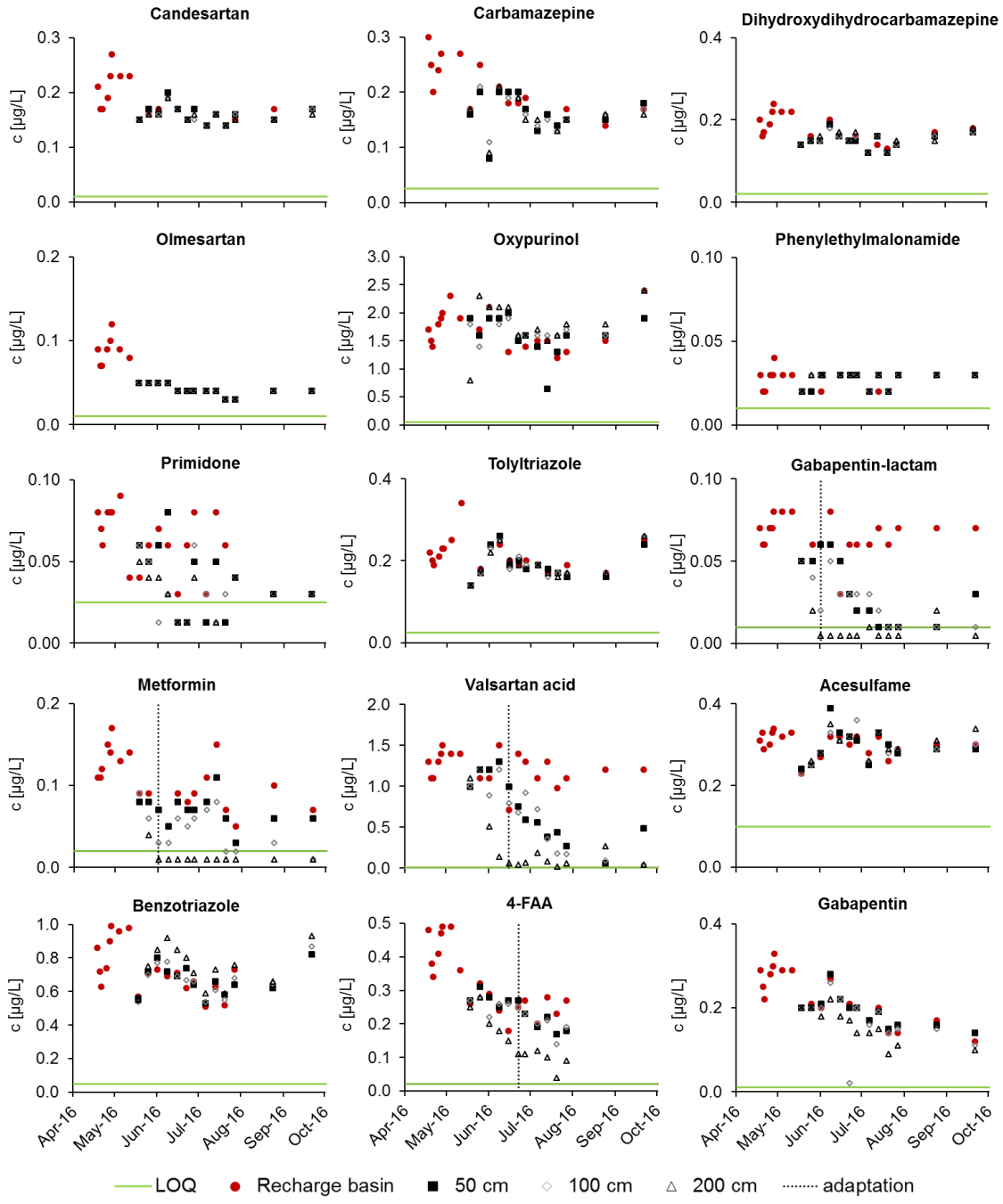

Figure SI-5 6: Concentration of all quantified TOrCs in the basin and in three different depths below the basin (50, 100, 200 cm) during the experimental period at the cMAR site. The vertical line indicates the estimated date of full adaptation.

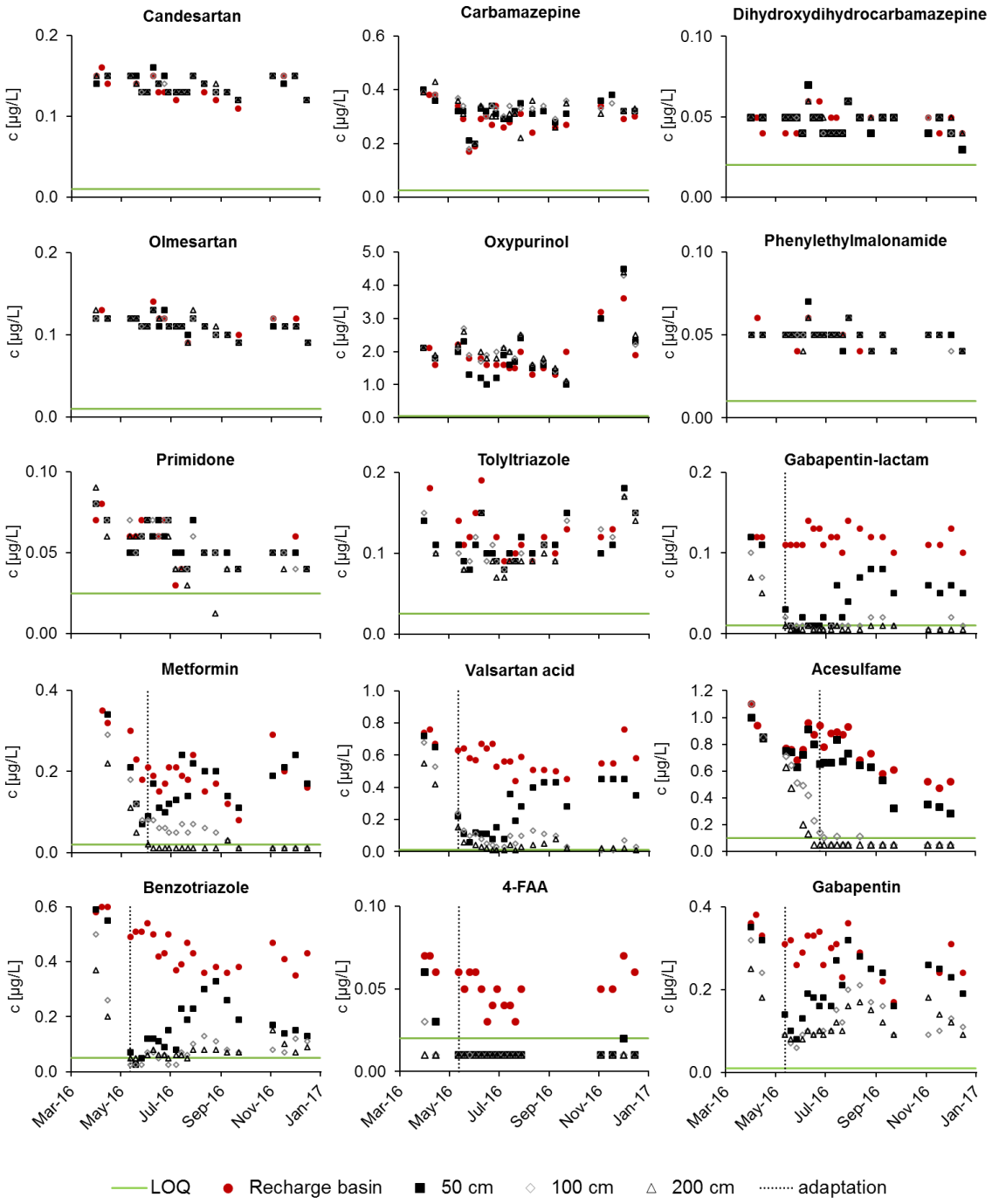

Figure SI-5 7: Concentration of all quantified TOrCs in the basin and in three different depths below the basin (50, 100, 200 cm) during the experimental period at the SMART site. The vertical line indicates the estimated date of full adaptation.

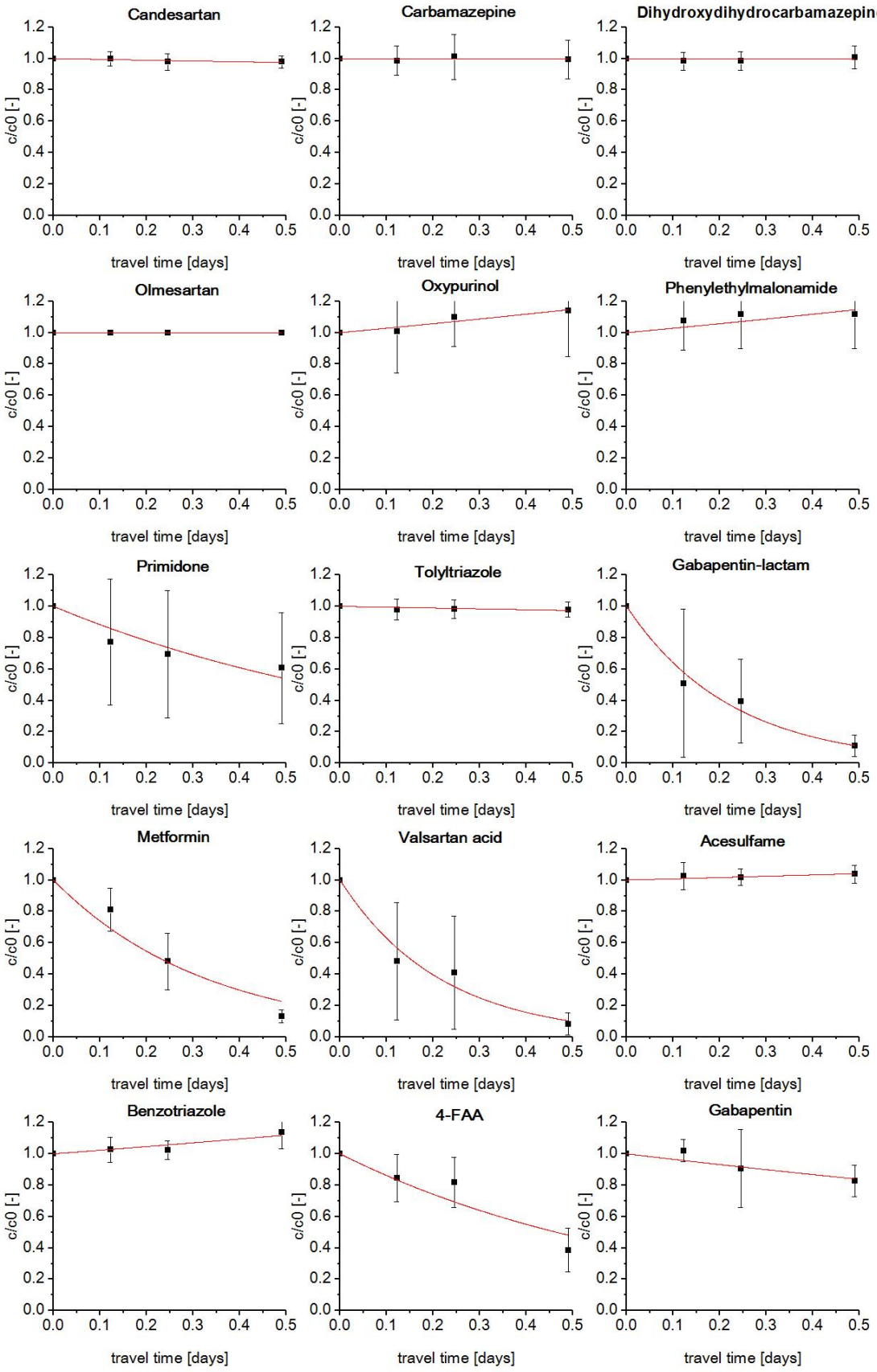

Figure SI-5 8: Fit of first-order kinetic of all quantified TOrCs at the cMAR site ($n \geq 6$).

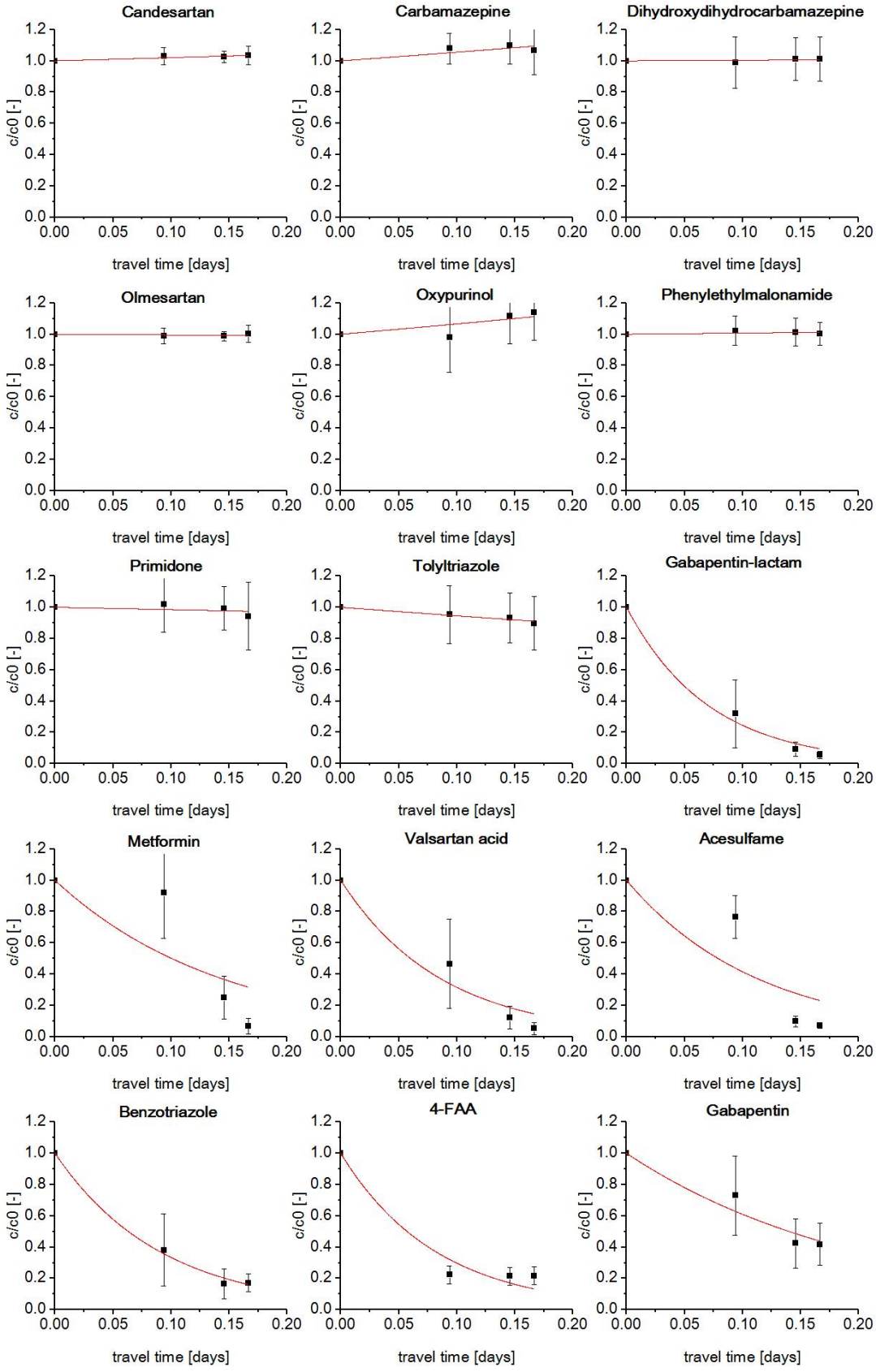

Figure SI-5 9: Fit of first-order kinetic of all quantified TOrCs at the SMART site ($n \geq 13$).

SI Chapter 6: Microbiome-triggered transformations of trace organic chemicals in the presence of effluent organic matter in managed aquifer recharge (MAR) systems

3D-fluorescence spectroscopy

The analyses of the samples were performed under specific settings as listed in Table SI-6 1. The blank was subtracted from the 3D-Excitation-emission-matrices (3D-EEM) of the sample and furthermore, the sample 3D-EEM were corrected by applying the inner filter effect algorithm as well as the first and second order Rayleigh masking as provided by the Aqualog® software. Finally, the 3D-EEM were normalized to Raman units (R.U.)[1].

Table SI-6 1: Settings chosen for the 3D-fluorescence spectroscopy.

Parameter	Setting
Integration time	1 s
Excitation increment	3 nm
Emission increment	1.64 nm
Excitation wavelength	230-599 nm
Emission wavelength	212-621 nm
Charge-coupled device (CCD)	medium

16S ribosomal RNA amplicon sequencing analysis

Merged and combined reads were processed using USEARCH v9.2.61[2]: i) quality filtering was done using the *fastq_filter* command[3] with default settings; ii) denoising was performed by the *derep_fulllength* command, whereby the *sizeout* option was chosen; iii) sequences were sorted by abundance (*sortbysize* command), a minimum size of 2 was set (*minsize 2*); iv) OTUs were clustered *de novo* by applying the *cluster_otus* command; v) the OTU table was created using *usearch_global* command setting an identity threshold of 0.97 and searching for hits on the forward strand only (*strand plus*).

PARAFAC analysis

The PARAFAC analysis was performed as described by Stahlschmidt et al. (2016)[1]. Due to interfering signals, only excitation wavelengths in the range of 239 - 599 nm were taken into account. Overall, 112 3D-EEM data were available of which 16 were excluded due to missing DOC concentrations and 9 were identified as outliers. The PARAFAC model was generated out of 28 and validated by 59 3D-EEM data. The quality of the model was assessed based on the Core Consistency, Total Variance and Split Half Analysis as proposed by Carvajal et al. (2017)[4].

FT-ICR-MS analysis

Samples were directly injected in the solariX FT-ICR-MS from Bruker (Bruker Daltonik GmbH, Germany) with a flow rate of 120 µL/h at a nebulizer gas pressure of 2.2 bar and a dry gas flow rate of 4 L/min at 180 °C. A capillary voltage of 3600 V was applied. 300 scans per sample were accumulated within a mass range of m/z 147.4 – 1500 with a time domain of 4 megawords. Spectra were first externally calibrated on clusters of a standard arginine solution and internal calibration was systematically done in the presence of natural organic matter reaching accuracy values lower than 1 ppm. Elemental formulae for each peak were calculated by an in-house written software tool[5] with respect to sensible chemical constraints: N rule, O/C ratio ≤ 1, H/C ratio ≤ 2n+2 (C_nH_{2n+2}), element counts: C ≤ 100, H ≤ 200, O ≤ 80, N ≤ 3, S ≤ 2 and mass accuracy window ± 0.5 ppm. Formulae were categorized into groups containing CHO, CHOS, CHNO and CHNOS molecular compositions.

Multivariate analysis

Table SI-6 2: All parameters from the OPLS model: residual sum of squares (SS), degrees of freedom (DF), mean squares (MS), the F-test (F), the p-values (p) and the standard deviation (SD). All the metadata that were included in the model are significant (p-values < 0.05).

Metadata	SS	DF	MS	F	p	SD
DOC [mg/L]						
Total corr	6	6	1			1
Regression	5.99995	5	1.19999	25338.5	0.0047695	1.09544
Residual	4.74E-05	1	4.74E-05			0.006882
UVA_{254} [1/m]						
Total corr	6	6	1			1
Regression	5.99995	5	1.19999	25001.4	0.0048015	1.09544
Residual	4.80E-05	1	4.80E-05			0.006928
Dissolved Oxygen						
Total corr	6	6	1			1
Regression	5.99983	5	1.19997	6859.82	0.0091663	1.09543
Residual	0.0001749	1	0.00017493			0.013226
Nitrate-N [mg/L]						
Total corr	6	6	1			1
Regression	5.99993	5	1.19999	16286.5	0.005949	1.09544
Residual	7.37E-05	1	7.37E-05			0.008584
Benzotriazole [-]						
Total corr	6	6	1			1
Regression	5.99983	5	1.19997	6992.22	0.0090791	1.09543
Residual	0.0001716	1	0.00017161			0.0131
Carbamazepine [-]						
Total corr	6	6	1			1
Regression	5.99987	5	1.19997	9001.11	0.0080021	1.09543
Residual	0.0001333	1	0.00013331			0.011546
Citalopram [-]						
Total corr	6	6	1			1
Regression	5.99998	5	1.2	52451.7	0.003315	1.09544
Residual	2.29E-05	1	2.29E-05			0.004783
Diclofenac [-]						
Total corr	6	6	1			1
Regression	5.99998	5	1.2	76813.8	0.0027393	1.09544
Residual	1.56E-05	1	1.56E-05			0.003952
Gabapentin [-]						
Total corr	6	6	1			1
Regression	5.99998	5	1.2	65804.1	0.0029596	1.09544
Residual	1.82E-05	1	1.82E-05			0.00427

Table SI-6 2 continued

Metoprolol [-]						
Total corr	6	6	1			1
Regression	5.99999	5	1.2	135454	0.0020629	1.09544
Residual	8.86E-06	1	8.86E-06			0.002976
Primidone [-]						
Total corr	6	6	1			1
Regression	5.99985	5	1.19997	8134.9	0.0084174	1.09543
Residual	0.0001475	1	0.00014751			0.012145
Sotalol [-]						
Total corr	6	6	1			1
Regression	5.99999	5	1.2	101601	0.0023819	1.09544
Residual	1.18E-05	1	1.18E-05			0.003437
Sulfamethoxazole [-]						
Total corr	6	6	1			1
Regression	5.99988	5	1.19998	10142	0.0075387	1.09543
Residual	0.0001183	1	0.00011832			0.010877
Tramadol [-]						
Total corr	6	6	1			1
Regression	5.99697	5	1.19939	395.379	0.0381626	1.09517
Residual	0.0030335	1	0.00303353			0.055078
Venlafaxine [-]						
Total corr	6	6	1			1
Regression	5.99966	5	1.19993	3483.48	0.0128627	1.09541
Residual	0.0003445	1	0.00034446			0.01856

Results

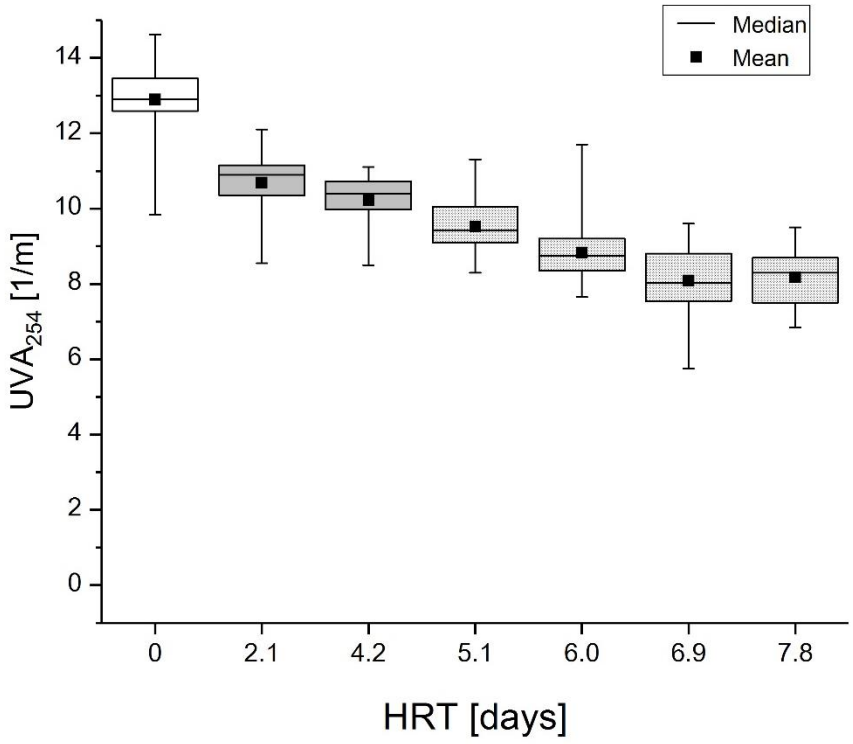

Figure SI-6 1: UV absorbance at 254 nm throughout the system with respect to the HRT ($n \geq 18$). The box represents the 25 – 75 percentiles, the whiskers indicate the maximum and minimum values.

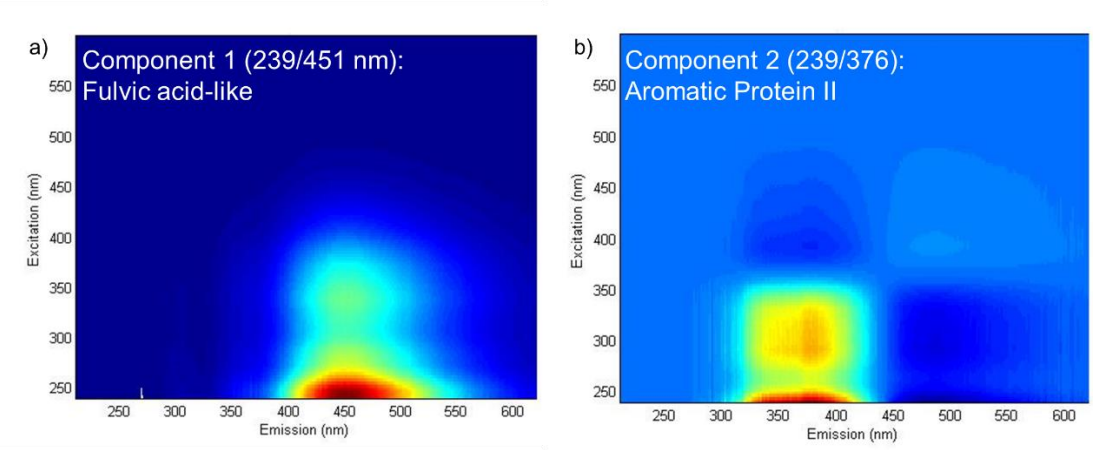

Figure SI-6 2: Two components identified by PARAFAC analysis: a) component 1 fulvic acid-like (λ_{Ex} 239/ λ_{Em} 451 nm), b) component 2 aromatic protein II (239/376 nm) as proposed by Chen et al. (2003)[6].

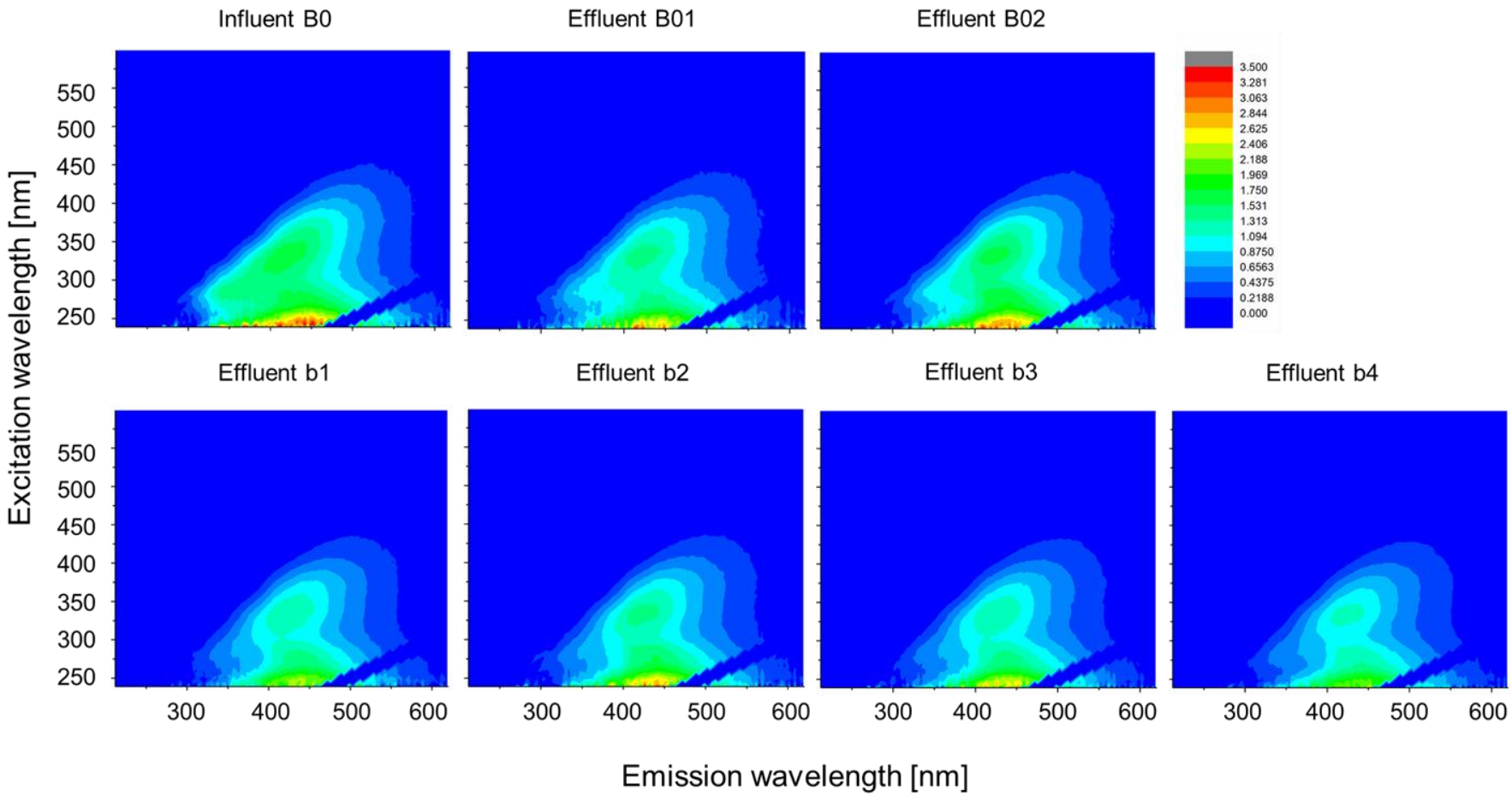

Figure SI-6 3: 3D-Excitation-Emission matrices of all samples throughout the infiltration system used for (-)ESI FT-ICR-MS analyses.

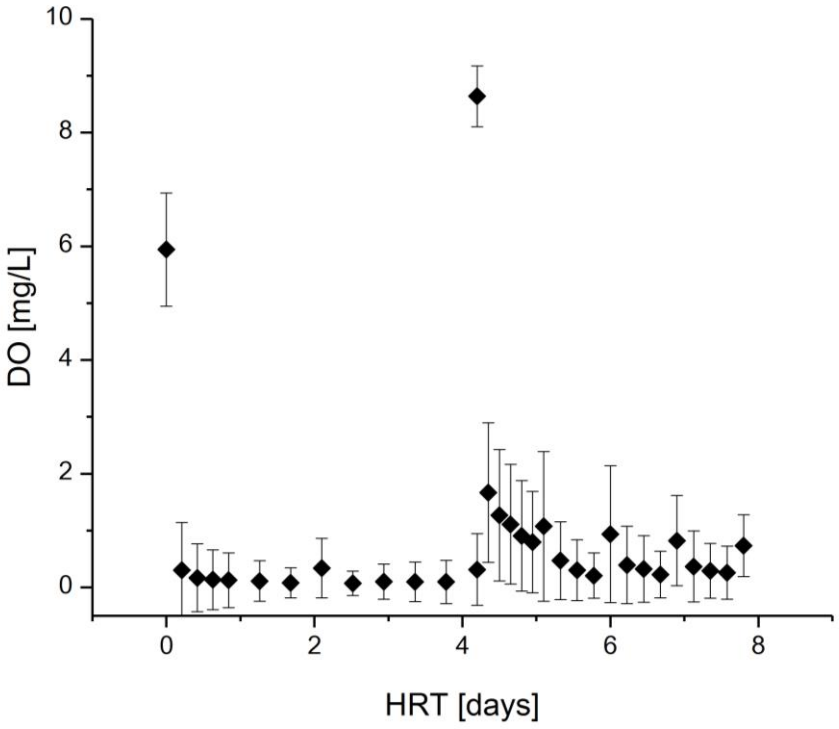

Figure SI-6 4: DO profile (*n* ≥ 22) throughout the system with respect to the HRT. Error bars indicate standard deviation.

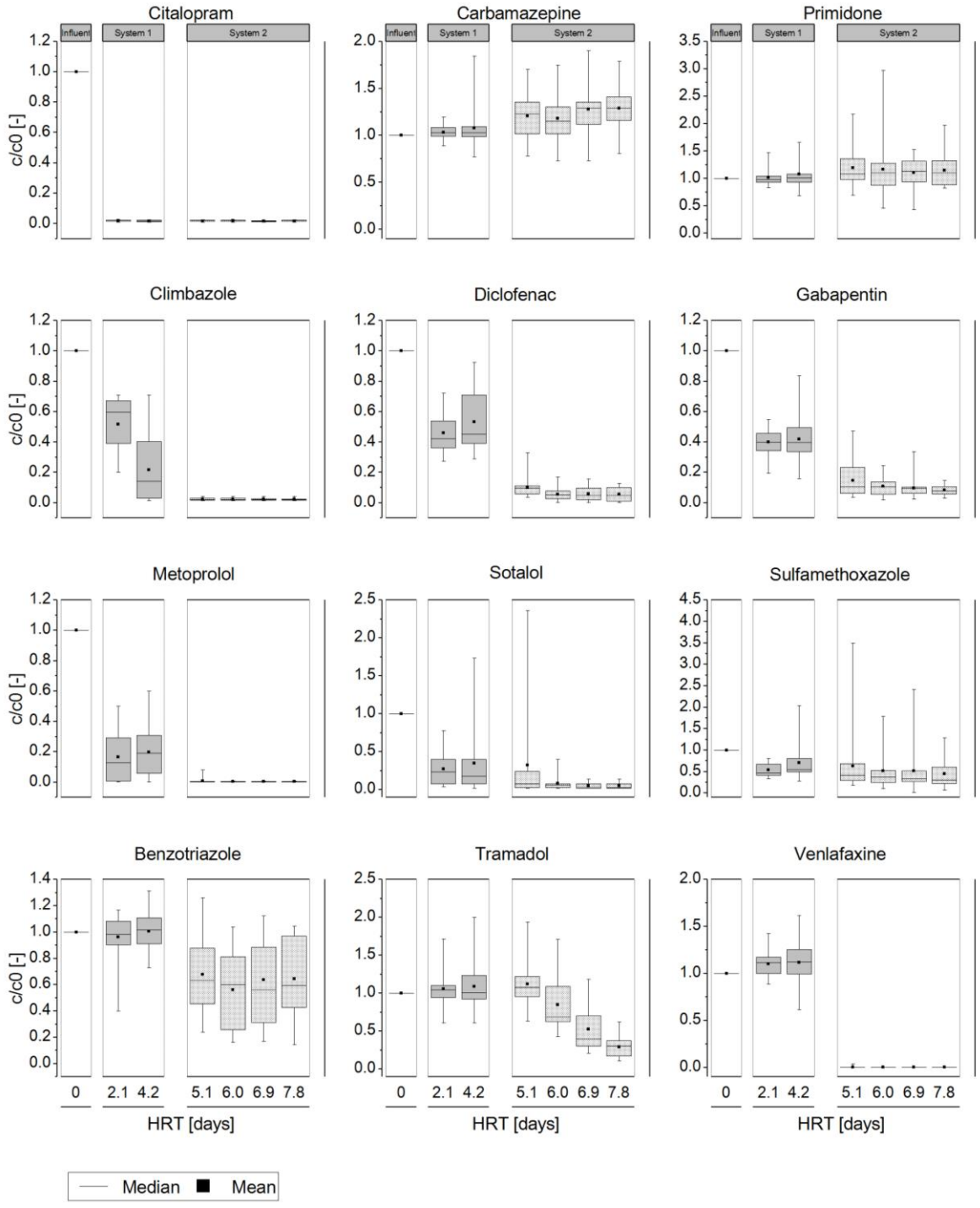

Figure SI-6 5: Relative removal of all targeted TOrCs throughout the infiltration system (*n* ≥ 7). The box represents the 25 – 75 percentiles. The whiskers indicate maximum and minimum values.

.

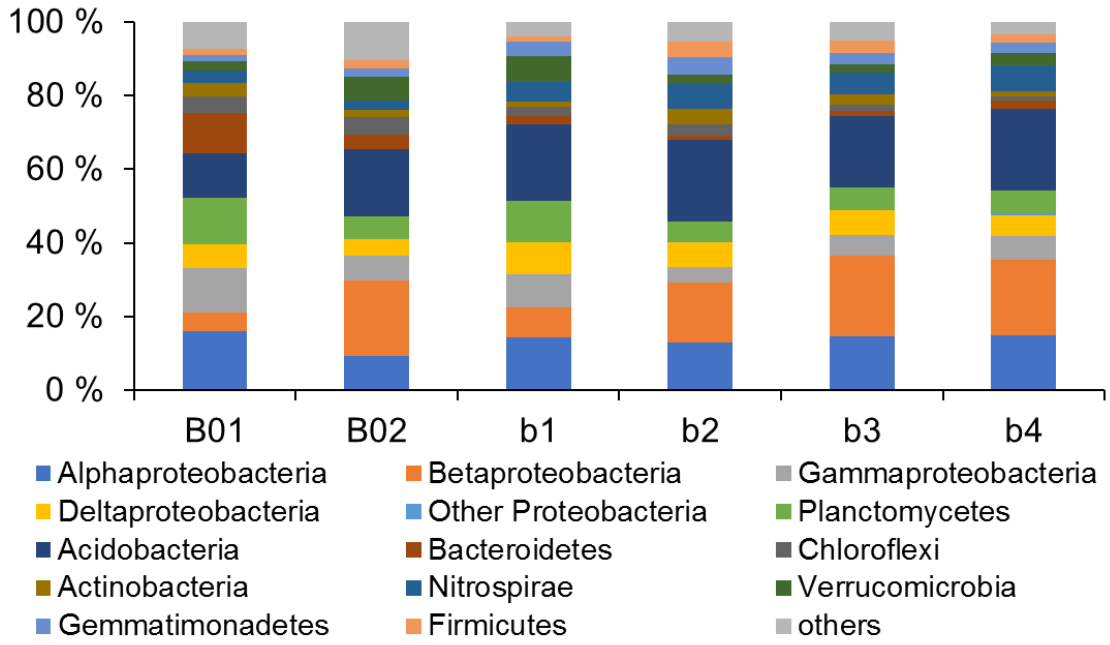

Figure SI-6 6: Percentage of most abundant microbial phyla throughout the system. Proteobacteria are shown in microbial classes.

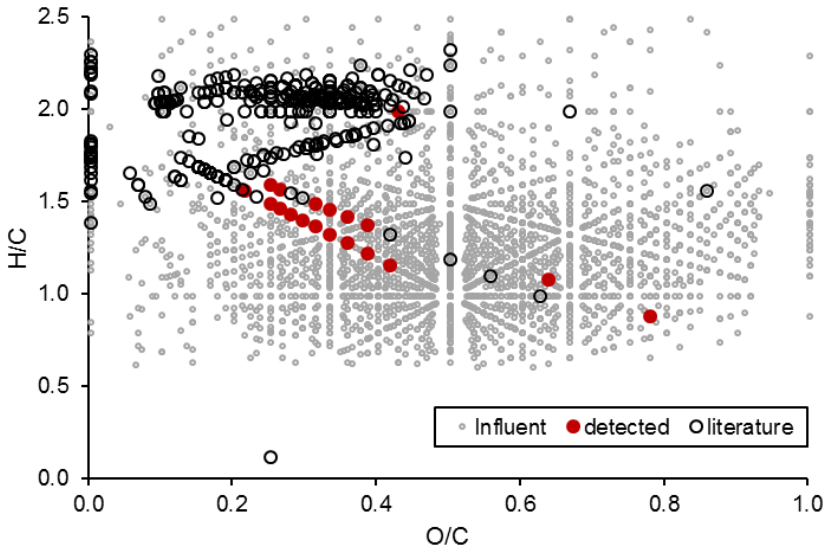

Figure SI-6 7: Surfactants and selected transformation products known from literature[7-13] (black circles) and those which were detected in EfOM (red dots) plotted according to their H/C and O/C ratios. Grey dots represent all masses which were detected in the EfOM meaning the influent to the system.

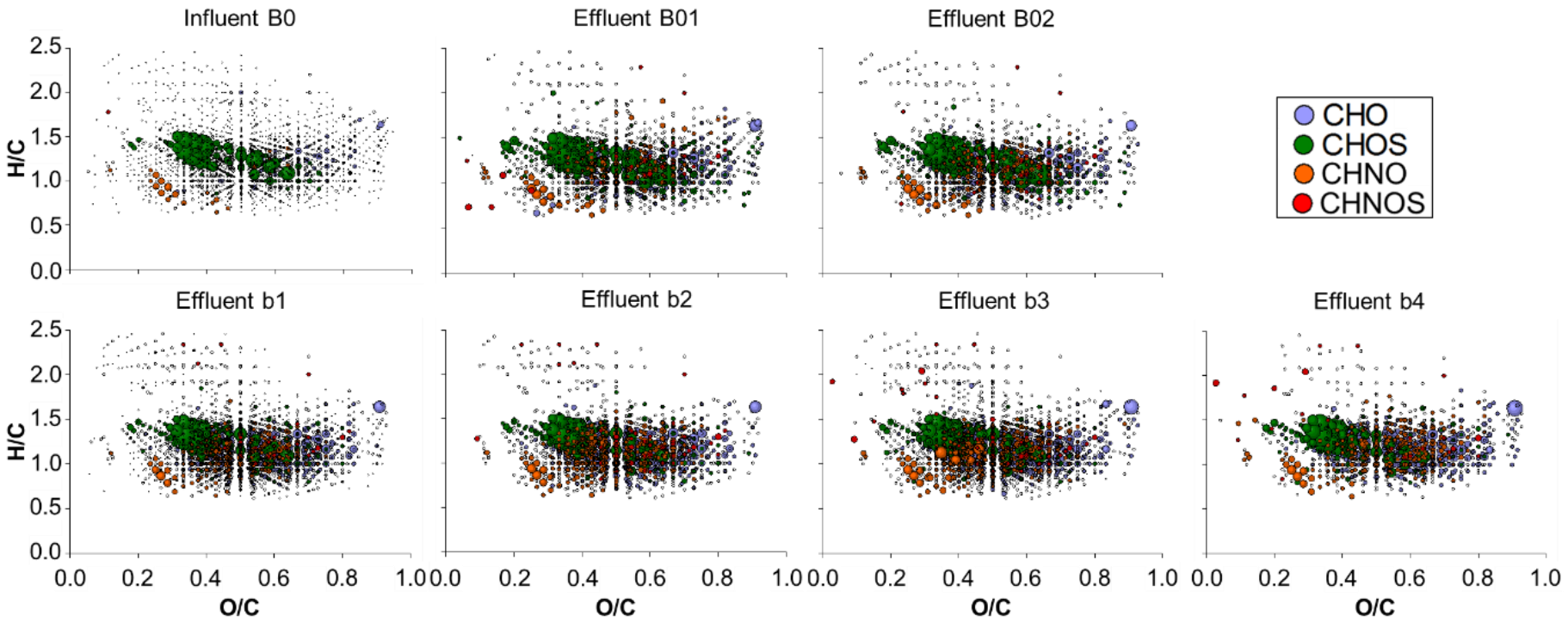

Figure SI-6 8: Results from (-)ESI FT-ICR-MS analyses plotted in van Krevelen diagrams as elemental compositions (CHO, CHOS, CHNO and CHNOS) for masses detected in the influent and effluent samples, respectively. Bubble sizes depict the absolute intensities of each mass.

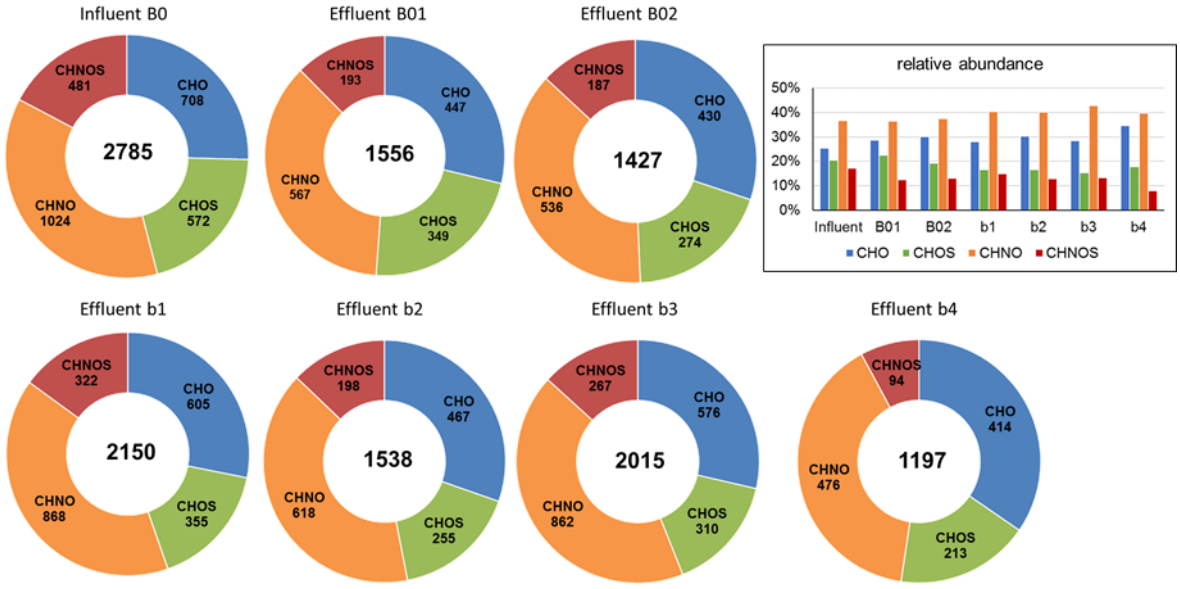

Figure SI-6 9: Molecular composition and the relative abundance of each sample throughout the infiltration based on (-)ESI FT-ICR-MS analyses.

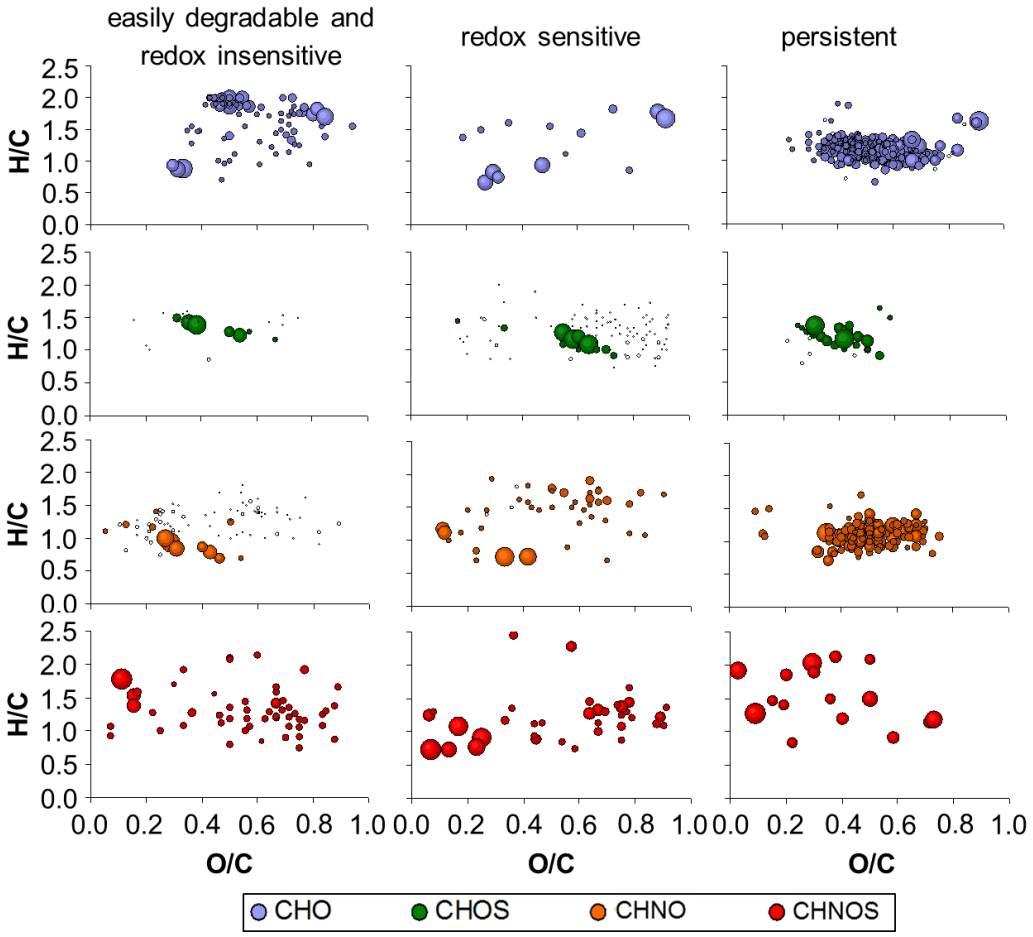

Figure SI-6 10: Van Krevelen plots for each elemental composition (CHO, CHOS, CHNO, CHNOS) of three identified clusters based on MCIA. Bubble sizes depict the absolute intensities of each mass.

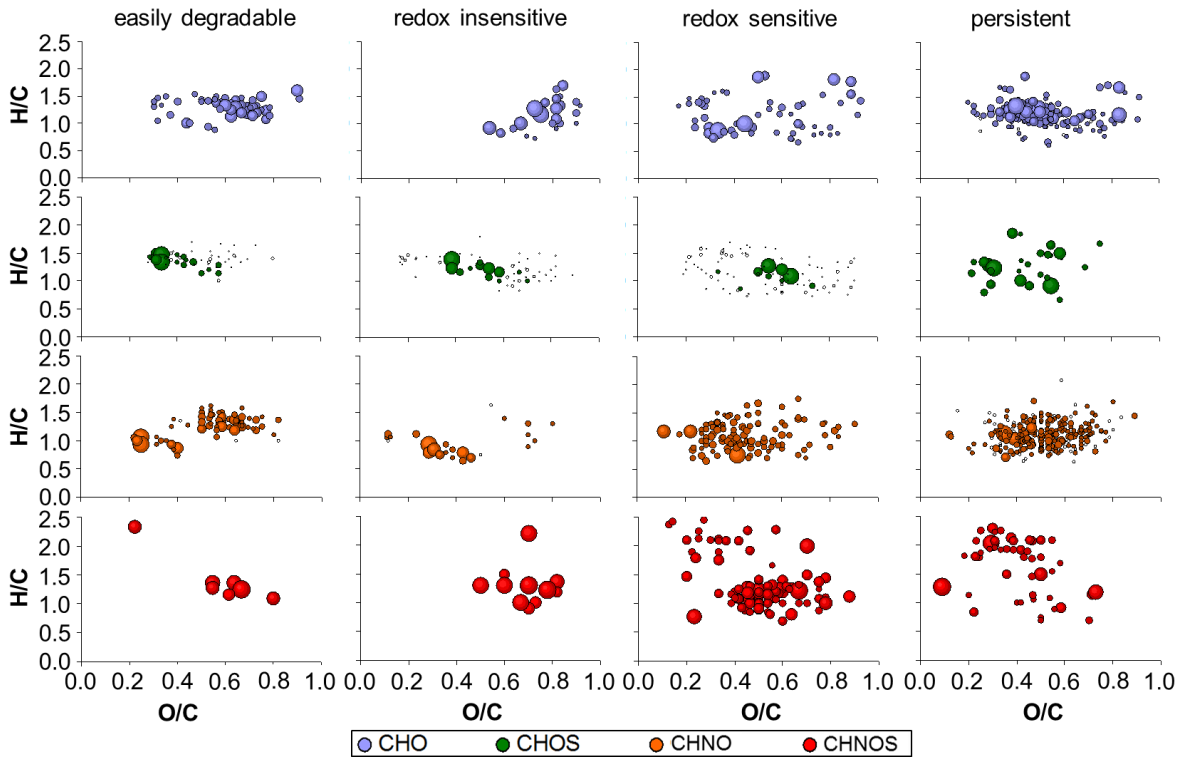

Figure SI-6 11: Van Krevelen plots for each elemental composition (CHO, CHOS, CHNO, CHNOS) of four identified clusters based on OPLS. Bubble sizes depict the absolute intensities of each mass.

References

(1) Stahlschmidt, M.; Regnery, J.; Campbell, A.; Drewes, J. E. Application of 3D-fluorescence/PARAFAC to monitor the performance of managed aquifer recharge facilities. *J. Water Reuse Desalination* **2016**, *6*, 249-263.

(2) Edgar, R. C. Search and clustering orders of magnitude faster than BLAST. Bioinformatics **2010**, *26*, 2460–2461.

(3) Edgar, R. C.; Flyvbjerg, H. Error filtering, pair assembly and error correction for next-generation sequencing reads. Bioinformatics **2015**, *31*, 3476–3482.

(4) Carvajal, G.; Branch, A.; Michel, P.; Sisson, S. A.; Roser, D. J.; Drewes, J. E.; Khan, S. J. Robust evaluation of performance monitoring options for ozone disinfection in water recycling using Bayesian analysis. *Water Res*. **2017**, *124*, 605–617.

(5) Tziotis, D.; Hertkorn, N.; Schmitt-Kopplin, P. Kendrick-analogous network visualisation of ion cyclotron resonance Fourier transform mass spectra: Improved options for the assignment of elemental compositions and the classification of organic molecular complexity. *Eur. J. Mass Spectrom. (Chichester)* **2011**, *17*, 415–421.

(6) Chen, W.; Westerhoff, P.; Leenheer, J. A.; Booksh, K. Fluorescence Excitation−Emission Matrix Regional Integration to Quantify Spectra for Dissolved Organic Matter. *Environ. Sci. Technol.* **2003**, *37*, 5701–5710.

(7) Terrabase Inc. Surfactants. http://www.terrabase-inc.com/ (accessed June 29, 2018).

(8) Riu, J.; Gonzalez-Mazo, E.; Gomez-Parra, A.; Barceló, D. Determination of parts per trillion level of carboxylic degradation products of linear alkylbenzenesulfonates in coastal

water by solid-phase extraction followed by liquid chromatography/ionspray/mass spectrometry using negative ion detection. *Chromatographia* **1999**, *50*, 275–281.

(9) González-Mazo, E.; Honing, M.; Barceló, D.; Gómez-Parra, A. Monitoring Long-Chain Intermediate Products from the Degradation of Linear Alkylbenzene Sulfonates in the Marine Environment by Solid-Phase Extraction Followed by Liquid Chromatography/Ionspray Mass Spectrometry. *Environ. Sci. Technol.* **1997**, *31*, 504–510.

(10) Crescenzi, C.; Di Corcia, A.; Marchiori, E.; Samperi, R.; Marcomini, A. Simultaneous determination of alkylbenzenesulfonates and dialkyltetralinsulfonates in water by liquid chromatography. *Water Res.* **1996**, *30*, 722–730.

(11) Trehy, M. L.; Gledhill, W. E.; Orth, R. G. Determination of linear alkylbenzenesulfonates and dialkyltetralinsulfonates in water and sediment by gas chromatography/mass spectrometry. *Anal. Chem.* **1990**, *62*, 2581–2586.

(12) Trehy, M. L.; Gledhill, W. E.; Mieure, J. P.; Adamove, J. E.; Nielsen, A. M.; Perkins, H. O.; Eckhoff, W. S. Environmental monitoring for linear alkylbenzene sulfonates, dialkyltetralin sulfonates and their biodegradation intermediates. *Environ. Toxicol. Chem.* **1996**, *15*, 233–240.

(13) Field, J. A.; Leenheer, J. A.; Thorn, K. A.; Barber, L. B.; Rostad, C.; Macalady, D. L.; Daniel, S. R. Identification of persistent anionic surfactant-derived chemicals in sewage effluent and groundwater. *J. Contam. Hydrol.* **1992**, *9*, 55–78.

SI Chapter 8: Genomic Bayesian networks identify trophic strategies in microbiomes of managed aquifer recharge (MAR) systems

Table SI-8 1: List of media and solution used for vortexing and media used for bacterial growth on agar plates as well as days of incubation after spreading 100 µL cell suspension.

Soil sample	Vortex medium	Plate medium	Days of incubation
WWTPE, WF	R2A	R2A	2
	R2A 1:10	R2A 1:10	6
	WWTPE	WWTPE	6
	WF	WF	6
DW, DW+HA	1x PBS	R2A	1.5
		R2A 1:10	2
		DW	5
		DW+HA	5

Table SI-8 2: Chemical composition of media used for vortexing and bacterial growth on agar plates.

R2A agar	
Difco™ R2A agar	9.1 g
Milli-Q water	500 mL
R2A 1:10 agar	
Difco™ R2A agar	0.91 g
Agar	8.25 g
Milli-Q water	500 mL
WWTPE/WF/DW/DW+HA agar	
Agar	9.0 g
Medium	500 mL
R2A Medium (pH 7.2 ± 0.2)	
Yeast extract	0.5 g
Proteose peptone	0.5 g
Peptone ex casein	0.5 g
Glucose	0.5 g
Starch, soluble	0.5 g
Sodium pyruvate	0.3 g
Dipotassium phosphate	0.3 g
Magnesium sulfate	0.05 g
Milli-Q water	1000 mL
1x PBS buffer, pH 7.4	
NaCl	8.00 g
KCl	0.20 g
Na_2HPO_4	1.44 g
KH_2PO_4	0.20 g
Milli-Q water	1000 mL

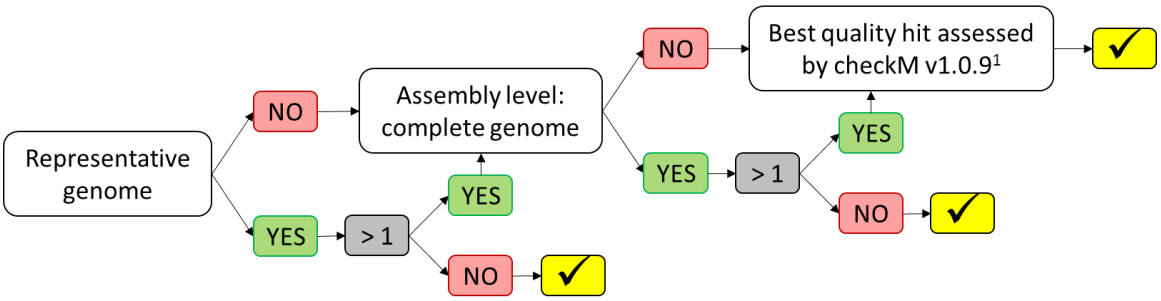

Figure SI-8 1: Workflow to select genome for identifying genomic markers. [1] Parks et al. (2015).

Table SI-8 3: Phylogenetic assignment based on phylogenetic trees built with MEGA7 (2) after aligning against type strains using MUSCLE (3). Bold written organisms represent genera of which genomes were available and had a completeness of > 95 % and < 3 % contamination.

	species	soil	plate medium	best-fit-model	closest relative
copiotrophs	*Flavobacterium*	WWTPE	R2A	K2+G[4]	***F. cauense; F. limnosediminis; F. saliperosum***
		WWTPE	R2A	GTR+G+I[5]	***F. cauense***
		WWTPE	R2A	GTR+G+I[5]	***F. cauense***
		WWTPE	WF	K2+G[4]	*F. eburneum*
		WWTPE	WF	K2+G[4]	*F. eburneum*
		WWTPE	WWTPE	GTR+G+I[5]	*F. inkyongense*
	Pseudomonas	WWTPE	R2A	K2+G+I[4]	***P. cichorii***
		WWTPE	R2A 1:10	K2+G+I[4]	*P. sp.;* ***P. vranovensis***
		WWTPE	R2A 1:10	K2+G+I[4]	*P. sp.;* ***P. vranovensis***
		WWTPE	R2A 1:10	K2+G+I[4]	*P. sp.;* ***P. vranovensis***
		WWTPE	WWTPE	K2+G+I[4]	***P. stutzeri***
		DW	R2A	K2+G[4]	***P. plecoglossicida; P. trivialis****; P. sp.;* ***P. lurida***
oligotrophs	*Microbacterium*	WF	R2A 1:10	K2+G+I[4]	***M. maritypicum; M. oxydans***
		WF	R2A 1:10	K2+G+I[4]	***M. maritypicum; M. oxydans;*** *A. liquefaciens*
		WF	WWTPE	K2+G+I[4]	***M. maritypicum; M. oxydans***
		WF	WWTPE	K2+G+I[4]	***M. maritypicum; M. oxydans***
		WF	WF	K2+G+I[4]	***M. maritypicum; M. oxydans***
	Nocardia	WF	R2A 1:10	T92+G+I[6]	***N. asteroides***
		WF	R2A 1:10	T92+G+I[6]	***N. asteroides***
		WF	R2A 1:10	K2+G+I[4]	***N. asteroides***
		DW	R2A 1:10	T92+G+I[6]	*N. salmonicida*
		DW+HA	R2A 1:10	T92+G+I[6]	***N. asteroides***
		DW+HA	R2A 1:10	T92+G+I[6]	***N. asteroides***
		DW+HA	DW	T92+G+I[6]	***N. asteroides***
		DW+HA	DW+HA	T92+G+I[6]	***N. asteroides***
	Sphingopyxis	WF	R2A 1:10	K2+G+I[4]	***S. bauzanensis***
		WF	WF	K2+G+I[4]	***S. bauzanensis***
		WF	WF	K2+G+I[4]	***S. bauzanensis***
		WF	WF	K2+G+I[4]	*S. fribergensis;* ***S. panaciterrae***
		DW	R2A 1:10	K2+G+I[4]	***S. panaciterra;*** *S. fribergensis*
		DW	DW+HA	K2+G+I[4]	*Sphingomonas sp.;* ***S. alaskensis***
		DW	DW+HA	K2+G+I[4]	*Sphingomonas sp.;* ***S. alaskensis***
		DW+HA	DW+HA	K2+G+I[4]	***S. indica; S. flava;*** *S. soli; S. taejonensis*

[4]Kimura M.A. (1980)
[5]Nei et al. (2000)
[6]Tamura K. (1992)

Table SI-8 3 continued

	species	soil	plate medium	best-fit-model	closest relative
oligotrophs	*Cupriavidus*	DW	R2A 1:10	TN93+G+I[7]	***R. oxalatica***
		DW	DW	TN93+G+I[7]	***R. oxalatica***
		DW	DW	TN93+G+I[7]	***R. oxalatica***
		DW	DW+HA	TN93+G+I[7]	***R. oxalatica***
		DW+HA	R2A 1:10	TN93+G+I[7]	***R. oxalatica***
		DW+HA	R2A 1:10	TN93+G+I[7]	***R. oxalatica***
		DW+HA	DW+HA	TN93+G+I[7]	***R. oxalatica***
	Brevundimonas	WF	R2A 1:10	K2+G+I[4]	***B. nasdae; B. vesicularis***
		DW	R2A 1:10	K2+G+I[4]	*Brevundimonas sp.*
		DW	DW	K2+G+I[4]	*Brevundimonas sp.*
		DW+HA	R2A	K2+G+I[4]	***B. nasdae; B. vesicularis***
		DW+HA	R2A	K2+G+I[4]	*Brevundimonas sp.*
		DW+HA	DW	K2+G+I[4]	*Brevundimonas sp.*
		DW+HA	DW+HA	K2+G+I[4]	*Brevundimonas sp.*
		DW+HA	DW+HA	K2+G+I[4]	*Brevundimonas sp.*
	Caulobacter	DW	R2A 1:10	K2+G+I[4]	***C. crescentus C. vibrioides***
		DW	DW+HA	K2+G[4]	***C. crescentus C. vibrioides C. segnis***
		DW	DW+HA	K2+G+I[4]	***C. crescentus C. vibrioides***
		DW+HA	DW	K2+G[4]	***C. crescentus C. vibrioides C. segnis***
	Tsuka-murella	WF	R2A 1:10	HKY+G[8]	***T. pulmonis;*** *T. sinensis*
		WF	R2A 1:10	TN93+G[7]	*T. spumae, T. sp.,* ***T. pseudospumae***
		WF	WF	TN93+G[7]	***T. pulmonis***
	Rheinheimera	WF	R2A	K2+G+I[4]	*R. chironomi; R. arenilitoris; R. tilapiae*
		WF	R2A	K2+G+I[4]	*R. chironomi; R. arenilitoris; R. tilapiae*
		WF	WWTPE	K2+G+I[4]	*R. mesophila ; R. aquamaris; R. japonica*
		WF	WF	K2+G+I[4]	*R. chironomi; R. arenilitoris; R. tilapiae*
		WF	WF	K2+G+I[4]	*R. tilapiae*
		WF	WF	K2+G+I[4]	*R. chironomi; R. arenilitoris*
		WF	WF	K2+G+I[4]	*R. chironomi; R. arenilitoris; R. tilapiae*

[4]Kimura M.A. (1980)
[7]Tamura and Nei (1993)
[8]Hasegawa et al. (1985)

Table SI-8 4: Species identified based on nucleotide blast of 16S sanger sequencing results. Blue: carbon-rich preferring organisms (copiotrophs); orange: carbon-limited preferring organisms (oligotrophs). WWTPE: soil from column receiving wastewater treatment plant effluent; WF: soil from column receiving biofiltrated WWTPE; DW: soil from column fed with biofiltrated drinking water; DW+HA: soil from column fed with biofiltrated drinking water augmented with humic acid. Numbers indicate identified species based on picked colonies.

soil sample	carbon-rich environment				carbon-limited environment											
	WWTPE				WF				DW				DW+HA			
plate medium	R2A	R2A 1:10	WWTPE	WF	R2A	R2A 1:10	WWTPE	WF	R2A	R2A 1:10	DW	DW+HA	R2A	R2A 1:10	DW	DW+HA
no result	5	3	8	7	1	7	18	7	0	0	0	0	0	2	2	0
Acidovorax	0	0	0	0	0	0	0	0	2	0	0	0	1	0	0	0
Aquabacterium	0	0	0	0	0	0	0	0	0	0	0	1	0	0	0	0
Bacillus	7	4	0	0	8	2	0	0	1	0	0	0	2	0	0	0
Bosea	0	0	1	0	0	0	0	0	0	0	0	0	0	0	0	0
Burkholderiales	0	0	0	0	0	0	1	0	0	0	0	0	0	0	0	0
Brevundimonas	0	0	0	0	0	1	0	0	0	1	1	0	2	0	1	2
Caulobacter	0	0	0	0	0	0	0	0	0	1	0	2	0	0	1	0
Chitinimonas	0	0	1	1	0	0	0	0	0	0	0	0	0	0	0	0
Chryseobacterium	0	0	0	0	3	0	0	0	0	0	0	0	0	0	0	0
Cupriavidus	0	0	0	0	0	0	0	0	0	1	2	1	0	2	0	1
Defluviimonas	0	0	0	0	0	0	1	0	0	0	0	0	0	0	0	0
Flavobacterium	3	0	1	2	0	0	0	0	0	0	0	0	0	0	0	0
Gordonia	0	0	0	1	0	0	0	0	0	0	0	0	0	0	0	0
Hydrogenophaga	0	0	0	0	0	0	0	0	0	0	0	0	1	0	0	0
Lysinibacillus	0	0	0	0	0	0	0	0	1	0	0	0	0	0	0	0
Microbacterium	0	0	0	0	0	2	2	1	0	0	0	0	0	0	0	0
Nocardia	0	0	0	0	0	3	0	0	0	1	0	0	0	2	1	1
Paenibacillus	1	2	0	0	2	0	0	0	1	0	1	1	0	0	1	0
Phenylobacterium	0	0	0	0	0	0	0	0	0	0	0	0	0	0	0	1
Polaromonas	0	0	1	0	0	0	0	0	0	0	0	0	0	0	0	0

Table SI-8 4 continued

soil sample	carbon-rich environment				carbon-limited environment											
	WWTPE				WF				DW				DW+HA			
plate medium	R2A	R2A 1:10	WWTPE	WF	R2A	R2A 1:10	WWTPE	WF	R2A	R2A 1:10	DW	DW+HA	R2A	R2A 1:10	DW	DW+HA
Pseudomonas	1	3	1	0	0	0	0	0	1	0	0	0	0	0	0	0
Pseudoxanthomonas	0	2	3	1	0	3	0	1	0	0	0	0	0	0	0	0
Rheinheimera	0	0	0	0	2	0	1	4	0	0	0	0	0	0	0	0
Rhodococcus	1	6	2	7	0	0	2	4	0	0	0	0	0	0	0	0
Shewanella	1	0	0	0	0	0	0	0	0	0	0	0	0	0	0	0
Sinorhizobium/ Ensifer group	1	0	0	0	0	0	0	0	0	0	0	0	0	0	0	0
Sphingomonas/ Sphingobium	0	0	1	3	0	0	0	0	0	0	0	0	0	0	0	0
Sphingobium	0	0	1	0	0	0	0	0	0	0	0	0	0	0	0	0
Sphingomonas	0	0	0	0	0	0	0	0	0	0	0	0	0	0	0	1
Sphingopyxis	0	0	0	0	0	1	0	3	0	1	0	2	0	0	0	1
Terribacillus	0	0	0	0	0	0	0	0	0	1	0	0	0	0	0	0
Tsukamurella	0	0	0	0	0	2	0	1	0	0	0	0	0	0	0	0

Table SI-8 5: Individual (Indiv.) COG categories significantly different between copiotrophs and oligotrophs based on one-sided White`s non-parametric t-test (9), p-value filter 0.05000 and Storey FDR (10) as multiple test correction (left "Bacterial genomes"); right ("Metagenomes"): relative abundance of Indiv. COGs of metagenomes.

			Bacterial genomes					Metagenomes				
Indiv. COG category	COG category	description	copiotroph (median)		oligotroph (median)		p-value	copiotroph (median)		oligotroph (median)		total median
COG0240	[C]	Glycerol-3-phosphate dehydrogenase	low	(0.03 %)	high	(0.04 %)	0.0186	high	(0.033 %)	low	(0.03 %)	(0.031 %)
COG0479	[C]	Succinate dehydrogenase/fumarate reductase, Fe-S protein subunit	low	(0.03 %)	high	(0.05 %)	0.0292	high	(0.04 %)	low	(0.034 %)	(0.035 %)
COG0584	[C]	Glycerophosphoryl diester phosphodiesterase	low	(0 %)	high	(0.05 %)	0.0186	low	(0.028 %)	high	(0.033 %)	(0.03 %)
COG0711	[C]	F0F1-type ATP synthase, subunit b	low	(0.01 %)	high	(0.08 %)	0.0292	low	(0.005 %)	high	(0.01 %)	(0.008 %)
COG0712	[C]	F0F1-type ATP synthase, delta subunit (mitochondrial oligomycin sensitivity protein)	low	(0 %)	high	(0.04 %)	0.0186	n.a.	(0.017 %)	n.a.	(0.017 %)	(0.017 %)
COG1014	[C]	Pyruvate:ferredoxin oxidoreductase and related 2-oxoacid:ferredoxin oxidoreductases, gamma subunit	low	(0 %)	high	(0.05 %)	0.0387	high	(0.103 %)	low	(0.067 %)	(0.075 %)
COG1053	[C]	Succinate dehydrogenase/fumarate reductase, flavoprotein subunit	low	(0.06 %)	high	(0.10 %)	0.0292	high	(0.162 %)	low	(0.144 %)	(0.158 %)
COG1062†	[C]	Zn-dependent alcohol dehydrogenases, class III	low	(0.03 %)	high	(0.09 %)	0.0292	low	(0.079 %)	high	(0.083 %)	(0.08 %)
COG1282	[C]	NAD/NADP transhydrogenase beta subunit	low	(0.03 %)	high	(0.05 %)	0.0186	high	(0.07 %)	low	(0.044 %)	(0.051 %)
COG1304	[C]	L-lactate dehydrogenase (FMN-dependent) and related alpha-hydroxy acid dehydrogenases	low	(0.03 %)	high	(0.09 %)	0.0186	low	(0.035 %)	high	(0.056 %)	(0.051 %)
COG2141	[C]	Coenzyme F420-dependent N5,N10-methylene tetrahydromethanopterin reductase and related flavin-dependent oxidoreductases	low	(0.03 %)	high	(0.06 %)	0.0428	low	(0.057 %)	high	(0.099 %)	(0.089 %)

Table SI-8 5 continued

COG2142	[C]	Succinate dehydrogenase, hydrophobic anchor subunit	low	(0 %)	high	(0.04 %)	0.0387	high	(0.006 %)	low	(0.004 %)	(0.005 %)
COG3288	[C]	NAD/NADP transhydrogenase alpha subunit	low	(0.05 %)	high	(0.10 %)	0.0186	high	(0.106 %)	low	(0.066 %)	(0.069 %)
COG3474	[C]	Cytochrome c2	low	(0 %)	high	(0.09 %)	0.0292	high	(0.013 %)	low	(0.007 %)	(0.01 %)
COG0554	[C]	Glycerol kinase	low	(0.03 %)	high	(0.05 %)	0.0292	low	(0.063 %)	high	(0.073 %)	(0.07 %)
COG3488	[C]	Predicted thiol oxidoreductase	high	(0.03 %)	low	(0 %)	0.0186	low	(0.003 %)	high	(0.009 %)	(0.007 %)
COG1042*	[C]	Acyl-CoA synthetase (NDP forming)	high	(0 %)	low	(0 %)	0.0387	high	(0.125 %)	low	(0.111 %)	(0.112 %)
COG1196	[D]	Chromosome segregation ATPases	low	(0.03 %)	high	(0.04 %)	0.0186	high	(0.069 %)	low	(0.064 %)	(0.068 %)
COG0014	[E]	Gamma-glutamyl phosphate reductase	low	(0.03 %)	high	(0.04 %)	0.0186	high	(0.058 %)	low	(0.041 %)	(0.043 %)
COG0066	[E]	3-isopropylmalate dehydratase small subunit	low	(0.03 %)	high	(0.05 %)	0.0186	low	(0.047 %)	high	(0.051 %)	(0.048 %)
COG0067	[E]	Glutamate synthase domain 1	low	(0.03 %)	high	(0.04 %)	0.0367	high	(0.061 %)	low	(0.056 %)	(0.057 %)
COG0070	[E]	Glutamate synthase domain 3	low	(0.03 %)	high	(0.04 %)	0.0367	high	(0.049 %)	low	(0.043 %)	(0.044 %)
COG0260	[E]	Leucyl aminopeptidase	low	(0.03 %)	high	(0.08 %)	0.0186	high	(0.074 %)	low	(0.06 %)	(0.063 %)
COG0263	[E]	Glutamate 5-kinase	low	(0.03 %)	high	(0.04 %)	0.0186	high	(0.045 %)	low	(0.026 %)	(0.033 %)
COG0347	[E]	Nitrogen regulatory protein PII	low	(0.03 %)	high	(0.06 %)	0.0367	high	(0.037 %)	low	(0.032 %)	(0.033 %)
COG1364	[E]	N-acetylglutamate synthase (N-acetylornithine aminotransferase)	low	(0.03 %)	high	(0.04 %)	0.0186	n.a.	(0.036 %)	n.a.	(0.034 %)	(0.034 %)
COG0119	[E]	Isopropylmalate/homocitrate/citramalate synthases	low	(0.04 %)	high	(0.05 %)	0.0387	high	(0.108 %)	low	(0.086 %)	(0.091 %)
COG0493	[ER]	NADPH-dependent glutamate synthase beta chain and related oxidoreductases	low	(0.05 %)	high	(0.10 %)	0.0367	high	(0.172 %)	low	(0.134 %)	(0.143 %)
COG0125	[F]	Thymidylate kinase	low	(0.03 %)	high	(0.04 %)	0.0186	high	(0.025 %)	low	(0.022 %)	(0.024 %)
COG0150	[F]	Phosphoribosylaminoimidazole (AIR) synthetase	low	(0.03 %)	high	(0.04 %)	0.0186	n.a.	(0.052 %)	n.a.	(0.046 %)	(0.046 %)
COG0248	[FP]	Exopolyphosphatase	low	(0 %)	high	(0.08 %)	0.0186	low	(0.032 %)	high	(0.034 %)	(0.033 %)
COG0380	[G]	Trehalose-6-phosphate synthase	low	(0 %)	high	(0.04 %)	0.0341	low	(0.024 %)	high	(0.044 %)	(0.03 %)
COG0800	[G]	2-keto-3-deoxy-6-phosphogluconate aldolase	low	(0 %)	high	(0.04 %)	0.0428	low	(0.003 %)	high	(0.013 %)	(0.012 %)
COG1877	[G]	Trehalose-6-phosphatase	low	(0 %)	high	(0.04 %)	0.0399	low	(0.006 %)	high	(0.013 %)	(0.008 %)

Table SI-8 5 continued

COG2301	[G]	Citrate lyase beta subunit	low	(0 %)	high	(0.06 %)	0.0186	high	(0.028 %)	low	(0.022 %)	(0.024 %)
COG2893	[G]	Phosphotransferase system, mannose/fructose-specific component IIA	low	(0 %)	high	(0.04 %)	0.0387	high	(0.01 %)	low	(0.007 %)	(0.008 %)
COG1070	[G]	Sugar (pentulose and hexulose) kinases	low	(0.03 %)	high	(0.05 %)	0.0186	low	(0.074 %)	high	(0.077 %)	(0.076 %)
COG0362*	[G]	6-phosphogluconate dehydrogenase	high	(0 %)	low	(0 %)	0.0387	low	(0.028 %)	high	(0.038 %)	(0.034 %)
COG1072*	[H]	Panthothenate kinase	high	(0 %)	low	(0 %)	0.0387	n.a.	(0.006 %)	n.a.	(0.007 %)	(0.007 %)
COG3572	[H]	Gamma-glutamylcysteine synthetase	low	(0 %)	high	(0.04 %)	0.0313	low	(0.013 %)	high	(0.016 %)	(0.015 %)
COG0301	[H]	Thiamine biosynthesis ATP pyrophosphatase	high	(0.03 %)	low	(0 %)	0.0387	n.a.	(0.001 %)	n.a.	(0.003 %)	(0.003 %)
COG0611	[H]	Thiamine monophosphate kinase	low	(0 %)	high	(0.03 %)	0.0387	high	(0.012 %)	low	(0.008 %)	(0.01 %)
COG0183	[I]	Acetyl-CoA acetyltransferase	low	(0.20 %)	high	(0.41 %)	0.0428	n.a.	(0.291 %)	n.a.	(0.282 %)	(0.282 %)
COG0245	[I]	2C-methyl-D-erythritol 2,4-cyclodiphosphate synthase	low	(0.03 %)	high	(0.04 %)	0.0186	n.a.	(0.024 %)	n.a.	(0.024 %)	(0.024 %)
COG0558	[I]	Phosphatidylglycerophosphate synthase	low	(0.03 %)	high	(0.08 %)	0.0186	n.a.	(0.037 %)	n.a.	(0.036 %)	(0.037 %)
COG0623	[I]	Enoyl-[acyl-carrier-protein] reductase (NADH)	low	(0 %)	high	(0.05 %)	0.0186	high	(0.062 %)	low	(0.057 %)	(0.061 %)
COG0657	[I]	Esterase/lipase	low	(0.07 %)	high	(0.34 %)	0.0186	low	(0.062 %)	high	(0.067 %)	(0.066 %)
COG0821	[I]	Enzyme involved in the deoxyxylulose pathway of isoprenoid biosynthesis	low	(0.03 %)	high	(0.04 %)	0.0186	low	(0.038 %)	high	(0.045 %)	(0.041 %)
COG1024	[I]	Enoyl-CoA hydratase/carnithine racemase	low	(0.30 %)	high	(0.66 %)	0.0186	high	(0.381 %)	low	(0.341 %)	(0.348 %)
COG1211	[I]	4-diphosphocytidyl-2-methyl-D-erithritol synthase	low	(0.03 %)	high	(0.04 %)	0.0186	n.a.	(0.024 %)	n.a.	(0.023 %)	(0.024 %)
COG2030	[I]	Acyl dehydratase	low	(0.09 %)	high	(0.17 %)	0.0186	high	(0.058 %)	low	(0.044 %)	(0.051 %)
COG2084	[I]	3-hydroxyisobutyrate dehydrogenase and related beta-hydroxyacid dehydrogenases	low	(0.05 %)	high	(0.11 %)	0.0186	low	(0.042 %)	high	(0.051 %)	(0.048 %)
COG4553	[I]	Poly-beta-hydroxyalkanoate depolymerase	low	(0 %)	high	(0.04 %)	0.0186	n.a.	(0.016 %)	n.a.	(0.013 %)	(0.016 %)
COG0671	[I]	Membrane-associated phospholipid phosphatase	low	(0.03 %)	high	(0.10 %)	0.0186	n.a.	(0.025 %)	n.a.	(0.025 %)	(0.025 %)

Table SI-8 5 continued

COG0736	[I]	Phosphopantetheinyl transferase (holo-ACP synthase)	low	(0 %)	high	(0.05 %)	0.0186	n.a.	(0.018 %)	n.a.	(0.014 %)	(0.014 %)
COG0743	[I]	1-deoxy-D-xylulose 5-phosphate reductoisomerase	low	(0.03 %)	high	(0.04 %)	0.0186	high	(0.046 %)	low	(0.042 %)	(0.043 %)
COG2031	[I]	Short chain fatty acids transporter	high	(0.03 %)	low	(0 %)	0.0387	low	(0.001 %)	high	(0.006 %)	(0.003 %)
COG0761†	[IM]	Penicillin tolerance protein	low	(0.03 %)	high	(0.05 %)	0.0186	high	(0.048 %)	low	(0.035 %)	(0.041 %)
COG0318	[IQ]	Acyl-CoA synthetases (AMP-forming)/AMP-acid ligases II	low	(0.16 %)	high	(0.66 %)	0.0387	high	(0.671 %)	low	(0.595 %)	(0.598 %)
COG1028†	[IQR]	Dehydrogenases with different specificities (related to short-chain alcohol dehydrogenases)	low	(1.00 %)	high	(1.75 %)	0.0186	low	(0.832 %)	high	(0.92 %)	(0.903 %)
COG0064	[J]	Asp-tRNAAsn/Glu-tRNAGln amidotransferase B subunit (PET112 homolog)	low	(0.03 %)	high	(0.04 %)	0.0186	high	(0.078 %)	low	(0.065 %)	(0.069 %)
COG0244	[J]	Ribosomal protein L10	low	(0.03 %)	high	(0.04 %)	0.0186	n.a.	(0.023 %)	n.a.	(0.022 %)	(0.022 %)
COG0721	[J]	Asp-tRNAAsn/Glu-tRNAGln amidotransferase C subunit	low	(0.03 %)	high	(0.04 %)	0.0186	high	(0.02 %)	low	(0.015 %)	(0.016 %)
COG0858	[J]	Ribosome-binding factor A	low	(0 %)	high	(0.04 %)	0.0313	n.a.	(0.006 %)	n.a.	(0.006 %)	(0.006 %)
COG1189	[J]	Predicted rRNA methylase	low	(0 %)	high	(0.05 %)	0.0186	high	(0.024 %)	low	(0.02 %)	(0.021 %)
COG1514	[J]	2'-5' RNA ligase	low	(0 %)	high	(0.05 %)	0.0219	n.a.	(0.009 %)	n.a.	(0.01 %)	(0.009 %)
COG0051	[J]	Ribosomal protein S10	low	(0.03 %)	high	(0.04 %)	0.0186	high	(0.018 %)	low	(0.011 %)	(0.013 %)
COG0018	[J]	Arginyl-tRNA synthetase	low	(0 %)	high	(0.04 %)	0.0219	high	(0.073 %)	low	(0.056 %)	(0.068 %)
COG0640†	[K]	Predicted transcriptional regulators	low	(0.17 %)	high	(0.34 %)	0.0186	low	(0.063 %)	high	(0.107 %)	(0.102 %)
COG1327	[K]	Predicted transcriptional regulator, consists of a Zn-ribbon and ATP-cone domains	low	(0.03 %)	high	(0.04 %)	0.0186	high	(0.03 %)	low	(0.024 %)	(0.025 %)
COG1329	[K]	Transcriptional regulators, similar to M. xanthus CarD	low	(0 %)	high	(0.04 %)	0.0219	n.a.	(0.009 %)	n.a.	(0.01 %)	(0.009 %)
COG1386	[K]	Predicted transcriptional regulator containing the HTH domain	low	(0.03 %)	high	(0.04 %)	0.0186	n.a.	(0.022 %)	n.a.	(0.022 %)	(0.022 %)
COG1396	[K]	Predicted transcriptional regulators	low	(0.10 %)	high	(0.25 %)	0.0428	high	(0.06 %)	low	(0.05 %)	(0.052 %)
COG1595†	[K]	DNA-directed RNA polymerase specialized sigma subunit, sigma24 homolog	low	(0.09 %)	high	(0.29 %)	0.0186	low	(0.089 %)	high	(0.117 %)	(0.104 %)
COG1733	[K]	Predicted transcriptional regulators	low	(0.01 %)	high	(0.23 %)	0.0186	low	(0.019 %)	high	(0.026 %)	(0.022 %)

Table SI-8 5 continued

COG1846	[K]	Transcriptional regulators	low	(0.17 %)	high	(0.32 %)	0.0292	low	(0.036 %)	high	(0.048 %)	(0.04 %)
COG1959	[K]	Predicted transcriptional regulator	low	(0 %)	high	(0.08 %)	0.0292	high	(0.035 %)	low	(0.025 %)	(0.028 %)
COG2188	[K]	Transcriptional regulators	low	(0.04 %)	high	(0.15 %)	0.0292	high	(0.049 %)	low	(0.037 %)	(0.04 %)
COG2378	[K]	Predicted transcriptional regulator	low	(0 %)	high	(0.04 %)	0.0186	low	(0.006 %)	high	(0.012 %)	(0.009 %)
COG4941†	[K]	Predicted RNA polymerase sigma factor containing a TPR repeat domain	low	(0.01 %)	high	(0.06 %)	0.0292	low	(0.015 %)	high	(0.049 %)	(0.041 %)
COG2740	[K]	Predicted nucleic-acid-binding protein implicated in transcription termination	low	(0 %)	high	(0.04 %)	0.0186	n.a.	(0.001 %)	n.a.	(0.003 %)	(0.003 %)
COG4957	[K]	Predicted transcriptional regulator	low	(0 %)	high	(0.05 %)	0.0186	n.a.	(0.014 %)	n.a.	(0.008 %)	(0.008 %)
COG0571	[K]	dsRNA-specific ribonuclease	low	(0.03 %)	high	(0.04 %)	0.0186	high	(0.026 %)	low	(0.022 %)	(0.023 %)
COG1940	[KG]	Transcriptional regulator/sugar kinase	low	(0 %)	high	(0.03 %)	0.0428	n.a.	(0.014 %)	n.a.	(0.015 %)	(0.014 %)
COG4219*	[KT]	Antirepressor regulating drug resistance, predicted signal transduction N-terminal membrane component	high	(0 %)	low	(0 %)	0.0387	low	(0.003 %)	high	(0.005 %)	(0.004 %)
COG0593	[L]	ATPase involved in DNA replication initiation	low	(0 %)	high	(0.05 %)	0.0186	n.a.	(0.005 %)	n.a.	(0.005 %)	(0.005 %)
COG0742	[L]	N6-adenine-specific methylase	low	(0.03 %)	high	(0.04 %)	0.0186	high	(0.018 %)	low	(0.011 %)	(0.015 %)
COG1195	[L]	Recombinational DNA repair ATPase (RecF pathway)	low	(0 %)	high	(0.04 %)	0.0399	n.a.	(0.014 %)	n.a.	(0.013 %)	(0.014 %)
COG1573	[L]	Uracil-DNA glycosylase	low	(0.01 %)	high	(0.09 %)	0.0292	low	(0.032 %)	high	(0.046 %)	(0.036 %)
COG1722	[L]	Exonuclease VII small subunit	low	(0.03 %)	high	(0.04 %)	0.0186	n.a.	(0.015 %)	n.a.	(0.01 %)	(0.01 %)
COG1793	[L]	ATP-dependent DNA ligase	low	(0.04 %)	high	(0.11 %)	0.0186	low	(0.042 %)	high	(0.102 %)	(0.086 %)
COG2256	[L]	ATPase related to the helicase subunit of the Holliday junction resolvase	low	(0.03 %)	high	(0.10 %)	0.0186	high	(0.081 %)	low	(0.076 %)	(0.079 %)
COG2887	[L]	RecB family exonuclease	low	(0 %)	high	(0.05 %)	0.0186	high	(0.021 %)	low	(0.017 %)	(0.018 %)
COG1570	[L]	Exonuclease VII, large subunit	low	(0.03 %)	high	(0.04 %)	0.0186	high	(0.036 %)	low	(0.032 %)	(0.033 %)
COG3285	[L]	Predicted eukaryotic-type DNA primase	low	(0.03 %)	high	(0.05 %)	0.0186	low	(0.028 %)	high	(0.057 %)	(0.039 %)
COG1112	[L]	Superfamily I DNA and RNA helicases and helicase subunits	low	(0 %)	high	(0.03 %)	0.0387	low	(0.013 %)	high	(0.023 %)	(0.02 %)
COG0494	[LR]	NTP pyrophosphohydrolases including oxidative damage repair enzymes	low	(0.18 %)	high	(0.25 %)	0.0186	high	(0.085 %)	low	(0.077 %)	(0.084 %)

Table SI-8 5 continued

COG0812	[M]	UDP-N-acetylmuramate dehydrogenase	low	(0 %)	high	(0.04 %)	0.0313	high	(0.023 %)	low	(0.021 %)	(0.022 %)
COG1207	[M]	N-acetylglucosamine-1-phosphate uridyltransferase (contains nucleotidyltransferase and I-patch acetyltransferase domains)	low	(0.03 %)	high	(0.05 %)	0.0387	high	(0.066 %)	low	(0.048 %)	(0.052 %)
COG2230	[M]	Cyclopropane fatty acid synthase and related methyltransferases	low	(0.04 %)	high	(0.10 %)	0.0428	high	(0.067 %)	low	(0.056 %)	(0.057 %)
COG3637	[M]	Opacity protein and related surface antigens	low	(0 %)	high	(0.04 %)	0.0186	n.a.	(0.005 %)	n.a.	(0.006 %)	(0.005 %)
COG3773	[M]	Cell wall hydrolyses involved in spore germination	low	(0 %)	high	(0.08 %)	0.0387	high	(0.01 %)	low	(0.008 %)	(0.009 %)
COG0787	[M]	Alanine racemase	low	(0.03 %)	high	(0.05 %)	0.0186	high	(0.031 %)	low	(0.028 %)	(0.029 %)
COG5479*	[M]	Uncharacterized protein potentially involved in peptidoglycan biosynthesis	high	(0 %)	low	(0 %)	0.0186	low	(0 %)	high	(0.003 %)	(0.002 %)
COG2064	[NU]	Flp pilus assembly protein TadC	low	(0 %)	high	(0.04 %)	0.0341	low	(0.007 %)	high	(0.024 %)	(0.019 %)
COG3170	[NU]	Tfp pilus assembly protein FimV	high	(0.03 %)	low	(0 %)	0.0387	n.a.	(0.003 %)	n.a.	(0.001 %)	(0.001 %)
COG0265†	[O]	Trypsin-like serine proteases, typically periplasmic, contain C-terminal PDZ domain	low	(0.07 %)	high	(0.11 %)	0.0387	low	(0.14 %)	high	(0.165 %)	(0.151 %)
COG0695	[O]	Glutaredoxin and related proteins	low	(0.03 %)	high	(0.09 %)	0.0186	n.a.	(0.018 %)	n.a.	(0.009 %)	(0.009 %)
COG1651	[O]	Protein-disulfide isomerase	low	(0 %)	high	(0.11 %)	0.0186	low	(0.025 %)	high	(0.033 %)	(0.029 %)
COG1764	[O]	Predicted redox protein, regulator of disulfide bond formation	low	(0.05 %)	high	(0.10 %)	0.0292	n.a.	(0.012 %)	n.a.	(0.011 %)	(0.012 %)
COG0501	[O]	Zn-dependent protease with chaperone function	low	(0 %)	high	(0.04 %)	0.0387	low	(0.014 %)	high	(0.018 %)	(0.017 %)
COG0735	[P]	Fe2+/Zn2+ uptake regulation proteins	low	(0.03 %)	high	(0.08 %)	0.0367	high	(0.018 %)	low	(0.013 %)	(0.015 %)
COG0783	[P]	DNA-binding ferritin-like protein (oxidative damage protectant)	low	(0 %)	high	(0.02 %)	0.0219	high	(0.008 %)	low	(0.006 %)	(0.007 %)
COG2072	[P]	Predicted flavoprotein involved in K+ transport	low	(0 %)	high	(0.05 %)	0.0186	low	(0.035 %)	high	(0.04 %)	(0.038 %)
COG0168	[P]	Trk-type K+ transport systems, membrane components	high	(0.03 %)	low	(0 %)	0.0292	high	(0.036 %)	low	(0.02 %)	(0.023 %)

Table SI-8 5 continued

COG0569	[P]	K+ transport systems, NAD-binding component	high	(0.03 %)	low	(0 %)	0.0387	high	(0.029 %)	low	(0.024 %)	(0.028 %)
COG2920	[P]	Dissimilatory sulfite reductase (desulfoviridin), gamma subunit	high	(0.03 %)	low	(0 %)	0.0387	high	(0.018 %)	low	(0.004 %)	(0.005 %)
COG3487	[P]	Uncharacterized iron-regulated protein	high	(0.03 %)	low	(0 %)	0.0387	n.a.	(0.004 %)	n.a.	(0.003 %)	(0.004 %)
COG4531	[P]	ABC-type Zn2+ transport system, periplasmic component/surface adhesin	high	(0.03 %)	low	(0 %)	0.0387	high	(0.008 %)	low	(0.006 %)	(0.007 %)
COG4985	[P]	ABC-type phosphate transport system, auxiliary component	high	(0.03 %)	low	(0 %)	0.0387	n.a.	(0.002 %)	n.a.	(0.002 %)	(0.002 %)
COG2124	[Q]	Cytochrome P450	low	(0 %)	high	(0.02 %)	0.0186	low	(0.04 %)	high	(0.088 %)	(0.075 %)
COG0491†	[R]	Zn-dependent hydrolases, including glyoxylases	low	(0.08 %)	high	(0.20 %)	0.0186	low	(0.133 %)	high	(0.165 %)	(0.154 %)
COG0595	[R]	Predicted hydrolase of the metallo-beta-lactamase superfamily	low	(0 %)	high	(0.04 %)	0.0186	high	(0.043 %)	low	(0.039 %)	(0.041 %)
COG0596†	[R]	Predicted hydrolases or acyltransferases (alpha/beta hydrolase superfamily)	low	(0.19 %)	high	(0.37 %)	0.0186	low	(0.204 %)	high	(0.245 %)	(0.225 %)
COG0637	[R]	Predicted phosphatase/phosphohexomutase	low	(0.01 %)	high	(0.06 %)	0.0428	n.a.	(0.025 %)	n.a.	(0.026 %)	(0.025 %)
COG1161	[R]	Predicted GTPases	low	(0 %)	high	(0.04 %)	0.0219	high	(0.017 %)	low	(0.01 %)	(0.012 %)
COG1286	[R]	Uncharacterized membrane protein, required for colicin V production	high	(0.03 %)	low	(0 %)	0.0387	low	(0.002 %)	high	(0.004 %)	(0.003 %)
COG1473	[R]	Metal-dependent amidase/aminoacylase/carboxypeptidase	low	(0.03 %)	high	(0.10 %)	0.0186	high	(0.074 %)	low	(0.063 %)	(0.068 %)
COG1611	[R]	Predicted Rossmann fold nucleotide-binding protein	low	(0.01 %)	high	(0.05 %)	0.0387	n.a.	(0.024 %)	n.a.	(0.024 %)	(0.024 %)
COG1750	[R]	Archaeal serine proteases	low	(0 %)	high	(0.04 %)	0.0341	low	(0.012 %)	high	(0.018 %)	(0.014 %)
COG1754	[R]	Uncharacterized C-terminal domain of topoisomerase IA	low	(0 %)	high	(0.04 %)	0.0186	n.a.	(0.03 %)	n.a.	(0.03 %)	(0.03 %)
COG2234	[R]	Predicted aminopeptidases	low	(0 %)	high	(0.10 %)	0.0292	low	(0.018 %)	high	(0.026 %)	(0.025 %)
COG4221	[R]	Short-chain alcohol dehydrogenase of unknown specificity	low	(0.24 %)	high	(0.47 %)	0.0292	n.a.	(0.204 %)	n.a.	(0.226 %)	(0.226 %)

Table SI-8 5 continued

COG4321	[R]	Uncharacterized protein related to arylsulfate sulfotransferase involved in siderophore biosynthesis	low	(0 %)	high	(0.04 %)	0.0387	n.a.	(0.003 %)	n.a.	(0.002 %)	(0.002 %)
COG0627	[R]	Predicted esterase	low	(0.03 %)	high	(0.05 %)	0.0186	n.a.	(0.023 %)	n.a.	(0.022 %)	(0.022 %)
COG3800	[R]	Predicted transcriptional regulator	low	(0 %)	high	(0.08 %)	0.0186	n.a.	(0.01 %)	n.a.	(0.009 %)	(0.009 %)
COG3030	[R]	Protein affecting phage T7 exclusion by the F plasmid	high	(0.03 %)	low	(0 %)	0.0387	n.a.	(0.001 %)	n.a.	(0.005 %)	(0.001 %)
COG3726	[R]	Uncharacterized membrane protein affecting hemolysin expression	high	(0.03 %)	low	(0 %)	0.0387	n.a.	(0 %)	n.a.	(0 %)	(0 %)
COG1418	[R]	Predicted HD superfamily hydrolase	high	(0.03 %)	low	(0 %)	0.0387	high	(0.006 %)	low	(0.004 %)	(0.005 %)
COG1832	[R]	Predicted CoA-binding protein	low	(0 %)	high	(0.04 %)	0.0387	n.a.	(0.014 %)	n.a.	(0.014 %)	(0.014 %)
COG3979*	[R]	Uncharacterized protein contain chitin-binding domain type 3	low	(0 %)	high	(0 %)	0.0428	low	(0.013 %)	high	(0.029 %)	(0.025 %)
COG1565	[S]	Uncharacterized conserved protein	low	(0 %)	high	(0.04 %)	0.0387	n.a.	(0.016 %)	n.a.	(0.016 %)	(0.016 %)
COG2261	[S]	Predicted membrane protein	low	(0 %)	high	(0.05 %)	0.0186	n.a.	(0.005 %)	n.a.	(0.002 %)	(0.002 %)
COG3349	[S]	Uncharacterized conserved protein	low	(0.01 %)	high	(0.05 %)	0.0367	high	(0.034 %)	low	(0.031 %)	(0.032 %)
COG3739	[S]	Uncharacterized integral membrane protein	low	(0 %)	high	(0.04 %)	0.0313	n.a.	(0.004 %)	n.a.	(0.002 %)	(0.002 %)
COG3750	[S]	Uncharacterized protein conserved in bacteria	low	(0 %)	high	(0.04 %)	0.0387	n.a.	(0.001 %)	n.a.	(0.001 %)	(0.001 %)
COG3795	[S]	Uncharacterized protein conserved in bacteria	low	(0 %)	high	(0.04 %)	0.0367	low	(0.007 %)	high	(0.018 %)	(0.017 %)
COG5349	[S]	Uncharacterized protein conserved in bacteria	low	(0 %)	high	(0.05 %)	0.0186	high	(0.006 %)	low	(0.004 %)	(0.005 %)
COG5394	[S]	Uncharacterized protein conserved in bacteria	low	(0 %)	high	(0.04 %)	0.0387	high	(0.016 %)	low	(0.009 %)	(0.01 %)
COG1872	[S]	Uncharacterized conserved protein	low	(0 %)	high	(0.04 %)	0.0313	n.a.	(0.006 %)	n.a.	(0.006 %)	(0.006 %)
COG2968	[S]	Uncharacterized conserved protein	low	(0 %)	high	(0.04 %)	0.0387	n.a.	(0.01 %)	n.a.	(0.009 %)	(0.009 %)
COG3346	[S]	Uncharacterized conserved protein	low	(0 %)	high	(0.02 %)	0.0387	n.a.	(0.004 %)	n.a.	(0.005 %)	(0.004 %)
COG1273	[S]	Uncharacterized conserved protein	low	(0.03 %)	high	(0.04 %)	0.0186	low	(0.006 %)	high	(0.026 %)	(0.021 %)

Table SI-8 5 continued

COG3266	[S]	Uncharacterized protein conserved in bacteria	high	(0.03 %)	low	(0 %)	0.0387	n.a.	(0 %)	n.a.	(0 %)	(0 %)
COG3490	[S]	Uncharacterized protein conserved in bacteria	high	(0.03 %)	low	(0 %)	0.0387	n.a.	(0.001 %)	n.a.	(0.001 %)	(0.001 %)
COG3930	[S]	Uncharacterized protein conserved in bacteria	high	(0.03 %)	low	(0 %)	0.0292	n.a.	(0.001 %)	n.a.	(0.002 %)	(0.002 %)
COG4642	[S]	Uncharacterized protein conserved in bacteria	high	(0.03 %)	low	(0 %)	0.0387	high	(0.005 %)	low	(0.003 %)	(0.004 %)
COG3397*	[S]	Uncharacterized protein conserved in bacteria	low	(0 %)	high	(0 %)	0.0428	low	(0.001 %)	high	(0.006 %)	(0.005 %)
COG3752	[S]	Predicted membrane protein	low	(0 %)	high	(0.04 %)	0.0313	n.a.	(0.007 %)	n.a.	(0.006 %)	(0.007 %)
COG0394	[T]	Protein-tyrosine-phosphatase	low	(0.01 %)	high	(0.07 %)	0.0367	low	(0.011 %)	high	(0.019 %)	(0.018 %)
COG0664	[T]	cAMP-binding proteins - catabolite gene activator and regulatory subunit of cAMP-dependent protein kinases	low	(0.01 %)	high	(0.11 %)	0.0367	low	(0.07 %)	high	(0.073 %)	(0.071 %)
COG3629*	[T]	DNA-binding transcriptional activator of the SARP family	high	(0 %)	low	(0 %)	0.0313	low	(0.009 %)	high	(0.029 %)	(0.025 %)
COG3745	[U]	Flp pilus assembly protein CpaB	low	(0 %)	high	(0.05 %)	0.0186	n.a.	(0.005 %)	n.a.	(0.006 %)	(0.006 %)
COG4962	[U]	Flp pilus assembly protein, ATPase CpaF	low	(0.03 %)	high	(0.10 %)	0.0186	low	(0.074 %)	high	(0.096 %)	(0.085 %)
COG4965	[U]	Flp pilus assembly protein TadB	low	(0 %)	high	(0.04 %)	0.0186	low	(0.009 %)	high	(0.016 %)	(0.015 %)
COG4961	[U]	Flp pilus assembly protein TadG	low	(0 %)	high	(0.02 %)	0.0387	n.a.	(0.001 %)	n.a.	(0.001 %)	(0.001 %)
COG1403	[V]	Restriction endonuclease	low	(0 %)	high	(0.05 %)	0.0186	low	(0.007 %)	high	(0.01 %)	(0.008 %)

†identified as markers within the Bayesian network analysis
*mean values significantly different even though median is zero in both cases.
n.a. same median observed for copio-/oligotrophs or same value for median of copio-/oligotroph and total median.

0

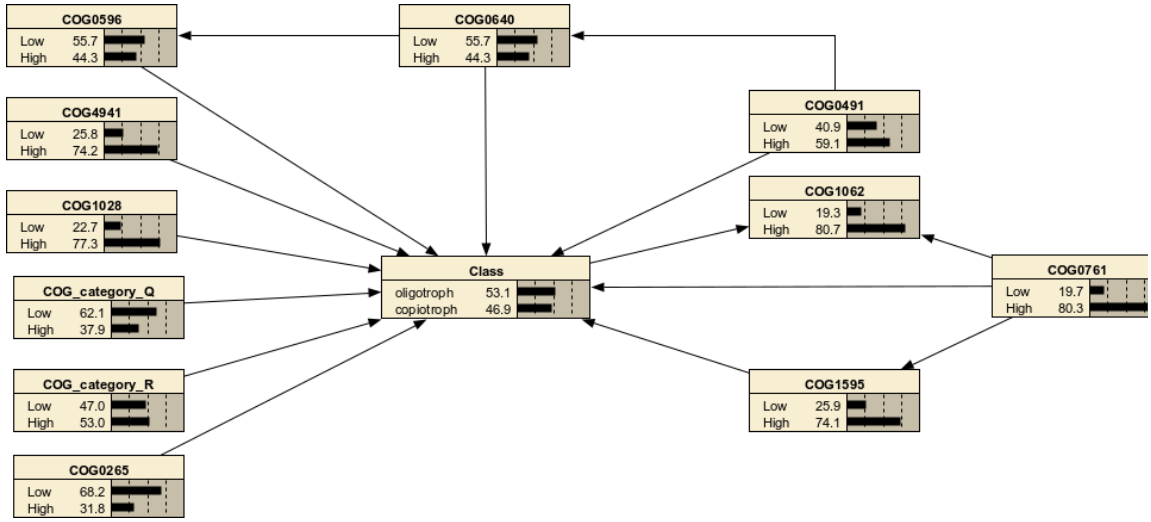

Figure SI-8 2: ICSS network for trophic strategy and genomic markers

Table SI-8 6: Sensitivity analysis of Bayes ICSS network

	Mutual Info	Percent	Variance of Belief
Class	0.99729	100	0.2490602
COG1062	0.036313	3.62	0.0122900
COG0640	0.00504	0.505	0.0017370
COG0596	0.00489	0.491	0.0016862
COG_category_R	0.00389	0.39	0.0013413
COG0491	0.00373	0.374	0.0012878
COG4941	0.00203	0.204	0.0007024
COG1028	0.00193	0.194	0.0006676
COG1595	0.00184	0.184	0.0006352
COG0761	0.00151	0.152	0.0005237
COG_category_Q	0.00046	0.0466	0.0001603
COG0265	0.00027	0.0275	0.0000946

References

1. Parks DH, Imelfort M, Skennerton CT, Hugenholtz P, Tyson GW. CheckM: Assessing the quality of microbial genomes recovered from isolates, single cells, and metagenomes. Genome Res 2015; 25(7):1043–55.
2. Kumar S, Stecher G, Tamura K. MEGA7: Molecular Evolutionary Genetics Analysis Version 7.0 for Bigger Datasets. Mol Biol Evol 2016; 33(7):1870–4.
3. Edgar RC. MUSCLE: Multiple sequence alignment with high accuracy and high throughput. Nucleic Acids Res 2004; 32(5):1792–7.
4. Kimura M. A simple method for estimating evolutionary rates of base substitutions through comparative studies of nucleotide sequences. J Mol Evol 1980; 16(2):111–20.
5. Nei M, Kumar S. Molecular evolution and phylogenetics. Oxford, New York: Oxford University Press; 2000.
6. Tamura K. Estimation of the number of nucleotide substitutions when there are strong transition-transversion and G+C-content biases. Mol Biol Evol 1992; 9(4):678–87.
7. Tamura K, Nei M. Estimation of the number of nucleotide substitutions in the control region of mitochondrial DNA in humans and chimpanzees. Mol Biol Evol 1993; 10(3):512–26.
8. Hasegawa M, Kishino H, Yano T-a. Dating of the human-ape splitting by a molecular clock of mitochondrial DNA. J Mol Evol 1985; 22(2):160–74.
9. White JR, Nagarajan N, Pop M. Statistical methods for detecting differentially abundant features in clinical metagenomic samples. PLoS Comput Biol 2009; 5(4):e1000352.
10. Storey JD, Tibshirani R. Statistical significance for genomewide studies. Proc Natl Acad Sci U S A 2003; 100(16):9440–5.